UNIVERSITÉ DU QUÉBEC

THÈSE PRÉSENTÉE À L'UNIVERSITÉ
DU QUÉBEC À TROIS-RIVIÈRES

COMME EXIGENCE PARTIELLE
DU DOCTORAT EN GÉNIE PAPETIER

PAR

S. Mehdi Manzour-ol-ajdad

ÉTUDE FONDAMENTALE DES CORRÉLATIONS ENTRE
L'OXYDATION DES FIBRES DE BAGASSE ET DE TREMBLE
PAR LE TÉTROXYDE D'AZOTE (N_2O_4)
ET LA RÉSISTANCE MÉCANIQUE DE LA FEUILLE

FUNDAMENTAL STUDY OF THE CORRELATION
BETWEEN N_2O_4 OXIDATION OF BAGASSE AND ASPEN FIBRES
AND THE MECHANICAL STRENGTH OF SHEETS

MARS 2000

Université du Québec à Trois-Rivières

Service de la bibliothèque

Ya Mahdi

ACKNOWLEDGEMENT

SUMMARY

By producing additional hydrogen bonds, due to the formation of carboxyl groups (COOH), we studied the effect of the N_2O_4 oxidation to the strength properties of the bleached kraft pulps. The main objective of this study was to observe the influence of the formation of carboxyl groups due to the nitrogen tetroxide (N_2O_4) oxidation to the bonding strength of the fibres, through the increasing the hydrophilic character and surface adhesion of the fibres. We intended to find out under what conditions of treatment, such as gas flow-rate, oxidation time, temperature and pulp consistency or by using the chemical substances, the improvement of the above properties may be obtained. The other objective was to determine whether the final achievements would be resulted to the higher paper strength of the sheet. An application of the page equation of $1/T=1/F +1/B$.

The experimental work first involved a three-design protocol applied to a standard bleached kraft softwood pulp as a reference. The designs used were the one factor at a time, the half-factorial and a 3-factor 5 level central composite design (CCD). It was found that carboxyl formation increased to a certain limit as the gas flow-rate, oxidation time increased. However, there was a simultaneous decrease in viscosity, which is a sign of fibre degradation. Regardless of the operating conditions, the decrease in viscosity was large enough to overcompensate the carboxyl formation effect, such that the overall effect was a decrease in tensile and z strength of the handsheets. The effect of temperature and consistency was to accelerate the viscosity loss.

The carboxyl formation was verified by inspection of FTIR spectra, which displayed a new peak at 1734-1738 cm^{-1}. The OH peak was perturbed due to the transformation of different carbons in the glucosidic rings to aldehyde and ketone groups. The ESCA showed that the O/C ratio increased during the oxidation, which is a

sign of greater hydrophilic character of the oxidised fibres. It was also found that the C1 component decreased and the C2 increased for all three fibres. The C3 representative the carbonyl groups formation increased for the softwood as well as for the bagasse oxidised fibres. However, it was not possible to detect carboxyl groups (at binding energy of 288.4 eV) on the surface by ESCA. At the same time, the specific acid-base interaction, I_{SP} of the softwood and bagasse fibres, as determined by IGC, increased due to the higher H-bonding formation. In the case of aspen fibres, there was neither an increase in O/C ratio nor in the specific acid-base interaction. This can be explained by the acidic character of the untreated aspen fibres (K_A= 2.9, K_B= 1.9) as compared to the basic character of the bagasse (K_A=1.7, K_B= 2.3) and to the amphoteric character of softwood bleached kraft fibres (K_A= 0.49, K_B= 0.55).

In order to determine the possibility of limiting the degradation of fibres by this oxidation, the oxidation was repeated in the presence of 1%-$MgCO_3$, a salt which has been reported to provide some protection to the cellulose fibres in other oxidative environments. It was found out that this salt limited the reduction of the viscosity of pulp. Even though the formation of carboxyls was also lower than that during oxidation without $MgCO_3$, the net effect was to improve the strength properties of the paper over and beyond those of papers made from the original untreated fibres. This occurred at oxidation rates of 0.8% and 2.5%-N_2O_4/fiber, for softwood and bagasse, respectively. The improvements in tensile and burst strength were 25, 5%, and 12% for the softwood and bagasse, respectively. Under the same conditions, it was also found that the treatment increased the opacity and the scattering coefficient of oxidised fibres.

The mathematical evaluation based on the Carrasco method, led to the same conclusions as the graphical interpretations of experiments. Essentially, the multiple regression analysis showed that a paper strength is more strongly influenced by the morphological and physical properties of fibres, (CSF, fibre length, viscosity), than by chemical changes induced by the oxidation process (carboxyl formation, O/C ratio, I_{sp}). However, the importance of the hydrophilic effect and surface adhesion of the fibres affecting the bonding strength of the oxidised fibres, B, on the tensile strength, T, in the

Page equation is clear when the viscosity is kept within a certain range by $MgCO_3$. Interpretation of the three-factor model showed that even though there is an obvious reduction in fibre length and in viscosity due to the N_2O_4 oxidation, it is still possible in the case of using a protective agent, to improve the paper strength due to the increase in the hydrophilic character and surface adhesion of the fibres.

RÉSUMÉ

a)   Problématique

L'amélioration des propriétés mécaniques de la feuille a toujours constitué un objectif souhaitable pour la fabrication du papier, et tout particulièrement pour les papiers fabriqués principalement de fibres courtes, tel que la bagasse ou le tremble. Divers traitements mécaniques, thermiques et chimiques de la pâte permettent d'arriver à cette fin. Il était évidant que par les simples traitements mécaniques, comme le raffinage ou le pressage, produisant un changement morphologique important des fibres, on obtient facilement de très bons résultats. En ce qui concerne le traitement chimique de la pâte, il entraîne une modification de la structure fine des fibres, ainsi que des propriétés mécaniques du papier, comme la résistance.

De nombreux chercheurs se sont penchés sur ces dernières. Ils ont obtenu une augmentation de la résistance du papier en utilisant, entre autres, divers substituants pour les groupements hydroxyles, un faible niveau d'oxydation (33) ou des réactions de greffage (1). Des recherches ont démontré qu'un faible taux de substitution des groupes hydrophobes permet d'augmenter la capacité de liaisons et d'améliorer la résistance du papier. Toutefois, lorsque le degré de substitution hydrophobe est élevé, la cellulose devient soluble.

Un autre type de traitement chimique utilisé pour améliorer la qualité de la cellulose est l'oxydation. La plupart des études portant sur ce procédé ont été effectuées dans le domaine du textile, et notamment sur les fibres de coton ou de linter (4,13). Diverses méthodes et différents niveaux d'oxydation de la cellulose ont été mis au point afin de permettre la formation de groupements carbonyles et carboxyles (8). Différents types de substances: chlore, hypochlorites, peroxydes de chlore, peroxyde d'hydrogène, ozone, rayonnement ultraviolet en présence d'eau, oxydent les fonctions alcooliques

cellulosiques et entraînent la formation de fonctions acides (COOH). On appelle oxycelluloses les produits relativement peu dégradés de ce procédé. Ce type d'oxydation fait partie des opérations de blanchiment (4,5,52).

L'oxydation par le périodate (11), par le tétroxyde de ruthénium (12) ou par l' héxanitratocérate d'ammonium.(13) constitue un autre type d'oxydation par lequel la structure chimique de la cellulose change énormément. Non seulement, il y a coupure des liens glucosidiques, ce qui réduit fortement le degré de polymérisation, mais aussi une production très élevée de groupements carbonyles aldéhydiques. Quand la concentration d'oxydants est élevée, le pH est alcalin et la durée d'oxydation longue, il se produit un clivage du cycle glucopyranique. Ce phénomène cause la dégradation totale de la cellulose et produit finalement de l'acide formique (H COOH) et des gaz tels que le dioxyde de carbone (CO_2) ou l'hydrogène (H_2).

On peut aussi recourir à l'oxydation par le tétroxyde d'azote (N_2O_4) à l'état gazeux. L'avantage de ce procédé est qu'il permet principalement d'oxyder les groupements hydroxyles de C-6, pour les transformer en groupement carboxyles (formation d'acide célluronique), et une quantité de groupement hydroxyles de C2 et/ou C3 pour les transformer en groupements cétoniques (15,16). Une légère éthérification entraîne un faible degré de nitration de la cellulose. Cette dernière est causée par l'acidité du dioxyde d'azote et l'humidité du coton (17)

L'objectif des expérimentations qui ont été effectuées à ce jour sur le coton, l'acétate de cellulose ou les oxycelluloses consistait à analyser les effets du procédé d'oxydation sur la cellulose et son mécanisme réactionnel sans tenir compte de ses effets sur les propriétés mécaniques. Mercer (15) a observé que l'oxydation de mannane B et de la cellulose régénérée a l'aide du tétroxyde d'azote permettait d'obtenir un contenu carboxylique de 24,1-25,4%; il a aussi mesuré la quantité de groupements cétoniques des substances utilisées. La carboxylation de la cellulose, par laquelle la fonction alcool (OH) se transforme en fonction acide (COOH), pourrait aussi augmenter l'énergie

d'adhésion entres les fibres et favoriserait une meilleure résistance des liaisons fibre à fibre.

Il est important de noter que la carboxycellulose est insoluble dans l'eau et dans les solvants organiques. Cependant, lorsque le contenu carboxylique augmente, elle devient soluble dans les solutions alcalines diluées, et la résistance des fibres diminue. Ainsi, pour arriver à une résistance de rétention acceptable, les conditions de traitement doivent être douces, la température ambiante, le pH du milieu presque neutre, et la durée du traitement longue (17).

Ces dernières années, beaucoup d'attention a été portée sur l'oxydation par le N_2O_4 comme un pré-traitement du blanchiment par l'oxygène ou par l'ozone (18,19). L'introduction du procédé de Prenox (20) a produit un effet positif pour les pâtes non blanchies. Kokta *et al.*(21) ont mesuré le contenu carboxylique de la pâte TMP oxydée par le N_2O_4. Ils ont rapporté que celui-ci augment en fonction de la durée d'oxydation. Beaucoup de questions se posent concernant l'effet de l'oxydation sur la viscosité de la pâte, sur l'adhésion à la surface des fibres, sur la résistance fibre à fibre et enfin sur les propriétés optiques de la pâte oxydée. Ceci constitue les objectifs de notre recherche définis ci-dessous.

b)   Objectifs de la thèse

-Étudier l'effet d'oxydation par N_2O_4 sur la formation des groupements carboxyliques (COOH) et sur la viscosité de la pâte

-Étudier l'effet de l'oxydation par le tétroxyde d'azote sur la structure chimique (masse et surface) des fibres de résineux, de la bagasse et du tremble.

-Évaluer l'influence de la formation des groupements carboxyliques (COOH) sur la contribution acido-basique au travail d'adhésion des fibres ci-dessus.

-Mesurer l'effet de l'oxydation sur la résistance des liaisons fibre à fibre et sur la résistance mécanique de la feuille(confirmation d'équation de Page).

-Évaluer si l'addition des agents chimiques tels que $MgCO_3$ pendant

l'oxydation a un effet positif sur la réduction de la dégradation de la cellulose et de la résistance de la feuille.

-Établir les corrélations entre les changements hydrophiles et la surface des fibres oxydées et les propriétés mécaniques et optiques du papier.

c)   Méthodologie

Tout d'abord, l'effet des quatre paramètres d'oxydation sur le contenu carboxylique et sur la viscosité des fibres a été étudié par trois plans expérimentaux d'un facteur à la fois, demi-factoriel et la désigne composite centrale(CCD). Cette démarche a été utilisée pour trouver une condition convenable pour rendre possible la formation des groupements carboxyliques dans la mesure où la viscosité intrinsèque reste au-dessus de 600 dm^3/kg (DP d'environ 540) ce qui permet de fabriquer la feuille. Par le plan d'un facteur à la fois, nous avons étudié l'effet de chaque variable sur la formation des groupements carboxyliques et la viscosité de la pâte en gardant les autres paramètres constants. Par le plan demi-factoriel, les quatre paramètres de l'oxydation sont comparés à deux niveaux. Les trois paramètres les plus importants sur la formation du contenu carboxylique sont comparés ensemble par un plan de CCD (Central Composite Design) à cinq niveaux. Ces essais ont été effectués sur la pâte kraft blanchie des résineux.

Après avoir choisi une condition raisonnable (COOH élevé entraînant la plus petite réduction de viscosité) pour les fibres kraft des résineux, on l'a appliquée pour les fibres kraft blanchies de bagasse et celles de tremble.

Pour évaluer l'effet de l'oxydation sur la structure chimique des fibres, on a utilisé la spectromètre infrarouge à transformée de Fourrier (FTIR). La spectrométrie électronique d'analyse chimique(ESCA) a aussi été utilisée pour connaître les composants chimiques et les caractères hydrophiliques de la surface des fibres oxydées. La technique de chromatographie gazeuse en phase inverse (IGC) a été mise au point, pour étudier l'effet de l'oxydation sur l'adhésion entre les fibres en utilisant les composants dispersifs de l'énergie de la surface, γ^D_S, ainsi que les constantes acide-base (K_A et K_B) des fibres oxydées. Finalement, les propriétés physiques et mécaniques des

fibres oxydées sont mesurées par les différents tests selon les méthodes du Tappi. Un modèle mathématique basé sur le coefficient de régression multiple a été utilisé pour établir une corrélation souhaitable entre les paramètres concernant les propriétés physiques et de la surface des fibres et les propriétés mécaniques et optiques de la feuille.

d)   Résultats

Les résultats obtenus par les différentes méthodes utilisées pendant cette recherche montrent que:

-Par l'augmentation du débit du gaz N_2O_4 pendant l'oxydation, la quantité du COOH peut augmenter jusqu'à une certaine limite. Pourtant, au-delà de 4 à 5 ml/min. (quand la température est maintenue à 5 degrés Celsius pour un poids de 30 grammes de fibres), il n'y a plus d'absorption du gaz et la formation de COOH n'augmente plus.

-Une durée d'oxydation égale ou inférieure à 2-heures favorise la formation du COOH. Au-delà de ce temps, l'oxydation cause une dégradation excessive.

-La température basse(5^oC) provoque une dégradation moindre, et la quantité de COOH est relativement élevée.

-La basse consistance (10%) de la pâte permet de mieux minimiser la dégradation et la perte de résistance des fibres pendant l'oxydation. Parallèlement, à cette faible consistance, on a observé un contenu carboxylique plus élevé qu'à la consistance de 35%.

Par l'étude des spectres obtenus de spectromètre infrarouge à transformée de Fourier (FTIR), on a observé un pic de COOH à 1734-1738 cm^{-1} apparaissant après l'oxydation. Pourtant, l'intensité du pic de COOH pour les fibres de tremble est beaucoup plus petite que pour les autres fibres. Il a aussi été observé que le pic du OH à 3330-3361 cm^{-1} est visiblement perturbé et que l'intensité du pic CH à 2900 cm^{-1} a été réduit, ce qui montre la transformation des groupements hydroxyls (CH_2OH et CHOH) en groupements carbonyles pendant l'oxydation. L'utilisation de $MgCO_3$ à 1% pendant l'oxydation a entraîné une réduction d'intensité du pic du COOH.

En même temps, l'intensité du pic du OH de l'eau d'adsorption à 1645cm^{-1} a été fortement diminuée en présence de MgCO$_3$ ainsi que la surface du pic de carbonyle à 1615-1630 cm^{-1}.

Par la technique de la spectrométrie électronique d'analyse chimique(ESCA), on a observé que le rapport de O/C, représentatif du caractère hydrophile des fibres augmente lors de l'oxydation pour les fibres des résineux ainsi que pour les fibres de bagasse. Pourtant, ce caractère ne varie pas pour les fibres du tremble. Pendant l'oxydation, le pourcentage de C1 représentatif de la lignine et des extractibles diminue, et celui de C2 représentatif des groupes hydroxyles augmente. Ce changement a été observé pour les trois fibres oxydées. Le pourcentage du C3, représentatif des groupements cétoniques et aldéhydes, a atteint 8,5% (de 12%) à 1,25% N$_2$O$_4$. Cela signifie que la dégradation maximum se fait à 1,25% N$_2$O$_4$. La présence de C4 représentatif des groupements carboxyliques (sur la bande de 288,4 eV), n'a pas été observé dans le spectre obtenu par ESCA.

En présence de 1% MgCO$_3$, la dégradation a diminué. Autrement dit, les pourcentages de C2 et C3 ont beaucoup moins augmenté (10,1% au lieu de 11,2% dans le cas de l'oxydation en l'absence de MgCO$_3$ à 1,25% N$_2$O$_4$/fibre). Dans le cas des fibres de bagasse, le pourcentage de C1 a plus diminué. De la même façon, les pourcentages de C2 et C3 ont augmenté en présence de MgCO$_3$. La raison de ce fait pourrait être la quantité élevée d'hémicelluloses dans les fibres de bagasse qui ont subi une transformation excessive de ses pentoses, produisant plus de C2 et C3. Le rapport de O/C a encore été augmenté pendant l'oxydation en présence de MgCO$_3$.

La technique de la chromatograghie inverse en phase gazeuse (IGC) permet d'observer une diminution de γ^D_s, $-\Delta G$ (-CH$_2$-) et $-\Delta H_A$ quand la température de la colonne augmente pour toutes les fibres non traitées et oxydées. Contrairement à ces fibres de résineux, dans le cas du bagasse et du tremble, plus le taux d'oxydation augmente, plus γ^D_s et $-\Delta G$(-CH$_2$-) augmentent également. Ces valeurs ont même dépassé celles des pâtes non traitées. Il est constaté que les valeurs de ΔH^{SP}, ainsi que les

constantes acide-base K_A et K_B, ont clairement augmenté pour les fibres oxydées. Cette augmentation est plus élevée pour les fibres de bagasse que pour les deux autres fibres. Dans le cas des fibres du tremble, l'acidité et la basicité ont varié de façon opposée. Par conséquent, l'interaction spécifique acide-base (I_{SP}), qui représente l'augmentation des liaisons hydrogène entres les fibres oxydées n'a pas augmenté.

Il est aussi observé que les fibres de résineux sont amphotères (K_A=0,49 et K_B=0,54) et que les fibres de la bagasse sont basiques (K_A=1,7 et K_B=2,25) et que celles du tremble sont acides (K_A=2,9 et K_B=1,9). On peut supposer que la basicité des fibres de bagasse a favorisé une augmentation des coefficients acide (K_A) et coefficients basiques (K_B) en absence ou en présence de $MgCO_3$. Ceci a abouti à une adhésion plus élevée entre les fibres et à une résistance relativement plus grande par rapport aux fibres de résineux et de tremble. Ceci indique l'amélioration du caractère hydrophile des fibres oxydées. Le caractère acide des fibres du tremble pourrait être la cause de l'absence d'augmentation de $I_{SP.}$

Par comparaison des propriétés mécaniques et optiques des fibres oxydées, on a montré que, par l'oxydation des fibres cellulosiques provoque l'augmentation du contenu carboxylique, diminue la viscosité de la pâte réduisent et affaiblit les propriétés mécaniques. On a observé que les fibres de bagasse étaient plus résistantes à de l'oxydation que celles des résineux. Ceci pourrait être dû à la quantité élevée d'hémicellulose et de lignine résiduelle dans les fibres de bagasse. En même temps l'amélioration de la blancheur et de l'opacité est beaucoup plus importante pour les fibres oxydées de bagasse que pour les deux autres fibres.

Après avoir utilisé 1% de $MgCO_3$ (pendant l'oxydation par le N_2O_4), la réduction de la viscosité a visiblement diminué, qui indique une dégradation limitée, et a permis une amélioration des propriétés mécaniques. On a même obtenu des valeurs plus élevées pour la résistance à la rupture et celle à la traction par rapport à la pâte non traitée. Ceci est essentiellement dû à l'amélioration des liaisons fibre à fibre (bonding

strength). Il est prouvé que, l'oxydation des fibres résineuses à 0,83% N_2O_4 et celle des fibres de bagasse à 2,5% N_2O_4 est favorisée par présence de 1% $MgCO_3$.

À l'aide d'un modèle mathématique, une corrélation entre les propriétés physiques (le C.S.F, la longueur des fibres, et la viscosité), le caractère hydrophile des fibres oxydées et les propriétés mécaniques et optiques de la feuille a été obtenu. Il est constaté que le CSF, la longueur de la fibre, la viscosité et la résistance intrinsèque ont une influence plus marquée sur la résistance de la fibre. Par contre, le contenu carboxylique, COOH, le rapport O/C, et l'interaction spécifique acide-base (I_{SP}) et la résistance interne ont une influence sur les liaisons fibre à fibre. La résistance à la rupture (T) est alors affectée par ces deux types de paramètres. Dans le cas d'addition de $MgCO_3$ la diminution de la résistance des fibres est moins marquée. Par conséquent, l'effet de l'amélioration des liaisons fibre à fibre peut être clairement observé. Le résultat final est l'amélioration de la résistance à la rupture, ce qui prouve la validité de l'équation de Page dans le cas de l'oxydation par N_2O_4 en présence de $MgCO_3$. Par contre ces dernières ont une influence plus élevée sur les propriétés optiques (la blancheur et l'opacité) de la feuille.

e)   Conclusion

L'oxydation par le N_2O_4 affaiblit généralement les fibres, ce qu'on peut observer par la réduction de la viscosité et de la résistance mécanique. Pourtant, cette dégradation est moindre pour les fibres de bagasse que pour les fibres de résineux et de tremble. Les conditions raisonnables pour obtenir la plus grande quantité de COOH et la plus faible diminution de la viscosité sont les suivantes : température de 5oC, débit du gaz de 4 à 5 ml/min, consistance de la pâte de 10% et la durée d'oxydation de 1 à 2 h.

L'oxydation des fibres kraft blanchies forme des groupements carboxyliques (COOH) sur les fibres. Ceci a été vérifié sur le spectre FTIR, par la formation du pic de COOH à 1734 cm^{-1}. On aussi observé la diminution de l'intensité des pics de OH à 3336cm^{-1} et la diminution des pics de CH à 2900 cm^{-1}. L'augmentation du rapport de

O/C et la valeur élevée de I_{SP}, indique l'augmentation du caractère hydrophile des fibres et l'amélioration de l'adhésion de la surface des fibres. Pourtant ceci n'est pas suffisant pour compenser la perte causée par la dégradation des fibres, en ce qui concerne la formation des aldéhydes et des cétones sur C-2 et C-4 et la coupure des liens glucosidiques C1-C4. Il est donc nécessaire de maintenir la viscosité des fibres suffisamment élevée pendant l'oxydation par N_2O_4 à l'aide d'un agent protecteur comme $MgCO_3$. Dans le cas où la viscosité des fibres résineuses serait maintenue à plus de 900 dm^3/kg (à 0,83% N_2O_4) ou celles de bagasse à plus de 600 dm^3/kg (à 2,5% N_2O_4), on a pu obtenir une augmentation de la résistance à la rupture. Ces résultats nous ont permis de vérifier l'influence de la résistance des fibres, ainsi que celle des liaisons fibre à fibre, sur la résistance à la rupture de la feuille. Un autre avantage de ce type d'oxydation est que l'opacité et la blancheur des fibres de bagasse (possède moins de 1,0 % lignine) ont augmenté dans la même sens, ce qui est souhaitable pour le papier d'impression à la base de bagasse.

On peut renommer l'originalité du travail comme les suivantes :

1   Les spéctres FTIR des fibres de la bagasse et du tremble(non traitées et oxydées par N_2O_4).

2   Détermination des coefficients acide-base de la pâte kraft blanchie des résineux, de la bagasse et du tremble:

	K_A	K_B	caractère acide-base
Résineux	0,49	0,55	amphotérique
Bagasse	1,7*	2,25*	basique
Tremble	2,9*	1,9*	acide

* indique ceux qui sont trouvés par ce travail

3   L'effet de la formation du COOH, du caractère hydrophile (O/C) et de l'interaction spécifique (I_{SP}) des fibres oxydées, sur la résistance des liaisons (B).

4   L'application de l'équation de Page concernant les facteurs qui affecte-la résistance des fibres (F) et les facteurs qui affectent la résistance des liaisons (B) sur la résistance à la rupture de la feuille dans cette recherche d'oxydation par N_2O_4.

5   L'effet positif de $MgCO_3$ en réduction de la dégradation des fibres cellulosiques.

6	Établissement d'une équation (avec un $R^2 > 0,90$) montrant la corrélation entre les caractéristiques physiques et de surface des fibres oxydées et la résistance à la rupture et l'opacité de la feuille.

Cette recherche pourrait avoir une application industrielle, surtout pour les pâtes semi-blanchies (contenant environs1% de la lignine), de préférence celles qui contiennent un pourcentage raisonnable d'hemicellulose, telles que les fibres de bagasse. Pour ces types des pâtes, en effet, la résistance mécanique, ainsi que les propriétés optiques peuvent être améliorées sans utilisation d'agents de blanchiment à base de chlore.

Pour atteindre à ces buts, il est nécessaire de poursuivre cette recherche en mesurant les propriétés mécaniques aux différents niveaux du raffinage. D'autres oxydants tels que le chlorite de sodium pourrait être essayé, et les résultats seraient comparés à ceux obtenus avec N_2O_4. L'efficacité d'autres agents protecteurs de la cellulose comme $MgSO_4$, moins cher que $MgCO_3$, peut être évaluée. Installer un pilote industriel et faire une analyse de la faisabilité sont nécessaires même dans le cas où l'on obtiendrait de meilleurs résultats.

CONTENTS

LIST OF TABLES

LIST OF FIGURES

ABBREVIATIONS

Å	Angstrom
AN	Acceptor number of polar liquids
C(1s)	Carbon components of first atomic layer
CCD	Composite Central Design
COOH	Carboxylic acid
CPPA	Canadian Pulp and Paper Association
CSF	Canadian Standard Freeness
Bl. k	Bleached kraft
d	Density
DN	Donor number of polar liquids
M	Molecular weight
E_B	Binding energy
E_K	Kinetic energy
ESCA	Electron Spectroscopy for Chemical Analysis
eV	Electronvolt
FTIR	Fourier Transform Infra-Red spectroscopy
G/L	Gauss Lorentz ratio
h	Hour
I_{SP}	Specific acid-base interaction
J	Joule
K	Kelvin
K_A and K_B	Acid constant and basic constant (of the fibres)
l	Litre
min.	Minute
nm	Nanometer
O/C	Oxygen-Carbon ratio
Pa	Pascal
TAPPI	Technical Association of the Pulp and Paper Industry
^oC	Degree Celsius

CHAPTER I

INTRODUCTION

a)   Background

The improvement of mechanical characteristics of paper has been one of the major challenges of the pulp and paper industry. This is all the more critical today since the industry must look to other sources of fibre than the traditional softwoods. Fibres from hardwoods such as aspen, and agricultural fibres from bagasse, straws or hemp can be used for making paper; however, their fibres are shorter and papers made from these sources tend to be weaker. Thus, there is a need to improve the strength of paper made from alternative sources of fibre.

Although mechanical defibrillation (refining) is used to produce papers with higher strength, this part of the process of making paper requires a great deal of energy. Chemical treatments that modify the fine structure of cellulose, its accessibility, reactivity, crystallinity, density, absorption, and mechanical characteristics could be used to reduce the process energy requirements or to increase even further the strength of papers made from mechanically refined pulps.

Many scientists obtained increases in paper strength by grafting (1), or by low degree of substitution (d.s.) of hyroxyl group with hydrophobic groups such as methoxyl or acetyl groups (2). The affinity for water of these substituted cellulose was increased , due perhaps to an opening up of the cellulosic structure, making more cellulosic hydroxyl groups available for bonding and for adsorption of water . However, as the degree of substitution was increased further, the affinity of the product for water and physical strength of handsheet decreased rapidly, due to the replacement of more and more of the hydroxyl groups with the hydrophobic methoxyl or acetyl groups (2). When hydrophilic groups instead of hydrophobic groups (such as the hydroxyethlation or

carboxymethylation) are substituted for the cellulosic hydroxyl, the resulting pulp should have properties that differ from the properties of both the original pulp and the pulp mentioned above (2, 3). If the substituted group were hydrophilic in nature, rather than hydrophobic, greater hydration (in the papermaking sense of the term) of the fibre surface might be obtained. Conceivably, such groups could participate in inter-fibre bonding. It should also be noted that internal fibrillation in CMC fibres and the more soluble character of the interior of the fibres would bring about an increase in bonding between cellulose chains within the fibre. This bonding within the fibre would create a more uniform structure, filling in some of the voids in the fibre, and creating a stronger cellulosic fibre. It is found that small number of hydroxyl groups of cellulose were substituted with hydrophilic carboxymethyl groups. Low d..s. CMC pulps retaining the insoluble fibrous nature of the original cellulose, and without excessive degradation. It was theorised that this change in properties with carboxymethlation was due to the hydrophilic nature of the carboxymethy group which increased the amount of water retained by the CMC pulp, the degree of swelling of these pulps, and their plasticity, in much the same manner as hemicelluloses increase these properties in wood pulp.

The bleaching process using agents such as chlorine, hypochlorite, chlorine dioxide, hydrogen peroxide, and ozone, is usually aimed at removing lignin. However, it also oxidises the alcoholic functions of cellulose to acid (COOH), aldehyde (CHO) or ketone (C=O) groups in varying proportions on the cellulosic macromolecules. The oxycellulose resulting from bleaching with these agents is only slightly degraded (4, 5, 6, 7). Although bleaching agents do oxidise cellulose, they do not usually help in improving paper strength of low yield pulps.

Many other oxidants have been studied in relation to their effect on cellulose fibres. The goal of many of the studies was to substitute alcohol groups with carbonyl and carboxyl groups (8,9,10). Substances such as periodate or periodic acid (11), ruthenium tetroxide (12) and ammonium hexanitratocerate (13) have been studied at different treatment intensities. Although these substances were found to be effective at increasing carboxyl groups, they also produced high degrees of aldehyde and carbonyl

groups and lead to substantial reductions in the degree of polymerisation. At high concentrations, alkaline pH and long reaction times, these substances caused cleavage of the glucopyranic chain, and the complete degradation of cellulose to produce formic acid (HCOOH), carbon dioxide (CO_2) and hydrogen (H_2).

An oxidation agent that has shown promise is nitrogen tetroxide (N_2O_4), which is applied in the gaseous state. The advantage of this substance is that it acts primarily on the C-6 hydroxyl group, transforming it to a carboxyl group (carboxylic acid). It also acts on the C-2 and /or C-3 hydroxyls to transform them to ketone groups (14, 15, 16). The research involving the effect of N_2O_4 on cellulose has been mainly directed at clarifying reaction mechanisms on cotton fibres (17) or cellulose acetate. The effects on the mechanical properties of the fibres were not taken into consideration. Mercer (15) observed that the N_2O_4 oxidation of Mannan B and regenerated cellulose resulted in carboxylic content of up to 25.4% and a low percentage of ketone groups. N_2O_4 oxidation has also been studied as a pre-treatment to remove lignin during oxygen and ozone bleaching (18, 19). It was shown that the Prenox process (20) applied to unbleached pulps helped to reduce the kappa number of the pulp during bleaching. Kokta et al (21) measured the carboxyl groups content of thermo-mechanical pulps (TMP) treated with N_2O_4, and reported that the carboxyl groups content of the pulp increased with oxidation time.

Nevertheless, it should be mentioned that some work has been done to determine whether the addition of the metal cations such as magnesium can limit cellulose degradation (22). It was shown that swelling of monocarboxycellulose in water increases with the amount of adsorbed cations and it is related closely to its degree of oxidation (23).

b)   Hypothesis

Although there has been some work concerning the possible uses of N_2O_4 in the pulp and paper industry, there are many questions left to be resolved. Here there is not the question of etherification of cellulose, but rather than the transformation of primary

alcohol groups along the cellulose polymer to carboxyl groups, that increases the hydrophilic character of the fibres and increases the number of hydrogen bonds. This could lead to an increase in the fiber-to-fiber bonding and surface adhesion of the fibres with a consequent increase in the tensile strength of the paper. The effect of a higher degree of bonding may be greater than the decrease in the viscosity caused by the depolymerization during the oxidation. In other word, verifying the Page equation of $1/T = 1/F + 1/B$ in the case of the oxidation treatment by N_2O_4.

The question addressed in this thesis is whether there are processing conditions (gas flow-rate, oxidation time, temperature, pulp consistency, presence of $MgCO_3$), under which the formation of carboxyl groups (COOH) and increasing the surface adhesion by the N_2O_4 oxidation can increase *bonding strength*, B, of the fibres, so as to compensate for any decrease in the degree of polymerisation that leads to a decrease in the *fibre strength*, F, due to the oxidation. Whether or not this can be used to improve the strength of paper made from short-fibres sources.

Herewith the main objectives of the research are summarised:

c)   **Objectives**

1)   **Study the effect of N_2O_4 oxidation on the formation of carboxyl groups (COOH) and on the viscosity of the bleached kraft pulp.**

2)   **Study the effect of nitrogen tetroxide oxidation on the chemical structure (mass and surface) of fibres of the initial softwood, bagasse and aspen pulps.**

3)   **Evaluate the influence of the formation of carboxyl groups (COOH) on the acid-base contribution to the work of adhesion of the above fibres.**

4)   **Measure the effect of oxidation on the fibre to fibre bonding and on the mechanical strength of the sheet (confirmation of the Page equation).**

5)   **Determine whether the addition of chemicals, such as $MgCO_3$ during oxidation has a positive effect on the diminution of the cellulose degradation.**

6)   **Derive a model relating the physical, surface and hydrophilic character of the oxidised fibres to the mechanical and optical properties of the paper.**

CHAPTER II

THEORETICAL CONSIDERATION OF THE RESEARCH

2.1   Strength of paper

The strength of paper is a function of the tensile strength of the individual fibres in a network and of the forces that bond the fibres together. The majority of polymeric chains of cellulose are oriented along the length of the fibres, so that the fibre strength may be expected to originate from strong covalent linkages within the cellulose molecules. In contrast, fibres adhere to one another in paper by much weaker inter-molecular hydrogen bonding. The highest tensile strength recorded for paper, even when based on the cross sectional area of the fibrous materials, is only about one quarter of that of the strength of a single fibre (24). Thus, the bonding strength is considered to be the limiting factor of the paper strength.

The tensile strength of paper has been defined by the following equation:

$$\frac{1}{T} = \frac{9}{8Z} + \frac{12A\rho g}{bPL(RBA)} \qquad [eq.2.1]$$

where,

T	tensile strength of the strip expressed as breaking length	N.m/g)
Z	zero span tensile strength	(N.m/g)
A	cross section of an average fibre	(mm^2)
ρ	density of fibrous material	(g/m^3)
g	acceleration due to gravity	
b	shearing bond strength per unit bonded area	(N/mm^2)
P	perimeter of the cross section of a fibre	(mm)
L	fibre length	(mm)
RBA	relative bonded area of the sheet	(%)

This relationship can be written in simplified form as:

$$\frac{1}{T} = \frac{1}{F} + \frac{1}{B}$$

[eq.2.2]

where,

F   an index of the resistance of fibres

B   an index of the resistance of bonds between fibres

Here, it is understood that both F and B are greater than zero. Thus, an improvement in either fibre or bond strength should lead to higher tensile strength. Since the influence of F is much greater than the effect of the fibre bonds, B, the tensile strength can be only maximised by increasing B. This can be done by refining, cooking or bleaching. An increase in bonding ratio (BR%) due to refining results in a corresponding increase in the relative bonded area (R.B.A) which in turn produces an increase in the tensile strength of paper (25) due to better fibrillation and to the formation of more fines. However, it has yet to be proved that the bond strength increases during refining (26).

According to Mayhood et al (27), refining does not affect the fibre to fibre bond strength. In fact, Mouhlin (28, 11) obtained lower bond strength for refined pulp than for non-refined pulp at the same bonding area. In the case of pulps with short fibres (eg. aspen and bagasse), conventional refining techniques result in even shorter fibres and lower fibre strength. This is why it is necessary to seek the methods that may improve bond strength. "Equation [2.1]" indicates that the tensile strength can be increased by increasing the bond strength per unit area, b. Divers values for b, from 1.1 to 5.9 dynes/cm$^2 \times 10^7$ are reported concerning different type of pulp (29, 30 and 31).

The bonding strength of fibres depends mainly on the hydrogen bonds of hydroxyl groups of cellulose and hemicellulose. A number of methods can be used to improve bonding strength in paper.

a)   To decrease the lignin content of the fibres by the cooking process (32, 11). Lignin is a hydrophobic material that is known to limit the formation of hydrogen bonds within the fibre structure.

b)   To maintain more hemicellulose in the fibre. Hemicellulose is known to swell easily, thus creating a greater possibility for fibre to fibre bonding after refining.

c)   To use certain chemical treatments, such as carboxymethylation, etherification, oxidation, or grafting (1, 3, 33, 34, 35) of cellulose fibres to increase hydrogen bonding

In this work, nitrogen tetroxide was used to treat different kinds of bleached kraft fibres. This is an oxidation reaction that is known to preferentially oxidise primary alcoholic groups. We expect that by the N_2O_4 oxidation, as the residual lignin is removed, and the of carboxyl groups (COOH) are formed, the number of H-bond be increased, so the bonding strength, b could be increased. This should result in turn an increase in tensile strength, T. The effect of the other parameters, such as zero span, Z, fibre length, L, relative bonded area, RBA and density, ρ on tensile strength will also be analysed to confirm the equations 2.1. and 2.2.

2.2   Cellulose oxidation

The paper industry has made many efforts to improve the physical and mechanical properties of paper through the chemical transformation of cellulose. It has been observed that if the substituents has hydrophobic character, such as acethyl or methoxyl and the degree of substitution is low, the resistance of paper increases. This is due to an opening of the fibre wall structure, followed by increasing possibilities of interfiber hydrogen bonding (11). Walecka (2) reported a better degree of fibrillation and higher strength for carboxymethylated pulp at a degree of substitution of 0.06. By hydroxyethylated of rayon fibres with ethylene dioxide (Fig. 2.1) a considerable increase in bond strength was obtained, while the fibre tensile strength was almost unaffected (11).

$$Cell - OH + CH_2 - CH_2 \xrightarrow{\hspace{3cm}} Cell - O - CH_2 - CH_2OH$$
$$\diagdown O \diagup$$

FIGURE 2.1 Cellulose hydroxyethylation by ethylene dioxide (9).

2.2.1 Methods of cellulose oxidation

Many methods of oxidation enable the transformation of the glucosidic structure of cellulose, which in turn modifies the strength of fibre to fibre bonds. Diverse experiments have shown that the degree of oxidation and the type of oxidant are the major factors determining the effectiveness of such treatments. When the degree of the oxidation is low, the lignin and hemicellulose, which are more amorphous and reactive than cellulose, will be oxidised first. This is typical during bleaching with oxidative agents such as H_2O_2, O_2, O_3 and ClO_2 (4, 5, 36, 37, 38, 39, 40, 41). The higher are the concentration of oxidants, the temperature and the oxidation time, the greater the degree of oxidation. Nevertheless, the effect of oxidation can be selective or complete. Another selective oxidation is metaperiodate oxidation of cellulose that leads to the preferential formation of aldehyde units at C-2 and C-3 (11).

In the case of N_2O_4, oxidation which is considered to be a selective treatment, C-6 is oxidised preferentially, which transforms the primary alcohol of CH_2OH to the carboxyl group, COOH (Fig.2.2). As a result, cellulose is protected from hemiacetal cleavage and there is little fibre degradation. Nevertheless breaking of the glucosidic bonds of C1-C4 may also occur during N_2O_4 oxidation (42, 43).
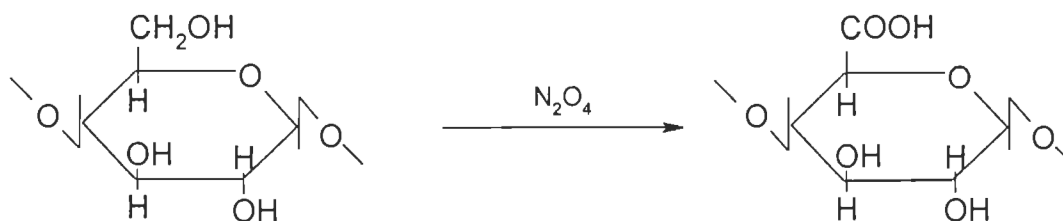
FIGURE 2.2 The oxidation of cotton cellulose by nitrogen tetroxide (42).

If the oxidation is strong, such as in the case of ruthenium tetroxide (30), periodate (16) or ammonium hexanitratocerate (13) (Fig.2.3), hemiacetyl chains (cycle) will open due to transformation of the secondary alcohol (C-2, C-3) to aldehyde or ketone, and substantial breaking of glucosidic bonds will occur.

$$Ce^{4+} + H_2O \underline{\hspace{4cm}} (CeOH)^{3+} + H^+$$

$$C_6H_{10}O_5 + 12Ce^{4+} + 7H_2O \underline{\hspace{2cm}} 6HCOOH + 12Ce^{3+} + 12H^+$$
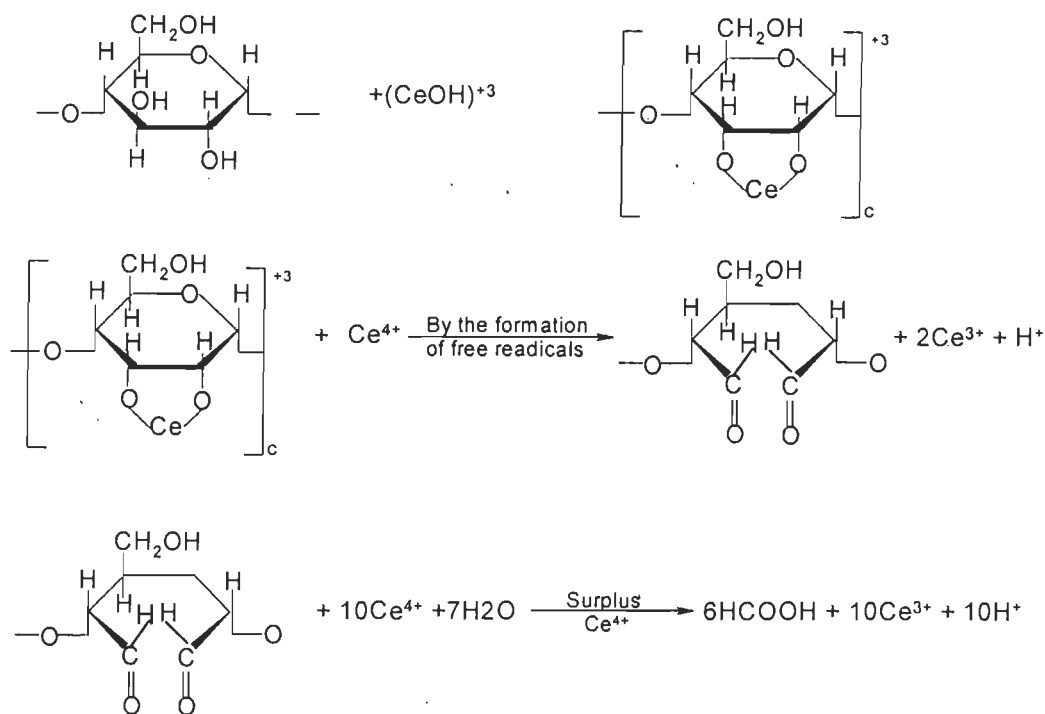
FIGURE 2.3   Cellulose acetate oxidation by the ammonium hexanitratocerate (13).

If the degree of polymerisation falls below 500, as in the case of ruthenium tetroxide oxidation (12), the interfibre bonding is weakened to such a degree that the fibre strength is no longer sufficient to make a sheet.

2.2.1.1 The formation of aldonic acid terminal groups

Upon radical oxidation, the reduced terminal group of the carbohydrate transforms itself into a glucose group (6). This group forms the an acid group, which stabilises the carbohydrate and prevents alkaline degradation. Another example of this

type of oxidation occurs when cellulose is soaked in a bromine solution, which results in formation of an aldonic acid (Fig.2.4).

D - Glucose   D-gluconic acid (Aldonic acid)
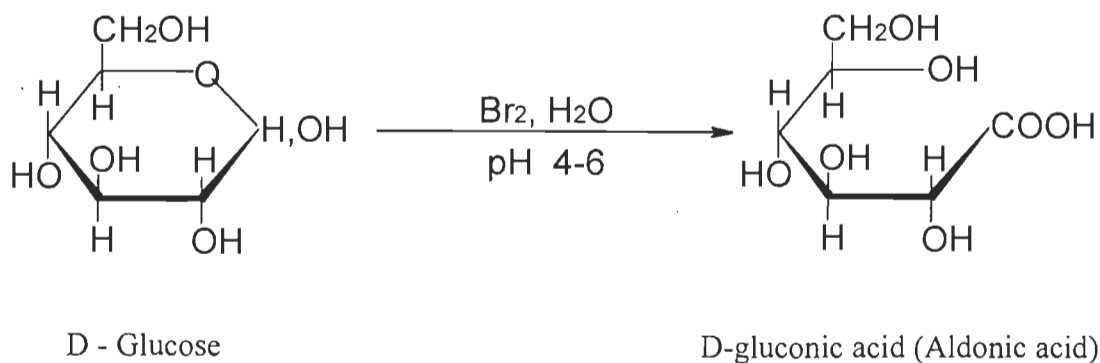
FIGURE 2.4   Oxidation by bromine in a solution (42).

The partial oxidation of cellulose can also be observed in the case of sodium chlorite ($NaClO_2$) oxidation. Dilute solutions of alkaline chlorite gently degrade the cellulose. In contrast, the warm concentrated solution transforms all parts of the cellulose by opening the glucopyranic cycle and the glucosidic bridges. This esterifies it at the C-1 position but allows the cellulose to maintain its macromolecular structure (Fig.2.5). If the ambient solution is acidic, there is some formation of glucuronic acid at the C-6 position. Here the proportion of glucuronic acid gluconic acid is 1/25 (44).
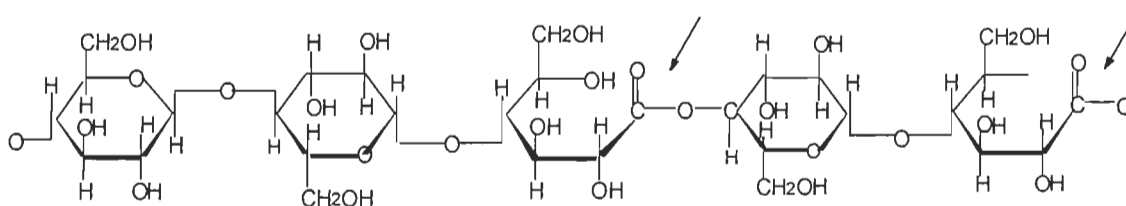
FIGURE 2.5   Partial oxidation of the cellulose by $NaClO_2$ (44).

2.2.1.2   Periodate oxidation

This type of oxidation may cause different levels of degradation in the cellulose including complete breakage of C-C bonds. At first, an aldehyde unit forms at C-2 and C-3 (Fig.2.6). Then, if the oxidation extends more, it leads to the formic acid, and later H_2 and CO_2 gases are obtained.

Cellulose   Cellulose dialdehyde
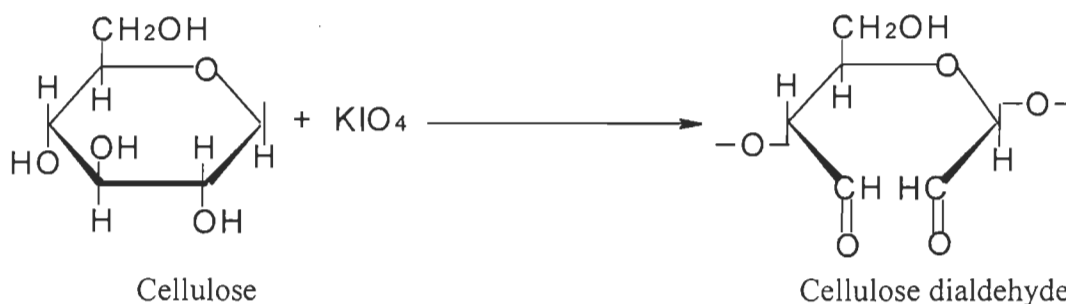
FIGURE 2.6   The formation of cellulose dialdehyde by periodates (16).

The bonding capacity of the fibre surface would not be modified by the periodate oxidation because the aldehyde groups of C-2 and C-3 are supposed to be *inactive* for the inter-fibre bonding. That is why this type of oxidation leads to contradictory results.

2.2.1.3   Glucuronic acid formation

Hypochlorite oxidation (Fig. 2.7) introduces carboxylic groups at C-2 and C-3. Although it opens the glucopyranic cycle, it hardly affects the cellulose fibres at a low concentration.

Cellulose dialdehyde   Dicarboxycellulose
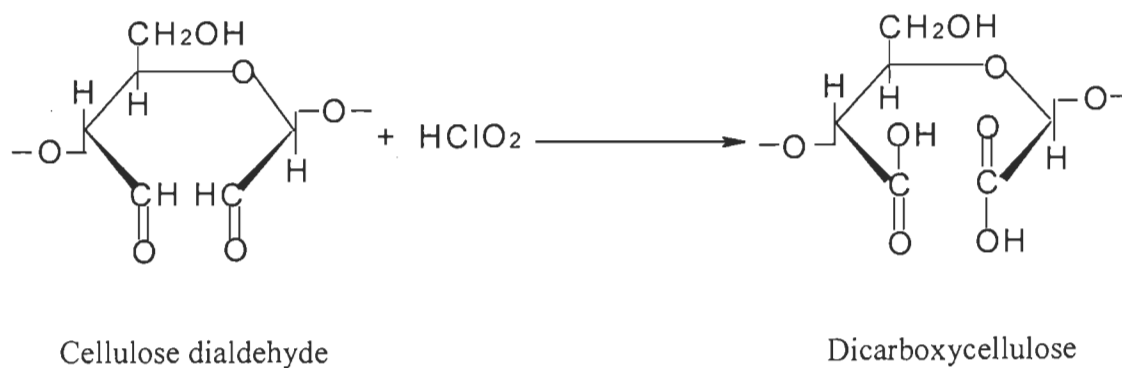
FIGURE 2.7   Formation of dicarboxycellulose (16).

It should be noted that carboxycellulose is not soluble in water or in organic solvents, Nevertheless it dissolves in dilute alkaline solutions of NaOH and Na_2CO_3 in NH_2RNH_2, when it contains more than 13% acid functions.

2.2.1.4 Oxidation by nitrogen tetroxide (NO_2, N_2O_4)

Few studies have been done on nitrogen tetroxide oxidation of bleached kraft pulp. In a study of cellulose oxidation of cotton linter, Friedlander et al (16) compared the periodate oxidation with nitrogen tetroxide oxidation. According to these results, the major products of NO_2 oxidation are the formation of carboxylic groups at C-6 and some ketones at C-2 and/or C-3 (Fig. 2.8).
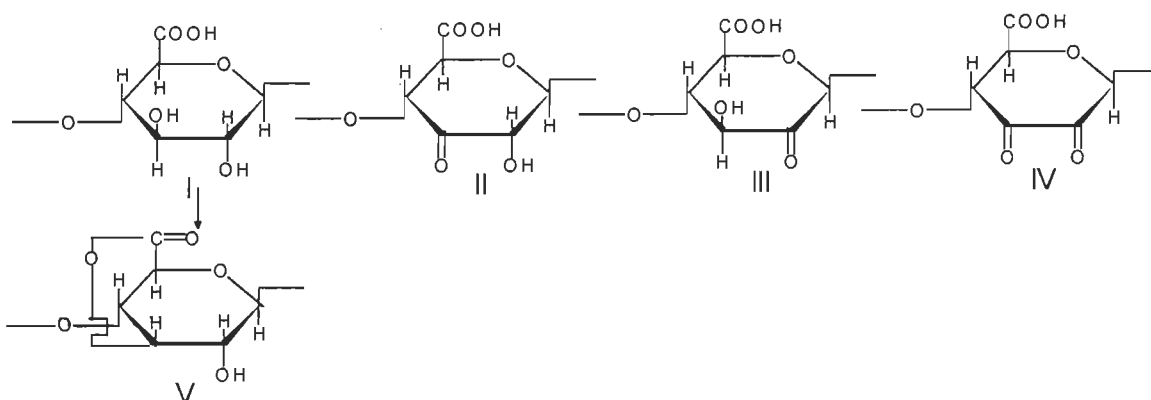
FIGURE 2.8   Nitrogen dioxide oxidation of the cotton (16).

Mercer and Bolker (15) used the N_2O_4 oxidation process for Mannan B and regenerated cellulose in CCl_4 solution. The oxidation consists primarily of the transformation of the primary alcohol at C-6 to carboxyl groups and of the secondary alcohols at C-2 and C-3 to ketones as a side reaction.

Svetlov et al (45) evaluated the rate of oxidation of cotton cellulose by N_2O_4 at temperatures of 80°C to 130°C. They observed that as NO_2 disappeared, different gases (N_2, NO, N_2O, CO and CO_2) appeared. The mechanism of the reaction is very complex and difficult to explain because the glucosidic groups are hydrolysed. These groups are

destroyed 5 to 10 times more slowly than the hydroxyl (OH) bonds. They could observe at least two kinds of oxidation. These were:

a)   Destruction of the glucopyranic cycle.

b)   Breakage of glucosidic chains and precipitation of the glucopyranic cycle.

It is believed that the alkyl radicals formed are capable of transforming NO_2 to N_2 and N_2O. It is possible to estimate the degree of destruction of glucopyranic cycle by measuring liberated N_2 , NO, N_2O, CO and CO_2 (45).

Laisha (46) studied the abilities of different solutions to increase oxygen absorption during this oxidation. Carbon tetrachloride was compared with nitromethane, nitrobenzene, acetonitrile, dimethyl acetamide and diethyl acetate. It was found that the rate of oxidation and the amount of adsorbed oxygen are higher for the solvents that have a higher dielectric constant and a lower donor number (ie. nitrobenzene, nitromethane and carbon tetrachloride).

Previous work on N_2O_4 oxidation was performed in CCl_4 solutions. The motivation was to study the reactivity of cellulose after carboxyl substitution, but papermaking properties were not considered. This oxidation with CCl_4 cannot be used in the paper industry due to environmental considerations. For a long time the pulp and paper industry has attempted to replace toxic chlorine products (Cl_2, ClONa, ClO_2, etc.) in bleaching. Substances such as O_2, O_3, and H_2O_2 have been used as alternatives. These were expected to satisfy the environmental requirements; however, these also cause significant fibre degradation. Nitrogen tetroxide has nevertheless been used in an aqueous pulp slurry as a pre-treatment to oxygen bleaching since about 1980. The ability of N_2O_4 to remove lignin reduces the consumption of oxygen or ozone in the bleaching process. In the present study also, the oxidation treatment is studied in an aqueous pulp slurry of 10 to 35% consistencies with and without additional chemicals.

a)   NO$_2$ pre-treatment in oxygen bleaching

According to the Samuelson and his colleges (47, 36, and 18), the pre-treatment of unbleached kraft pulp by NO$_2$, followed by oxygen bleaching, makes it possible to remove over 80% of the lignin without excessive depolymerisation of the cellulose. This rate could be compared with a 40-50% lignin removal by the classic bleaching by oxygen. Thus, by using N$_2$O$_4$ in the gas phase with nitric acid solution, it is possible to obtain a kappa number of 4 at a viscosity of 950 dm^3/kg. Based on the Samuelson experiments (20), the Prenox project was realised by 4 Swedish companies (AGA, EKA-Nobel, Mooch Domsjo AB and Sunds Defibrator AB) in 1984.

The results of that study have been considered for industrial application since the new process offered remarkable results. According to Swedish environmental regulations, the rate of total organic chlorine or acceptable AOX is 1.5 kg/ ton of dry pulp (20). To achieve this limit, there should be a chlorine substitution of 90% ClO$_2$ at a kappa number of 24. With the aid of a pre-treatment with N$_2$O$_4$, it is possible to decrease the kappa number to 10 with 15% ClO$_2$ substitution.

When the Prenox process is compared with a classic bleaching, it can also be observed that the rate of trichlorinated and tetrachlorinated phenolic components is much lower for the same charge of chlorine (20). Fig. 2.9 shows the industrial installation diagram of Prenox as it is used by the Sunds Defibrator Company. Nitric acid has also been used as a pre-treatment to oxygen bleaching for CMP of eucalyptus (48).
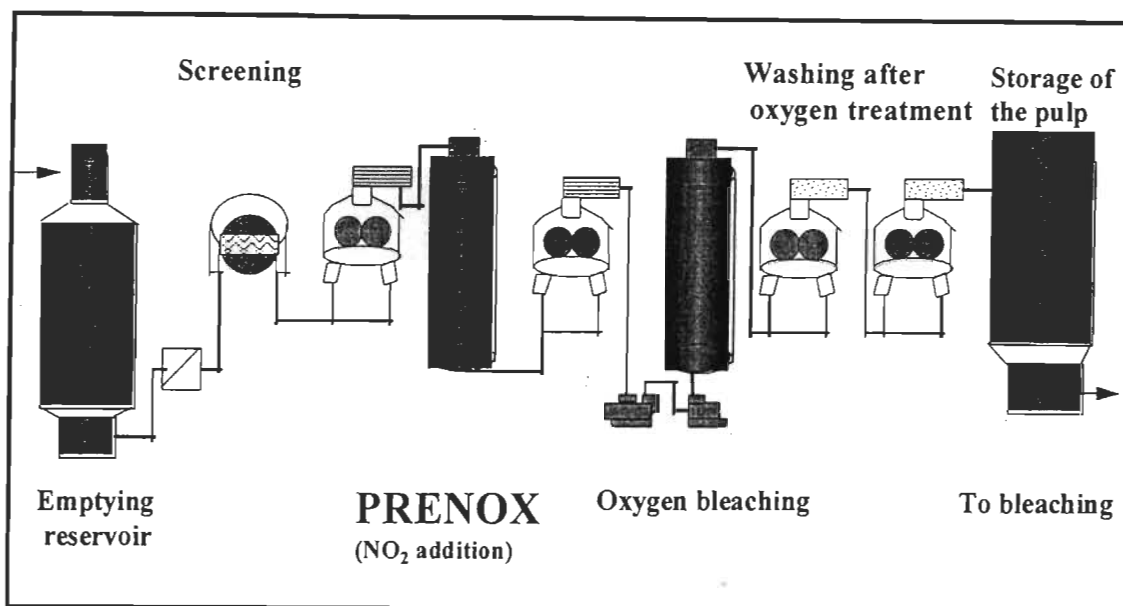
FIGURE 2.9   Installation diagram of Prenox (17).

b)   **NO$_2$ pre-treatment of bleaching by ozone**

Pulp bleaching by chemicals without chlorine is largely sought after to decrease pollution (5, 39, 40). A number of ozone-based processes were proposed, but although ozone can remove lignin, it is not selective enough and degrades carbohydrates as well. This means that the yield and viscosity of the treated pulp are lower than those obtained by bleaching with chlorine products. NO$_2$ pre-treatment has also been suggested as a method to improve ozone bleaching. In this new process, delignification occurs with 1.5% sulphuric acid (or 10% acetic acid) and 2% NO$_2$. These acids react by acidolysis and NO$_2$ by nitration and oxidation. The above process is called «ANZE», «NAZE» or NZE (39).

The positive effects of NO$_2$ in reducing cellulose degradation during delignification of unbleached pulp and during bleaching are well established. However, the effect of NO$_2$ on fibre to fibre bonding has not yet been verified. In a study concerning the oxidation of TMP with N$_2$O$_4$ in a gas phase, Kokta et al (21) reported

that the carboxyl content of the pulp increased gradually as the oxidation time increased (Fig.2.10).
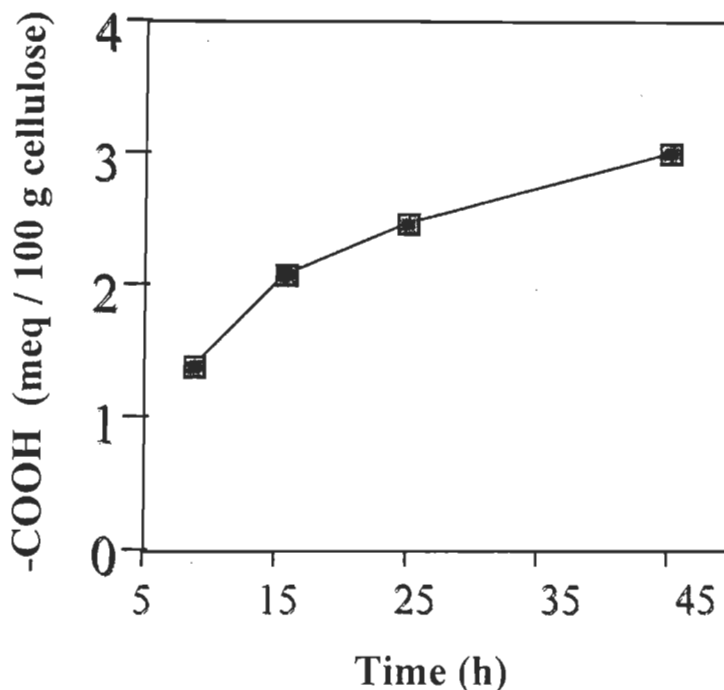
FIGURE 2.10   Dependence of carboxylic content of TMP to the oxidation time during N$_2$O$_4$ oxidation (21).

Based on the above research and on the literature review, the main objective of the present study is to verify the effects of N$_2$O$_4$ oxidation on the formation of carboxyl groups (COOH) on the bleached kraft pulp originating from bagasse and aspen, using a softwood pulp as reference. The research deals with the chemical modification of cellulose, inter-fibre surface adhesion , and the degree of bonding strength with the final strength properties of the paper.

2.2.2   Reaction mechanism of the oxidation reaction

The reaction mechanism of the N$_2$O$_4$ oxidation of cellulose is very complicated. This is especially true for unbleached pulp that contains significant quantities of residual lignin and hemicellulose. Different mechanisms of lignin and carbohydrate oxidation have been recently suggested, and the formation of ROOH groups is proposed. These

compounds are also strong oxidisers and decompose to different radicals under the effect of transition metal ions present in the wood (6).

The degradation of cellulose is mainly due to the action of such radicals. It should also be mentioned that the presence of lignin in the pulp considerably increases the production of radical species. Lignin is much more easily oxidised by the oxidants than are the carbohydrates. It is preferentially attacked by radicals and plays the role of radical scavenger. That is why this research focuses rather on the effect of N_2O_4 oxidation on bleached kraft pulps with less than 0.5% lignin content. This approach will permit the evaluation of the direct effect of N_2O_4 on cellulose fibres.

2.2.2.1 Reaction mechanism of oxygen with cellulose

The mechanisms of reaction of oxygen and nitrogen tetroxide with cellulose fibres are similar. It was reported (6) that oxygen attacks the glucose unit of the cellulose chains. This is the major cause of depolymerisation. Radical oxidation by oxygen leads to the formation of carbonyl groups in the first step (Fig. 2.11).
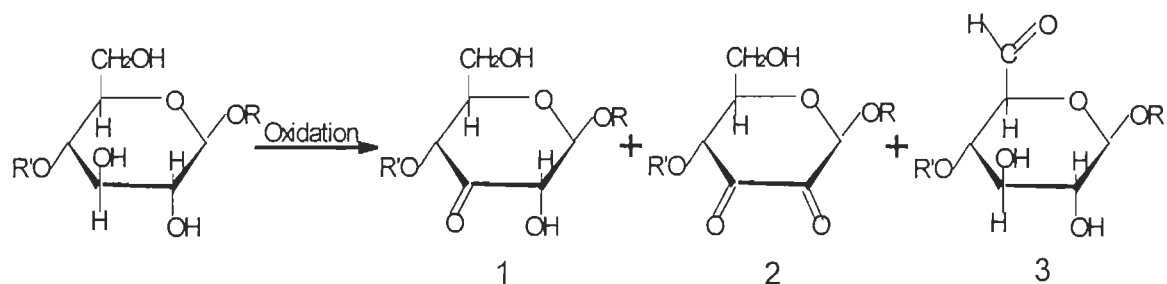
FIGURE 2.11 Oxidation mechanism through formation of the carbonyl groups (6).

Radicals are produced preferentially on carbons with the secondary alcohol at the C-2 or C-3 positions. The compounds numbered 1 and 3, which are not stable in alkaline conditions, are cleaved into β carbonyl groups. The cellulose is then depolymerised as follows (Fig. 2.12 and 2.13):
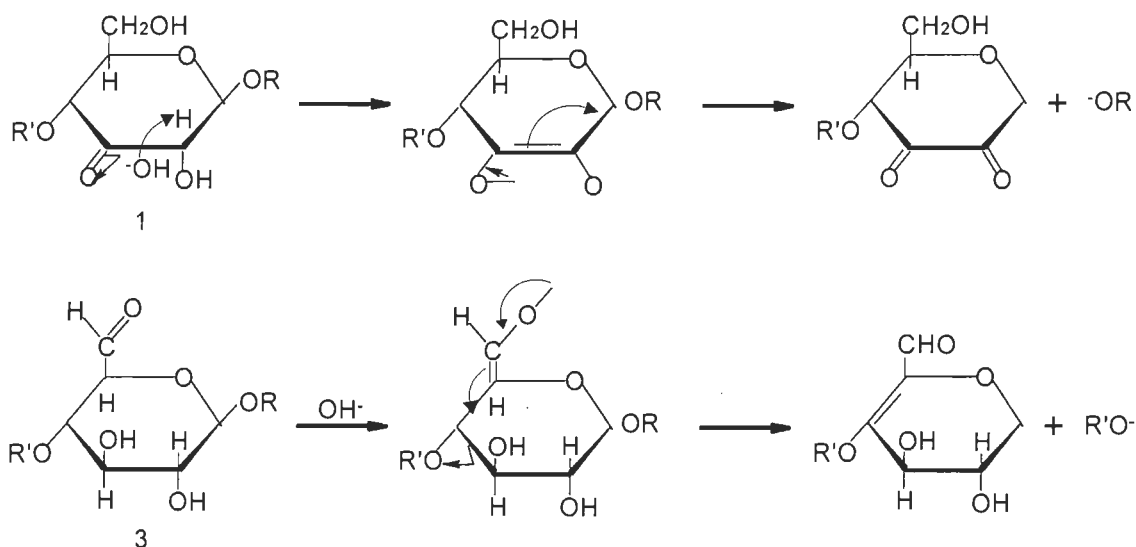
FIGURE 2.12 **Depolymerisation of number 1 and 3 compounds, unstable in the alkaline medium (6).**

Compound number 2 then in turn forms two COOH groups by direct oxidation. It can be oxidised to diacid or be subjected to a benzylic transformation that forms a pentafurasonidic acid. This is therefore a complicated reaction.
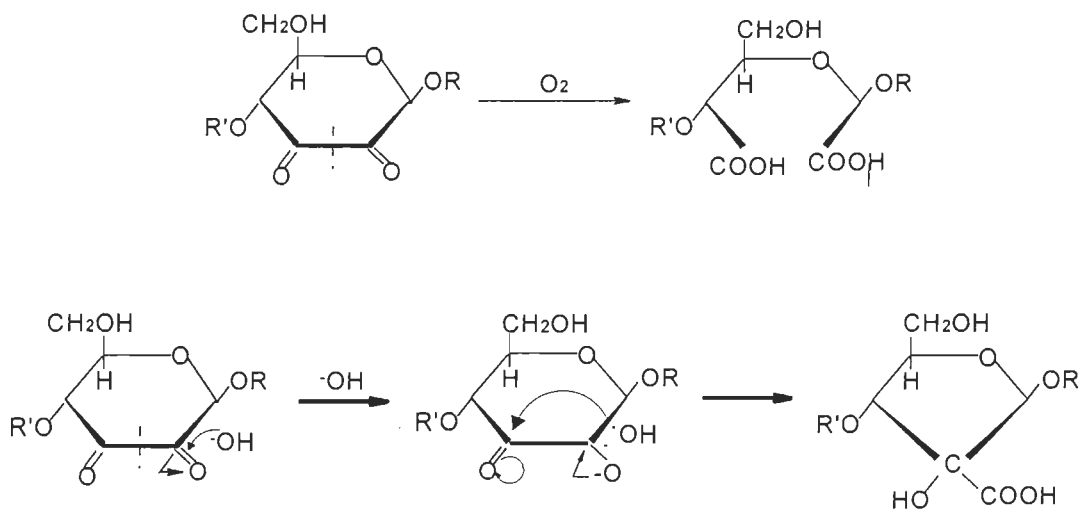
FIGURE 2.13 **Formation of a diacid or a pentafurasonsidic acid by direct oxidation (6)**

2.2.2.2 Reaction mechanism of oxidation by nitrogen tetroxide

The reaction mechanism of cellulose oxidation by N_2O_4 depends on the oxidation conditions. These include temperature, N_2O_4 /fibre percentage, oxidation time and type of solvent. Nevertheless, the major change is the formation of carboxylic groups at C-6. This occurs through an intermediate transformation to cellulose nitrite. This hypothesis has been proposed by Svetlov et al (45) for the reaction of N_2O_4 oxidation of cotton cellulose in gas phase (Fig.2.14).

$$ROH + N_2O_4 \rightleftharpoons RONO + HNO_3.$$

$$RCH_2ONO \xrightarrow{N_2O_4,\ N_2O_3} RC\begin{smallmatrix} \diagup\!\!\diagup NOH \\ \diagdown ONO \end{smallmatrix} \xrightarrow{H_2O} RCOOH$$
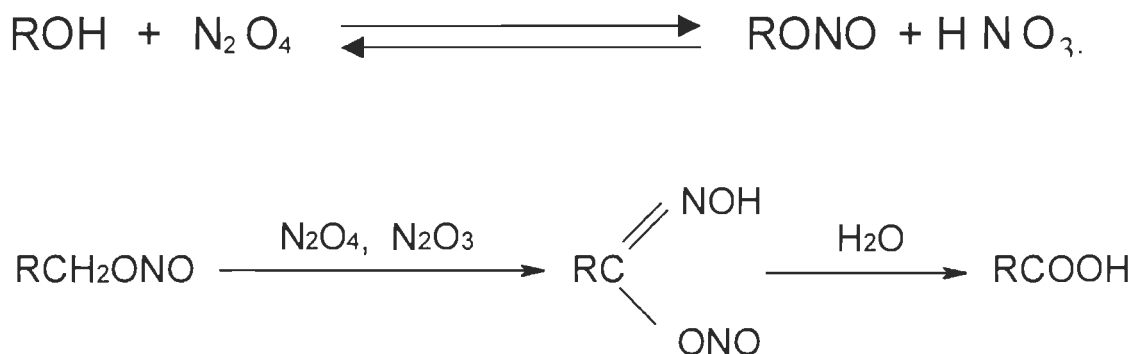
FIGURE 2.14 Cellulose oxidation by the N_2O_4 (45).

Svetlov (45) proposed equation 2.3 to explain the rate of disappearance of NO_2.

$$W = k_1.C_{cell}.C_{N2O4} + k_2.C_n.C_{N2O4} \qquad [eq.2.3]$$

where,

W	Reaction rate
k_1, k_2	Constants
Ccell	Concentration of cellulose
Cn	Concentration of the nitrite
$C.N_2O_4$	Concentration of N_2O_4

A similar oxidation was confirmed by Gert et al (50) for the oxidation of chromatographic paper by N_2O_4 in diethyl alcohol (DE) solution (2.15).

$$\text{C- (OH)}_3 + 3N_2O_4 \underset{\longleftarrow}{\overset{S}{\longrightarrow}} \text{C-(ONO)}_3 + 3HNO_3\,.S$$

FIGURE 2.15 Cellulose oxidation by the N_2O_4 (50).

In a study of the oxidation of chromatographic paper by N_2O_4 in a CCl_4 solution, Grinshpan et al (51) confirmed that the cleavage of the C-H bond of the methyl group at C-6 removes a free radical that adds an intermediate isomer to the hydroxamic acid (Fig. 2.16).

$$3N2O4 + 3H2O \longrightarrow 3HNO3 + 3HNO2$$

$$3HNO2 \longrightarrow 2NO + HNO3 + H2O$$

$$RCH2OH + HNO2 \longrightarrow RCHOH + NO + H2O$$

$$RCHOH + NO \longrightarrow \underset{\underset{NO}{|}}{RCHOH}$$

$$\underset{\underset{NO}{|}}{RCHOH} \longrightarrow \underset{\underset{NOH}{|}}{RCOH}$$

$$\underset{\underset{NOH}{|}}{RCOH} \longrightarrow \underset{\underset{NHOH}{|}}{RCO}$$

$$\underset{\underset{NHOH}{|}}{RCO +} \xrightarrow[H2O]{OH^-, H^+} RCOOH + NH2OH$$
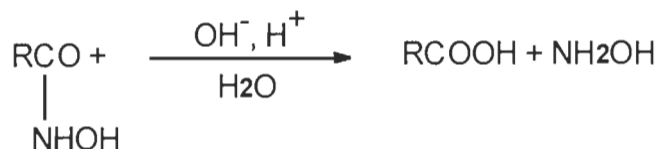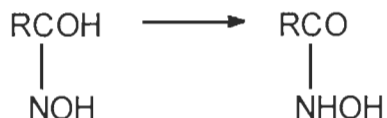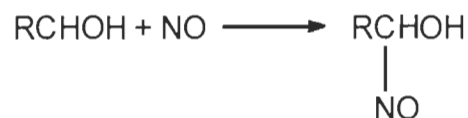
**FIGURE 2.16   Mechanism of reaction of N_2O_4 with the cellulose of
       chromatographic paper (51).**

The above formula can be simplified as follows:

$$RCH_2OH + HNO_2 \longrightarrow RCOO^-H^+ + NH_2^+OH^-$$

This is in fact the principal reaction that takes place between cellulose and nitrous acid, HNO_2. In other words, an alcohol (base) and an acid are transformed to a new acid and a new base via a Lewis-Bronsted type reaction. This must also be an explanation for the acid-base contribution to the adhesion of the oxidised fibre. The presence of hydroxamic acid and carboxylic acid simultaneously leads to the formation of intermolecular hydrogen bonds. New IR peaks can be observed for COOH($1730cm^{-1}$) and for hydroxamic acid (1580-1610 cm^{-1}). The addition of nitric acid at the start, or its regeneration during the reaction, eliminates hydroxamic acid by transforming it to carboxylic acid. This is why the amount of COOH increases during the addition of nitric acid and explains the disappearance of the hydroxamic acid peak at 1610 cm^{-1} (52).

In our research, the pulp consistency varied from 10 to 35% in water with no other chemicals (such as CCl_4). Thus, it is only water that accompanies the fibres during the oxidation reaction. Consequently, the reaction is similar to the acid-base mechanism just described, and there are fibres which have had some hydroxyl groups transformed to carboxyl groups. It is important to select relatively mild conditions for the oxidation by N_2O_4 in order to reduce the degradation of cellulose. The effect of carboxylic groups on the bond strength is described in the next section.

2.2.3   Effects of the carboxylic groups (COOH) on the inter fibre bond strength.

On the basis of certain principles of molecular chemistry to be elaborated in this section, it is postulated that the oxidative transformation of primary alcohol groups to carboxyls should lead to an increase in the surface adhesion among fibres. This should result in an improvement in the bonding strength of the paper.

The chemical modification of cellulose by the oxidation treatment should:
-Increase the cohesive energy density

-Increase the energy of hydrogen bonds by conversion of alcohol groups to carboxylic groups

-Increase the work of adhesion

2.2.3.1   Cohesive energy density

Some researchers (54, 58) calculated the cohesive energy density of materials from their evaporation energy, which is directly related to the value of a solubility parameter, δ.

$$CED = \delta^2 \qquad\qquad [eq.2.4]$$

For polymers such as cellulose, δ can be calculated by the following equation (27):

$$\delta = (\Sigma G)\, d/M \qquad\qquad [eq.2.5]$$

where,

G   molar attraction constant of the basic group of the polymer according to Table 2.1

d   polymer density

M   molecular weight of polymer

According to equation 2.5 and Table 2.1, one may calculate the theoretical change in the solubility of cellulose due to the conversion of alcohol groups to acid groups.

Cellulose in alcohol state

-CH_2OH- 4(CHOH)-CHO

-CH_2OH=(CH_2)+(O)+(H)=133+70+90=<u>293</u>

-4 (CHOH)=4((CH)+(O)+(H))=4 (28+70+90)=<u>672</u>

-CHO=(C) +(H) +(O)= 19+90+70=<u>179</u>

$(\Sigma G)_1$ = (293) + (672) + (179) = <u>1144</u>

Cellulose in acid state

-COOH- 4(CHOH)-CHO

-COOH=(CO)+(O)+(H)=275+70+90=<u>402</u>

-4CHOH= <u>672</u>

-CHO=<u>179</u>

$(\Sigma G)_2$ = (402) + (672)+ (179) = <u>1253</u>

In the case that the ratio of density to molecular weight does not change, the following results could be obtained:

$$d_2M_1/d_1M_2=1$$

as
$$\delta_2/\delta_1 = \Sigma G_2 d_2 M_1/\Sigma G_1 d_1 M_2$$

This yields: $\delta_2/\delta_1 = \Sigma G_2/\Sigma G_1 = 1253:1144 = 1.095$

ΣG is 1.095 times higher for the oxidised fibres (with carboxyl groups) than for untreated fibres (with hydroxyl groups). The solubility parameter δ will also be 1.095

Table 2.1   Molar attraction constant of different groups (55).

Group		G	Group		G
-CH$_3$		214	CO	Ketone	275
-CH$_2$	Single bond	133	COO	Esters	310
-CH<		28	CN		410
>C<		-93	Cl	(average)	260
CH$_2$=	Double bonds	190	Cl	Single	270
>C=		19	Br	Single	340
CH=C-		285	I	Single	425
-C=C-		222	CF$_2$	N fluorocarbons	150
Phenyl		735	CF$_3$	" " " "	274
Phenyl(o,m,p)		658	S	Sulphides	225
Naphtyl		1146	SH	Thiols	315
Chain of 5 members		105-115	ONO$_2$	Nitrates	~440
Chain of 6 members		95-105	NO$_2$	Nitro-aliphatic compounds	~440
Conjugation		20-30	PO$_4$	Organic phosphates	~500
H	(variable)	80-100	Si	Silicones	-38
O	Ethers	70			

times greater (assuming that the ratio of d/M was not changed). Thus, according to equation "[2.6]", the *CED* of cellulose with carboxyl groups would be 1.2 times greater than cellulose with hydroxyl groups as a result of oxidation:

$$CED_2 / CED_1 = (\delta_2)^2 / (\delta_1)^2 = (\delta_2 / \delta_1)^2 = (1.095)^2 = 1.2 \qquad \text{[eq.2.6]}$$

Now, both the molecular weight, M and density, d increase during the oxidation treatment. The molecular weight of an anhydroglucose unit will increase upon substitution of alcohol groups with carboxyl groups as follows:

162 (131 + 31)   176 (131 + 45)
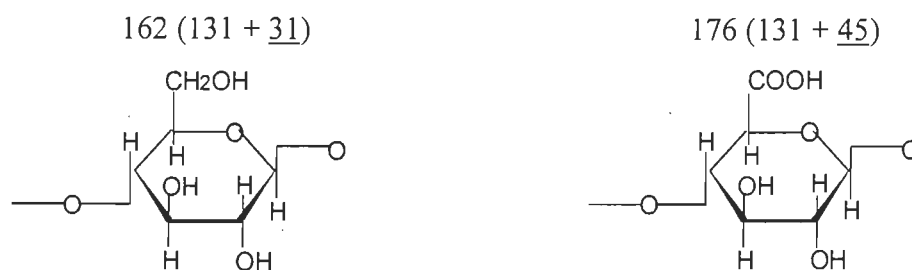
FIGURE 2.17 **Cellulose structure before and after oxidation during passage from hydroxyl to carboxyl state.**
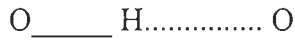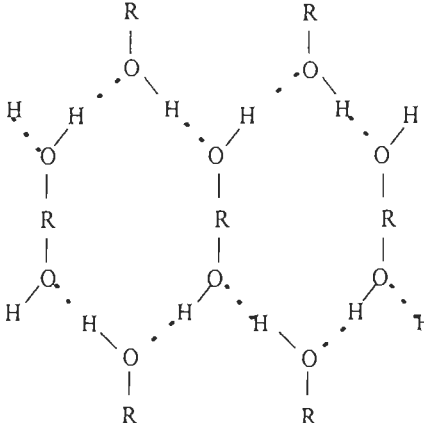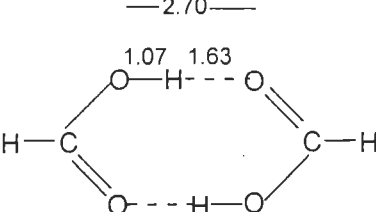
Increasing molecular weight of a defined cellulosic chains could result in an increase in the density, if the total volume remains constant, or even decrease.
So the effect of the greater "Cohesive energy density " and fibre density due to the transformation of the hydroxyl to the carboxyl at C6 of the, as mentioned above, might be observed in the reduction of specific surface area of the oxidised fibres and the density of the sheet. Decrease in the specific surface area can be interpreted as an increase in the relative bonded area, RBA, resultant higher tensile strength in turn. An Increase in density can also lead to an increase in tensile strength (56, 57). This would be true if the cellulose degradation due to the chain scission is not to high.

2.2.3.2   Hydrogen bonding force

The hydrogen bonding force is related to factors such as the distance between two molecules of oxygen O___H……..O, the angle and the shape of the hydrogen-

oxygen bond, all of which depend on the overall structure of the molecule in question. Examples of the hydrogen bond forces in water, ethanol and formic acid are given below (58).

It can be stated that the energy of the H........O bond in formic acid (including COOH) is 1.4 times higher than in the ethanol molecule. The state of cellulose before and after N_2O_4 oxidation can be simulated to the state of ethyl alcohol and formic acid or acetic acid. Before oxidation, the energy due to H-bonds is weak because it is produced only by the hydroxyl groups. In contrast, the post-oxidation force is much stronger because it is produced mainly by the carboxyl group and by the residual hydroxyl groups. It is clear that as the number of H-bonds increases the total bond energy should also increase.

	Bond length (A^o)	**Bond shape**	**Energy of H-bond** (kcal/mole)
Ice, H_2O	2.76		5.0
Ethanol, C_2H_5OH	2.60		5.64
Formic acid, HCOOH	2.70		7.6

The formation of COOH peaks at 1734 cm^{-1} for the oxidised fibres can be clearly seen and verified by observation of the FTIR peaks. Shifting the OH band towards lower energy also proves a higher number of H-bonds and a higher inter fibre-bonding, b, in the Page equation, due to the formation of COOH peaks (59).

2.2.3.3 Work of adhesion according to the acid-base theory

Another way of demonstrating the influence of different intermolecular forces on the surface structure of the fibre is through the acid-base theory of Bronsted (58). According to this theory, an acid is a proton donor and a base is a proton acceptor. This can be illustrated as follows:

$$Acid \longrightarrow Base + Proton$$

$$Base + Proton \longrightarrow Acid$$

$$Acid\ 1\ +\ Base\ 1 \longrightarrow Base\ 2\ +\ Acid\ 2 \quad [eq.2.7]$$
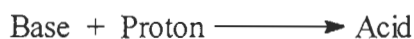
One may consider cellulose to be a base (R-OH) prior to N_2O_4 oxidation. During the reaction with HNO_2, it becomes a new acid (RCOOH), leaving a new base (NH_2OH) in the process.

$$RCH_2OH + HNO_2 \underline{\hspace{3cm}} RCOO^-H^+ + NH_2^+OH^-$$

FIGURE 2.18   Acid-base reaction of cellulosic fibres during N_2O_4 oxidation.

As the reaction advances, the number of $RCOO^-$ groups increases and the number of RCH_2OH groups decreases. Nevertheless, there is always a certain quantity of CH_2OH on the cellulose chains. These groups may react in an acid-base fashion with the COOH groups that have been formed. Consequently, the acidity and basicity of the treated fibres are gradually modified as a result of the oxidation treatment. It is possible that this increases the inter-fibre bonding. This is why it is necessary to measure this change of acidity and basicity and verify whether it has a positive effect on the final surface adhesion of the oxidised fibres.

a)   Acid-base contribution to the work of adhesion

For many years it was believed that H-bonds were due to dipole interactions. However, it is now believed that the H-bonds are too strong to be explained by this phenomenon. Rather, H-bonds are more likely to be due to acid-base interactions, and their strength is dependent on the acidity of the hydrogen donor and the basicity of the hydrogen acceptor, neither of which depends on the dipole moment (60). The hydrogen bonds are in fact exothermic acid-base interactions that have no relation to the dipole. In other words, hydrogen bonds are a subdivision of Lewis acid-base interactions, where hydrogen is responsible for the acid character (ie. acts as the electron acceptor or proton-donor.

Another delicate point is the degree of auto-association that may occur. Some solids and liquids possess both acidic and basic characters that lead to a greater or lesser degree of association depending on the strength of acidity or basicity. This is true of amphoteric liquids such as water, glycerol and glycol, all of which display high degrees of auto-association due to the equilibrium between the oxygen (base) and the active hydrogen (acid). In these kinds of liquids, auto-association increases the dielectric constant, surface tension and evaporation energy, while decreasing the solubility in non-polar liquids. In contrast, an acid such as chloroform has little basic character and the degree of auto-association is negligible.

In auto-associated liquids in which hydrogen-bonding occurs, surface energy is due to two components. These are the dispersive forces γ^d, which exclude hydrogen bonds, and the acid-base surface energy γ^{ab} which includes all types of hydrogen bonds. One of the advanced theories of surface and interface energy was proposed by Fowkes (60). According to him, the surface energy of a material γ consists of:

$$\gamma = \gamma^d + \gamma^p \qquad \text{[eq.2.8]}$$

where, γ^d represents the dispersive component of surface energy and γ^p, the polar component of surface energy, as was shown earlier by γ^{ab}. The following equation represents the attraction forces acting through the interface of two non-polar materials:

$$\gamma_{12} = \gamma_1 + \gamma_2 - 2(\gamma_1^d \gamma_2^d)^{1/2} \qquad [eq.2.9]$$

These interactions are generally represented under the form of the work of adhesion as follows:

$$W_a = W_a^d + W_a^p + W_a^i + W_a^h \qquad [eq.2.10]$$

where,

d   dispersion force

p   dipole interaction

i   induced dipole interaction

h   hydrogen bonds

When p and i are very small, equation 2.10 can be simplified to:

$$W_a = W_a^{lw} + W_a^{ab} \qquad [eq.2.11]$$

W_a^{lw} contribution of the combined dispersion force with dipole and induced dipole forces to the work of adhesion

W_a^{ab} contribution of acid-base interaction including hydrogen bonds to the work of adhesion.

Where, the dispersion force combined with dipole and induced dipole forces are called *Lifshitz-van der Waals* (LW) forces(61). All other forces can be considered to result from acid-base interactions. Lewis acid-base interactions which were previously called Bronsted interactions (62) cover all kinds of interactions related to the contribution of one pair of electrons including the hydrogen bonds.

b)   **Acidity and basicity of a polymer surface**

Dasgupta (63) reported that ozonation of dilute aqueous polypropylene pulps generates carboxyl groups and this yields better responses towards the wet strength resins of a paper. Better fibrillation and higher resistance are obtained (2) for the carboxymethylated and hydroxyethylated pulp. The hydrolysis effect of the oxidation treatment would not generally increase the strength properties of paper. However, because of the formation of carboxyl groups that increase the polarity and hydrophility

of the fibre surface, the bonding strength and consequently the paper strength may increase.

The contribution of acid-base interactions to the work of adhesion is measured by the changes in acidity or basicity of a liquid on a known solid (polymer). Vrbanac and Berg (64) studied the effect of certain bases (0.1% sodium hydroxide, dimethylsulfoxide, dimethylfluoride) and an acid (35% to 72% phenol in triphenyl sulfide) on a solid polymer having an acid behaviour (such as acrylic acid in copolymer). After measuring the value of W^{ab}, they observed that the greater the increase in basicity, the greater is $W_{SL}-W^d_{SL} =W^{ab}_{SL}$.

Where,

W_{SL} work of adhesion between a solid and a liquid

W^d_{SL} contribution of dispersion force to the work of adhesion

W^{ab}_{SL} contribution of acid-base interaction to the work of adhesion

Nevertheless, the effect of 35% phenol on this acid polymer is zero. By the same argument, the acid-base contribution of pyridine (a basic liquid) on a solid polymer having the same basic behaviour (such as vinyl acetate) will be zero.

These results reveal how the acidity or the basicity of a solid polymer can be characterised via compounds with known acidity or basicity, such as dimethylsulfoxide (DMSO), dimethylfluoride (DMF) and an acid (35% to 72% phenol) in triphenyl sulfide (TPS). It is convenient that in the case of cellulose, whose surface is dominated by hydroxyl groups, the acid-base interactions can be expressed by hydrogen bonds. This new approach has been listed in certain practical methods, such as the measurement of the contact angle or the acid-base characteristics of fibres by inverse gas chromatography (IGC).

c)   **Thermodynamic characteristics of the fibres surface by IGC technique**

Inverse Gas Chromatography (IGC) is often used to measure the thermodynamic

Characteristics of solid surfaces. It permits the study of an unknown stationary surface via an injection of known gas solvents. The solvent is distributed through a mobile gas phase and a stationary solid phase (65, 66, 67, 68, 69, 70). In these studies the stationary phase is the polymer or cellulose fibres whereas the gas phase is N_2.

There should be a high degree of exchange surface between these two phases. This condition is obtained by using a long column containing the stationary phase through which the gas is transported. The elution time that the solvent needs to pass through the column depends on the partition coefficient of the solvent between the two phases. IGC is not only used for regular surfaces such as polymers, but also for rough and irregular hydrophyl surfaces such as cellulosic fibre (68). This technique also permits an evaluation of the acidity or basicity of surfaces. These characters indicate the specific interactions attributable to the polar components. Specific surface energy, γ^{sp}, expresses the concept of acid-base interaction or acceptor/donor one (71). To determine the contribution of the specific interaction to the total surface energy, the polar probes should be injected in addition to the n-alkanes in the column. It is supposed that the n-alkanes, which are non-polar, favour these exchanges, because of their dispersion interactions. On the other hand, the dispersive and polar surface energies are additive. The straight line corresponding to alkanes can be taken as a reference to determine the dispersive component of polar probes. Consequently, the distance between the observed ΔG_A and the straight line of the alkane probes is the specific surface free energy of the polar probe, ΔG^{SP}_A (72). The adsorption enthalpy ΔH_A, and the adsorption enthalpy corresponding to a specific interaction ΔH^{sp}_A, may be obtained by IGC measurements at different temperatures. Schultz et al (71) proposed the following equation:

$$-\Delta H^{SP}_A = K_A DN + K_B AN \qquad\qquad [eq.2.12]$$

$$-\Delta H^{SP}_A / AN = K_A . DN/AN + K_B$$

where,

DN   polar probes donor number

AN   polar probes acid number

K_A acid constant of the stationary solid

K_B·   basic constant of the stationary solid

By plotting $-\Delta H^{SP}_A /AN$ on the y axis, and DN/AN on the X axis for different points of the polar probes, a straight-line relationship can be obtained. Then the acid and base constants K_A and K_B are calculated as the *slope* and *intercept* of this line. It is therefore possible to determine whether the treated fibre has become acid, basic or amphoteric. In the case that both acid and basic character of the fibres are increased, the specific acid base interaction, I_{SP} is increased respectively. This leads to an increase in the work of adhesion through the fibres, which interpreted as an increase in the bonding strength, b, in the Page equation.

CHAPTER III

EXPERIMENTAL METHODOLOGY

3.1   Materials

A softwood bleached kraft pulp sheet made mainly from spruce (5-6% moisture content) was selected as a reference pulp. The reason for this choice was that there were sufficient Fourier Transform Infra Red (FTIR), Electron Spectroscopy Chemical Analysis (ESCA) and Inverse Gas Chromatography (IGC) data for this pulp, which would permit evaluation of the results of preliminary tests and the comparisons with the short-fibres pulps.

The short-fibre pulps used in this study were a bleached kraft bagasse pulp from the Pars Paper Co., Iran, and a bleached kraft aspen pulp from Avenor Inc. of Thunder Bay, Ontario. Bleached kraft pulps were chosen to test the effect of the N_2O_4 oxidation on the fibres independently of lignin content since that component has been removed by more than 99%. The chemical compositions of the three pulps were measured according to the Tappi standard procedures, T 223, om-84, and T 452. The results are reported in Table 3.1. The oxidation parameters were evaluated on the softwood pulp by three different designs: the one factor at a time design, the half-factorial and the composite central design (CCD).

TABLE 3.1   **Chemical compositions and brightness of the fibres used for the oxidation study with N_2O_4.**

	Pentosan (% of pulp)	Lignin (% of pulp)	Brightness (%ISO)
Softwood	8.4 ± 0.5	0.18	85.7
Bagasse	22.2 ± 1	0.42	72.25
Aspen	18.5 ± 1	0.50	75.10

After finding the reasonable condition; flow-rate of N_2O_4 gas (4.04 l/min), pulp consistency (10%), and ambient temperature (5°C), where the formation of COOH was at higher and viscosity reduction was relatively at lower level, another set of tests was done at different oxidation times. Since the sample weight (30 grams bon dry)was constant for all trials, it was possible to calculate the N_2O_4/fiber ratio (expressed as a percentage) by equation 3.1, thus combining flow-rate and time into the single parameter.

$$N_2O_4/\text{Fiber (\%)} = \frac{1\,\text{molecular weight of N}_2\text{O}_4(g) \times \text{gas flow (ml/min)} \times \text{oxidation time (min)} \times 100}{\text{weight of the fibers (g)} \times 22400} \quad [\text{eq.3.1}]$$

Oxidation treatments were carried out at N_2O_4/fibre ratios of: 0.0%, 0.83%, 1.25%, 1.66% and 2.50% for bagasse and aspen as well as for the softwood fibres in the same conditions of pulp consistency and temperature. FTIR, ESCA and IGC studies were performed on samples of the treated fibres. The results are reported in the second, third and fourth section of chapter 4. Table 3.2 shows the code numbers and descriptions of the fiber samples used in these analyses.

TABLE 3.2 The description of samples used for FTIR, ESCA and IGC analysis.

Run No.	Fibre species	N_2O_4/Fiber(%)
S-0	Bleached kraft softwood	0
S-1	« « «	0.83
S-2	« « «	1.25
S-3	« « «	1.66
S-4	« « «	2.50
B-0	Bleached kraft bagasse	0
B-1	« « «	0.83
B-2	« « «	1.25
B-3	« « «	1.66
B-4	« « «	2.50
A-0	Bleached kraft aspen	0
A-1	« « «	0.83
A-2	« « «	1.25
A-3	« « «	1.66
A-4	« « «	2.50

The samples were not washed and neither any post-treatment were carried to the samples after the oxidation The oxidised fibres were dried in the air at room condition, collected in the plastic bags and kept in the cool area to be used for the further physical tests and FTIR, ESCA and IGC analysis.

For the evaluation of the fibre and paper properties, one more points (0.42% N_2O_4 /fibre) were added to the experiments. The results are reported in the fifth section of chapter 4.

The effect of Mg salts was also studied for softwood and bagasse fibres with the same oxidation conditions as above. The $MgCO_3$ was present at a percentage of 1% by weight of pulp (0.3 grams). These samples were coded as S-0, S-1, S-2, S-3, B-0, B-1, B-2 and B-3 correspond to the 0-%, 0.83-%, 1.25-% and 2.5-% N_2O_4 /fibre respectively. The comparative results are presented in each section of chapter 4.

The gas used for the oxidation treatment was nitrogen tetroxide. This is a poisonous oxidising gas that causes the eyes and skin to burn, and is extremely dangerous to inhale. It should only be used under a fume hood with full security precautions. It is colourless when pure, but obtains a yellow colour when mixed with NO_2. For security reasons, it is supplied as a pressurised liquid mixture with NO_2. The proportions of N_2O_4 and NO_2 are controlled by the manufacturer (Matheson Inc., USA) but were not given. As the ambient temperature goes up, the proportion of N_2O_4 gas reduces; however, the temperature of the cylinder should not exceed 52°C. It can be transferred to gas phase at room temperature. The $MgCO_3$ used in this study was in a powder form with 99% purity with the following formula:

$$MgCO_3 * Mg(OH)_2 * 5H_2O$$
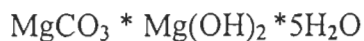
A gas feeding system was set up to carry out the oxidation treatment and to permit modification of the oxidation parameters (Fig.3.1). The gas flow was controlled by two manual valves. Gas was passed through a glass u-tube containing calcium chloride and phosphorous pentoxide to capture the water vapour present in the gas. The

final flow was controlled by a flow meter (0-150 ml/min) with a glass float placed before the rotating balloon that contained pulp fibres.
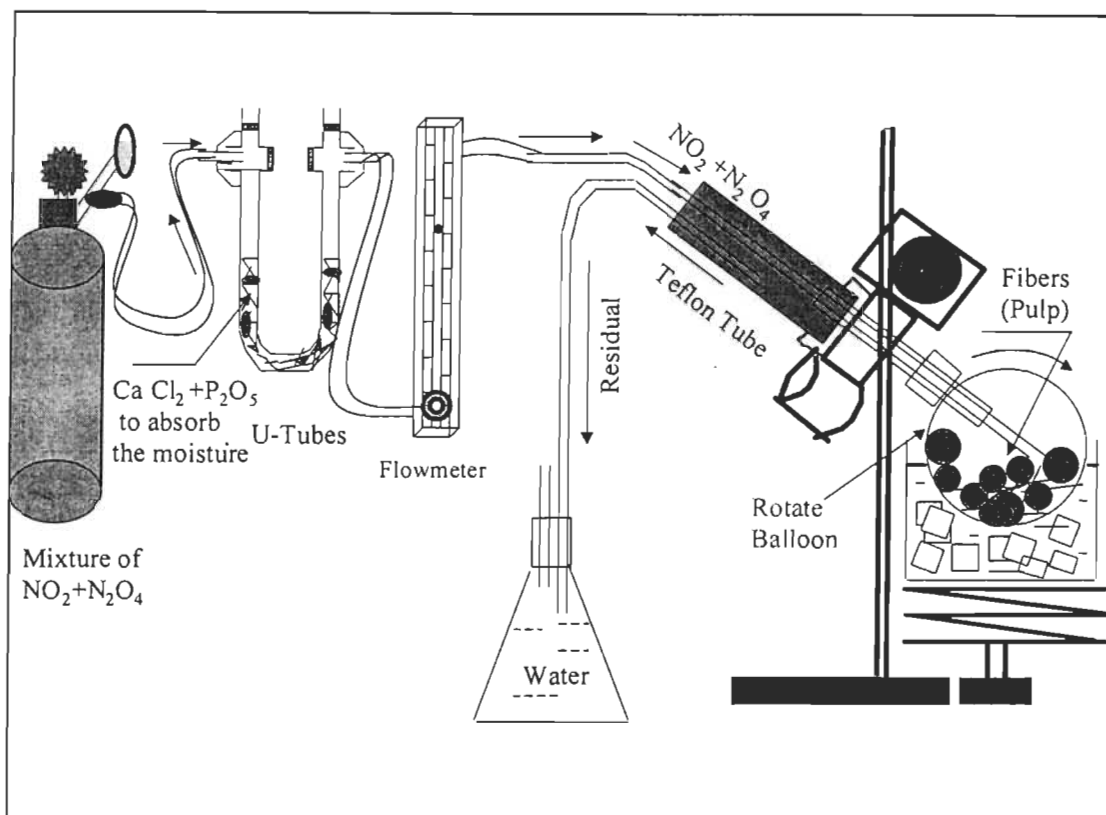
FIGURE 3.1 Apparatus for the N_2O_4 treatment of cellulosic fibres.

The treatment temperature was controlled by a water bath. Gas flow-rate was controlled by two manual valves and finally by a flow meter model 150. A 1000 ml rotating flask, with variable speed controller assured direct contact between the pulp and the N_2O_4 gas. The excess gas was returned to an Erlenmeyer flask containing water, and its water vapour was sent to the atmosphere. This assured constant gas pressure. The two other oxidation parameters, including the time of oxidation and the pulp consistency were measured and changed as needed. The bon dry weight of the fibres without any pre-treatment was constant (30 grams) for all experiments.

3.2   Methods

The test methods used in this study were FTIR, ESCA, and IGC. The chemical

and physical properties of the fibres were also evaluated as will be described further on.

3.2.1 Chemical analysis
3.2.1.1. Lignin content

The lignin content of bleached fibres was measured according to Tappi standard methods T 236 cm 85 (73). The kappa number was measured first. The kappa number is the volume (in millilitres) of 0.1N potassium permanganate solution consumed by one gram of moisture-free pulp under the conditions specified in the method. The lignin content is calculated using a coefficient of 0.13. This method is valid for pulps with less than 60% yield. The results are corrected to 50% permanganate consumed.

$$k = \frac{pf}{w}\left[1 + 0.013(25 - t)\right] \qquad \text{[eq.3.2]}$$

% of Klason lignin in the bleached kraft fibres = $k \times 0.13$

where,

k   kappa number

f   factor for a 50% permanganate consumption (Table 1 in T 236 cm85)

w   weight of moisture-free pulp in the specimen, g

t   actual reaction temperature in Celsius (20 –30 °C)

p   amount of 0.1N permanganate actually consumed by the test specimen, ml

3.2.1.2 Pentosans content

Wood pulps contain a certain amount of non-cellulosic carbohydrates, which are called hemicellulose. Softwood hemicellulose consists mainly of hexosans, while the hemicelluloses of hardwood consist mainly of pentosans. Thus, the pentosans content in pulp indicates the loss of hemicellulose during pulping and bleaching of hardwood fibres. Since hemicellulose is known to contribute to the development of the paper strength, pulps with high pentosan or hexosan content are desirable.

According to Tappi standard T 223 cm-84, the calibration graph was plotted for different concentrations of xylose in water versus its light absorbance at 630 nm. The relation between xylose and xylan content is expressed as follows:

$$\text{Xylan (mg)} = \text{Xylose (mg)} \times 0.88$$

The xylan content of a solution may be determined by measuring its absorbance in a colorimeter. The xylose and xylan contents may then be obtained from the calibration graph mentioned above..

For each pulp, the distillate is prepared by the distillation method using hydrochloric acid. Then its absorbance is measured. Finally, the xylan content and the pentosan percentage of the fibres are calculated with the aid of the calibration graph and equation 3.3 (73).

$$\text{Pentosans, \%} = \frac{A}{10 \times w} \qquad \text{[eq.3.3]}$$

where,

A   xylan in test specimen, mg

w   oven-dry weight of the test specimen, g

3.2.1.3   Carboxyl content

Grams of three oven-dried (OD) pulp were soaked twice in 0.1M hydrochloric acid for 60 minutes to convert to proton of the anioni the ionic groups to hydrogen form. It is assumed that this time is sufficient to obtain constant conductance. Each soaking was followed by washing with deionised water. The pulp was then drained and dispersed in 450 ml of 0.001M sodium chloride solution prepared in deionised water. Titration of 5 ml acid chlorhidric was carried out with 0.1 M sodium hydroxide by a computer-controlled automatic–burette, while the pulp suspension was stirred under a nitrogen atmosphere. Alkali was then added at a rate of 0.5 ml every 5 minutes so as to allow sufficient time for equilibrium to be reached between readings. Following titration, the pulp was washed, dried at 105°C and weighed (74). Data from the potentiometer were

processed on a computer and the content in carboxyl groups was computed based on the response curve. Two measurements were taken for each sample and the average value was reported.

3.2.1.4   Viscosity

Oven-dry pulp samples weighing 250 ±0.1mg were placed into 118-ml dark brown tubes containing 25 ml water. Then, 25 ml of 0.5M cuprethylendiamine (CED) solution was added to each tube. These were then put under a Burell Wirst action shaker for a period of 8 hours to ensure that all fibres were well separated, and no aggregate was seen during the measurement. The Tappi procedure proposes that this be done for 45 minutes, instead of the 8 hours employed in this study. The solution is poured into a viscometer, which in turn is placed into a Julabo water basin. After 5 minutes of equilibration, the solution is drawn up into the measuring leg of a viscometer, until it reaches a marked line. The solution is then drained down the viscometer. The time required for the solution to pass from the top line to the bottom line is measured at a precision of ± 0.2 second. When the flux time falls between 100 and 800 seconds, the read value is considered to be reliable. Once the readings fall out of this range, another type of viscometer is used. The average of three readings is taken for the calculation of the dynamic viscosity, V, using equation 3.4.

$$V = Ctd \hspace{3cm} [\text{eq. 3.4}]$$

where, V is the viscosity of cuprethylendiamine solution as $25°C$ mPa s.(cP), C is the viscometer constant found by calibration, t is the average efflux time of the solution in seconds, and d is the pulp density in cuprethylendiamine (CED) solution equal to 1.052 g/cm^3 at a 0.5% pulp consistency.

The test was prepared also at pulp concentrations of 0.3, 0.5, 0.7 and 0.9% to determine the intrinsic viscosity (equation 3.5).

$$[\eta] = \lim_{C \to 0} \eta_{sp}/C \hspace{3cm} [\text{eq.3.5}]$$

where,

η the intrinsic viscosity

$$\eta_{spec.} = \frac{\tau - \tau_0}{\tau_0} \Big/ C$$

τ the dynamic viscosity of the rest solution

τ_0 the dynamic viscosity of the solvent

C   the concentration of the solution mass of dissolved substance per unit volume of solution

A plot of η_{sp} versus the concentration of the solution produces a linear function. As C tends to zero the intrinsic viscosity, η, is obtained by the intercept value of this curve. In the other hand with the aid of Mark-Hawink equations (eq. 3.6), it is also possible to calculate the molecular weight, M of the cellulose (42).

$$\eta = kM^{\alpha} \qquad\qquad [eq.3.6]$$

k and α are the constant, which usually are found for each substance and in any specific solvent by the light scattering or centrifugation techniques. For the materials such as cellulose, α is taken as 0.9 and even 1 for cellulose trinitrate. k is taken as 6.9×10^{-3} dl/g in the case of Cuen solution (138). As the oxidised bleached kraft fibres used in the experiments are similar to the cellulose nitrate, it might be assuming that $\alpha = 1$ and $k = 6.9 \times 10^{-3}$.

The DP can be further computed as DP $= M/162$. Since most of the OH groups of the cellulose are converted into aldehyde, ketone or carboxyl groups during the oxidation reaction, the assumed value of 162 for the molecular weight of the modified glucose unit is no longer valid. Therefore, the DP values calculated by the above equation become doubtful. This is why it is preferred to report just the intrinsic viscosity in dm^3/kg, rather than DP values.

3.2.2   The evaluation of pulp and fibre quality

3.2.2.1 Freeness

Canadian Standard Freeness (CSF) is a measure of the drainage rate at which a dilute suspension of fibres may be dewatered. It is generally a useful index of the amount of mechanical treatment given to a pulp and may even correlate with the drainage behaviour of pulp material on the wire of a paper machine. CSF is determined according to the CPPA standard testing method C.1. The test consists of thoroughly wetting the whole freeness tester with water at the temperature of the stock to be tested. A 1000 ml sample of disintegrated pulp with a consistency of 0.3% is poured into the tester chamber gently, but as rapidly as possible. The top lid and air-cock is then closed and the bottom lid is opened. After 5 seconds the air-cock is fully opened to let the stock drain through the bottom screen. The volume of the discharged liquid form the side orifice of the funnel under the chamber is read in millilitres. This volume is the Canadian Standard Freeness after a correction for temperature to 20 °C. In order to eliminate the effect of mechanical treatment, pulp samples were not refined in this study. Their CSF values were determined as described above.

3.2.2.2 Paper sheet formation

Seven hand-sheets per sample were formed according to the Tappi hand-sheet making procedure. Five of them were selected based on the quality of formation. These sheets were then weighed to give the grammage and tested for density, tensile index, burst index, zero-span, z strength and for the optical properties.

3.2.2.3 Fibre physical properties

According to Tappi procedure T 271 pm-91, pulp samples were prepared at 0.005-% consistency for hardwood and at 0.002-% for softwood. Then 100 ml of this well-mixed sample was placed in a 4-litre container and water was added to reach 500 ml. This was done to test the apparatus. The manual of the machine recommended a

0.0002% concentration to minimise the risk of plugging the wire. This enables the passage of 10-40 fibres, and minimises the risk of plugging. The data obtained by this apparatus then plotted on a graph, yielding an arithmetic average of fibre length, fine percentage, curl and kink index.

The weighted average fibre length by weight is calculated automatically by the machine, based on the following equation:

$$L_W = \frac{\sum_{i=1}^{144} n_i l_i^3}{\sum_{i=1}^{144} n_i l_i^2} \qquad [eq. 3.7]$$

where, n is the number of the fibres in each category, l is the average fibre length, in each category and 144 is the number of the categories.

All samples used for the strength properties and optical measurements were made according to the Tappi standard procedure, but without any refining. Thus, any change in the strength properties can be attributed to the chemical treatment itself.

3.2.2.4 Mechanical properties of handsheets

These measurements were made on handsheets made from non-treated and oxidised fibres. The tests included the tensile strength, burst strength, z strength and zero-span strength.

Tensile strength is calculated from the maximum load that a narrow strip of specimen can support before failure. The tensile strength is measured according to Tappi standard T 494 om-88 with an Instron tester using a constant rate of loading. The load required to rupture the specimen is corrected for the basis weight, and reported as the tensile index.

Burst strength is also measured by the Tappi test, T 403, om-91 with a Mullen tester. Here, a specimen is held between annular clamps through a rubber diaphragm to the circular area defined by clamps and subjected to a pressure from one side. This causes the specimen to deform into an approximately spherical shape until failure occurs by rupture. Once the corrections are made for the basis weight, the burst strength is reported as burst index in $kPa.m^2/g$. The burst strength is designated as the hydrostatic pressure in kilopascal required to produce rupture in the sheet when the pressure is increased at a constant rate of loading.

The *Z strength;* In the case of this test the paper sample is placed between two solid bodies with the help of a double face adhesive paper, 3M, number 610. The solid parts have an area of 645,16 mm ^{2}. Acetone is used to remove any dirt from the solid surfaces. In order to assure a good adhesion between paper and the adhesive solid, 345 kPa pressure is applied to the entire assembly during one minute. According to Koubaa (76, 77) this is the optimal pressure from the point of view of fibre bonding in paper. The sample was then placed in the apparatus and the test is carried out at 20 kg load at a constant speed of 10 mm/min. The data are then been transferred automatically to the computer, to be saved and analysed according to the program number 66. For the sake of comparison, the resistance of the adhesives to the solid part was measured and was found to be 1000 kPa. In comparison a highly resistant paperboard measures 600 kPa. The Z strength is usually expressed in kPa. The breaking energy can also be calculated from equation 3.8.

$$W_Z = \int_0^\varepsilon \sigma d\varepsilon \qquad [eq. 3.8]$$

where σ is the breaking stress in Pa and ε is the displacement during the breakage.

Zero-span strength measurement is done with The Pulmac apparatus. At first, the apparatus is left with open air for 15 min, then the zero setting is verified. The air pressure is then activated to an outlet pressure of 100 psi and the start button is placed to the GO position. A metal is used to calibrate the clamping pressure at a value of 85.5

psi. The metal is then replaced by a paper sample and the average of 10 readings is inserted into the equation below:

Zero-span breaking length (km) = (reading value–2) × 24.8/basis weight in g/m^2

The average of 6 sheets is used with 3 significant figures.

In comparison, Tappi standard T231 cm-85 proposes the following equation.

Zero span breaking length=200000 p/3r

where p is load in pounds and r is the average weight of 3 moisture free samples.

3.2.2.5 Optical properties

Brightness of a sheet is defined as the reflectance of a bulk light with a specified spectral distribution peak at 457 nm as compared to that of the perfectly reflecting surface of $MgSO_4$. The pulp brightness was evaluated on 1.2-gram hand-sheets made with deionized water using a Zeiss Elerpho photometer. The same instrument was used for the measure of opacity and the light scattering coefficient.

Transmittance *opacity* is defined as the amount of light not transmitted by a sheet of paper. However, it is usually determined by measuring the reflectance of the sheet. The reflectance was also measured with a Zeiss Elerpho photometer. The opacity in this study is expressed as printing opacity, R_0/R_∞, where R_0 is the reflectance of a single sheet backed by a black-velvet-lined cavity. R_∞ is the reflectance when the sheet is backed with enough of the same or similar coloured sheets to make the pile opaque paper.

Light scattering coefficient is a measurement of the ability of the interior empty space of the sheet to scatter light. It is also determined by R_0 and R_∞, but using the following equation:

$$S = \frac{10^4 R_\infty}{\left(1 - R_\infty{}^2\right)W} \ln\frac{\left(1 - R_0 R_\infty\right)}{\left(1 - R_0/R_\infty\right)} \qquad \text{[eq. 3.9]}$$

where S is the light scattering coefficient; W is the basis weight of the sheet in g/m^2. All of the physical tests were carried out in a conditioning chamber at 23 °C and 50% relative humidity.

3.2.3   Method of FTIR Spectroscopy

Infrared spectroscopy is one of the most commonly used techniques for the identification and characterisation of the chemical structure of the fibre constituents. This technique measures the vibration energy level of molecules, which are usually in the range of middle infrared radiation (Fig. 3.2).

Infrared absorption spectroscopy of cellulose at room temperature provides useful information about the molecular structure of the fibre. This technique can be used to monitor the chemical modifications of cellulose fibres as a result of chemical treatment such as oxidation.

It is known that the N_2O_4 oxidation attacks the OH groups of the primary and secondary alcohol of the treated fibres. As a result, the chemical structure of the fibres changes. It is possible to verify these changes by observing the displacement of the OH peak or formation of COOH peak in the FTIR spectra.

3.2.3.1   Apparatus

The conventional instrument uses a dispersive technique in which the IR radiation passes through a narrow slit and grating system to limit the frequency of the radiation reaching the detector to one resolution. Thus, the detector only receives a tiny part of the radiation source. Therefore, the intensity of the final signal is very weak.
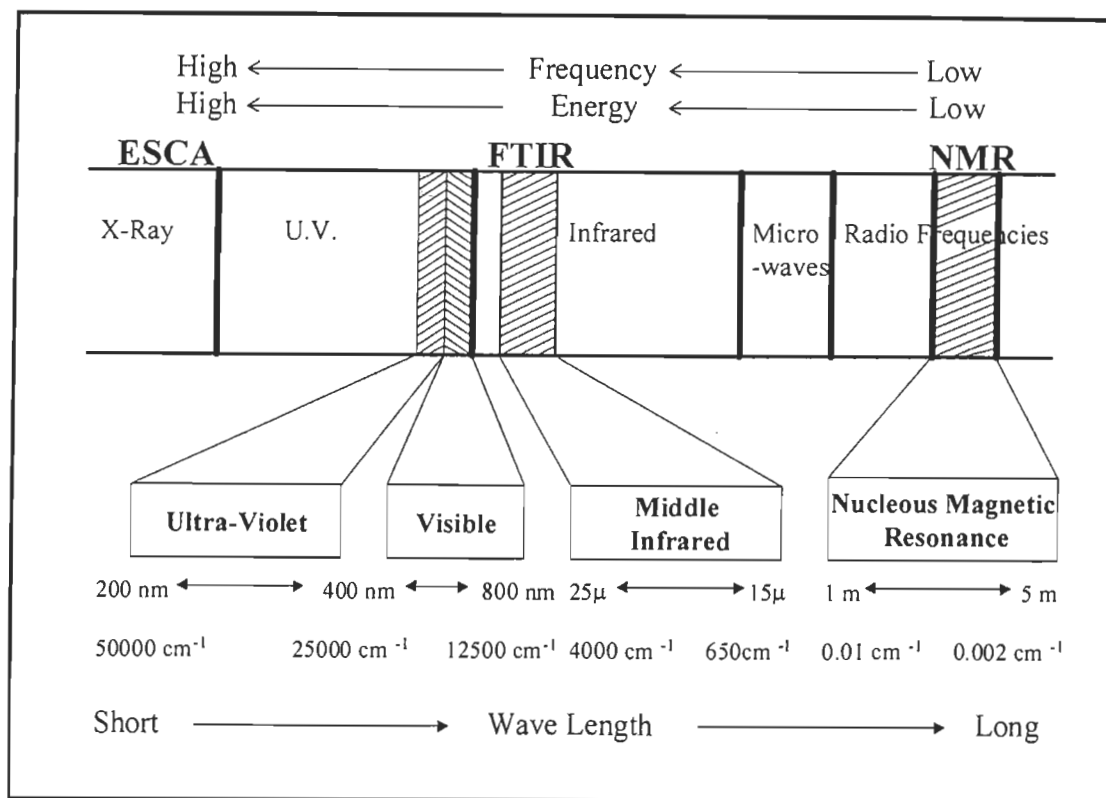
Figure 3.2   Electromagnetic radiation spectrum (78).

This drawback is overcome by Fourier transform infrared spectroscopy (FTIR), where an interferometer of the Michelson type is used instead of a grating system. The intensity of the detected signal depends on the radiation frequency and on the displacement of the moving mirror in the interferometer. The resulting interferogram contains the necessary information on the intensity of each frequency in the system.

This interferogram can be calculated by the Fourier transform to yield the IR spectrum. Since the FTIR instrument uses a laser to monitor the position of the moving mirror, the frequency of the measured spectrum is very accurate and the risk of drift during multiple scanning is absent. Moreover, the computational ability is improved since the data are the in digital forms. This allows spectrum to be subjected to mathematical treatment, such as spectral subtraction, differentiation and deconvolution. FTIR spectra were recorded using the 510P spectrometer from Nicolet firm in the middle IR range 4800-400cm^{-1}. The resolution was 2 cm^{-1} at 20 scans per second.
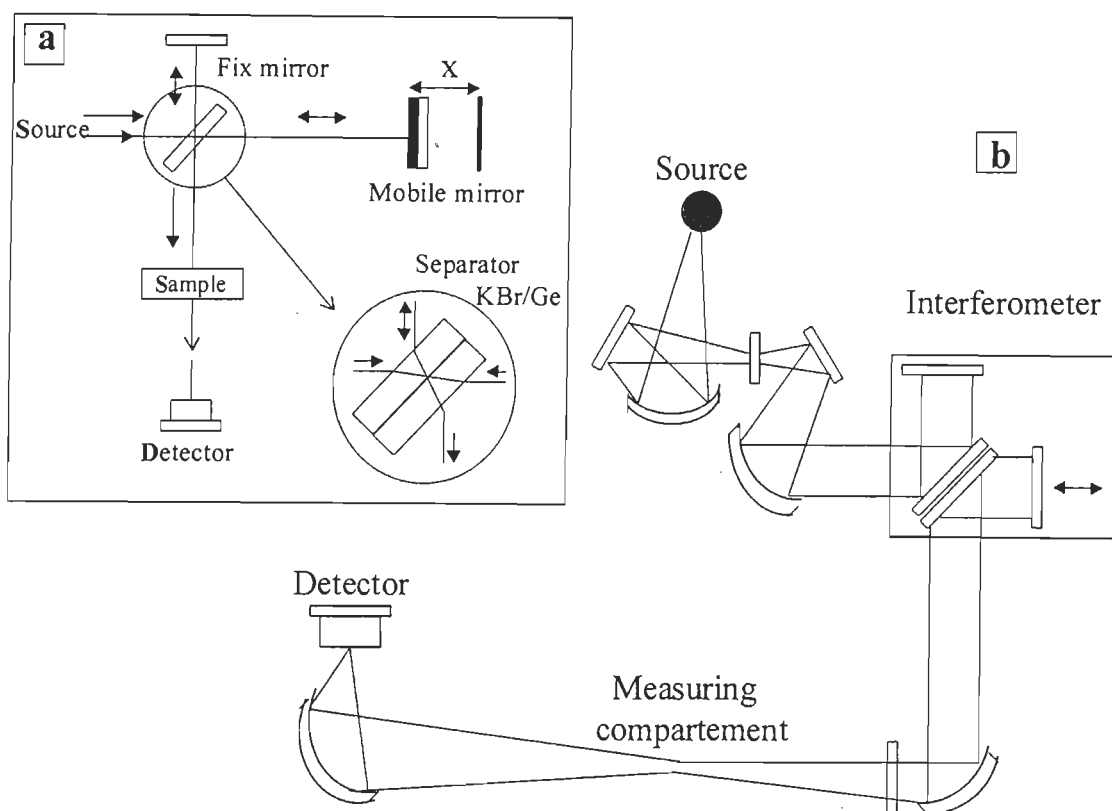
FIGURE 3.3 Optical assembling of Fourier transformer. a) 90° Michelson Interferometer. b) Optical diagram of spectrometer with single beam of Fourier transformer IFS 25 (Bruker association) (79).

The samples were prepared by the procedure used by Friedlander et al (16). Two mg of cellulosic fibres have been ground to 40 mesh, then mixed with 350 mg KBr. The mixture was then compressed in a transparent tablet. The compressing time and pressure were 8 min and 110000 psi, respectively.

3.2.4   Electron Spectroscopy for Chemical Analysis (ESCA)

Even though the chemical composition of a fibrous material is well known, much less is known about its surface chemistry. This is important since it affects the final properties of the paper. More precisely the strength of fibre bonding is closely related to the chemical nature of the fibre surface. This in turn determines its final paper physical strength and its resistance to photochemical degradation.

ESCA analysis of the surfaces of fibres enables to obtain chemical data of the fibre surface at a resolution less than 10 angstrom (Å). ESCA, which is also called X-ray Photoelectron Spectroscopy (XPS), has been used as a powerful instrument for surface chemistry analysis of synthetic and natural polymers as well as modified fibres (80, 81, 82, 83). This technique was also used in this work to verify the oxidation treatment of the bleached kraft fibres from the point of view of the surface chemistry and the hydrophilic character of the surface.

3.2.4.1   Apparatus

An ESCA-LAB MK II Spectrometer fitted on a Microlab system from V. G. Scientific was used for the characterisation of fibre surfaces. It was equipped with a non-monochromatized dual Mg-Al anode X-ray source. Kinetic energy was measured with a hemispherical electrostatic analyser, which has a 150-mm radius. This works in a constant pass energy mode at 20 eV for C_{1S} and O_{1S} peak, 50 eV for S_{2P} and survey spectra. No flood gun was used in this study. A 10^{-8} torr vacuum was maintained in the test chamber. A small sample of pulp pad was pressed in an indium disk with maximum care to prevent the contamination of the sample. Spectra could be produced using an Mg anode at 300 W, with typical accumulation time of 275-300 seconds for carbon C_{1S} peaks, 130-210 seconds for O_{1S} peak and 225-250 seconds for S_{2P} peak (83). Spectra were acquired to check the stability of the fibre surface as a function of exposure time. During the test a sample of 10×15 mm area was exposed to X-ray. The spectrometer was operated in a computer controlled scanning mode. A computer with VGS 1000 software was used for peak synthesis. This is a curve fitting technique for resolving the complex spectra, The ratio of the Gaussian to the Lorenzian function was around 60% for the C1S and O1S peaks and the FWHM was about 2 eV as mentioned for each of the sample in Table 4.3. FWHM is the full width at half maximum of formed peaks.

3.2.4.2   Principle of ESCA

Siegbahn et al (84), obtained the first X-ray photoelectron spectrum from cleaved

sodium chloride. At this time, the goal of using XPS for atomic structure investigation had been realised. As the effect of chemical shift and other field of electron spectroscopy were studied, commercial instruments started to appear between 1969-1970 (129). A solid sample is placed on a mount under high vacuum and is irradiated with X-ray photons. Some of these photons collide elastically with the inner shell electrons of atoms in the sample. Upon the impact with the photons, the electrons leave the atoms with a kinetic energy that is equal to that of the photons, minus the binding energy, E_B, which holds an electron to its parent atom (Fig.3.4). This binding energy is different for every electronic shell of each element in the periodic table. Thus, it is possible to determine which elements are present in the sample by measuring the energy of emitted electrons, E_K (81). This energy, E_B, is in the range of 20 to 1400 eV for different elements, and it can be calculated by the following equation (85):

$$E_B = E_X - (E_K + Q + E_C) \qquad \text{[eq. 3.10]}$$

where,

E_K kinetic energy as measured with respect to the vacuum level

E_X or hv is the energy of incident photon

E_B binding energy of the electron at its original level

Q work function of the spectrometer

E_C energy lost in counteracting the potential associated with the steady state charging of the surface.

Although the X-ray may penetrate deep into the sample, the electrons emitted in the bulk of the material soon lose their energy through repeated collisions. Thus, only atoms of a surface layer of very limited depth contribute to the intensity of measured electron emission. Because this 'escape depth' is between 1 and 5 nm, depending on the chemical nature of the solid under study, this technique is very sensitive to the surface constituents. Thus, the energy of the emitted electrons characterises the elements present in the surface layer and the intensity of the signal indicates their abundance (81).
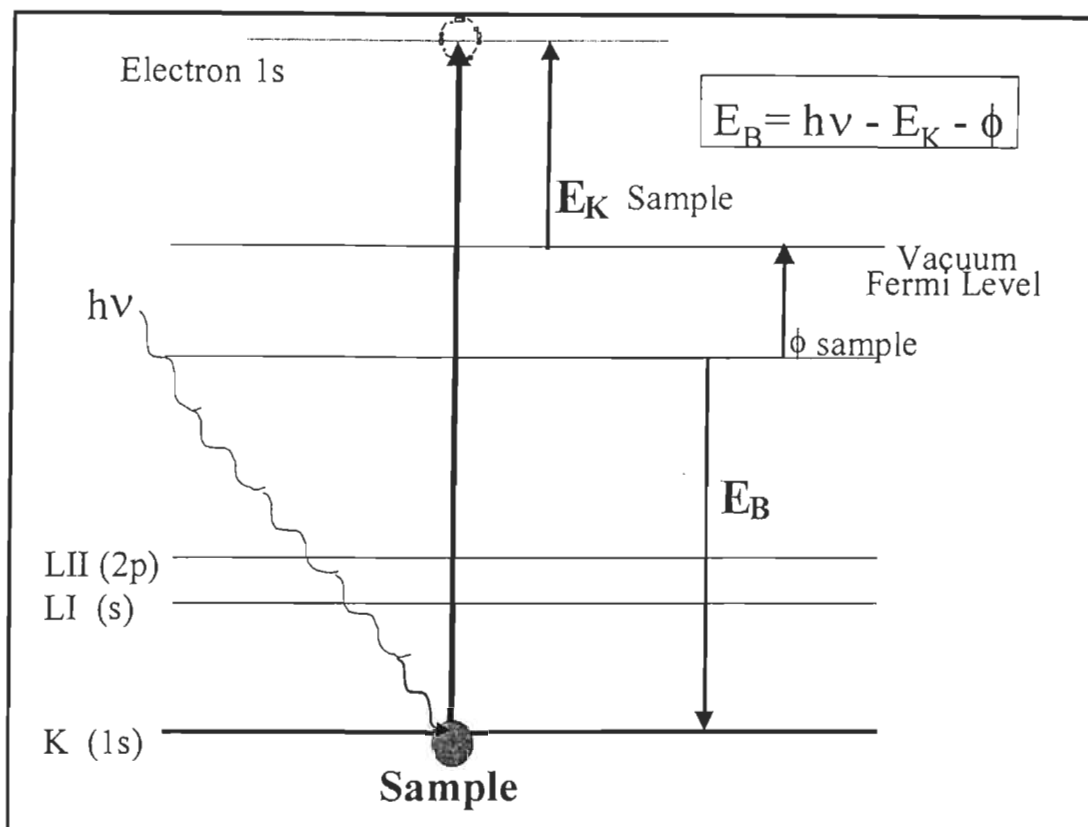
FIGURE 3.4 Principle of the emission of photoelectrons by X-ray (86).

The atomic ratio of two elements in the surface region analysed by ESCA can be approximately estimated from the ratio of their peak intensity, for example,

$$\frac{O}{C} = \frac{\delta_c D_c \lambda_c I_O}{\delta_o D_o \lambda_o I_c} \qquad \text{[eq3.11]}$$

where,

δ cross section for the generation of photoelectrons

λ mean free path of photoelectrons, which depends on their kinetic energy

D spectrometer transmission

I integrated intensity of the ESCA peak

The following relation can be derived for equation 3.11 for the C1s and O1s peaks by the using of Scofield's cross-section (85, 87):

$$O/C \quad \text{or} \quad N_O/N_C = \frac{1}{2.85}\left(\frac{I_{O1s}}{I_{C1s}}\right) \qquad \text{[eq.3.12]}$$

where, I_{O1s} and I_{C1s} are the areas under the respective ESCA peaks. The factor 2.85 or 2.93 as reported by Dorris (81) , sometimes referred to as the « sensitive ratio », depends on the design of the spectrometer. By the same way, the S/O and S/C values are calculated as follows(88):

$$S/O = \frac{1}{1.497}\frac{I_S}{I_{O1s}}$$ [eq.3.13]

$$S/C = \frac{1}{0.525}\frac{I_S}{I_{C1s}}$$ [eq.3.14]

The binding energy and chemical shifts for the carbon (1s) atoms in organic compounds have already been measured and tabulated. Based on these data, Dorris and Gray (81) classified the carbon atoms in the wood components into four broad classes in order of increasing chemical shifts (Fig. 3.5).

I   carbon atoms bonded to a carbon and/or hydrogen

II   carbon atoms bonded to single oxygen, other than carbonyl oxygen

III   carbon atoms bonded to two non-carbonyl oxygen, or to a single carbonyl oxygen

IV   carbon atoms bonded to carbonyl and non-carbonyl oxygen

C(1S) CHEMICAL SHIFTS   (eV)
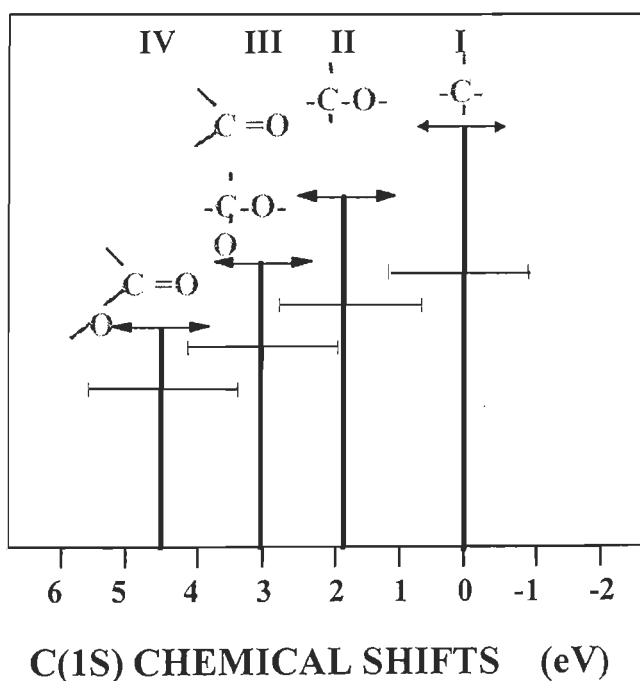
FIGURE 3.5   Diagram representing the range of C (1s) binding energies expected for carbon-oxygen bonds. The solid state peak width at half height are indicated by the upper and lower arrows, respectively (81).

Upon the above classification many researchers have interpreted C1, C2, C3 and C4 for lignocellulosic materials as follows:

C1 is the indication of the presence of lignin and extractives

C2 is the indication of the presence of cellulose and hemicellulose

C3 is the indication of the presence of ketone on the surface

C4 is the indication of the carboxyl content on the surface

The oxygen peaks are much less sensitive than the carbon peaks to the effect of the chemical shift for the type of organic bonds under consideration. Thus, it is necessary to bring the $O(1_S)$ signal in line with the irradiation values. The approximate chemical shifts associated with the $C(1_S)$ atoms may then be calculated. Under favourable circumstances, this « chemical shift », may indicate the type of chemical bonds present in the surface.

Even after correction, the exact values of the binding energies for C1, C2, C3 and C4 still display a large range of variation, which overlap with one another. This has given different interpretations as to the composition of the lignocellulosic materials concerned. For example, a base binding energy of 285.0 eV is proposed for C1. The values for C2, C3, and C4 are calculated upon their chemical shift. Consequently, the peak at a binding energy of 286.6 refers to C2 and indicates the presence of cellulose. The peak at a binding energy of 288.4 ± 0.4 eV refers to C3 and indicates the presence of ketone groups in many works (80, 82,83). The binding energy of 289 ± 0.2 eV refers to C4 and indicates the presence of carboxyl groups. Chtourou named this band C3b (80), but it could be named C4 referring to the classification of Dorris (81). It is however agreed that it indicates the carboxyls.

3.2.5 Inverse gas chromatography (IGC).

The surface properties of cellulose fibres could be altered by a variety of treatments, such as N_2O_4 oxidation. Of particular interest is the resulting change in acid and base constants K_A and K_B, since these are an indication of the change in surface adhesion and of the hydrophilic character of the cellulose. These constants can be determined by IGC. To prepare the columns, the oxidised fibres were first passed through a 40 mesh ball mill. Then, after becoming powder, 1.5 grams of samples were introduced under vacuum to facilitate packing into a 4 mm and 1.2 meters long copper tubing that have been previously washed with methanol and rinsed with acetone. Columns were conditioned for 24 hours at 80 °C under nitrogen flow.

3.2.5.1 Apparatus

A Hewlett Packard 5700A gas chromatograph equipped with a dual hydrogen flame ionisation detector (FID) was used to obtain the experimental data. A circulating water bath (Julabo, Model UC-5b) was used to maintain the temperature of the column to within ±0.5°C, as monitored with an Omega digital thermometer. To ensure flash vaporisation, the temperature at the injection ports of the chromatograph was around 300°C, which is 50°C above the highest boiling point of the alkane probes. Measurements were performed at temperatures ranging from 30 to 90 °C. Nitrogen was used as the carrier gas in the mobile phase with a flow rate about 30 l/min. The dead volume of the column was estimated by injecting methane in the column. The probes used to evaluate the dispersive component of the surface energy of the stationary phases were n-alkanes ranging from n-hexane to n-nonane in these experiments. A very small quantity of probe vapour was injected to ensure conditions near zero coverage to obey Henry's law. Injections were made from 1 μl Hamilton syringes was filled with vapour, emptied several times and the remaining probe injected into the column. Injections were repeated 3 times to determine whether the elution peaks were reproducible. The retention times measured at the peak maximum. For the determination of ΔH^{SP}, and subsequently K_A and K_B, measurements were performed at 30, 50, 70 and 90 °C. The

probes used in this work were purchased in a chromatographically pure state from Aldrich without any further purification.

Surfaces are characterised by a thermodynamic parameter called surface tension or surface energy (γ_s). For many years it was accepted that surface energy is the sum of a dispersive component (γ^D_s) due to London dispersive intermolecular interactions, and a non-dispersive polar component (γ^P_s) due to all other intermolecular interactions (89). These two components of surface energy were used to predict the work of adhesion between two phases (solid/solid or solid/liquid) based on wetting adsorption theory and the contact angle technique, which were widely used to study adhesion phenomena (131). However, the assumption that $\gamma_s = \gamma^D_s + \gamma^P_s$ was not sufficient to predict the adhesion and interactions. Furthermore, the contact angle measurement lacks rigor in case of surface roughness.

More recently, adsorptive interactions have been discussed in terms of acid-base properties (90). It appears that the specific interactions responsible for the γ^P_s term could be better described using the concept of acid/base or acceptor/donor interactions (71). Since the acidity and basicity of a surface can be well estimated by IGC, this technique can be used to obtain better estimates of the surface adhesion components. The surface properties of pigments and various types of cellulose materials have been studied with IGC (66, 69, 70, 72, 91, 92, 93, 94, 95, 96).

3.2.5.2   Interpretation of the results

The term "inverse" derives from the fact that IGC does not characterise the injected probe as in traditional gas chromatography, but characterises the stationary phase in the column. In this study, the stationary phase was oxidised or untreated fibres. Experiments yield the residence time in the column of known probes with defined neutral, acidic, basic or amphoteric characteristics (Table 3.3). The retention time (peak maximal value) (97) of the injected probes was used to calculate the net retention

volume (V_N) by the following equation:

$$V_N = K_S \, A = Q(t_r - t_m) \qquad \text{[eq.3.15]}$$

K_S surface partition coefficient of the given probes between the stationary and mobile phase

A   surface area of the stationary phase

Q   corrected flow rate of the carrier gas (N_2) at column temperature and at 760 mm Hg obtained by equation 3.16

t_r retention time of injected probes

t_m retention time measured for a practically non-adsorbing probe, such as methane.

$$Q = Q_0 J \frac{T_c}{T_a}\left(1 - \frac{P_w}{P_a}\right) \qquad \text{[eq.3.16]}$$

where, Q_0 is the measured flow rate (ml/min), T_c and T_a are the experimental (313, 323, 343 and 363 K) and ambient temperature (k), respectively. P_a and P_w are the atmospheric and saturated vapour pressure of water and J the James-Martin compression correction value determined as follows (98):

$$J = \frac{3}{2}\frac{1 - \left(\dfrac{P_1}{P_a}\right)^2}{1 - \left(\dfrac{P_1}{P_a}\right)^3} \qquad \text{[eq. 3.17]}$$

where P_1 is equal to P_a (760 mm Hg) plus the pressure drop in the column.

It is common to find that $-\Delta G^0_A$ or $RT\ln V_N$ is a linear function of the number of carbon atoms in the non-polar probes (n-alkanes). The free energy of adsorption corresponding to one methylene group, $-\Delta G^0_A$ (-CH_2-), was obtained by the injection of a homologous series of n-alkanes probes.

$$- \Delta G^0_A(-CH_2-) = RTLn \frac{V_N\left(C_{n+1}H_{2n+4}\right)}{V_N\left(C_nH_{2n+2}\right)} \qquad \text{[eq.3.18]}$$

The London dispersive component (γ^D_S) of the surface energy of the stationary phases is calculated by equation 3.19 proposed by Dorris and Gray (66).

$$\gamma^D_S = \frac{1}{4}\frac{\Delta G^0_A(-CH_2-)^2}{\gamma(-CH_2-)N^2a^2} \qquad [eq.3.19]$$

where, N is Avogadro's number, a is the surface area of a single methylene group, (66) $\gamma(CH_2) = 35.6 + 0.058(293-T)$, in mJ/m^2. $-\Delta G^0_A$ ($-CH_2-$) and γ^D_S for all untreated and oxidised fibres were calculated and reported in section 4 (Table 4.8).

Considering each sample weight (w), the specific net retention volumes (V^0_g) at $0^\circ C$ were calculated using equation 3.20.

$$V^0_g = \frac{273.15 V_N}{T_C w} \qquad [eq.3.20]$$

The thermodynamic characteristics of treated fibres could then be measured. These are the standard free energy (ΔG^0_A), the enthalpy (ΔH_A) and the standard entropy (ΔS^0_A) of adsorption (91).

$$-\Delta G^0_A = RTLnV^0_g + C = RTLn\left(K_s \cdot \frac{P_{s,g}}{\Pi_s}\right) \qquad [eq.3\,21]$$

$$-\Delta H_A = R\frac{d\left(LnV^0_g\right)}{d\left(\frac{1}{T}\right)} \qquad [eq.3.22]$$

$$-\Delta S^0_A = \frac{\Delta G^0_A - \Delta H_A}{T} \qquad [eq.3.23]$$

where, $P_{s,g}$ is the adsorptive vapour pressure in the gaseous standard state, equal to 101

kN/m^2 , and $\prod_S$ is the spreading pressure of the adsorbed film to a reference gas phase state. This is defined by the pressure $P_{s,g}$ of the solute, equal to 0.338 mN/m (99).

To calculate K_S, ΔG^0_A, and ΔS^0_A it is necessary to measure the specific surface area, (A). However, this is not needed to find the acid-base constants, K_A and K_B of the fibres, since the ΔH_A values are sufficient to measure them.

An investigation was carried out by Schreiber and Panzer (100) to compare different procedures for IGC data to measure. The results were obtained by applying three methods:

1- $RTLnV_N$ as a function of $a(\gamma^D_L)^{1/2}$, proposed by Schultz (71)

2- $RTLnV_N$ as a function of $Ln (P_0)$, proposed by St.Flour and Papirer (101)

3- $RTLnV_N$ as a function of T_b, proposed by Sawyer and Brookman (102)

The differences found between the γ^D_S values obtained from the three above methods are small.

The dependence of LnV^0_g as a function of $a(\gamma^D_L)^{1/2}$ is also linear, what was used by Papirer (104) and later by Chtourou and Riedl (72). We used this approach, that would be preferable as compared with those mentioned above, when the weight of treated fibres (w) is taken into consideration (eq.3.20). γ^D_L, is the dispersive component and a is the surface area of the alkanes and the polar probes used, which their values (Table 3.3) are found in the literature (100, 103). In order to determine the contribution of the surface interactions in the total surface free energy (ΔG^0_A), it is necessary to inject polar probes in the column, in addition to n-alkanes. Assuming that the alkanes exchange only dispersive interactions and that the dispersive and polar components of surface energy are additive, the alkanes line may be taken as a reference for the determination of the dispersive components for polar components. Thus, the difference of ordinate between the alkanes line and the polar probes gives, ΔG^{SP}_A, which corresponds to the specific interactions.

On the other hand, as for the evaluation of the same fibres, the environment does not change, ΔS^0_A can be neglected. Consequently, the variation of ΔG^0_A is related to the variation of ΔH_A. Thus oxidation evaluation was based on the changes of ΔH_A instead of ΔG^0_A. Similarly to the calculation of ΔG^{SP}_A, by plotting ΔH_A versus $a(\gamma^D_L)^{1/2}$, ΔH^{SP}_A is obtained for each probe as the distance between the observed ΔH_A and the straight line for the n-alkanes.

The specific interactions are all acid-base types as noted by Fowkes (60). Later, Martin and Schultz (71) characterised solid surfaces by acid K_A and base K_B constants, using Gutmann's acid-base concept, and proposed the following equation (previously 2.12):

$$-\Delta H^{SP}_A = K_A.DN + K_B.AN \qquad \text{[eq. 3.24]}$$

where $-\Delta H^{SP}_A$ is the specific enthalpy of adsorption and K_A and K_B correspond to the acid-base interaction constants, related to AN (acceptor number) and DN (donor number) of molecules. The above formula has also been mentioned (105) as follows:

$$-\Delta G^{SP}_A = C\,(DN) + C^*(AN) \qquad \text{[eq. 3.25]}$$

where C and C* like K_A and K_B are constants which determine the acidity and basicity strength of the solid. Equation 3.24 can be written as follows:

$$-\Delta H^{SP}_A\,/AN = DN/AN.K_A + K_B \qquad \text{[eq. 3.26]}$$

According to Gutmann's acid-base concept (106), a Lewis base is an electron pair donor (EPD) which is characterised by the donor number (DN). Similarly, a Lewis acid is an electron pair acceptor (EPA) characterised by the acceptor number (AN). On the other hand, the donor number DN is defined by Gutmann as the molar enthalpy of

the reaction between the base and a reference acceptor, antimony pentachloride (SbCl$_5$) in a dilute solution of 1,2-dichloroethane.

$$DN = -\Delta H_{SbCl5} - base \qquad \text{[eq. 3.27]}$$

The acceptor numbers AN of the solvent are defined as the relative ^{31}P NMR chemical shift, $\Delta\delta$, induced in triethylphosphine oxide (Et$_3$PO), when it is dissolved in an acceptor solvent (107). The AN values are arbitrarily scaled by assigning a value of 0 to the shift induced by hexane and a value of 100 to the shift induced when antimony pentachloride (SbCl$_5$) is in a dilute solution of 1,2-dichloroethane.

Obviously, DN and AN are expressed in different units. Recently, Riddle and Fowkes (103) showed that the ^{31}P NMR shift $\Delta\delta$ of Et$_3$PO dissolved in an acidic solvent is made up of a dispersion contribution, $\Delta\delta$, and a Lewis acid-base contribution, $\Delta\delta^{ab}$. Consequently, the AN values have to be corrected for the dispersion effect. In many cases the correction is quite substantial. They have also found that the acid-base contribution $\Delta\delta^{ab}$ is directly proportional to the enthalpies of acid-base interactions between Et$_3$PO and acid liquids. This results in new acceptor number, AN*, with the same units as DN.

$$AN^* = -\Delta H_{acid} - Et_3PO \qquad \text{[eq. 3.28]}$$

They (103) further linked AN* with the original AN numbers by equation 3.29.

$$AN^* = 0.288 \, (AN - AN^d) \qquad \text{[eq. 3.29]}$$

where AN^d is the dispersion contributions. It was also noted (103) that DN is free of the effect of dispersion force. The values used referred to The values proposed by Riddle and Fowkes for DN, AN, and AN* of the probes were used in this work (Table 3.3). The values for the acid-base constants, K_A and K_B of the oxidised fibres have been calculated by using these values in equation 3.26.

TABLE 3.3 Acid-Base Contributions to Acceptor Numbers of Solutes used in this work according to Riddle-Fowkes (72) and (103).

Liquid probes	a (Å)^2	γ^D_L (mJ/m^2)	DN (kcal/mol)	AN	AN^d	AN-AN^d	AN* (kcal/mol)	DN/AN*	Probes characteristics
Hexane(C6) (C$_6$H$_{14}$)	51.5	18.4	0	0	0	0	0	∞	Non-polar
Heptane(C7) C$_7$H$_{16}$)	57.0	20.3	0	0	0	0	0	∞	
Octane(C8) (C$_8$H$_{18}$)	62.8	21.3	0	0	0	0	0	∞	
Nonane(C9) (C$_9$H$_{20}$)	68.9	22.7	0	0	0	0	0	∞	
Nitromethane (CH$_3$NO$_2$)	37.8	26.2	2.7	20.5	5.7	14.8	4.3	0.63	Acidic
Dichloromethane (CH$_2$Cl$_2$)	31.5	27.6	0	20.4	6.9	13.5	3.9	0	
Tetrahydrofuran (T .H .F.)	45.0	26.5	20.0	8.0	6.1	1.9	0.5	40	Basic
Diethyl ether (D.E.E.)	47.0	16.9	19.2	3.9	-1.0	4.9	1.4	13.7	
Acetone (CH$_3$)$_2$O	42.5	23.6	17.0	12.5	3.8	8.7	2.5	6.8	Amphoteric
Ethyl acetate (CH$_3$-COO)C$_2$H$_5$	48.0	23.7	17.1	9.3	4.0	5.3	1.5	11.4	

d and *, see text for the definitions

3.3   Experimental designs for the evaluation of the oxidation parameters

The experimental design was carried out in three stages. First, a simple design of "one factor at the time" was used to evaluate the oxidation variables. The treatment variables were the flow rate of N_2O_4 gas, oxidation time, ambient temperature, and the pulp consistency. Once the desirable range was determined for each factor, a "half factorial" screening design was employed. This permitted the determination of which of the four factors have the greatest effects on the characteristics of the fibres.

Once the least important of the four factors was identified, the Composite Central Design (CCD) was applied to the three most important factors within a more limited range. This in turn was expected to eliminate the next least important factor. This left only two important factors, the gas flow-rate and the oxidation time. These were lumped to one combined factor, namely the ratio of N_2O_4 to fibre weight, expressed as a percentage. This factor was finally varied while keeping the ambient temperature and pulp consistency constant. The same set of conditions was used for softwood, bagasse and aspen fibres.

Mercer (15) had obtained maximum percentage (25.4 %) of carboxyl groups for regenerated cellulose for a 24-hour period of oxidation by N_2O_4. In this case, the degree of polymerisation was well below the critical value of 500. This means that the mechanical properties of the fibres deteriorated to the point where it was no longer possible to make a sheet of paper. Thus, in the first stage of the experiments (one factor at a time), the oxidation factors (gas flow-rate, oxidation time, temperature and consistency) were varied within ranges expected to maintain a DP above 540 (about 600 dm^3/kg). Table 3.4 shows all of the different combinations of the oxidation factors that were tried. For each experiment, carboxylic content, viscosity, tensile index, and the z directional strength of the sheet were determined.

TABLE 3.4   Preliminary experiments with the design of the one-factor-at a time

Run No.	Flow (A) (ml/min)	Time (B) (min)	Temp. (C) (^{0}C)	Cons. (D) (%)	NO$_2$/Fiber (%) [eq.3.1]
1	2.6	120	45	10	3.56
2	3.3	120	45	10	4.52
3	4.2	120	45	10	5.75
4	5.5	120	45	10	7.53
5	6.5	120	45	10	8.90
6	8.9	120	45	10	12.18
7	2.6	60	5	10	1.78
8	2.6	120	5	10	3.56
9	2.6	240	5	10	7.11
10	2.6	480	5	10	14.22
11	2.6	60	45	10	1.78
12	2.6	120	45	10	3.56
13	2.6	240	45	10	7.11
14	2.6	480	45	10	14.22
15	2.6	120	5	10	3.56
16	2.6	120	25	10	3.56
17	2.6	120	45	10	3.56
18	2.6	120	65	10	3.56
19	2.6	120	5	35	3.56
20	2.6	120	25	35	3.56
21	2.6	120	45	35	3.56
22	2.6	120	65	35	3.56
23	2.6	120	5	10	3.56
24	2.6	120	5	22.5	3.56
25	2.6	120	5	35	3.56
26	2,6	120	5	95	3,56

As a result of the first series of studies, it was found that the next series of experiments should be carried out at about 4 l/min gas flow-rate, one hour oxidation time, and at about 25°C. The target value for viscosity was over 600 dm³/kg,. The experiments were planned according to the screening type half-factorial design. The model, coded and standard values of the above design are shown in Table 3.5. The half-factorial design has a resolution of IV (109), which is convenient for the evaluation of the effect of main factors on the fibre characteristics. The statistical analysis of this design is reported in Table 4.1.

According to the results obtained by the half-factorial screening design, it was concluded that the high temperature (45 °C) was a negative factor for the viscosity and that it was less important than the three other factors relative to the formation of carboxyl groups. After finding the most effective factors for the formation of COOH that lead to a minimum decrease in the strength properties, a Composite Central Design (CCD) was used. This method also gives an optimum of surface response for each factor of the oxidation reaction.

TABLE 3.5 The model of the "Half Factorial Design" for the evaluation of four oxidation factors at two levels (2^{4-1}) with coded and treated values.

Run No.	Coded values				Treated values				Response		
	Flow (A) (ml/min)	Time (B) (min)	Temp. (C) (°C)	Cons. (D) (%)	Flow (A) (ml/min)	Time (B) (min)	Temp. (C) (°C)	Cons. (D) (%)	y_1	y_2	y_3
1	-1	-1	-1	-1	2.6	30	5	10			
2	-1	-1	+1	+1	2.6	30	45	35			
3	-1	+1	-1	+1	2.6	90	5	35			
4	-1	+1	+1	-1	2.6	90	45	10			
5	+1	-1	-1	+1	6.5	30	5	35			
6	+1	-1	+1	-1	6.5	30	45	10			
7	+1	+1	-1	-1	6.5	90	5	10			
8	+1	+1	+1	+1	6.5	90	45	35			

The CCD model with the coded and treated values is presented in Table 3.6.

TABLE 3.6   The model of CCD design for three oxidation factors at 5 levels with coded and treated values.

Run No.	Coded values			Treated values			Response	
	Flow (A) (ml/min)	Time (B) (min)	Cons. (C) (%)	Flow (A) (ml/min)	Time (B) (min)	Cons. (C) (%)	y_1	y_2
1	-1	-1	-1	2.6	30	10		
2	-1	-1	+1	2.6	30	35		
3	-1	+1	-1	2.6	60	10		
4	-1	+1	+1	2.6	60	35		
5	+1	-1	-1	5.5	30	10		
6	+1	-1	+1	5.5	30	35		
7	+1	+1	-1	5.5	60	10		
8	+1	+1	+1	5.5	60	35		
9	0	0	0	4.04	45	22.5		
10	0	0	0	4.04	45	22.5		
11	$+\alpha$	0	0	6.49	45	22.5		
12	$-\alpha$	0	0	1.61	45	22.5		
13	0	$+\alpha$	0	4.04	70.2	22.5		
14	0	$-\alpha$	0	4.04	19.8	22.5		
15	0	0	$+\alpha$	4.04	45	43.5		
16	0	0	$-\alpha$	4.04	45	1.48		

Total number of runs as shown in Figure 3.6 consists of 16. These are:

8 factorial points
2 central points and
6 axial points, where $\alpha=1.688$
Results are reported and discussed in the first part of chapter 4.
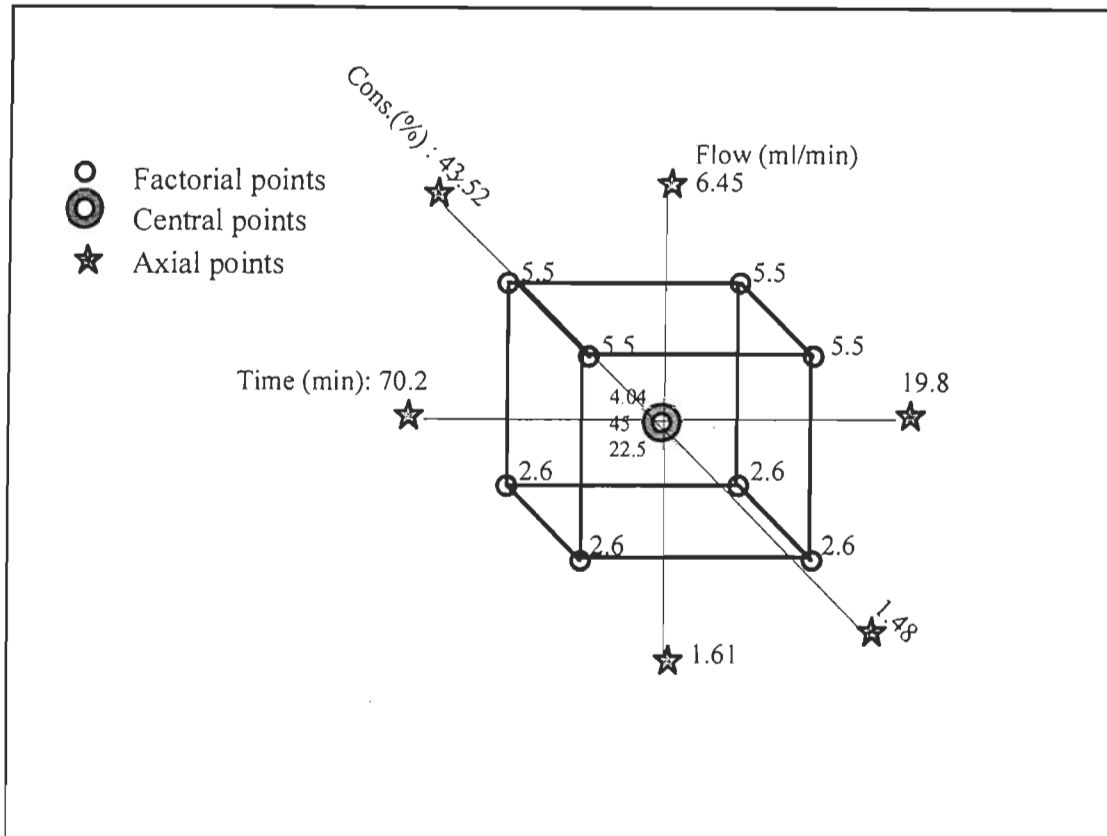
FIGURE. 3.6 A CCD model for the three-variable parameters of the N_2O_4 oxidation. These are gas flow-rate, oxidation time and pulp consistency, each one at five levels, 3^{4-1}.

To plot the Pareto charts for the half-factorial design and the three dimensional curves upon Surface Response Methodology for the Composit Central Design (CCD), we used the software of STATGRAPHIC PLUS. This allowed us to create different type of the experimental designs to analyse three or more factors in two and five levels (109).

A two-factor regression model proposed by Carrasco *et al* (110) was used to derive a mathematical relationship between the fibre characteristics after oxidation and the paper properties. The equations are reported in the sixth part of chapter 4.

CHAPTER IV

RESULTS AND DISCUSSION

The results and discussion of this research are presented in 6 major sections in this chapter.

Evaluation of the N_2O_4 oxidation parameters on softwood.

FTIR spectroscopy

ESCA analysis

IGC analysis

Comparison of the chemical and physical properties of the oxidised fibres

Mathematical evaluation of data

4.1 Evaluation of the oxidation parameters

The first part of the study involved the determination of optimal conditions of gas flow-rate, oxidation time, temperature of treatment and consistency of pulp for oxidation of the softwood bleached kraft fibres in terms of carboxyl content and viscosity. The optimisation study was performed in a three-step approach involving a one-factor-at-a-time design, followed by a half-factorial and then a composite central design (CCD). In all statistical analyses, a significance level of a= 0.05 was considered.

4.1.1 One factor at a time

The N_2O_4 oxidation was carried out according to the treatment conditions listed in Table 3.4. The effects of each parameter on the carboxyl group content, viscosity, tensile index and z strength of the handsheet are presented and discussed in the following subsections.

4.1.1.1   Gas flow-rate

Figure 4.1 shows that an increase in flow-rate produced a corresponding increase in carboxyl content. However, beyond 4.5 ml/min, the gas absorption reduced, resulting in a decrease in the formation of COOH groups. It can be observed that viscosity and tensile index dropped after a small increase in the flow-rate. It should be pointed out that the reduction in the viscosity and the tensile index usually change in the same direction and are linearly related over a certain range. The z strength, which essentially represents fibre to fibre bonding, followed the same trends as the tensile index of the fibres. Nevertheless, it direction is not always similar with tensile index.
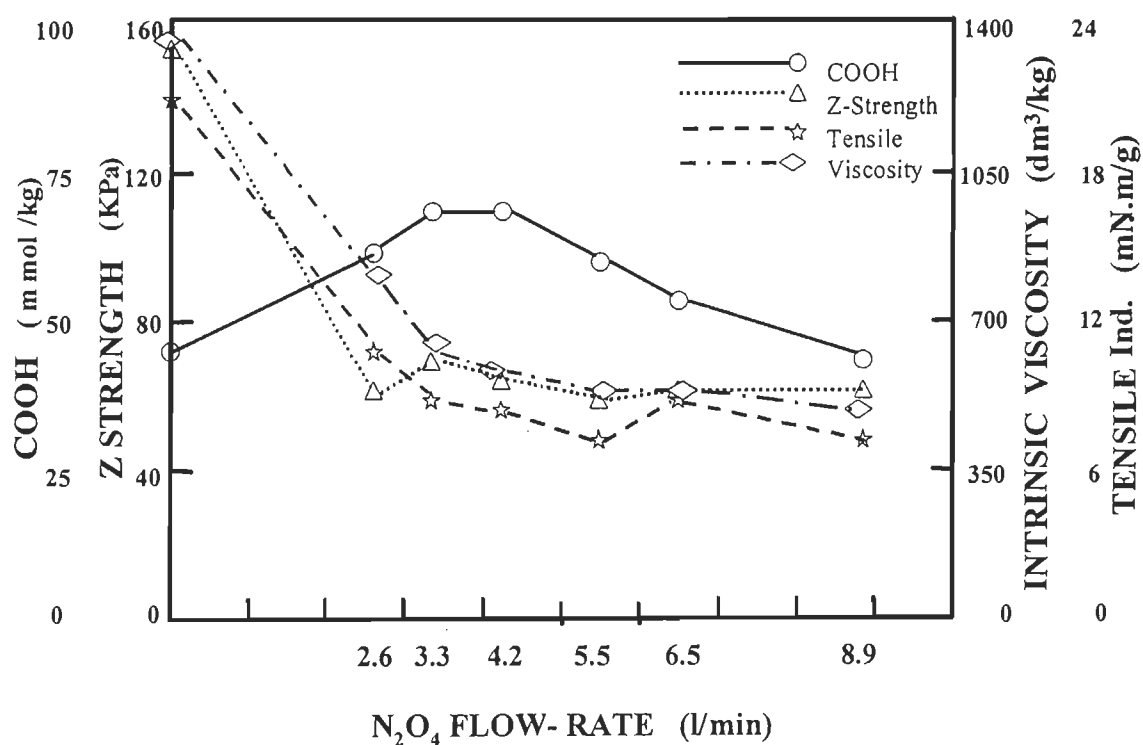
FIGURE 4.1   **Fibre characteristics as a function of the gas flow-rate during oxidation by the N_2O_4 (oxidation time 120 min. temperature 45°C, consistency 10%).**

4.1.1.2   Oxidation time

The fibre oxidation was done for different periods of time. These periods varied from 60 to 480 minutes for temperatures of 5 °C and 45°C (Fig. 4.2 & 4.3). Here, it can
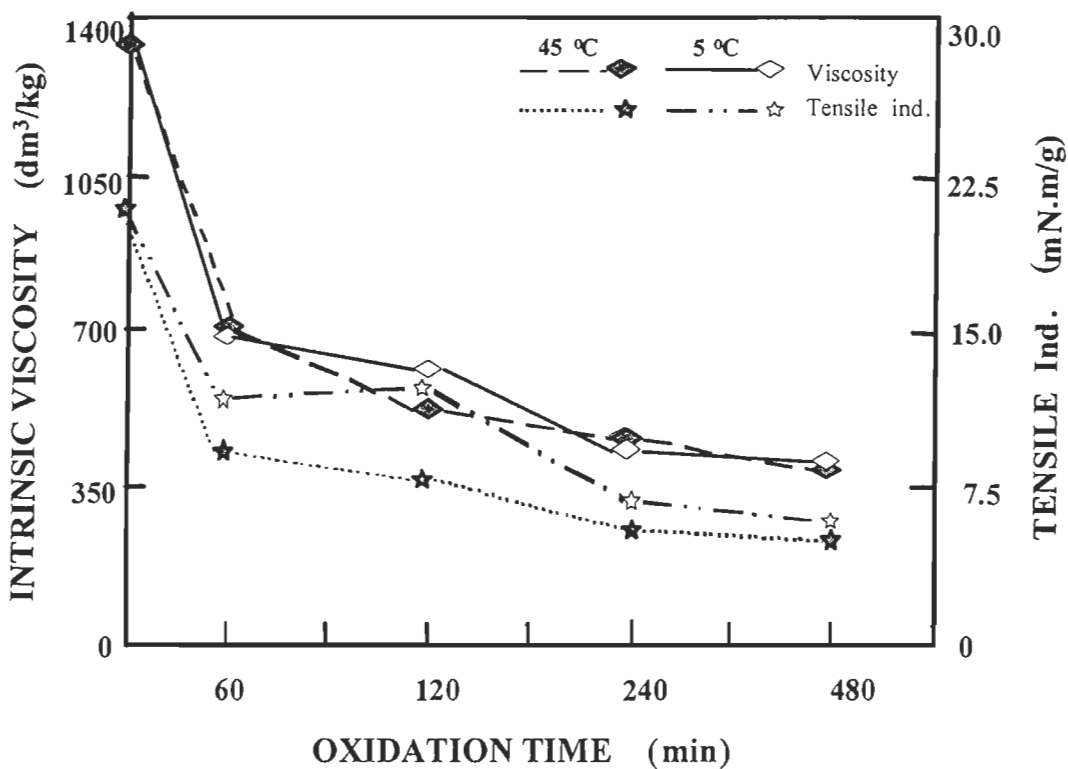
FIGURE 4.2 Intrinsic viscosity and tensile index as a function of the time of oxidation by N_2O_4 at 5°C and 45 °C (10% pulp consistency).
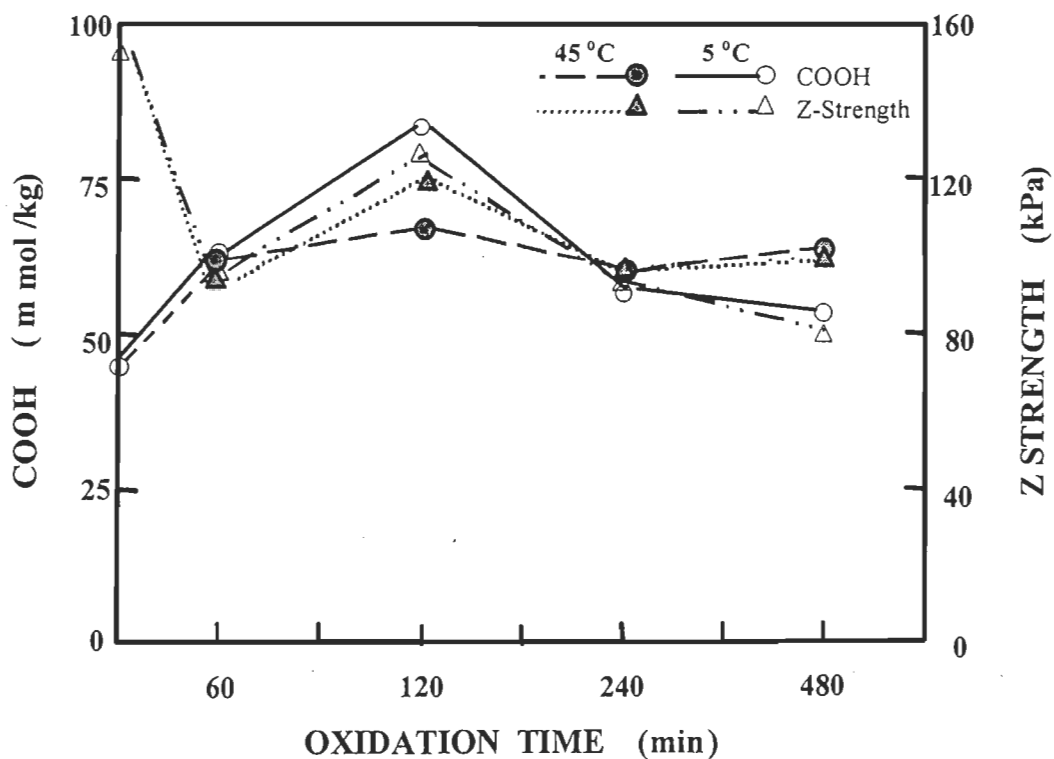
FIGURE 4.3 COOH and z strength as a function of the time of oxidation by N_2O_4 at 5 °C and 45°C (10% pulp consistency)..

be observed that after about 60 min., the oxidation causes a drastic reduction in viscosity and tensile index as compared to the initial untreated pulp (zero oxidation time). This reduction is much greater at 45°C than at 5°C. Slightly improvement in z strength was observed about 120 minutes of oxidation which can be interpreted as higher bond strength due to the formation of COOH.

4.1.1.3 Consistency of pulp

Fig. 4.4 shows that, the fibre properties and paper strength decrease with an increase in consistency. This is likely due to more direct contact of the N_2O_4 gas with the fibres in high consistency of the pulp. When the consistency is low (10%), the nitrous acid HNO_2 concentration due to reaction of N_2O_4 gas with water will be lower due to the greater dilution factor.
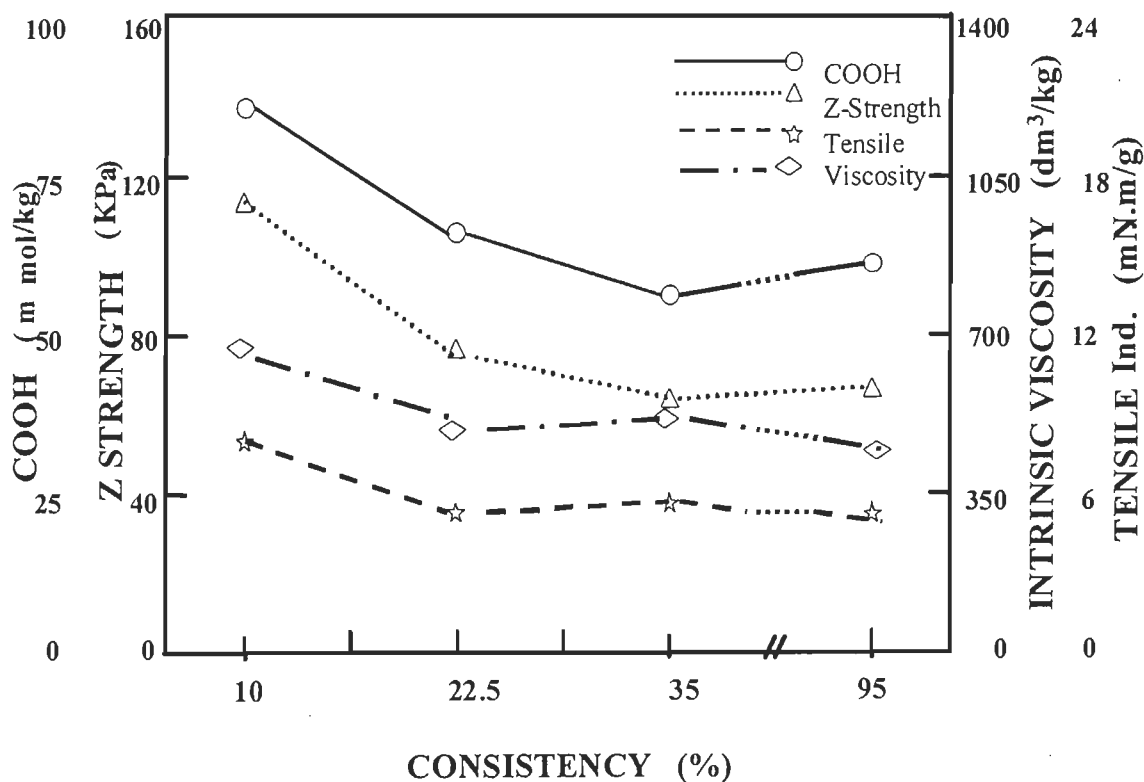
FIGURE 4.4 Fibre characteristics as a function of the pulp consistency during oxidation by N_2O_4 (2.6 ml/min, 120 min, 5°C).

That might be the reason for lower degradation at 10% consistency compared to that at 35% consistency. A very high consistency (95%) also results in low viscosity and tensile index, but relatively higher COOH and z strength compared to those at 35% consistency.

4.1.1.4 Ambient Temperature

In other experiments, the oxidation was carried out at 5, 25, 45 and 65 °C and two pulp consistencies 10 and 35%. In these trials, the flow-rate and oxidation time were kept constant. Figs. 4.5 & 4.6 show that, as the temperature increases, all of the four characteristics decrease. In general the 10% samples give higher COOH, viscosity and tensile index, but z strength is lower at this consistency.

It is clear that the temperature is a factor that increases the rate of the chemical reaction. It affects the reaction in two ways: degradation and oxidation of the cellulosic fibres. Degradation is due to the hydrolysis effect (45) that leads to the breakage the glucosidic bond of C1-C4. This in turn causes a reduction in viscosity (degree of polymerisation). Oxidation, in turn, forms carboxyl groups at C-6 and ketone group at C-2 and/or C-3. As the temperature increases, the degradation rate accelerates and dominate the effect of the oxidation. Consequently the formation of COOH groups reduces too When the temperature approaches 70, 90 and 100 °C, formic acid, carbon dioxide (CO_2) and hydrogen (H_2) gases are produced (45). The reaction mechanism, the speed and the activation energy are beyond the scope of this research.

4.1.1.5 Discussion

According to the above experiments it can be concluded that:

a)   An increase in the gas flow-rate produces more COOH up to a flow-rate of 4-6-l/min. At higher rates, the formation of COOH no longer increases since the fibres are likely to be saturated. Viscosity is reduced by an increase in flow-rate, perhaps due to more rapid nitrous acid formation which would lead to greater
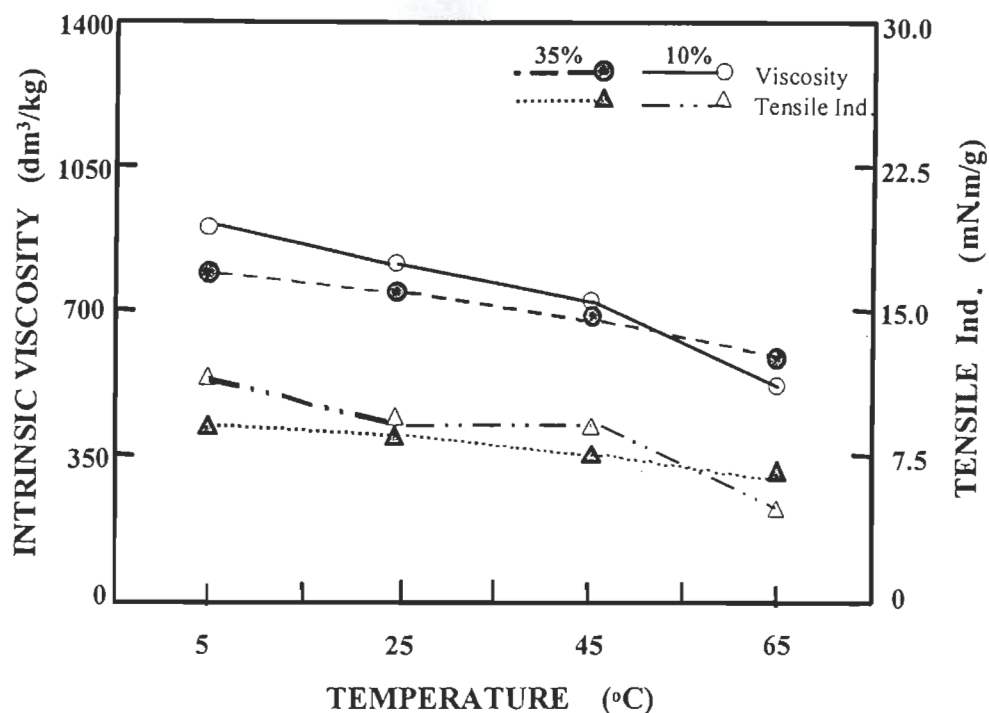
FIGURE 4.5 Intrinsic viscosity and tensile index as a function of ambient temperature during oxidation by N_2O_4 at 10% and 35 % pulp consistency (2.6 ml/min, 120 min).
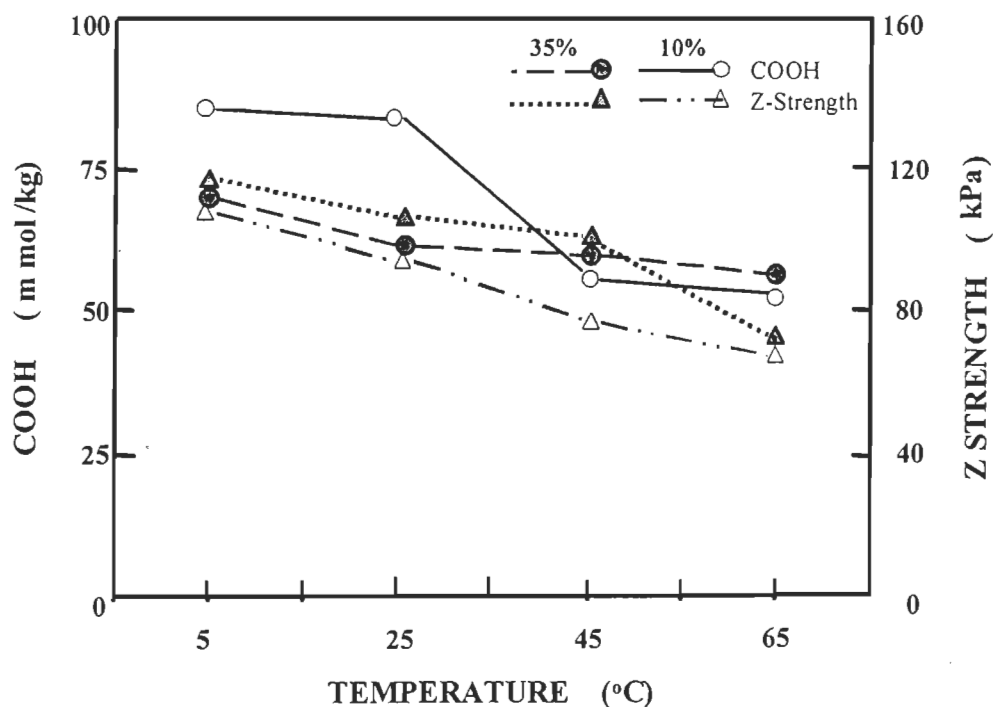
FIGURE 4.6 COOH and z strength as a function of ambient temperature during oxidation by N_2O_4 at 10% and 35% pulp consistency (2.6 ml/min, 120 min).

chain scission.

b) An increase in the oxidation time up to 2 hours produces higher COOH. At longer oxidation times, COOH levels off. However, the viscosity continues to decrease. The difference in tensile index at 5°C and 45°C is not greater than the standard deviations (±2.1), thus it may be considered that the difference is not significant.

c) An increase in temperature produces decreases in COOH formation and in viscosity and tensile index. The rate of decrease at 10% consistency is nearly the same as at 35% consistency

d) An increase in the consistency also produces a decrease in COOH formation. The Viscosity and the tensile index drop as pulp consistency increases, up to a point. At higher consistencies, these properties stabilize.

By the preliminary experiments, the approximate range for the gas flow and oxidation time was determined. The negative effect of the high temperature for viscosity and tensile strength was noticed, but the effect of pulp consistency at different temperatures was not clear. Specially for the z strength, that the contradiction results were obtained. We faced with the relatively higher z strength for 35% consistency as compared to 10% consistency. This did not support the former experiments of comparing 4 different consistencies of 10, 25, 35 and 95% at 5°C temperature, where the z strength for 35% consistency was lower than that for 10% consistency. Even though all the samples were dried after the treatment in the room temperature and kept in the plastic bags, but as all the experiments of one series did not do at the same day, the variations in the air humidity during the treatment and during the period waiting for the physical and mechanical tests, may interfered the reaction rate, its mechanism and produced some unexpected variations in the results. Specially the variations in the COOH content and z strength, the factors being more sensible to the humidity. There were also some interactions between two factors of temperature and consistency that could not be verified by the one factor at a time design. In order to verify the results of the first design regarding the effect of the consistency and study the interactions, the half-factorial and CCD designs were then implemented, the results being presented bellow.

4.1.2   Half factorial design

The half-factorial experiment of plan was designed taking into account the conditions under which intrinsic viscosity could be maintained above to 600 dm^3/kg (DP environ 540). Here, the gas flow rates were 2.6 and 6.5 l/min, the oxidation time were 30 and 90 min., the temperatures were 5 and 45 °C and the pulp consistencies were 10 and 35%. Each combination of these four factors was replicated three times. The coded and actual levels of the factors were given in Table 3.5(p.61). The results are reported using Pareto charts as follows.

4.1.2.1   Carboxyl content (COOH)

Based on the Pareto diagram (Fig. 4.7) it can be concluded that the factors A (gas flow-rate), B (oxidation time) and D (pulp consistency) have significant positive effects on the carboxyl content (Table 4.1). This means that increases in gas flow-rate, oxidation time and pulp consistency result in corresponding increases in carboxyl content. In contrast, factor C (temperature) does not have a significant effect on COOH. Certain combinations of the interactions of gas flow (A), oxidation times (B) with temperature and pulp consistency, such as AB+CD, AC+BD and AD+BC are also significant, and should be analysed. Other experiments are needed to clarify the effect of the above interactions on the characteristics of the fibres. The effect of temperature (C) is not significant to COOH formation, but it has negatively significant effect on the viscosity and z strength. So, it was decided to study the interactions of the other three factors, at the low temperature (5°C). This was done using the CCD design.

4.1.2.2   Viscosity

The Pareto diagram of viscosity (Fig. 4.8) shows that increases in the oxidation time (B), gas flow-rate (A), and temperature (C), produce significant decreases in the viscosity. However, consistency (D) does not have a significant effect on viscosity.

TABLE 4.1 **Analysis of variance (ANOVA) of four oxidation factors according to the half-factorial design at two levels, 2^{4-1} ($\alpha=0.05$).**

Dependent Responses	Principal effects	Parameter coefficient	F ratio	P>F	Significant	R^2 (%)
COOH	constant	61.449	-	-	-	
	A	4.86	122.69	0.000	Sig.	
	B	5.12	135.89	0.000	Sig.	94.56
	C	-0.039	0.01	0.930	N.Sig.	
	D	1.57	12.82	0.003	Sig.	
Viscosity	constant	686.62	-	-	-	
	A	-130.0	235.62	0.000	Sig.	
	B	-275.5	237.25	0.000	Sig.	96.33
	C	-54.33	34.74	0.000	Sig.	
	D	-10.17	2.07	0.170	N.Sig.	
Tensile index	constant	12.545	-	-	-	
	A	-2.86	102.84	0.000	Sig.	
	B	-3,11	100,80	0.000	Sig.	91.73
	C	-1,20	20,02	0.001	Sig.	
	D	0,13	0,75	0.410	N.Sig.	
Z Strength	constant	91.359	-	-	-	
	A	21.86	71.69	0.000	Sig.	
	B	28.02	610.87	0.000	Sig.	98.52
	C	-11.77	107.81	0.000	Sig.	
	D	-7.51	43.93	0.000	Sig.	

4.1.2.3 Tensile strength

The Pareto diagram of tensile index (Fig. 4.9) shows that increases in factors B, A and C, decrease the tensile index as was the case for viscosity. Again, factor D (consistency) does not have any significant effect on the tensile index, as was the case for viscosity.

4.1.2.4 Z strength

Increasing the time of oxidation (B), flow-rate (A) have a significant positive effect on z strength (Fig 4.10), but the temperature (C) and consistency (D) have a negative effect on z strength.

Standardized Pareto Chart for COOH
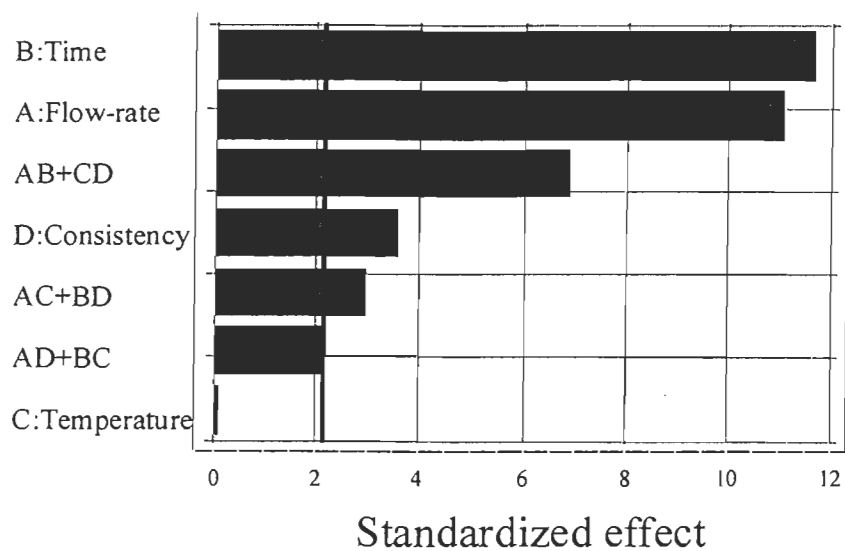
FIGURE 4.7   **Standardised Pareto chart for the carboxyl content of oxidised fibres of bleached kraft softwood.**

Standardized Pareto Chart for Viscosity
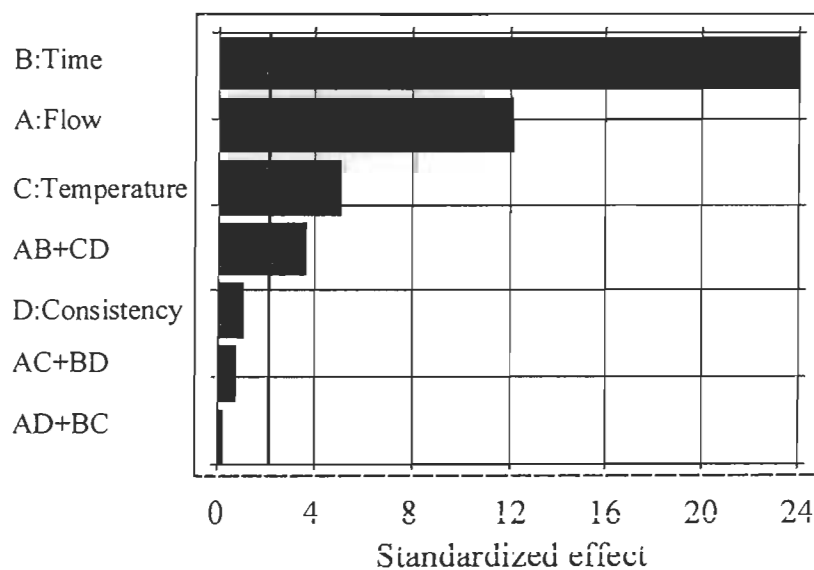
FIGURE 4.8   **Standardised Pareto chart for the viscosiy of oxidised fibres of bleached kraft softwood.**

Standardized Pareto Chart for Tensile Index

Standardized effect
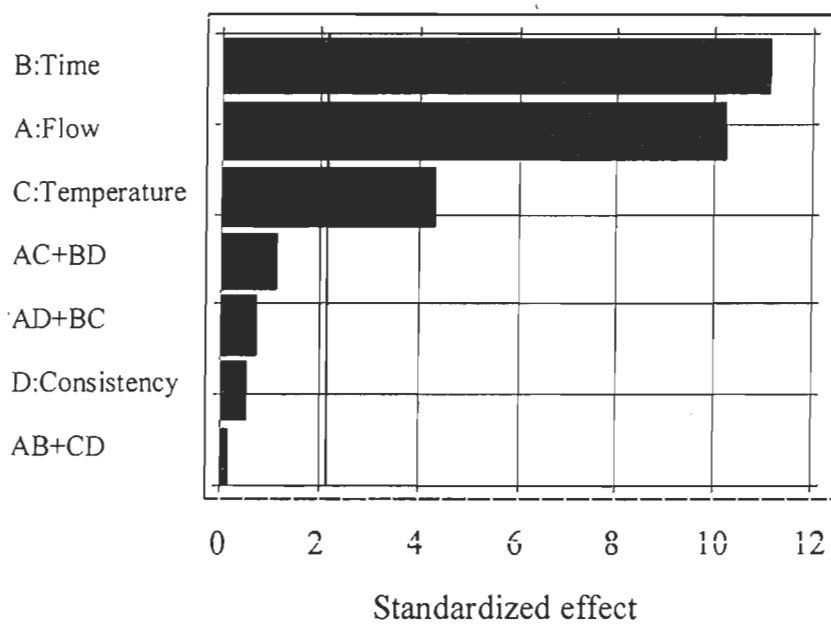
FIGURE 4.9 **Standardised Pareto chart for the tensile index of oxidised fibres of bleached kraft softwood.**

Standardized Pareto Chart for Z Strength

Standardized effect
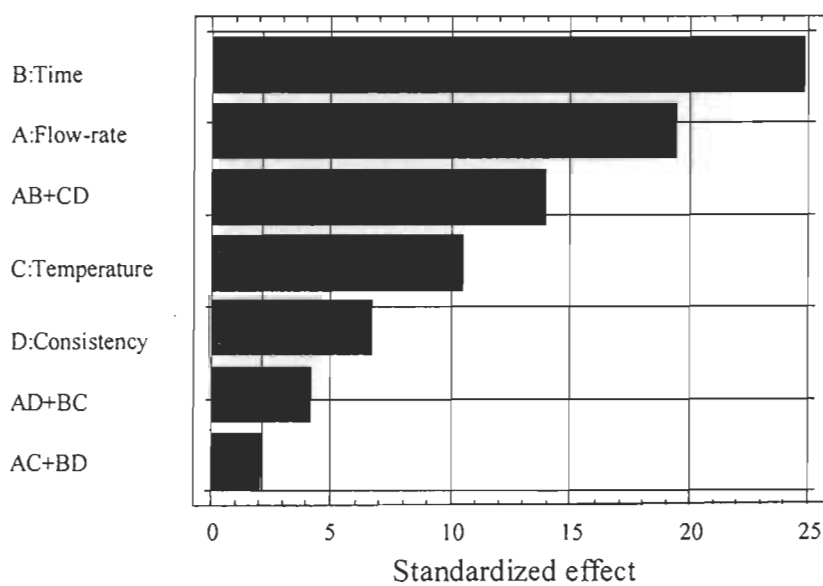
FIGURE 4.10 **Standardised Pareto chart for the z strength of oxidised fibres of bleached kraft softwood.**

4.1.2.5   Discussion

The half-factorial design (Table 4.1) shows that the two factors, A and B have significant effects on all of the fibre characteristics. However, the effect of temperature (C) on the formation of COOH was not found to be significant. In addition, the effect of temperature on viscosity, the critical character of the oxidised fibres, is negatively significant with R^2 over 96%. Thus, this factor should be kept at the minimum level (5 $^\circ$C) for further investigations in order to have lower reductions in the viscosity It was also observed that the reductions in the viscosity and in the tensile index were usually similar, as the gas flow or the oxidation time was increased.

The effect of consistency (D) on viscosity was found to be not significant. Furthermore the effect of consistency on the formation of COOH and z strength, were different. At pulp consistency of 35% higher amounts of COOH produced, but lower values of z strength representing the fibre to fibre bonding (Table 4.1). Thus, it is not yet possible to judge at which percentage of consistency one may obtain both lower viscosity decrease and higher formation of COOH. It is necessary to study the effect of consistency on the above fibre properties using a design with more precision and involving more levels of the relevant factors (five levels instead of two levels). Data are annexed (Table A.5).

4.1.3   Composite central design (CCD)

In this experiment, the effects of the gas flow-rate, oxidation time and pulp consistency on fibre properties was studied in more detail. Five levels of each of these factors were used as given in Table 3.6. The results of ANOVA for these experiments are presented in Table 4.2. The Pareto charts and the graphs concerning the response surfaces of these factors are shown in the Figures 4.11 to 4. 23. Data are annexed (Table A.6).

4.1.3.1   Carboxyl content

The Pareto chart of COOH (Fig. 4.11) shows that the only significant variable

was the AB interaction (i.e. Flow-rate and oxidation time), that indicates that the response surface should be curvilinear as shown in (Fig. 4.12). This combined factor can be interpreted to represent the total amount of gas flowing through the fibres in a given time. Fig.4.12 shows that high carboxyl content is obtained at a gas flow about 4 to 5 l/min and 60 minutes oxidation time. Thus a high gas flow-rate will not guarantee high gas absorption nor a high COOH formation on the cellulose fibres. In fact, there is a limit for the gas flow, and above this limit the fibres will no longer absorb of the added. gas. This has also been observed during the oxidation experiments. When the gas flow increased to 5 l/min or more, there was an accumulation of the N_2O_4 gas in the flask. Then the gas pushed back the water to the Erlene and the water line through the tube also moved back (Fig. 3.1). By the way, the low consistency of 10 % could lead to a greater COOH formation.

4.1.3.2 Viscosity

The Pareto diagram of viscosity (Fig. 4.13) and Table 4.2 show that all three factors of the oxidation, A, B and C have a significant negative effect on the viscosity with an $R^2 = 0.94$. Thus the increase in oxidation time (B), gas flow-rate (A) and in consistency (C) produces increasingly more reductions in the viscosity of the fibres (Figs. 4.14, 4.15 and 4.16). It means that the N_2O_4 oxidation leads to a somewhat lower viscosity. In other words, the low flow-rate of 2.6 l/min and the 30-45 minutes oxidation time can maintain the viscosity at higher level. The formation of COOH is at a very low level in this case. On the other hand, Fig. 4.16 shows that a 10% consistency is the optimal value to maintain the higher viscosity.

4.1.3.3 Tensile Index

The flow-rate was found to have the most significant effect on the tensile strength (Fig. 4.17). Thus, the tensile strength drops more when gas flow-rate increases. The other factors of oxidation did not have a significant effect on tensile index. However they have a negative effect on the tensile index (Table 4.2). As far as oxidation time is concerned, the maximum reduction in the tensile index occurred at about 40 to 50.

Standardized Pareto Chart for COOH
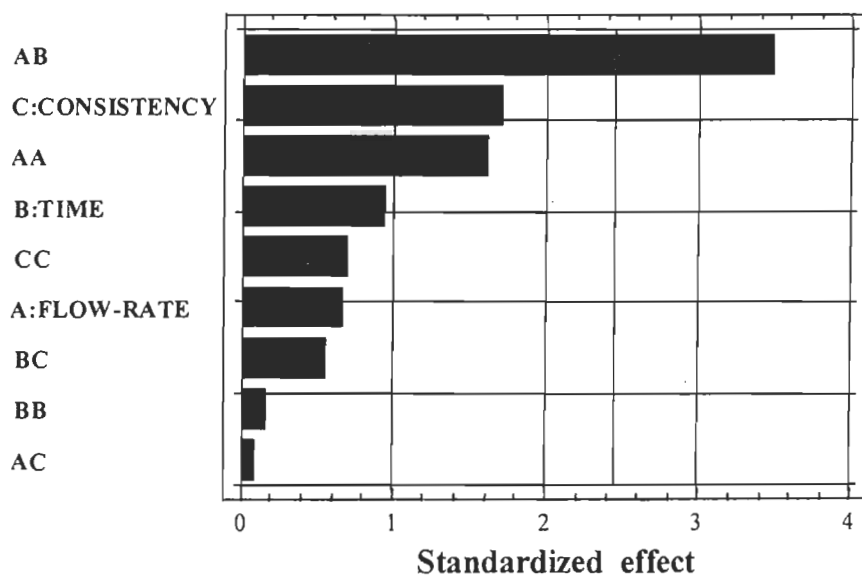
FIGURE 4.11   Standardised Pareto chart of carboxyl content for the
oxidation factors.
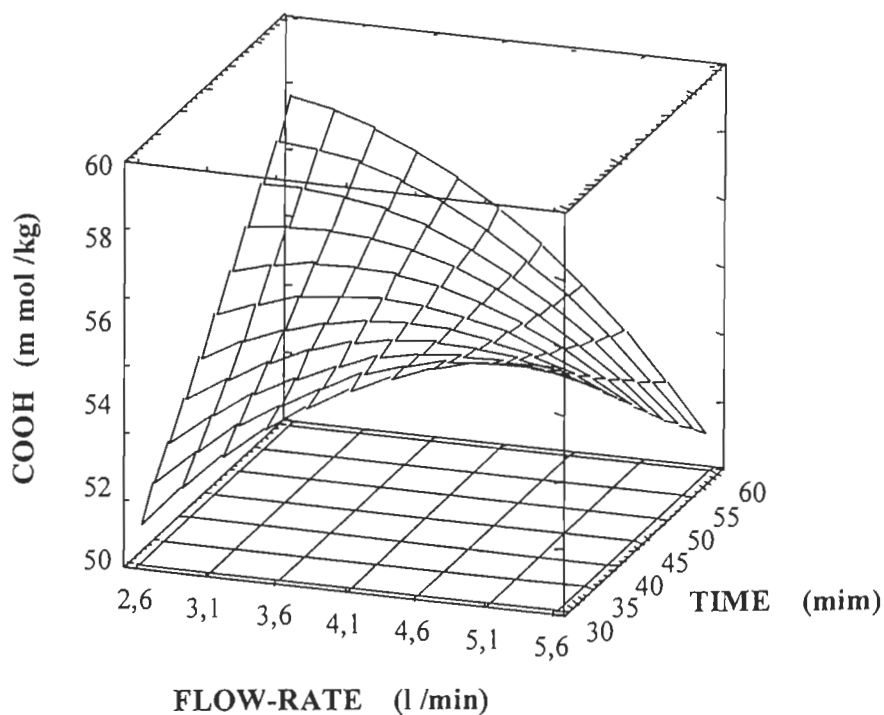
FIGURE 4.12   The estimated surface response of carboxyl content as a function of
gas flow-rate and the oxidation time.

TABLE 4.2 Analyse of variance (ANOVA) for the three oxidation factors upon CCD design at five levels.

Dependent Responses	Principal effects	Parameter Coefficient	F ratio	P value	Significant	R^2 (%)
COOH	Constant	55.279	-	-	-	78.56
	A	0.871	0.45	0.540	N.Sig.	
	B	1.021	0.88	0.400	N.Sig.	
	C	-2.219	2.94	0.140	N.Sig.	
	A.B	-5.9	12.19	0.013	Sig.	
Viscosity	Constant	662.499	-	-	-	94.10
	A	-247.51	53.91	0.000	Sig.	
	B	-145.01	15.50	0.005	Sig.	
	C	-91.19	7.32	0.035	Sig.	
	A.B	151.25	11.79	0.014	Sig.	
Tensile Ind.	Constant	11.629	-	-	-	74.75
	A	-2.71	7.09	0.037	Sig.	
	B	-0.56	0.30	0.610	N.Sig.	
	C	-1.94	3.62	0.110	N.Sig.	
Opacity	Constant	77.75	-	-	-	90.09
	A	1.41	10.33	0.020	Sig.	
	B	1.92	19.15	0.005	Sig.	
	C	0.23	0.28	0.620	N.Sig.	
	A.A	-2.17	16.67	0.006	Sig.	
	A.B	1.24	4.69	0.070	Sig.	
	C.C	-0.75	10.79	0.020	Sig.	
L. Scattering Coefficient.	Constant	38.75	-	-	-	70.59
	A	4.23	7.34	0.035	Sig.	
	B	1.51	0.94	0.379	N.Sig.	
	C	1.54	0.97	0.373	N.Sig.	

Standardized Pareto Chart for Viscosity
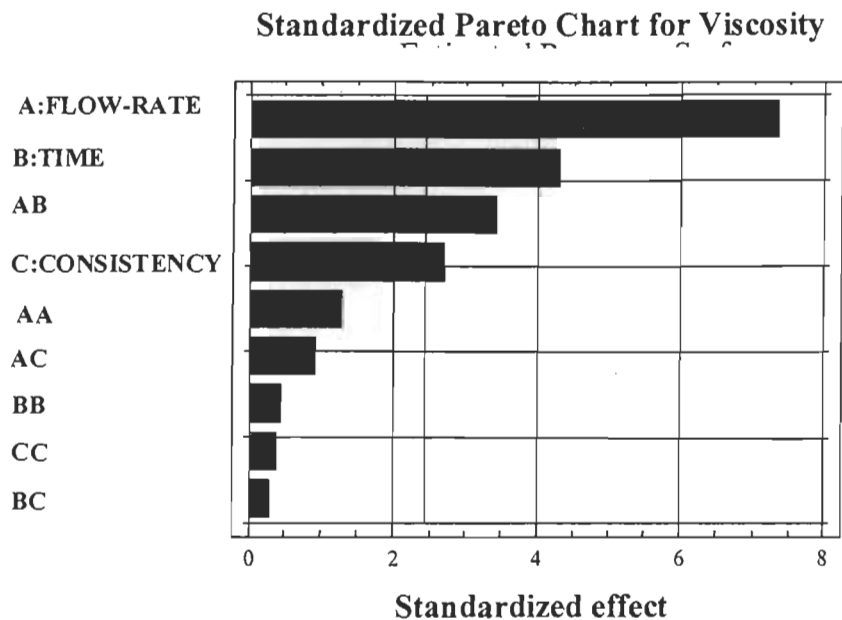
FIGURE 4.13   The standardised Pareto chart of viscosity for the oxidation
factors.
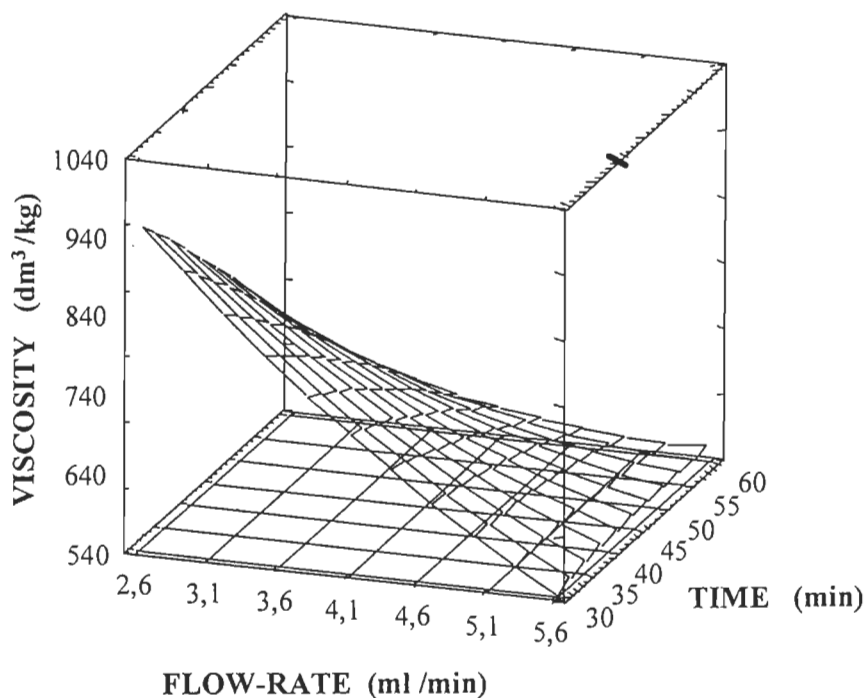
FIGURE 4.14   The estimated surface response of viscosity as a function of gas
flow-rate and oxidation time.
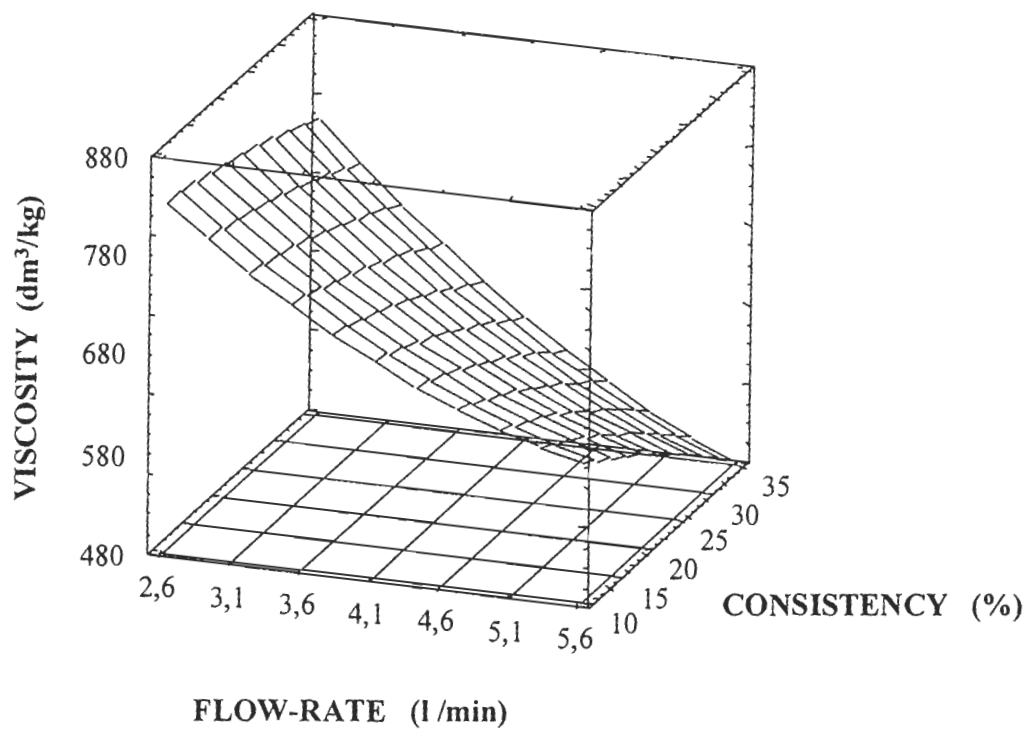
FIGURE 4.15 The estimated surface response of viscosity as a function of gas flow-rate and pulp consistency.
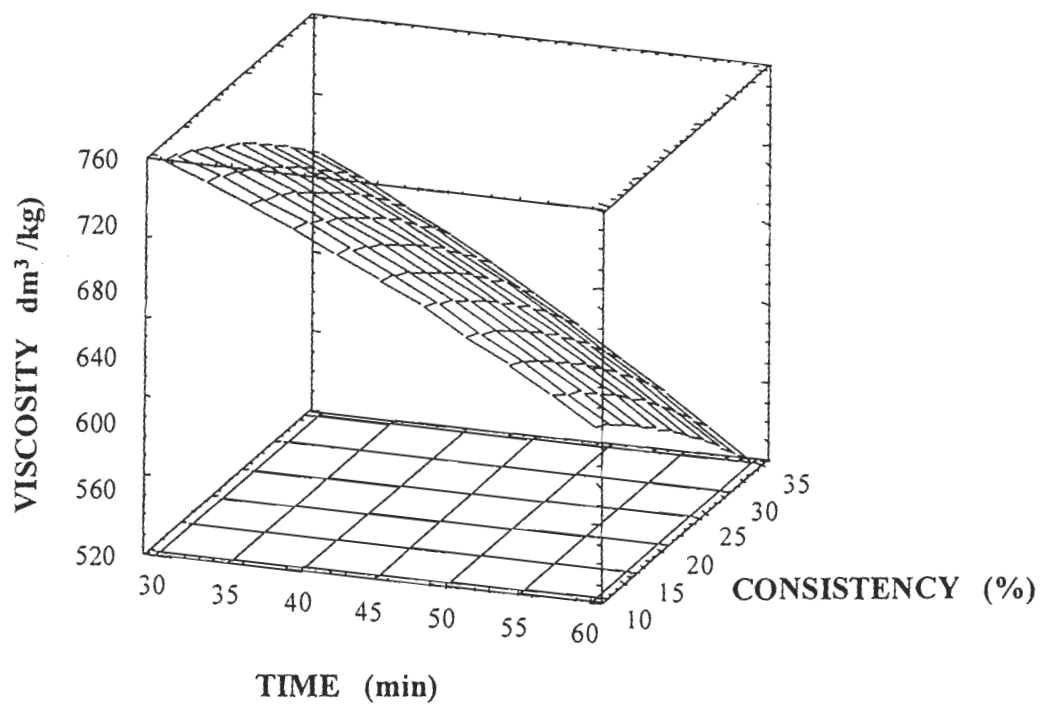
FIGURE 4.16 The estimated surface response of viscosity as a function of pulp consistency and oxidation time.

minutes oxidation time. (Fig. 4.18). It is important to note that the tensile index increases at longer oxidation times. This will be clarified later.

4.1.3.4   Brightness

The N_2O_4 oxidation of the cellulosic fibres also has a notable effect on the optical properties of the paper sheet, especially for the fibres containing some residual lignin. It has already been proven that the NO_2 pre-treatment for oxygen bleaching itself alters the optical properties (18, 19). Figure 4.19 shows that the oxidation parameters have no significant effect on brightness since the fibres used have already been bleached to maximum brightness (85% ISO) and a minimum lignin content (0.18%).

4.1.3.5   Opacity

The Pareto diagram for opacity (Fig. 4.20) shows that the significant factors are the flow-rate and oxidation time, the square of flow-rate and the square of consistency. The response surfaces (Figs. 4.21 and 4.22) are sharply curved in consequence. Since the linear effect of consistency was not significant (Fig. 4.20), the corresponding response surface showed that the opacity was the same at 10% and 35%, with a maximum at the

Standardized Pareto Chart for Tensile Index
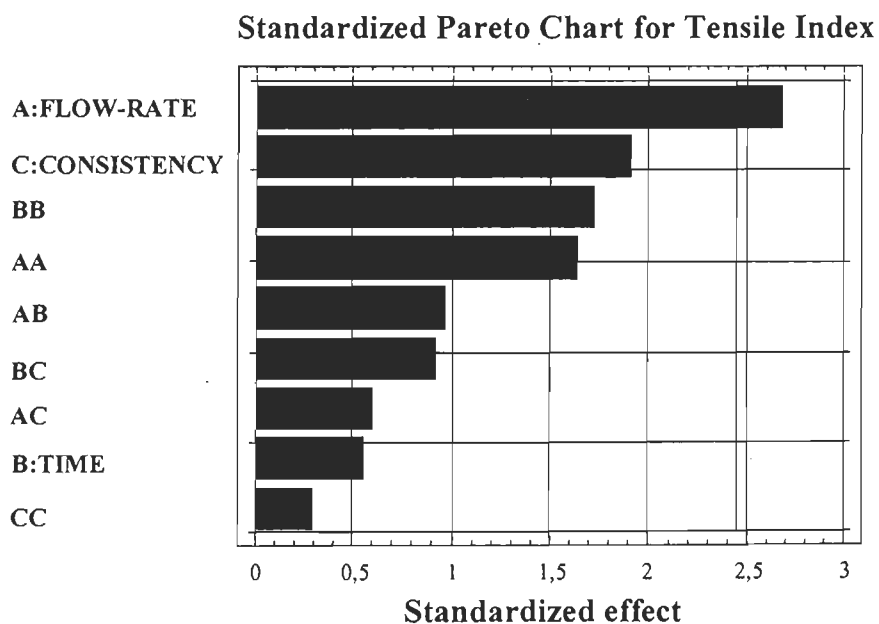
FIGURE 4.17   The standardised Pareto chart of tensile index for the oxidation factors.
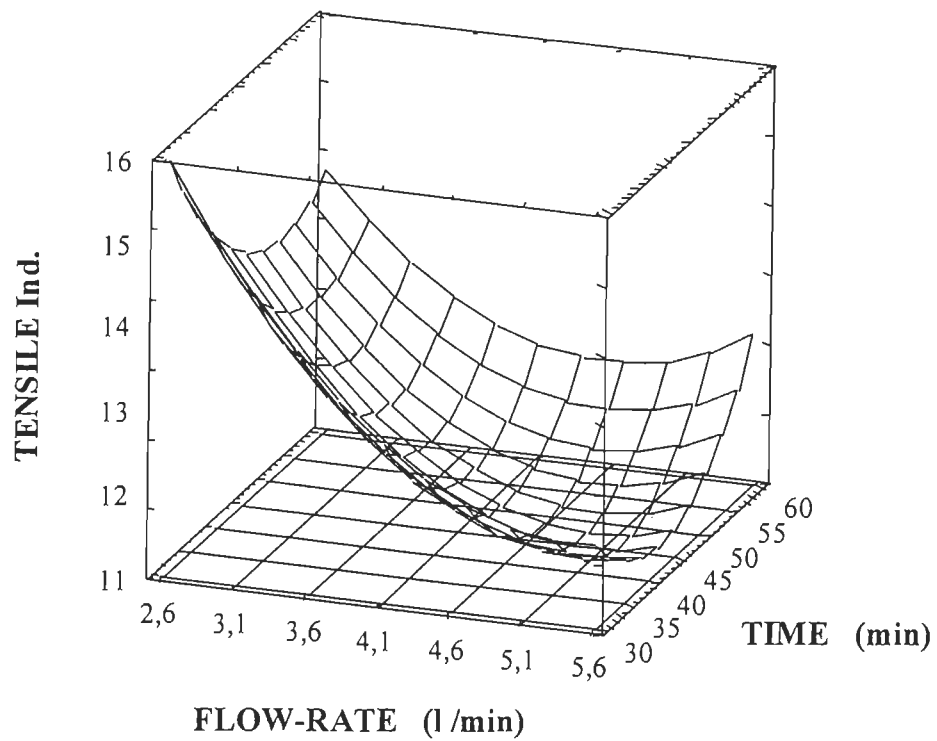
FIGURE 4.18 The estimated surface response of tensile index as a function of gas flow-rate and oxidation time.

Standardized Pareto Chart for Brightness
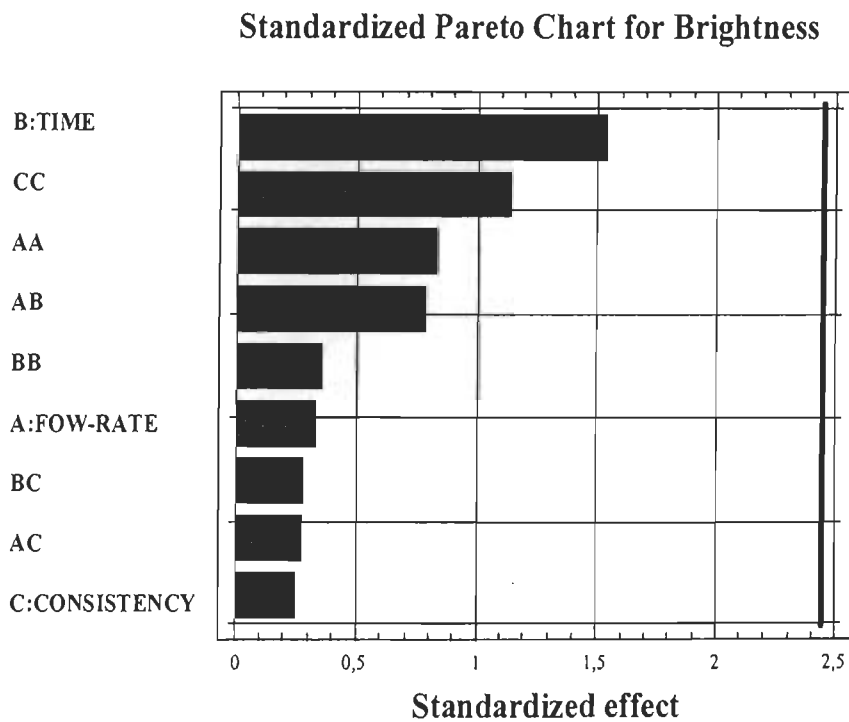
FIGURE 4.19 The standardised Pareto chart of brightness for the oxidation factors.

Standardized Pareto Chart for Opacity
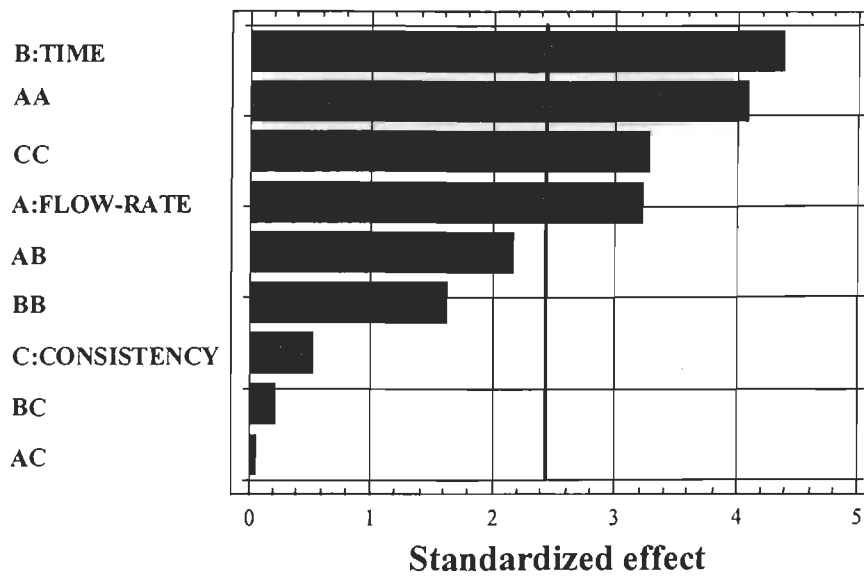
FIGURE 4.20   The standardised Pareto chart of opacity for the oxidation factors.
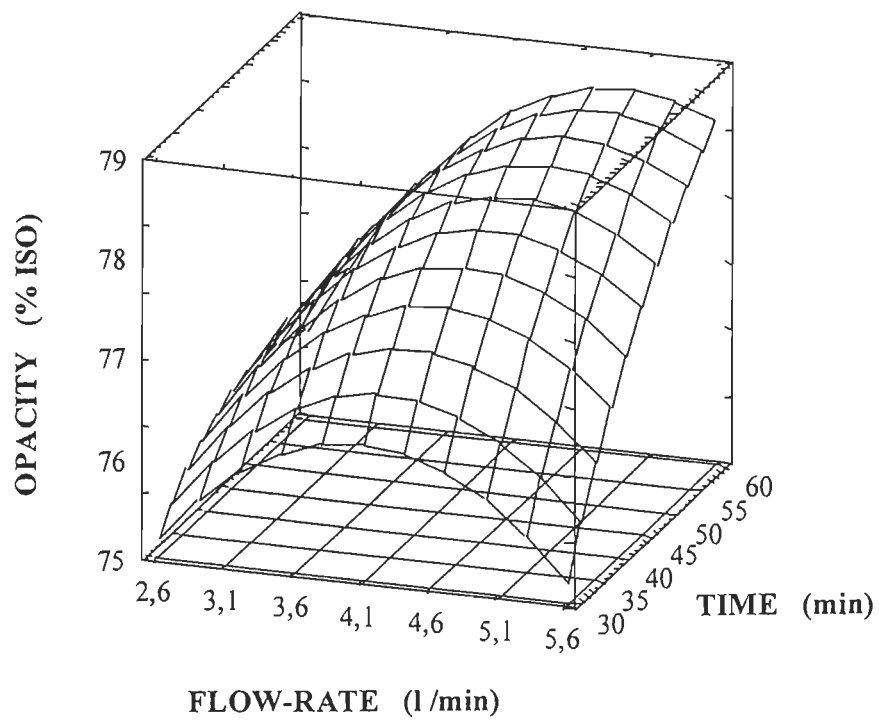
FIGURE 4.21 The estimated surface response of opacity as a function of gas
flow-rate and oxidation time.
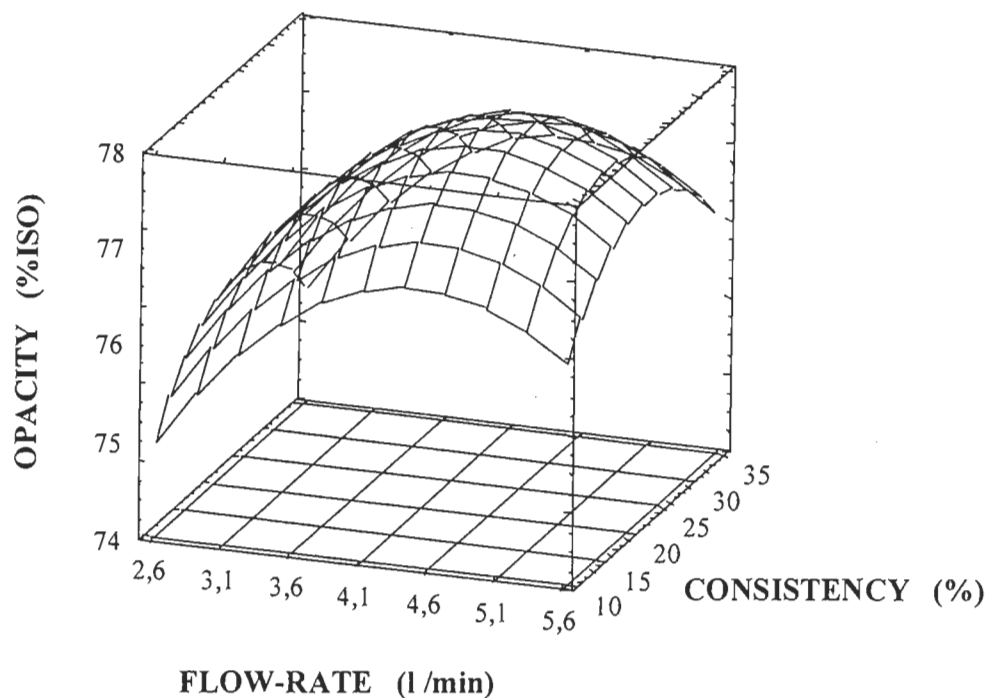
Figure 4.22   The estimated surface response of opacity as a function of gas
flow-rate and pulp consistency.

\

Standardized Pareto Chart for Light Scattering Coefficient
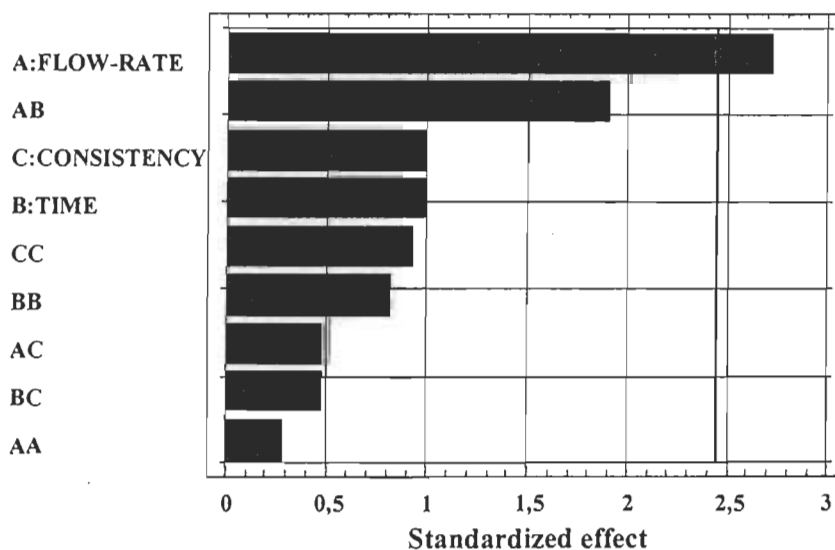
Figure 4.23   The standardised Pareto chart of light scattering coefficient for the
oxidation factors.

midpoint (22.5%), corresponding to the strong quadratic effect. So the 10% consistency leads to the smaller degradation.

The other important point is that for the medium gas flow-rate (4-5 l/min), the opacity is at maximum, whereas the tensile index is at a minimum. This also shows that the degradation is highest when the opacity is highest (at 22.5-% consistency).

4.1.3.6　　Light scattering coefficient

According to the Pareto chart (Fig. 4.23), only the gas flow-rate has a significant positive effect on the light scattering coefficient. This is due to the corresponding cellulose degradation and a reduction in bonding strength.

4.1.3.7　　Discussion

According to the response surfaces (Fig. 4.12), and the statistical analysis presented in Table 4.2, it can be pointed out that the effects of gas flow and oxidation time on COOH formation are not significant individually, but their interaction (AB) is significant. The same result was obtained in the one-factor-at-a-time design which showed that when gas flow increased above 4-5 ml/min, the COOH formation decreased (Fig. 4.1), and that when oxidation time increased up to 120 min (Fig. 4.3), the COOH increased. This means that the factor, which has the negative coefficient (gas flow-rate), should be kept at lower levels, while the factor having the positive coefficient (oxidation time), should be at a higher level. Under these conditions, one should obtain the maximum formation of COOH. The equations obtained from Table 4.2 were:

$y = \bar{y} - 0.871A + 1.021B - 5.90AB - 2.219C$

$y = 55.279 - 0.871(-1) + 1.021(+1) - 5.9(-1)(+1) - 2.219(-1) = 65.290$

where, y is the carboxyl content, $\bar{y}$ is the average, A is the gas flow rate at the low level (-1), B is the oxidation time at high level (+1). The highest carboxyl content should then be obtained at 10% consistency (C) (i.e. level of -1).

Based on the results of three experimental designs, it can briefly be concluded that:

Gas flow-rates about 4-5 l/min produces greatest increase in the formation of COOH.

An increase in oxidation time beyond 2 hours also results in an important loss of viscosity. Although high oxidation time causes lower viscosity, it is the only way to increase the carboxyl content during oxidation.

Lower pulp consistency (10-20%) leads to a higher COOH formation, viscosity and tensile index. However high consistency (35% or more) produced high z strength.

High temperature (40-60 ^{o}C) drastically decreases the viscosity of pulp. This could be because a rise in temperature reduces the ratio of N_2O_4 in the mixture with NO_2. This leads to a higher degradation effect due to greater ratio of NO_2. Therefore, it would be better to work at ambient temperatures or lower.

Based on the above considerations, the comparison of the effect of N_2O_4 oxidation among three different types of fibres (softwood, bagasse and aspen) was done under the following conditions:

-Constant temperature at 5°C, at the minimum level
-Constant consistency at 10%, at the minimum level
-Constant gas flow-rate, at 4.05 l/min, at the medium level
-Variable time of oxidation from 30 min to 180 min.

Keeping gas flow-rate constant and modifying the oxidation time for the same weight of fibre permits the consideration of a combined variable factor, the percentage of N_2O_4 /fibre. (Table 3.2, p.33). All of the samples prepared under these conditions were analysed by FTIR, ESCA, and IGC. The optical and mechanical properties of handsheets made from these samples were determined.

4.2   Fourier Transform Infra-Red (FTIR) Spectroscopy

It is possible to verify changes to the chemical structure of the fibres due to the oxidation treatment by FTIR spectroscopy. The spectra of the 3 untreated fibres were referenced to published cellulose spectra (111, 112, 113) to check the presence and the location of the OH, CH, and CH_2 peaks.

The following changes due to N_2O_4 oxidation were expected:

a   carboxyl band formation at 1738cm^{-1}.

b   shift of the OH band of cellulose towards lower energy due to carboxyl group
        formation.

c   modification of the OH peak intensity due to carboxyl, aldehyde and ketone
        formation at C6, C2 or/and C3 positions.   .

d   Modification of CH peak intensity due to the aldehyde and ketone formation at
        C2 or/and C3 positions.

As the oxidation rate increases the intensity of the COOH peak increases (12, 16, and 59). H-bonded OH shows a broad and strong peak component of free OH. However, in most situations, H-bonds have a serious overlap with free OH, making it difficult to separate them on the FTIR. At the same time, the OH peak at 3333 cm^{-1} will shift to lower frequency and its intensity will be reduced (114). This is a sign of more intermolecular bonding. There is also another OH peak related to the adsorbed water that appears at 1640-1650 cm^{-1} (111). The peak of OH, which exists on cellulose and not on D-glucose spectra (112, 115), was also, affected by the N_2O_4 oxidation and Mg salts used in the treatment. The OH transformation during N_2O_4 oxidation is due to the formation of aldehyde or ketone at C2/C3 or to the formation of carboxyl groups at C6. The spectra of the full energy range of 400-4800cm^{-1}, and the enlarged spectra at 1580-

1780 cm^{-1} are shown in the Figures 4.24 to 4.33. These demonstrate the perturbed peaks due the oxidation. To enable a proper comparison of the spectra, a common base line through two unchanged points was selected and common intensity scales are maintained for all spectra.

4.2.1 N$_2$O$_4$ oxidation of the fibres

4.2.1.1 The spectra of softwood oxidised fibres

According to the IR spectra in Figure 4.24, the OH peak of untreated softwood fibres appears at 3337 cm^{-1}. As N$_2$O$_4$/fiber increased, the intensity of this peak varied. This demonstrated some transformation of the hydroxyl (OH) units of cellulose. At the same time, the OH peak at 1650 cm^{-1} increased, except in the case of S-3. This may indicate the formation of aldehyde end chains, which were produced due to the C1-C4 glucosidic scission. Even though the variations in intensity of the OH peaks do not correlate exactly with the concentration values of N$_2$O$_4$, but in all types of oxidised fibres, the OH intensities were reduced, They illustrate the oxidation effects and indicate the direction of N$_2$O$_4$/fiber addition. This could be acceptable for a qualitative conclusion. It should be reminded that each series of the samples, the softwood samples for example were prepared at the same day, following exactly the testing procedure (according to the ref.16) to minimise the effect of the air humidity during pellet preparation and handling. Nevertheless as the fibres are hygroscopic, they absorb a bit quantity of the water vapour existing in air during getting the IR spectra. Taking into consideration that the interval of the formation of COOH was also small and the sample is a natural substance, the minimum absorption of air humidity, water molecules can interfere the intensity of the OH peaks. As the result, the reduction in the intensity of the OH peaks may not match exactly to the percentage of N$_2$O$_4$ addition. The pellet sampling method cannot keep the thickness of the pellet constant. In other words, it is not possible to fix an exact quantity of cellulose molecules to be exposed to the FTIR radiation, even though the fibre weights were the same for all samples. Samples made by the film method could have been more appropriate for quantitative analysis.

The carbonyl (ketone) peak which normally appears at 1715-1730 cm^{-1}, is very sharp and identifiable (78,116). In the spectra of bleached kraft fibres used in this study, the peak was not visible; however the baseline in this region (1690-1720 cm^{-1}) was raised after oxidation. That could be interpreted as a continuation of the carboxyl peak or the indication of the formation of carbonyl by the N_2O_4 oxidation. Mercer (15) and Friedlander (16) have already reported the formation of carbonyl groups during N_2O_4 oxidation. At the same time, production of carbonyl groups was reported as the major factor of cellulose fibres degradation (118) in ozone bleaching. This could be the reason why the maximum reduction in the strength properties was observed for all types of oxidised fibres at 1.25% N_2O_4/fiber, S-2, B-2, A-2 (see fibre and paper properties in part 4.5).

Meanwhile, the formation of COOH peaks at 1734-1738 cm^{-1} resulting from N_2O_4 oxidation have been observed for all of the oxidised fibres (except for S-3 and A-3). This peak was formed in the region of the bands of carboxyl groups, as reported earlier (102). Increasing the intensity of COOH peaks with an increase in the oxidation rate (N_2O_4/fiber) is well demonstrated in Figures 4.25, 4.27 and 4.29. This shows the direct relation of COOH formation to the rate of oxidation. As the percentage of N_2O_4 increases, the height of the COOH peaks generally increased. The results obtained are also in agreement with the O/C ratio found by the ESCA analysis.

4.2.1.2 The spectra of the oxidised bagasse fibres

Contrary to the softwood OH peak intensities, the OH peaks of the bagasse fibres showed a decrease either at 3354 cm^{-1} or at 1628 cm^{-1}. It might be concluded that in the case of bagasse fibres, there were less glucosidic scissions (less degradation effect) and relatively higher formation of carboxyl and ketone groups (oxidation effect). The intensity of OH vibration peaks at 1628 cm^{-1} were reduced and shifted about 10-20 cm^{-1} towards higher energy (COOH), which could be an indication of higher H-bonding in this case.
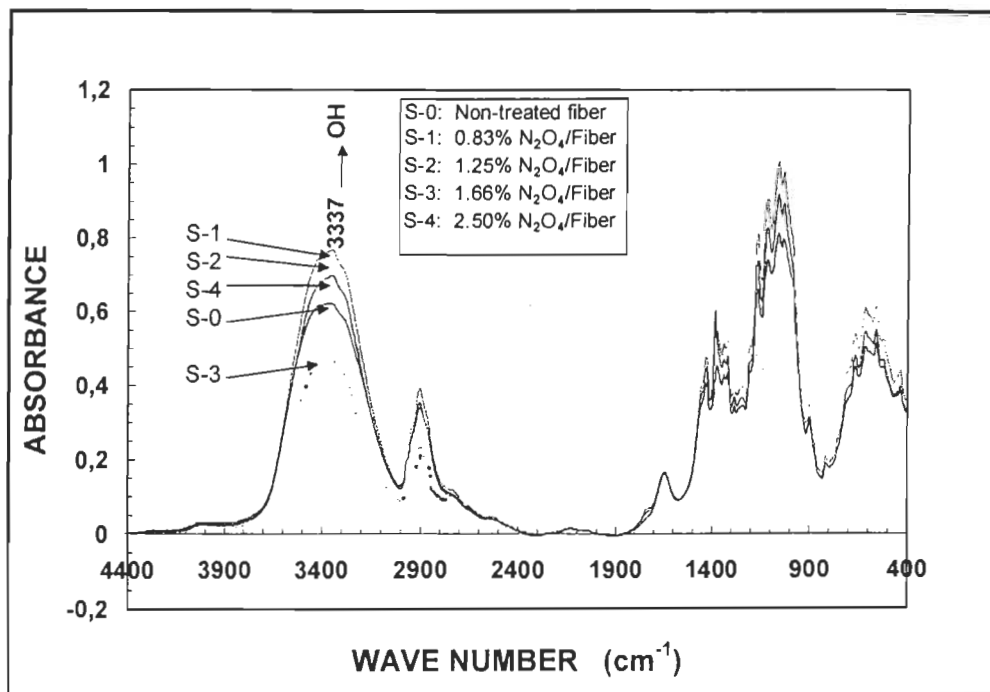
FIGUE 4.24 FTIR absorbance peaks of oxidised bleached kraft softwood fibres at different oxidation rates of 0, 0.83, 1.25, 1.66 and 2.50% N_2O_4 /fiber.
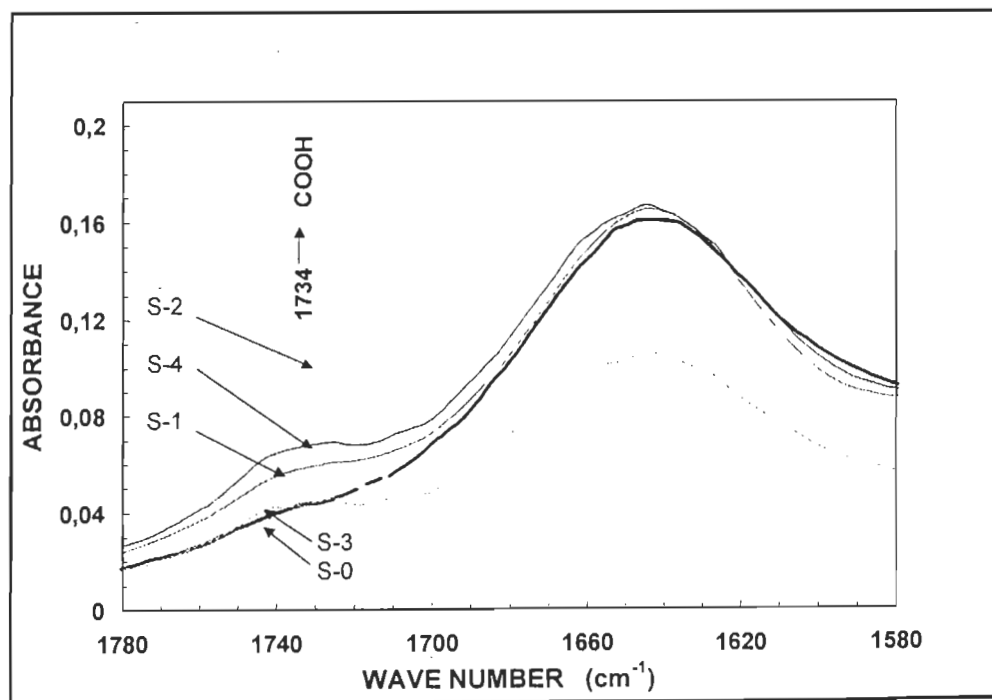
FIGURE 4.25 FTIR absorbance peaks of oxidised bleached kraft softwood fibres at different oxidation rates of 0, 0.83, 1.25, 1.66 and 2.50 % N_2O_4 /fibre (Enlarged for 1580-1780 cm^{-1}).
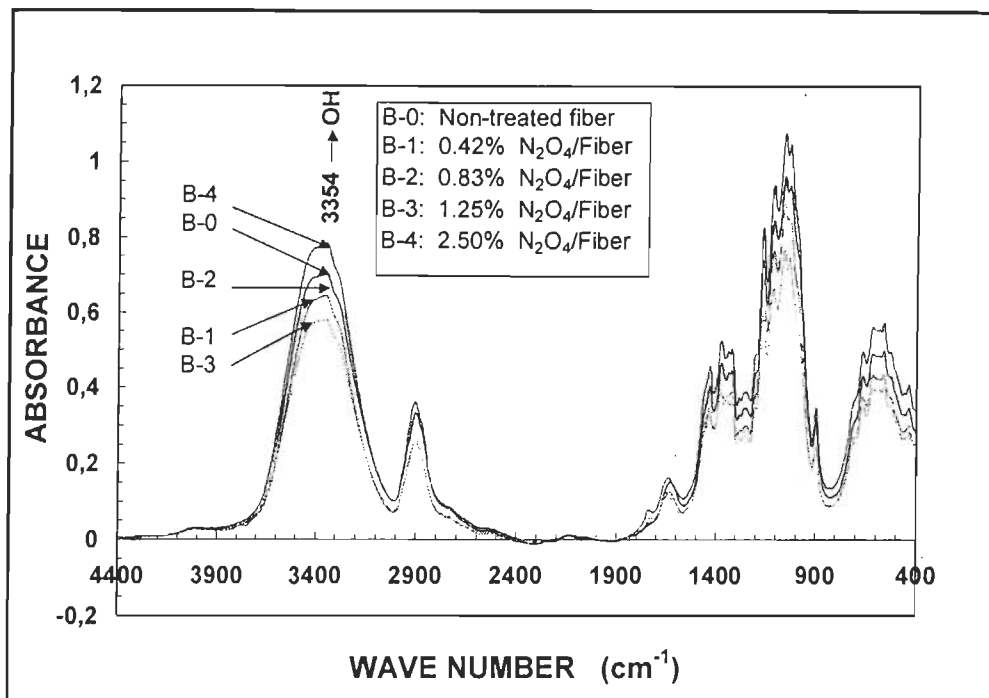
FIGURE 4.26 FTIR absorbance peaks of oxidised bleached kraft bagasse fibres
at different oxidation rates of 0, 0.83, 1.25, 1.66 and 2.50 % N₂O₄
/fibre.
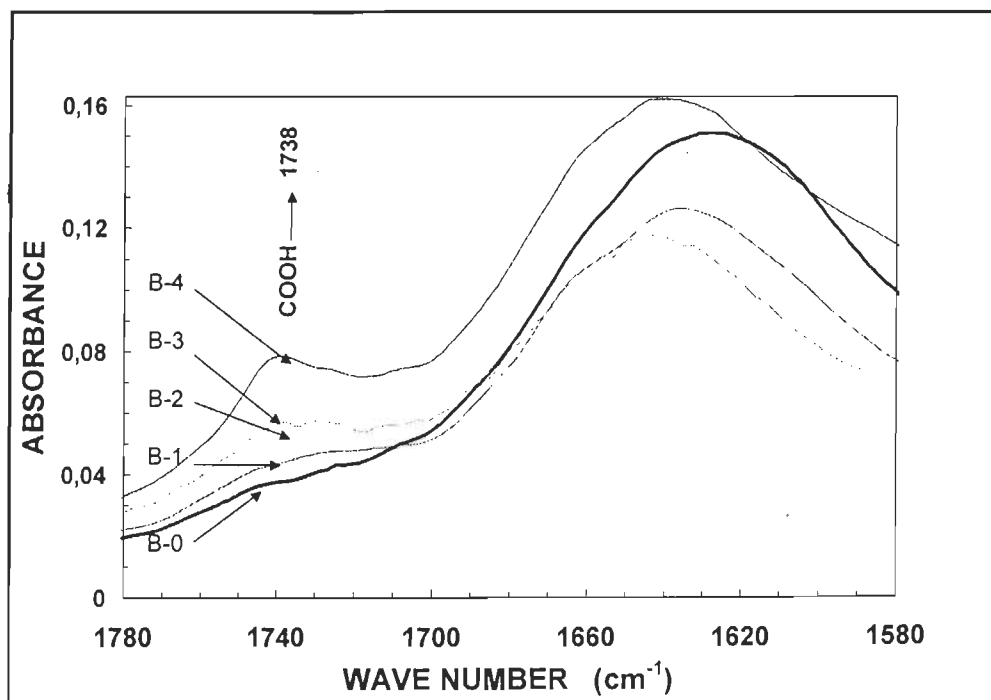
FIGURE 4.27 FTIR absorbance peaks of oxidised bleached kraft bagasse fibres
at different oxidation rates of 0, 0.83, 1.25, 1.66 and 2.50% N₂O₄
/fibre (Enlarged for 1580-1780-cm⁻¹).
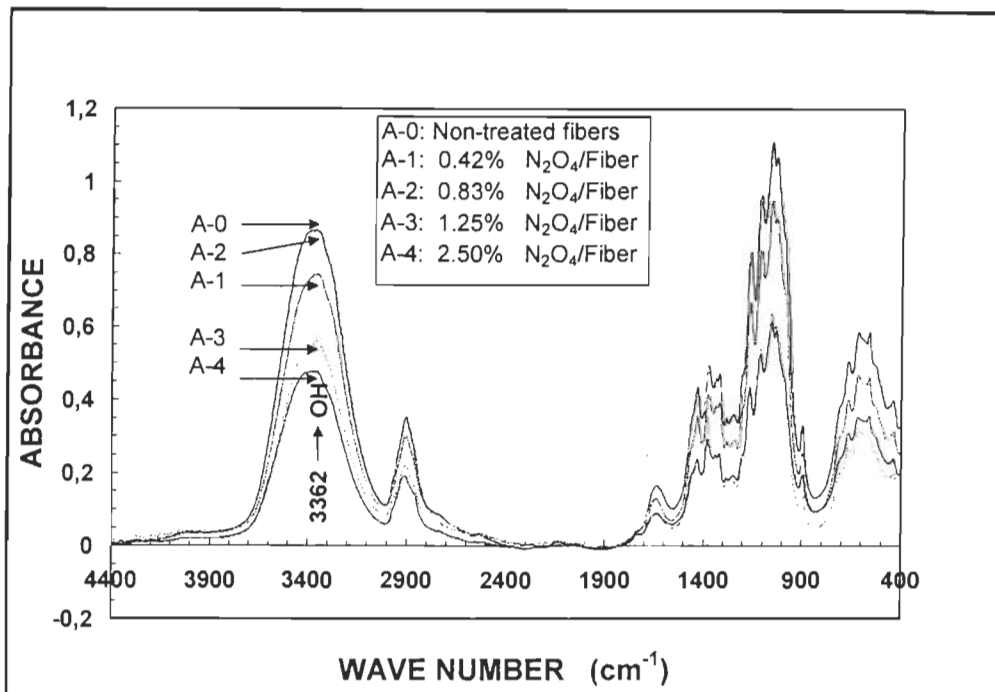
FIGUR 4.28 FTIR absorbance peaks of oxidised bleached kraft aspen fibres at different oxidation rates (0, 0.83, 1.25, 1.66 and 2.50 %N$_2$O$_4$ /fiber).
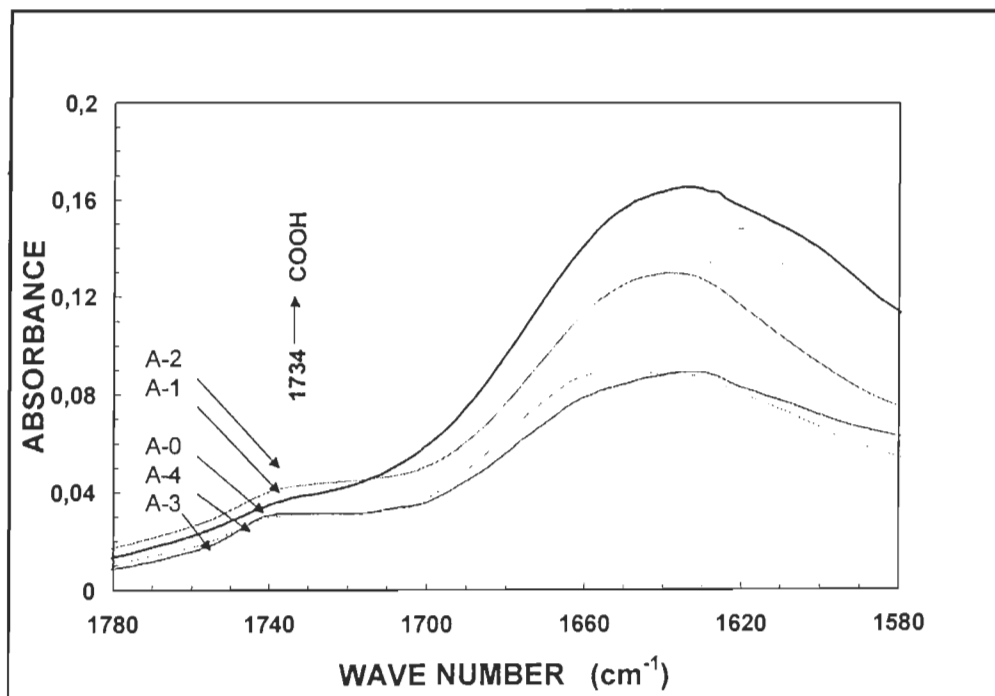
FIGUR 4.29 FTIR absorbance peaks of oxidised bleached kraft aspen fibres at different oxidation rates (0, 0.83, 1.25, 1.66 and 2.50 %N$_2$O$_4$/fiber (Enlarged for 1580-1780 cm^{-1}).

The COOH peaks related to higher oxidation rates have been well demonstrated in Fig. 4.27. Comparing these intensities to the softwood COOH peaks, they are formed at higher energy (1738-1740 cm^{-1}), where hemicellulose peaks at 1740 cm^{-1} are reported. This implies that the location of the COOH peak may be influenced by hemicellulose content.

4.2.1.3 The spectra of the aspen oxidised fibres

Fig. 4.28 shows that the intensity of OH peaks at 3362 cm^{-1} for the oxidised aspen fibres decreased as the oxidation rate increased. The OH intensity at 1641 cm^{-1} was also reduced as the oxidation rate increased and they shifted towards higher energy. This may be due to its higher percentage of hemicelulose (like bagasse) compared to the softwood OH peaks at this point. COOH peaks were formed by the oxidation, but the intensity increases of the peaks were less than 50% of those for bagasse and softwood (Fig. 4.29). This shows that aspen did not react as effectively as bagasse to form COOH groups. Consequently, there would be lower H-bond formation for the aspen fibres during the oxidation. This may explain why the reduction in strength properties was relatively greater for aspen (section 4.5). The minimum formation of COOH was also confirmed by the unchanged ESCA values of O/C ratio of the aspen fibres (section 4.3).

The reduction in the intensity of the CH peak at 2900 cm^{-1} is also very identical.. This reductions demonstrates the transformation of the secondary alcohols (CH-OH) of the oxidised fibres at C-2 and C-3 positions to the ketone or aldehyde groups. The reduction in the intensity of the CH peaks were about 4-5 times more than that of the fo COOH peaks for all three types of fibres; softwood, bagasse and aspen. However the amount of intensity reduction for aspen and softwood are greater than that for bagasse oxidised fibres. This might indicate that the formation of carbonyl groups (negative effect) is more than the formation of carboxyl groups (positive effect) during the N_2O_4 oxidation.

4.2.2 The effect of the addition of Mg CO_3 during N_2O_4 oxidation on the FTIR spectra.

The addition of 1% $MgCO_3$ during N_2O_4 oxidation of softwood and bagasse fibres was carried out as mentioned previously. Here, the situation of their IR spectra is discussed.

4.2.2.1 Oxidised fibres of softwood

OH peaks for softwood fibres were nearly identical to those corresponding to the fibres oxidised by N_2O_4 alone. The OH intensities at 3337 cm^{-1} and at 1645 cm^{-1} decreased upon oxidation(Figs. 4.30 and 4.31). Here the reduction in the intensity of OH peak at 1645 cm^{-1} is an indication of a great loss of adsorbed water due to the presence of $MgCO_3$. It is known that magnesium has a higher co-ordination potential than the sodium and potassium salts and its salts have an extreme affinity to water. (More hygroscopic) Therefore, they could have absorbed the adsorbed water of cellulose, which would reduce the OH peak at 1645 cm^{-1}. This gives less chance to N_2O_4 gas to form acid nitrous and acid nitric. Consequently the acid hydrolysis effect was reduced, so the degradation effect was decreased, and at the same time the formation of COOH groups was also reduced. Loosing the adsorbed water of cellulose could help the cellulose chains to approach each other (increase in cohesive energy) and compress the individual fibres together.

The intensities of carbonyl peaks at 1715-1730 cm^{-1} region showed a notable decrease compared to those for oxidised fibres without $MgCO_3$ addition. This lower carbonyl formation could be the cause of lower reduction in viscosity reduction or minimum degradation in presence of the $MgCO_3$. The large reduction in cellulose degradation, the formation of COOH groups at C6 and the reduction in the intensity of OH peak of the adsorbed water are the reasons for increasing the strength properties in this case (section 4.5).
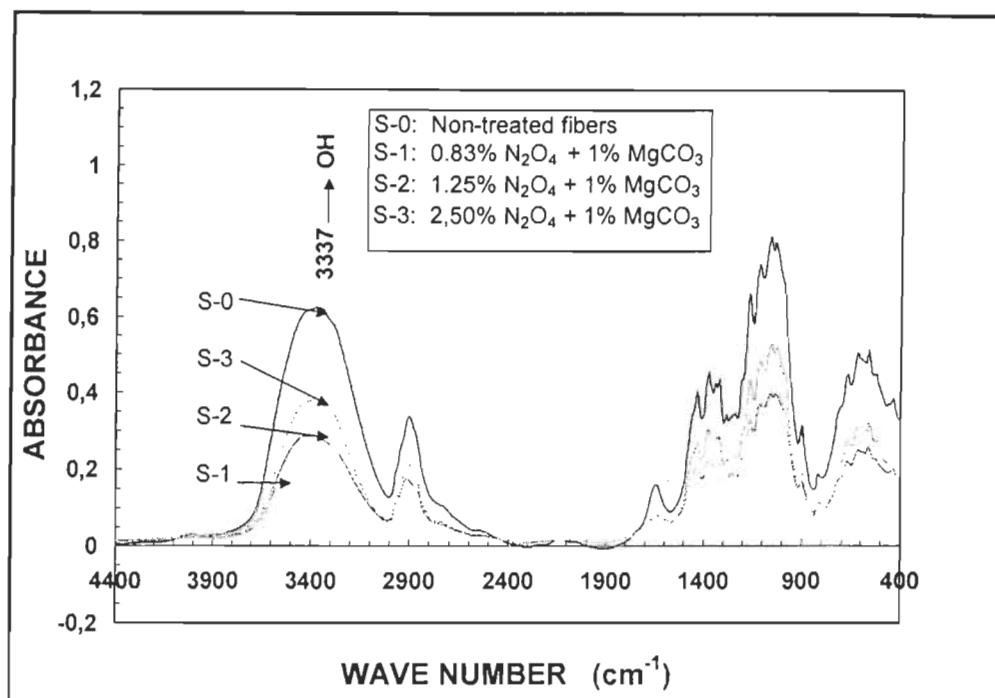
FIGURE 4.30 FTIR absorbance peaks of oxidised bleached kraft softwood fibres at oxidation rates of 0, 0.83, 1.25 and 2.50% N_2O_4/fiber + 1% $MgCO_3$.
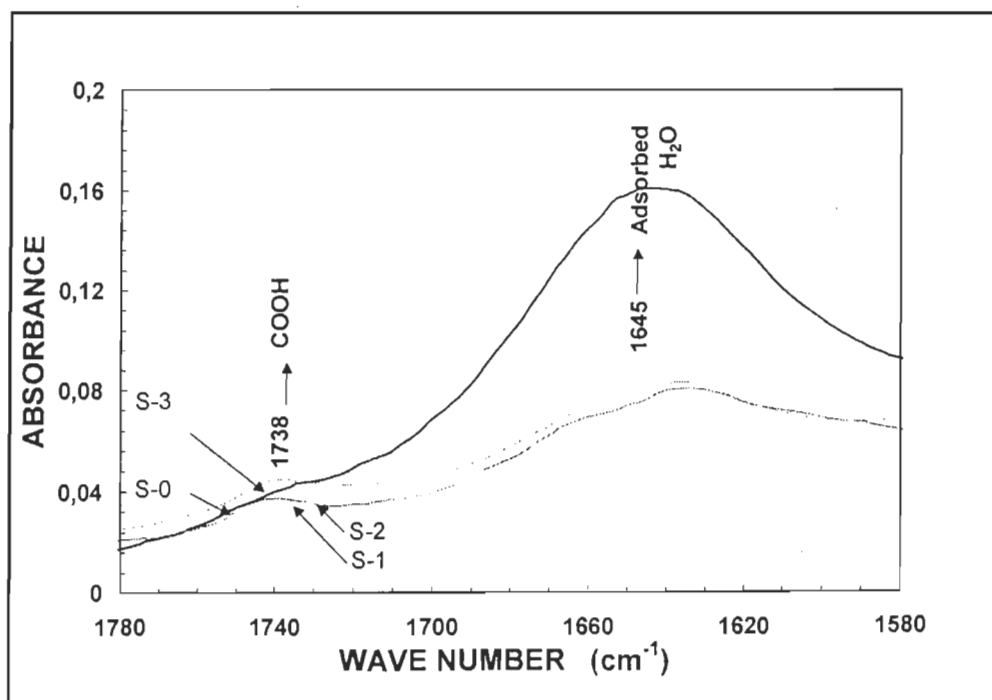
FIGURE 4.31 FTIR absorbance peaks of oxidised blleached kraft softwood fibres at oxidation rates of 0, 0.83, 1.25 and 2.50 %N_2O_4/fiber + 1% $MgCO_3$ (Enlarged for 1580-1780 cm^{-1}).
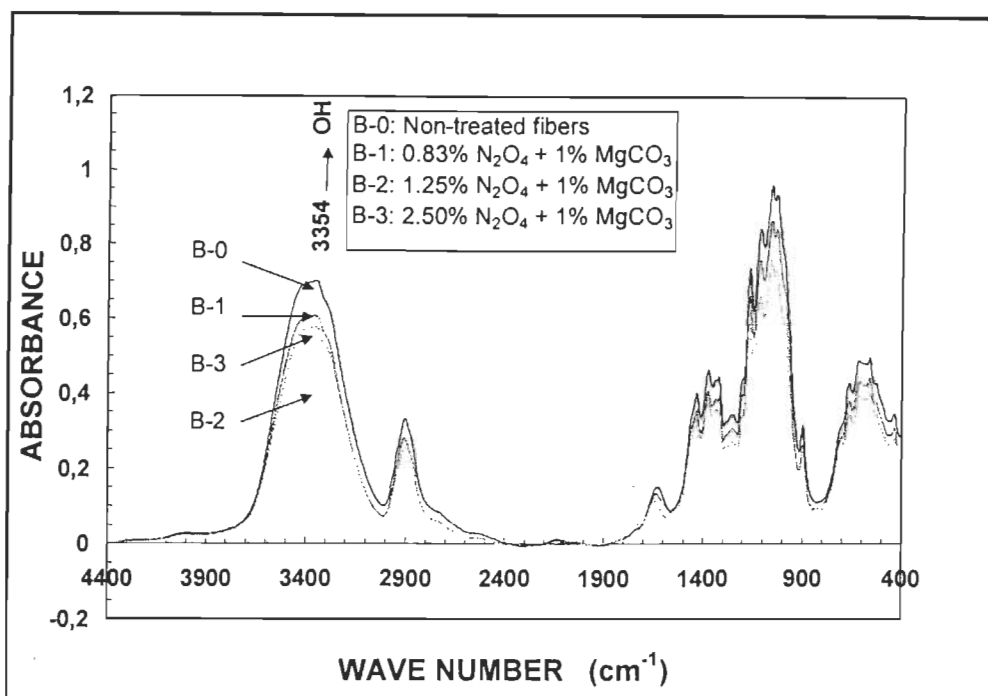
FIGURE 4.32 FTIR absorbance peaks of oxidised fibers of bleached kraft bagasse with oxidation rates of 0, 0.83, 1.25 and 2.50 %N_2O_4/fiber + 1% $MgCO_3$.
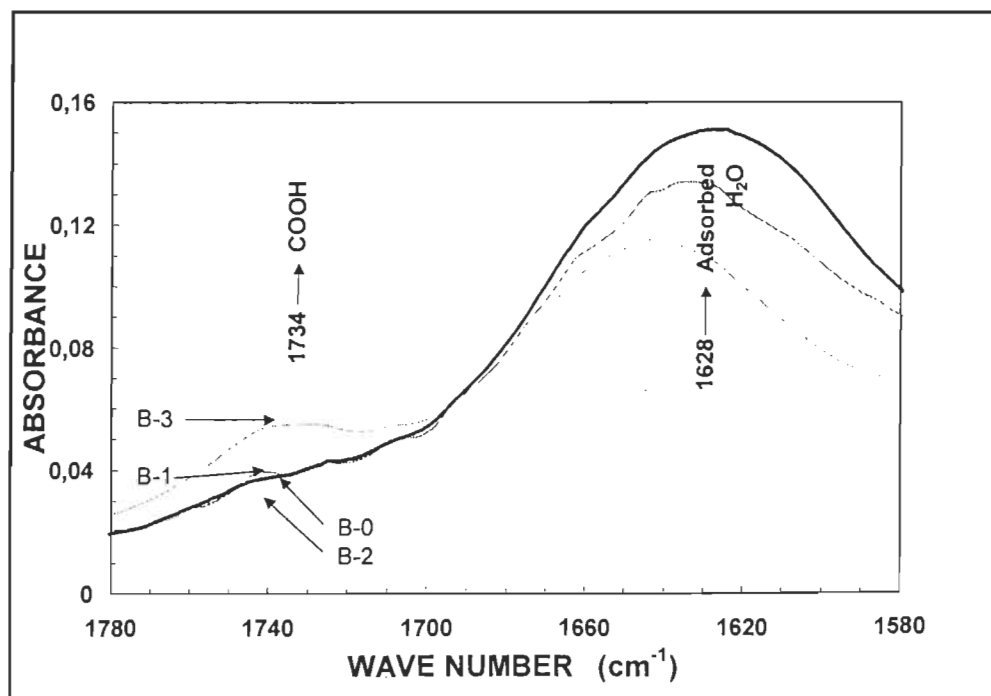
FIGURE 4.33 FTIR absorbance peaks of oxidised bleached kraft bagasse fibres at oxidation rates of 0, 0.83, 1.25 and 2.50 %N_2O_4/fibre + 1% $MgCO_3$ (Enlarged for 1580-1780 cm^{-1}).

4.2.2.2   Oxidised fibres of bagasse

The same changes in OH peak intensities due to the addition of 1-% $MgCO_3$ were observed for bagasse fibres as were observed for softwood fibres (Figs. 4.32 and 4.33).

The reduction in the intensity of the carbonyl and OH of adsorbed water peaks could be favourable to an increase in the strength properties. In addition, the formation of COOH peaks in this case could result in the higher strength properties at 1.25% and 2.5% N_2O_4 /fibre (see part 4.52). If the oxidation rate was raised to 5-10% N_2O_4/fiber in the presence of $MgCO_3$, higher amounts of COOH might be formed; however, it would not be possible to predict the viscosity. Furthermore, the additional consumption of N_2O_4 gas would probably be very uneconomical. It may be briefly concluded that FTIR spectra were useful to verify the chemical changes occurring in the fibres during N_2O_4 oxidation. The formation of COOH groups was proven by identification of the peak at 1734-1738 cm^{-1} for all oxidised fibres. On the other hand, the intensities of the peaks at 3333-3360 cm^{-1}, which represent the different OH groups of the glucosidic chains, were perturbed during the oxidation. This could indicate the transformation of the different alcohol groups of cellulose to aldehyde, ketone and carboxyl groups. This transformation was homogeneous, but not selective. The formation of carbonyl peaks was not observed. However, in the region of 1715-1730 cm^{-1}, which is the standard location for these groups, the intensity increased substantially after oxidation. The technique of peak deconvolution could permit these changes in intensity to be observable as peaks.

The effect of $MgCO_3$ was associated with a remarkable decrease of the OH intensity at 1645 cm^{-1} (location of adsorbed water) as well as by an increase in the COOH peak at 1734-1738 cm^{-1}. However, the intensities of COOH peaks were lower than in the case of N_2O_4 oxidation without $MgCO_3$. The FTIR evaluation of the oxidised fibres introduced fairly good qualitative information, but the variability induced by the pellet sampling method of fibres did not permit more precise quantitative results.

4.3 Electron spectroscopy for chemical analysis (ESCA)

Oxidation treatment changes the chemical structure of the celluloseic fibres not only in the bulk, but also on the surface.lectron spectroscopy for chemical analysis (ESCA) is a technique well known and mostly used to verify the chemical composition of the solid, synthetic polymers and cellulosic fibres, through their carbon, oxygen, sulphur and metal components on the surface . The bleached kraft fibres of softwood, bagasse and aspen which have been oxidised by N_2O_4 as described in Table 3.3, are analysed by the ESCA apparatus according to the procedure mentioned in the chapter 3. The C(1s) peaks, their carbon components, and peaks of other elements detected on the surface of the oxidised fibres are reported respectively.

4.3.1 N_2O_4 oxidation of the fibres

4.3.1.1   Carbon components

The ESCA results of the of the three series of oxidised fibres concerning binding energies, of the carbon components and the O/C ratio appear in the Table 4.3. In the experiment the bleached kraft fibres were used, in which the lignin content were at the minimum level.Consequently the observation of carbon components and their O/C ratio were sufficient for the evaluation of the treatment. This is why the evaluation of O1 and O2 components of the lignin were not verified seprately. Values of 0% for C1, 83% for C2, and 17% for C3 for pure celulose, also for the values of 0.33 as the O/C ratio for lthe pure ignin and 0.83 as the O/C ratio for the pure cellulose are reported in the literature (81, part I, 85). Furthermore, these values of C1, C2 and C3 vary for the different pulps, bleached or unbleached, TMP, CTMP or kraft. In this work, the values of 34.5, 39.8 and 41.1 for C1, 56.9, 52.7 and 50.3% for C2, and 8.6, 7.5 and 8.7% for C3

are obtained for different bleached kraft fibres of softwood, bagasse and aspen (Table 4.3). The related peaks are shown in Figs. 4.34, 4.35 and 4.36 for C1, C2 and C3 of the untreated and oxidised fibres of softwood, bagasse and aspen respectively. The values obtained for the C1(0.345) of the softwood bleached kraft due to low content of lignin (less than 0.2%) was expected to be closer to the cellulose, or whatmann paper with C1 values about 2 to 7 % (82, 119), but due to the presence of extraxtive and fatty acids on the surface, the higher amount of C1 was observed. This was close to the values of C1 obtained for TMP (0.40, Ref. 81, or 0.41 Ref 120), or to the CTMP (0.41 Ref. 82). The C1 values for bagasse and aspen bleached kraft, which were measured and reported only in this work, due to their higher lignin content, were more than that of softwood as it was expected (0.398, 0.411 as compared to 0.345 for softwood fibres). C1 correspond to the carbon component bonded only to another carbon or hydrogen, and represnting the lignin and the extractives, was reduced to 0.204 , 0.278 and 0.337 for the oxidised fibres of softwood, bagasse and aspen respectively. It shows, that the slihtly residual lignin and extracives materials (fatty acids, abietic acids and wax materials) existing with the fibres were also reduced, but these hydrocarbons were still presennt on the surface of the oxidised fibres. This might be the reason why the existance of the carboxyl groups (C4) formed was not observed on the ESCA spectra.

The values of C2 correspond to a carbon bonded to a single oxygen other than carbonyl oxygen, represents mainly the carbohdrates (cellulose and hemicllulose) as CH-OH or lignin as β-ether,-C-OH (85). As the total surface area of C1s compenent peaks are taken as 100, decreasing the percentage of the C1, would lead to higher percentage of C2 and C3. That is why the values for C2 for all three series of fibres were increased as it was expected. It is clear that C2 increase by the N_2O_4 oxidation, is an indication of an increase in polysaccarides, and not due to the lignin augmentation, as the residual lignin is the first composant to be removed by the NO_2 (18, 38). Nevertheless C2 increase did not result to the higher sheet strength, as there were considerable degradation of the oxidised fibres during the N_2O_4 oxidation. Figures 4.37 shows the maximum reduction in the percentage of C1 (and maximum increase in the percentage of C2) at 1.25% N_2O_4 for all three types of the fibres.
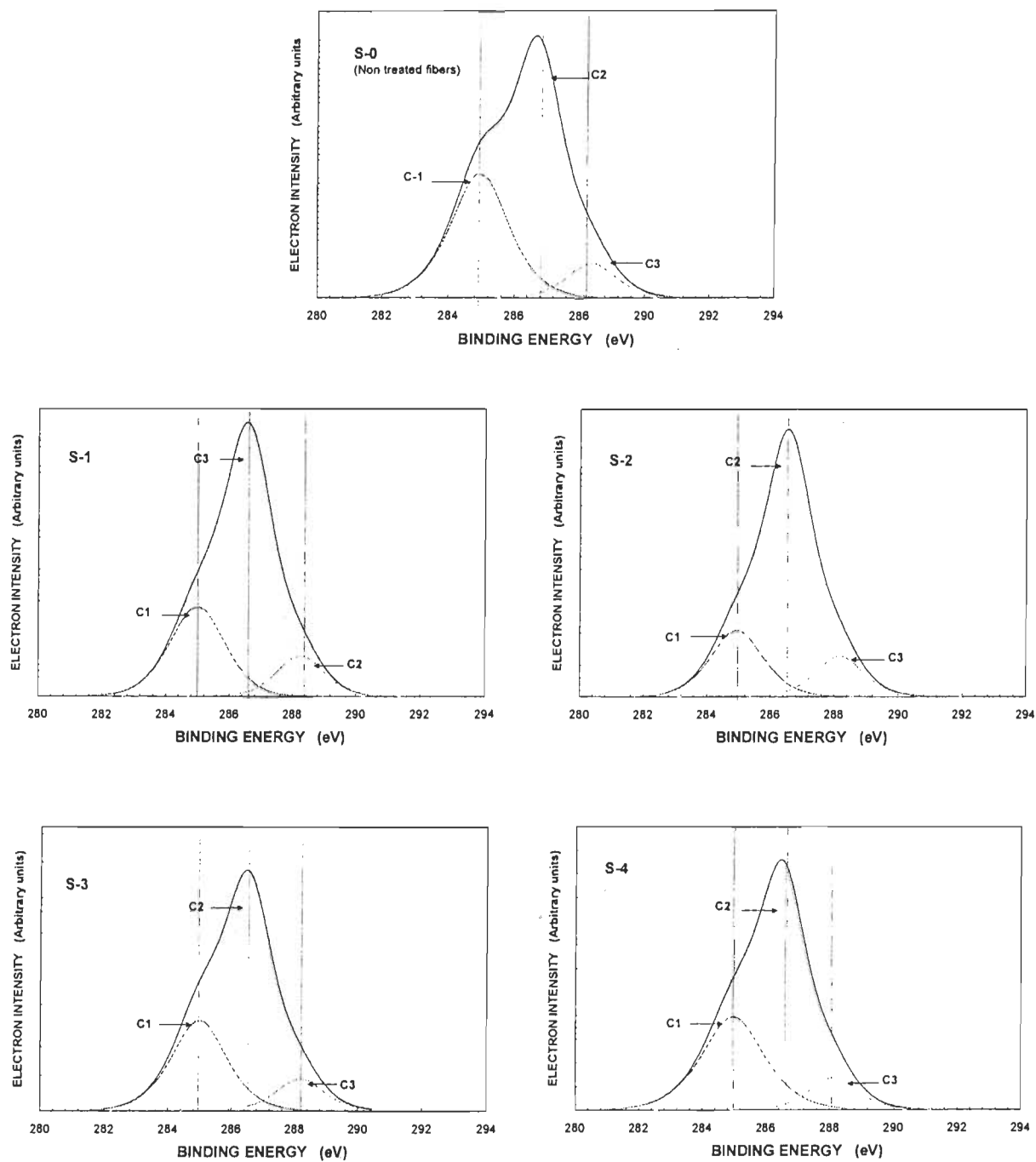
FIGURE 4.34 C (1s) peaks obtained from ESCA spectra for softwood oxidised by N_2O_4 at oxidation rates of 0.0% (S-0), 0.83% (S-1), 1.25% (S- 2), 1.66% (S-3) and 2.50% (S-4).
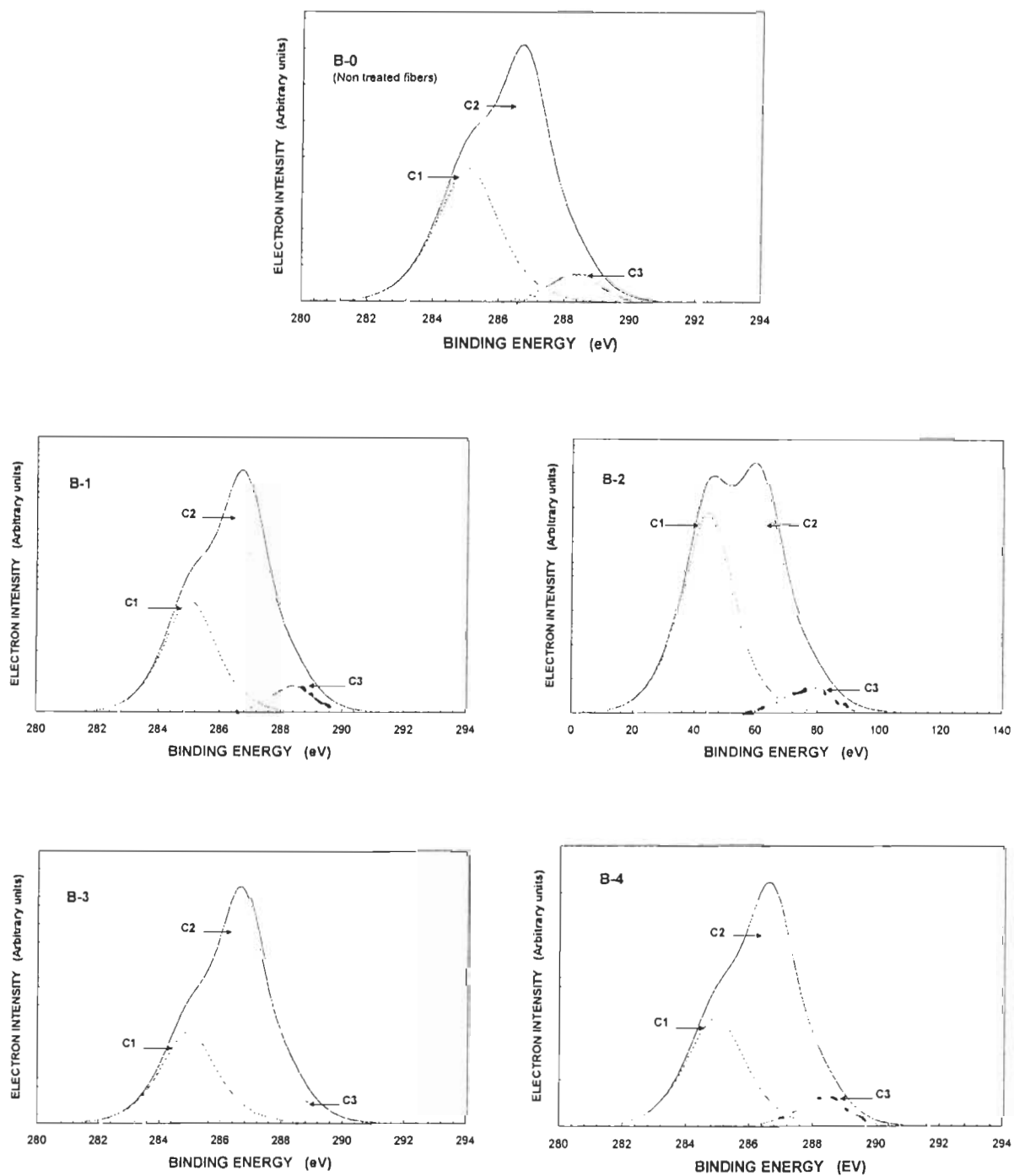
FIGURE 4.35 C (1s) peaks obtained from ESCA spectra for bagasse oxidized by N_2O_4 at oxidation rates of 0.0% (B-0), 0.83% (B-1), 1.25% (B-2), 1.66% (B-3) and 2.50% (B-4).
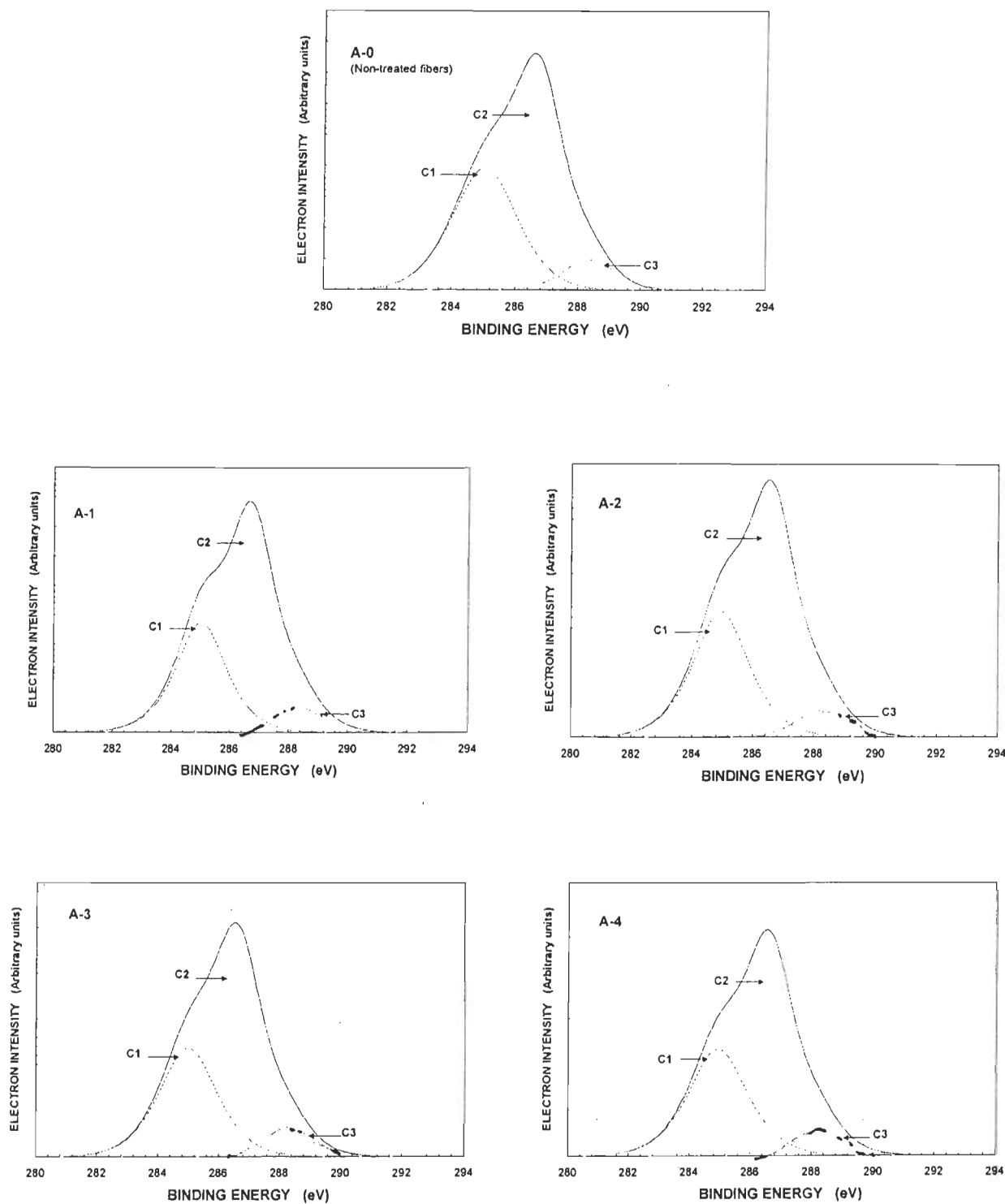
FIGURE 4.36   C(1s) peaks obtained from ESCA spectra of aspen oxidised by by N_2O_4 at oxidation rates of 0 .0% (A-0), 0.83% (A-1), 1.25%   (A-2), 1.66% (A-3) and 2.50% (A-4).

For the S1 and S2, the left shoulder of spectra was reduced, or completely eliminated (3/4 loss in peak height as shown in dash line), whereas for bagasse there was little modification of this shoulder. This confirms the previous assumption of higher reduction of the C1 percentage for the softwood fibres as compared with that for bagasse fibres (Table 4.4).

By accepting the binding energy of 288.2-288.4 eV to be an indication of carbon with double bonds on the surface, as this represent the presence of the ketone and aldehyde groups (carbonyl), no improvement in the fibre bonding should be expected (120). Increases in C3 of up to 2.65-% were obtained for softwood fibres, up to1.15-% for bagasse fibre and no increase for aspen fibres. The highest percentage of C3 was 11.2-% at 1.25-% N_2O_4, the point at which the lowest tensile strength and burst index were obtained (section 4.51). Figure 4.38 shows the relation between the percentage of N_2O_4/fibre and C3/C1 ratio. This permits the interpretation of lower degradation of the bagasse oxidised fibres during the N_2O_4 oxidation, as the increase of C3/C1 ratio for bagasse fibres (from 0.188 to 0.266) were much less than those for the softwood fibres (from 0.249 up to 0.549).

The B-2 spectra in Figure 4.35 showed that the percentage of C1 increased unexpectedly. Similarly, the percentage of C2, C3 and O/C ratio dropped for this treatment. This might be due to some error in the graphical computation of C1 that affected the other values. Using the four other points, a new value was interpolated. The location of C1 for B-2 is illustrated by dash-line in Fig. 4.37. For aspen, a small, decrease was obtained for the percentage of C3 for all ratio of oxidation, but this did not result in an improvement in the strength properties.

4.3.1.2   O/C Ratio

The O/C ratio is an indication of the effect of oxidation, and one can see that it has increased for all oxidised fibres except aspen (Fig.4.39), even though the percentage

of C1 decreased and the percentage of C2 increased for all of the fibres. This means that the N_2O_4 oxidation of the aspen fibres modified the chemical structure of its cellulose and hemicellulose, but the O/C ratio representing the hydrophilic character of the fibres did not improved. This is in agreement with the FTIR results, where the formation of carboxyl groups of the aspen fibres was lowest. It might be concluded that the O/C ratio demonstrates the oxidation effect, and C2 and C3 percentages illustrate the degradation effect of fibres during N_2O_4 oxidation.

4.3.2   The effect of the addition of $MgCO_3$ during N_2O_4 oxidation

The ESCA results obtained for the fibres oxidised in the presence of 1% $MgCO_3$ are presented in Table 4.5.

4.3.2.1   Carbon components

Based on the results reported in Table 4.5, and on the observation of the C (1s) peaks in Figures 4.40 and 4.41, it was found that an addition of 1% $MgCO_3$ resulted in the conservation of higher C1 and in the formation of lower C2. In other words by the addition of 1% $MgCO_3$ during the oxidation, the changes in chemical structure were much less pronounced than those without $MgCO_3$ (Fig. 4.42). The percentage increase of C2 in this case was lower than that obtained during the oxidation without $MgCO_3$ (58.1% as compared to 68.3% at 1.25-% N_2O_4 for the softwood fibres). This is also shown in Figures 4.42 and 4.43 where the modifications of C1 and C2 were less than those in the absence of $MgCO_3$. Figure 4.44 illustrates the C3/C1 ratio, indicating the lower formation of C3 after the addition of $MgCO_3$ for the softwood fibres.
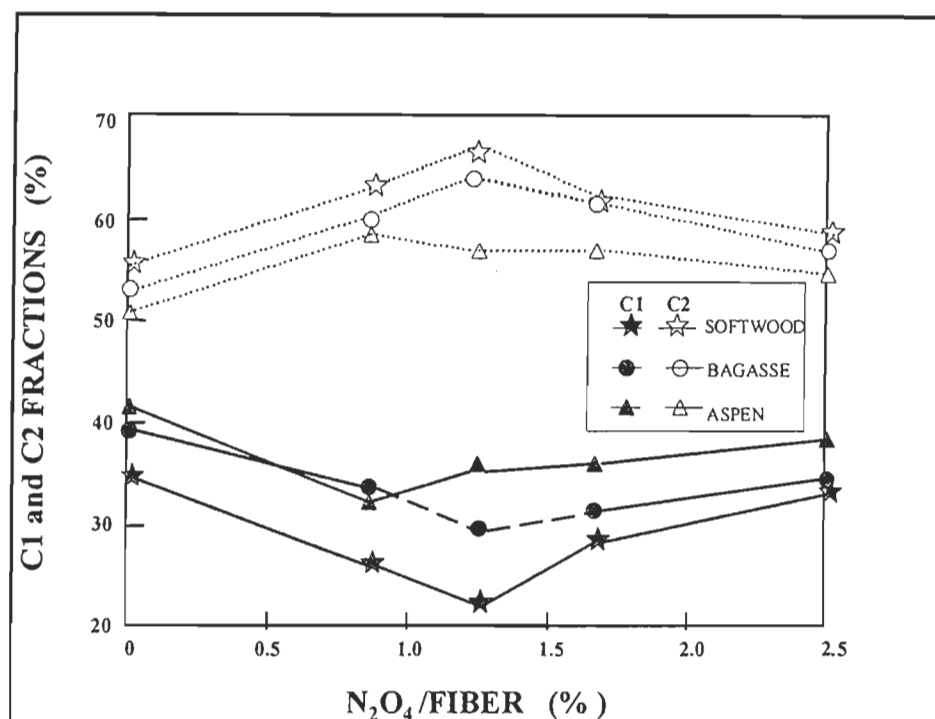
FIGURE 4.37 The effect of N_2O_4 oxidation of bleached kraft softwood, bagasse and aspen fibres on C1 and C2 fractions.
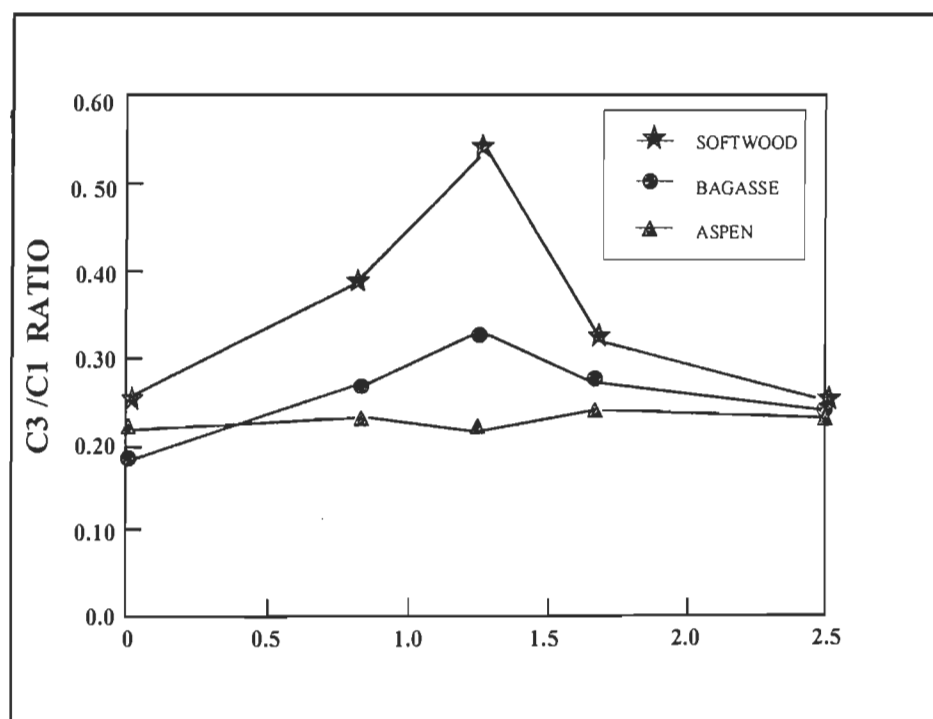
FIGURE 4.38 The effect of N_2O_4 oxidation of bleached kraft softwood, bagasse and aspen fibres on C3/C1 ratio.
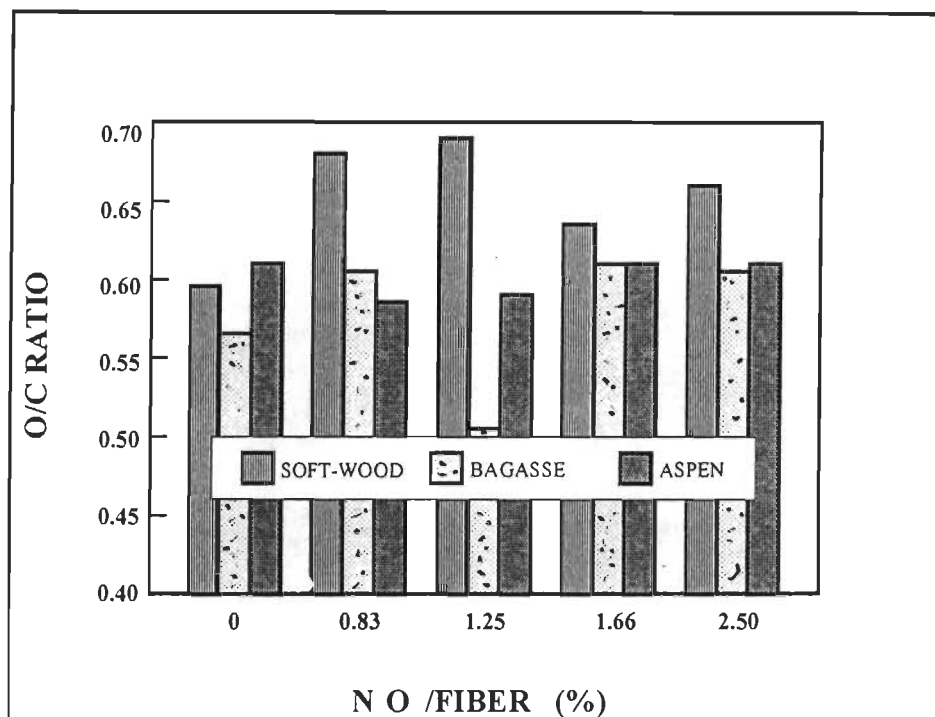
FIGURE 4.39 The effect of N_2O_4 oxidation of the bleached kraft fibres of softwood, bagasse and aspen on the O/C ratio.
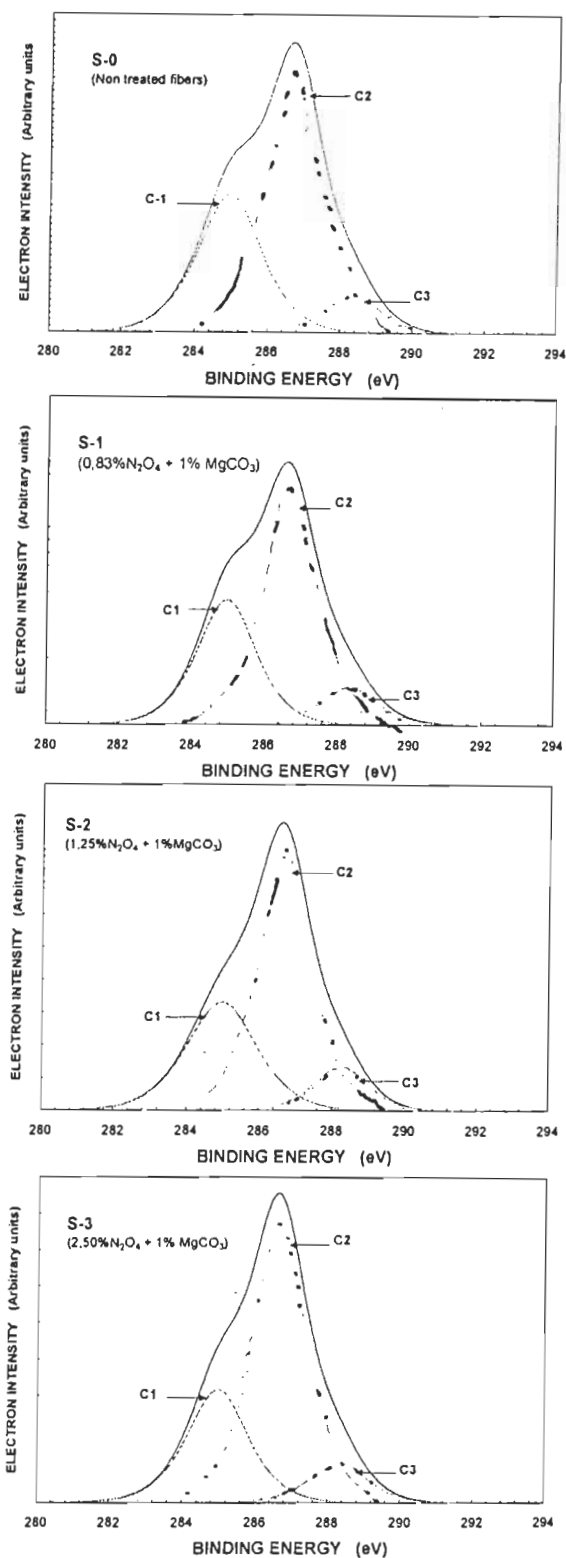
FIGURE 4.40 C (1s) peaks obtained from ESCA spectra for bleached kraft softwood fibres oxidised by N_2O_4, at oxidation rates of 0.0% (S-0), 0.83%, (S-1), 1.25% (S-2), and 2.50% (S-3) plus 1% $MgCO_3$.
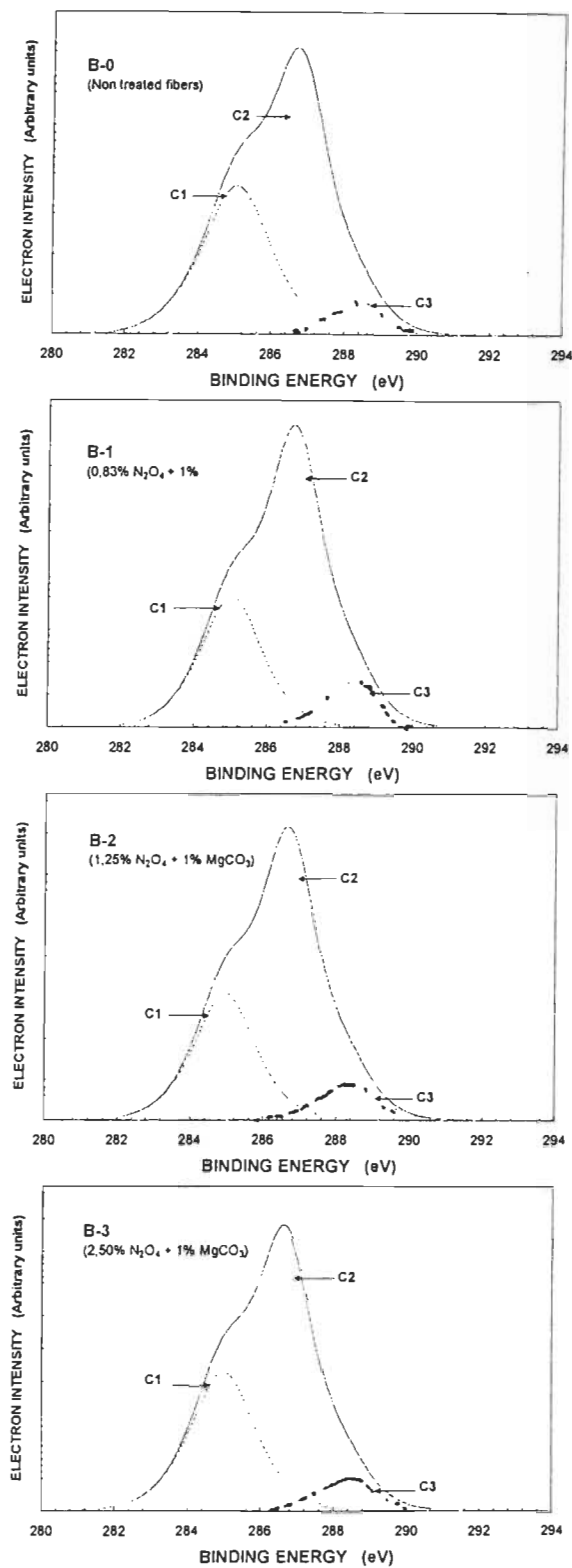
FIGURE 4.41 C (1s) peaks obtained from ESCA spectra for bleached kraft bagasse fibres at different oxidation rates: 0.0% (B-0), 0.83% (B-1), 1.25% (B-2), and 2.50% (B-3) plus 1% $MgCO_3$.

For the bagasse fibres (Fig 4.43), the C1 component decrease was lower and the percentage of C2 increase was lower too. The presence of 1% $MgCO_3$ caused a 0.0-2.4% increase in the formation of C3 at a lower rate of oxidation and a 1.0% increase at a higher rate (2.5% N_2O_4 /fibre). The higher percentage of C3 might be due to its higher hemicellulose content, so there is more chance that C2 correspond to the hydroxyl groups (C-OH) converts to the carbonyl groups (C=O). This is why the C3/C1 ratio increased for bagasse fibres in the presence of $MgCO_3$. This can be observed in Figure 4.44 and Table 4.5, where the C3/C1 ratios were increased from 0.133 to 0.291 at 1.25% N_2O_4, and from 0.151% to 0.362 at 2.5% N_2O_4.

4.3.2.2   O/C ratio

Figure 4.45 shows the O/C ratios of the softwood and bagasse fibres as a function of the percentage of N_2O_4/fibre. The O/C ratio again represents the hydrophilic character of the fibres due to the oxidation, which increases by the formation of the carboxyl groups. As the formation of the carboxyl groups was reduced by the addition of $MgCO_3$, the increase in the O/C ratio was lower than in the case of the oxidation without $MgCO_3$. The reason could be due to the reduction of the acid hydrolysis of the N_2O_4 oxidation after the addition of (basic) $MgCO_3$. The value of O/C for softwood fibres was reduced from 0.662 to 0.612, whereas it dropped from 0.606 to 0.579 at 2.5 % N_2O_4/fibre for bagasse fibres.

4.3.3   Apparent concentration of the elements on the fibre surface

In addition to the main oxygen (O) and carbon (C) atoms, Tables 4.4 and 4.6 demonstrate the presence of other elements at low concentrations on the surface. The presence of Cl in all three fibres is an indication of the effect of chlorine or chlorine dioxide bleaching. For the bagasse, the presence of the Na ions relates to the sodium hypochlorite bleaching process (125). There are also traces of nitrogen on the surfaces of
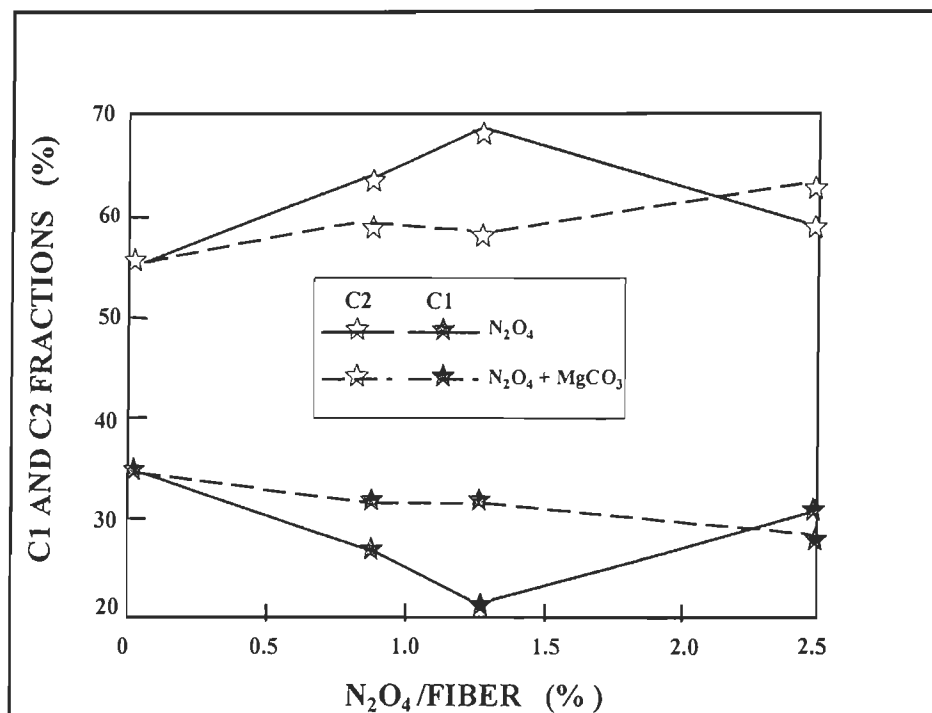
FIGURE 4.42   The percentage of C1 and C2 of bleached kraft fibres of softwood as a function of the oxidation rate.
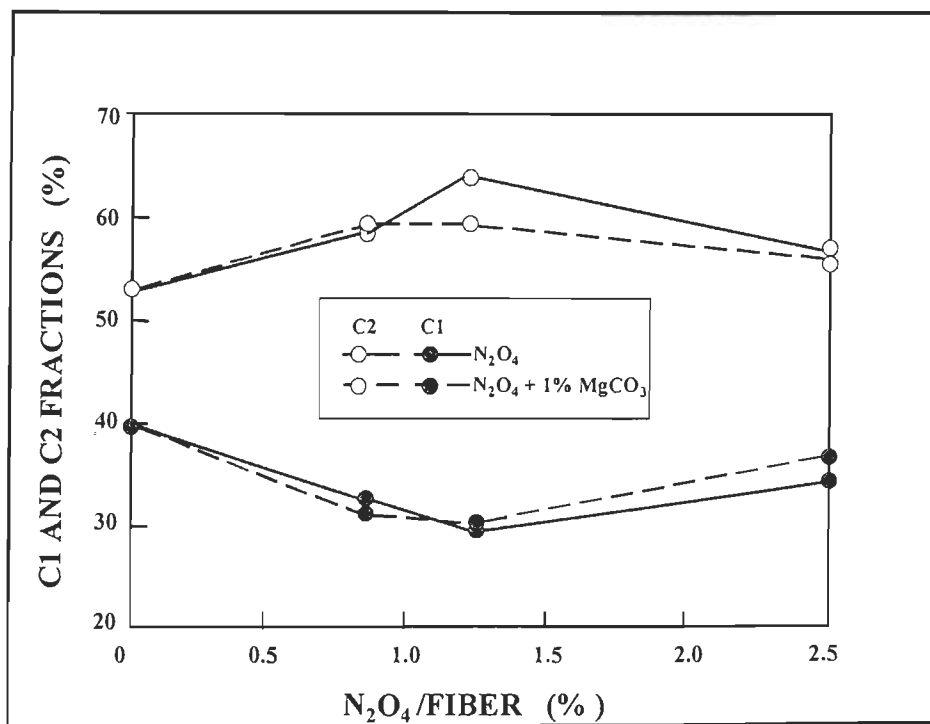
FIGURE 4.43   The percentage of C1 and C2 of bleached kraft fibres of bagasse as a function of the oxidation rate.
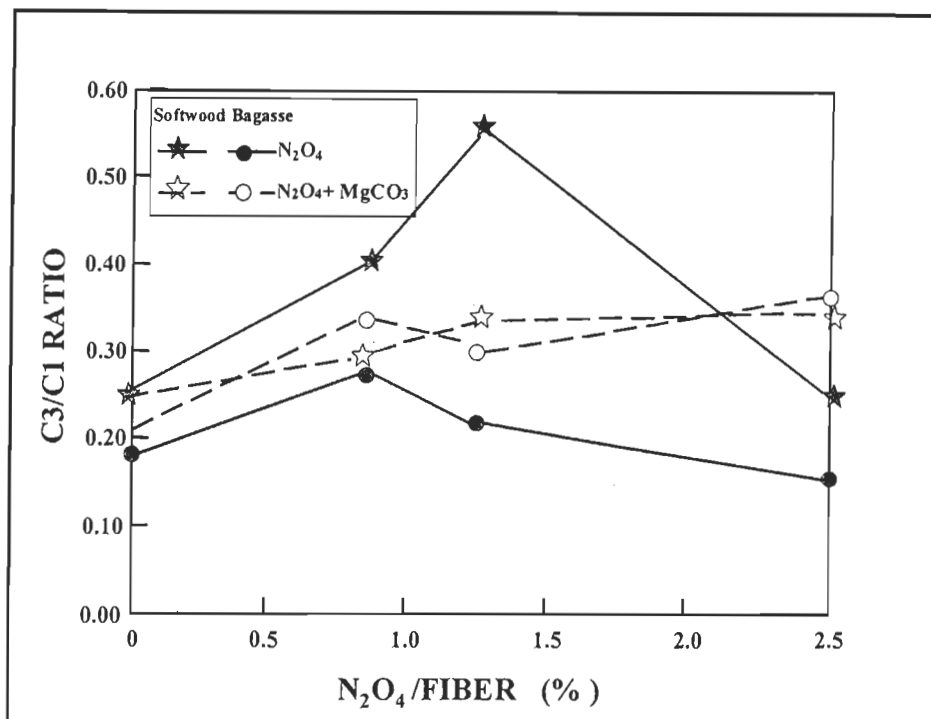
FIGURE 4.44   Plot of C3/C1 ratio of bleached kraft fibres of softwood and bagasse, versus the N_2O_4 oxidation rate, in presence of 1% $MgCO_3$.
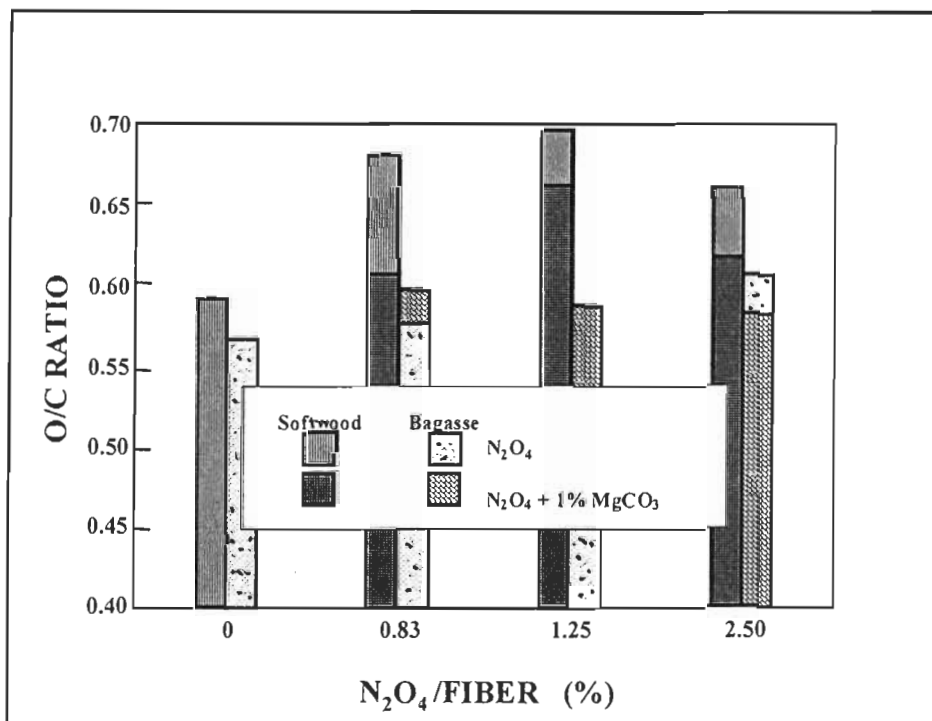
FIGURE 4.45   Plot of O/C ratio of beached kraft fibres of softwood and bagasse versus the N_2O_4 oxidation rate, in presence of 1% $MgCO_3$.

the N_2O_4 oxidised fibres. Finally, the presence of silicon on the bagasse fibres (115). Case of $MgCO_3$ is justified, since sugarcane is known to carry this element.

4.3.4   Discussion

Instead of classifying different carbon components by C1, C2, C3 and C4, Dilk (127) proposed the binding energies for each carbon functional group as presented in Table 4.7. These are 286.6 eV for hydroxyl groups (C-OH), 287.9 eV for ketone group (C=O) and 289.0 eV for carboxyl groups (O=C-O). In this work, binding energies of 285.0, 286.6-286.7 and 288.2-288.4 eV were observed for these groups, respectively. Thus, a binding energy of 285.0 eV was considered as C1, representing C-C or C-H bonds, 286.6 eV as C2 representing the C-OH bonds, and 288.4 eV as C3 representing the ketone groups. No peak was observed at 289.1 eV, which is representative of the carboxyl groups. Thus, there was apparently no observation of carboxyl groups on the surface of the oxidised fibres. Nevertheless, the COOH peaks observed by the FTIR spectra suggest that carboxyl groups were formed in the bulk of the fibres during the N_2O_4 oxidation.

Dorris (81) noted that the binding energies of each category vary within 1-1.5 eV (Fig. 4.14), which indicates that the binding energy peaks of each category of the carbon component may overlap. It might therefore be assumed that the peak observed at the binding energy of 288.4 eV (C3) results from the peaks for the binding energy of ketone at 287.9 eV and of carboxyl at 289.0 eV. Consequently the binding energy of 288.4 eV in this work could represent the contribution of both C3 (C=O) and carboxyl groups C4 (O=C-OH) in a 1:1 ratio. This assumption agrees better with the IR findings of the other researchers (15, 16), who claim that both ketone and carboxyl groups are produced during the N_2O_4 oxidation of cellulose. It would also confirm the formation of COOH that observed in the FTIR spectra in this work. Consequently, the values of C3 reported here represent the formation of ketone and carboxyl during oxidation. When the percentage of C3 changes, it is difficult to know which one of the two increases more.

This is because the change in percentage of C3 during the oxidation treatments is very small (+2.6% for softwood, +1.1% for bagasse and -1.2% for aspen).

TABLE 4.7 Binding Energies of Oxygen-containing Structural Features (127).

Feature	Material	Binding energy C1s (eV)
C-OH	**Ethanol , Methanol**	**286.6**
C=O	**Acetone**	**287.9**
C-O-C	Diethyl ether	286.5
-C=O Ò-C	Acetates	289.2 286.6
-C=O Ò-H	**Polyacrylic acid**	**289.1**
-C=O Ò-C	Polyalkylacrylates	288.9 286.6
-C=O Ò-C	Polyalkylmethacrylates	288.8 286.7
-C-O-C-O-	Polymethyleneoxide	287.8
C=O	Polyacetyl-p-xylylene	287.6
-O C=O -O	Polycarbonates	290.6

It may be briefly concluded that the values of C1, C2 and C3 were not related to the formation of COOH, since no peak was observed in the binding energy of 289.2 eV representing the carboxyl groups. The decrease in C1 and the increase in C2 were in agreement with the effect of the oxidation. At 1.25-1.66% N_2O_4 /fibre, C1 showed the maximum decrease for all of the oxidised fibres. This implies a maximum reduction of the lignin and extractives. The O/C ratio showed the effect of the oxidation and the increasing the hydrophilic character of the oxidised fibres on the fibres surface. This ratio remained constant for the aspen, which had a minimum formation of carboxyl groups. This implies that the hydrophilic character of the aspen fibres did not improved as a result of the N_2O_4 oxidation. The addition of 1% $MgCO_3$ lowered the decrease in C1 and the increase in C2. This is an indication of lower transformation of C1, C2 and C3 in the presence of $MgCO_3$. At the same time the O/C ratios were reduced.

4.4   IGC Technique

After being ground, the oxidised fibres (Table 3.2) were screened (40 mesh) and weighed. They were then placed in IGC copper columns and the retention times of alkane and polar probes as listed in table 3.3 were measured at 30, 50, 70 and 90 $^{\circ}$C. The vapour volume injection varied in the beginning to see the change in the retention time. No change was observed in the retention time, indicating that retention volume is independent of sample size. This proves that Henry's law indeed reached. The alkane probes were hexane, heptane octane and nonane, and the polar probes were nitromethane and dichloromethane having acid character, tetrahydrofurane and diethyl ether having basic character and acetone and ethyl acetate having amphoteric character. These different type of the polar probes were selected as we did not aware the acid base character of the three types of the oxidised fibres. The fibres oxidised by the N_2O_4 gas in the presence of $MgCO_3$ were prepared similarly, and the retention times were measured for comparison. Finally the acid-base constants were computed as described in section three, and reported in Tables 4.11 and 4.13.

4.4.1 N_2O_4 oxidation of the fibres

4.4.1.1   Surface specific area

The surface areas of the untreated and oxidised softwood fibres were measured at 5°C, 10% consistency and at 3.65-% N_2O_4 /Fibre.

The specific surface areas of the untreated and treated softwood fibres were determined using the BET equation and the nitrogen adsorption isotherm, and were 1.600 m^2/g and 1.365 m^2/g, respectively. The reduction in surface area due to oxidation was thus determined to be 14.7%. The lower specific surface area obtained for the treated fibres could be explained by the fact that the pores of the fibres shrink during oxidation. This might have produced higher density,ρ, in the Page equation which could lead to the greater tensile strength.

4.4.1.2 Dispersion Component of the Surface Energy

Table 4.8 shows the measured $-\Delta G_A$ ($-CH_2-$) and γ^D_S for all of the untreated and oxidised fibres. To measure the values of $-\Delta G_A$ ($-CH_2-$) and γ^D_S for each type of the untreated or oxidised fibres, the retention volume of the alkane probes corresponding to that special fibres were used. The values obtained for $-\Delta G_A$ ($-CH_2-$) of the untreated bleached kraft softwood are close to those reported in the literature. Gurnagul and Gray (128) reported a value of 2.90 kJ/mol for kraft pulp and Dorris (91) a value of 2.70 kJ/mol for TMP, both at 25 °C column temperature.

	This work	Ref. (128)
°C	$-\Delta G_A(-CH_2-)$	$-\Delta G_A(-CH_2-)$
30	2.58	2.90 (25°C)
50	2.12	-
70	1.77	-
90	1.61	-

Fibre species and its chemical composition after the bleaching process also affect the final values of $-\Delta G$ ($-CH_2-$) and γ^D_S. It can be observed that the values of $-\Delta G_A$ ($-CH_2-$) obtained for all untreated and treated fibres decrease with an increase in the temperature of the column. This means that the standard free energy of adsorption of one methylene group has an inverse linear relation with temperature regardless of the nature of the cellulosic fibres. The same phenomena are seen for the dispersive component of the surface energy, γ^D_S of the different fibres. These values also decrease with an increase in the column temperature. This is in agreement with previous results (66, 71, 72, 100, 129, 130, 131, 132) that showed decreases in the values of $-\Delta G$ ($-CH_2-$) and γ^D_S with an increase in column temperature.

Standard error in the retention volume, V_N measuresd for the untreated fibres of three type of the fibres due to the column dead volume, column characteristics and loading were up to 3.5%.

TABLE 4.8 Column description, $-\Delta G^0_A$ (-CH$_2$-) and γ^D_S obtained by the IGC measurements for different bleached kraft fibres.

Samples	W (g)	Q^0(50°C) (ml/min)	J	Q(50°C) (ml/min)	$-\Delta G^0_A$(-CH$_2$-) (kJ/mol)				γ^A_S(mJ/m^2)			
					30 (°C)	50 (°C)	70 (°C)	90 (°C)	30 (°C)	50 (°C)	70 (°C)	90 (°C)
S-0	1.603	34,68	0,80	28.53	2.58	2.12	1.77	1.61	27.33	19.25	13.84	11.89
S-1	1.611	50.00	0.82	42.15	1.48	0.88	0.44	0.28	9.09	3.31	0.96	0.37
S-2	1.607	66.66	0.86	60.21	1.15	0.81	0.79	0.75	5.49	2.81	2.78	2.58
S-3	1.393	35.09	0.80	29.17	1.22	0.83	0.43	0.26	6.16	2.96	0.82	0.31
S-4	1.618	23.04	0.94	22.45	2.05	1.10	0.37	0.35	17.56	5.23	0.60	0.56
B-0	1.634	34.68	0.95	34.64	3.01	2.26	1.10	1.04	37.59	21.97	5.33	4.99
B-1	1.592	51.95	0.92	50.08	1.42	0.87	0.65	0.62	8.44	3.26	1.87	1.78
B-2	1.639	30.56	0.95	30.21	2.22	1.37	0.81	0.66	20.38	8.08	2.90	2.01
B-3	1.940	24.22	0.97	24.49	2.28	1.49	1.10	0.60	21.58	9.51	5.38	1.68
B-4	1.645	22.77	0.96	22.68	3.41	2.69	1.41	1.20	48.32	31.08	8.82	6.64
A-0	1.502	34.78	0.58	21.35	2.08	1.08	0.93	0.90	17.96	4.98	3.86	3.75
A-1	1.629	22.64	0.96	22.86	2.00	1.15	0.86	0.44	16.60	5.67	3.26	0.91
A-2	1.617	22.47	0.93	22.03	2.15	1.67	1.59	1.54	19.11	11.95	11.21	10.94
A-3	1.607	30.17	0.82	25.77	2.07	1.60	1.41	1.12	17.39	10.98	8.83	5.78
A-4	1.620	20.99	0.95	20.76	2.55	1.41	0.92	0.90	26.97	8.55	3.77	3.73

The other important point is the different γ^D_S values obtained for each type of fibre at the same temperatures (30, 50, 70 and 90°C). Reduction in the values of γ^D_S when the temperature increased was observed. For each degree increase in the temperature, the of $d\gamma^D_S/dT$ was -0.26 mJ m^{-2} K^{-1} for the softwood. This values was near the value of –0.21 mJ m^{-2} K^{-1} for cellulose (67). The values of γ^D_S as a function of the temperature (increase) is plotted for all three non treated fibres and annexed. The standard error measured for three different fibres was around 15% as temperature increased from 30 to 90 °C and some data were not closed to the curve. This might be explained because of the difficulty we faced during temperature achievement of the column at 90 °C. As the column temperature should be maintained by the Julabo circulating water bath, and the heat loss was high at this temperature, so it might be affected few data concerning the peak maxima and the related calculation for the γ^D_S. It would be preferable to work with this type of apparatus. in the temperature of 20 to 70°C rather than 30-90°C. The values of γ^D_S for the bagasse are somewhat higher than those for softwood and aspen. When the N_2O_4 oxidation ratio is increased from 0.83% to 1.25%, the γ^D_S values decrease, and then increase at higher oxidation ratios. The decrease of γ^D_S for softwood fibres, especially at 1.25% N_2O_4 /fibre is pronounced. Reduction of γ^D_S values of the softwood oxidised fibres might be related to the reduction in the hydrocarbon (extractives) components interactions of these fibres after the oxidation, what has been also observed during reduction in C1 percentage of ESCA. Table 4.8 shows that for the bagasse and aspen fibres, the γ^D_S values of B4 and A4 even exceed the initial values of untreated fibres values of γ^D_S for the bagasse fibres at 2.5% N_2O_4/fibre, B-4, were 48.3, 31.1, 8.8, 6.6 mJ/m^2 as compared to the untreated bagasse fibres, B-0, which were 37.5, 21.9, 5.3, 4.9 mJ/m^2.

4.4.1.3 Surface thermodynamic functions of adsorption

The plots of Ln (V^0_g) versus a $(\gamma^D_L)^{1/2}$ corresponding to the number of carbon atoms of 6,7 and 8 are linear at all temperatures and for all fibres (Figs. 4.46 to 4.51). Linearity is also obtained by plotting Ln(V^0_g) versus 1/T for alkanes and polar probes (Figs. 4.52 to 4.57). This proves the validity of equation 3.22 in these experiments.Only.

the figures related to untreated and oxidised fibres at 2.5% N_2O_4 are reported here in Figs 4.58 to 4.63. Additional figures related to other oxidation ratios are annexed at the end of the thesis. The enthalpy of adsorption, ΔH_A (using the equation 3.22) of the samples is plotted as a function of $a(\gamma^D_L)^{1/2}$ in Figures 4.58 to 4.63. These plots are also linear for all the treated and untreated fibres. This shows that the standard enthalpy of adsorption of the n-alkanes may also be interpreted to be the dispersive value of polar probes. The polar probes react differently in the oxidised softwood, bagasse and aspen fibres, as the oxidation ratio increases. As in the calculation of $-\Delta G$ (-CH_2-), the slope of $\Delta \dot{H}_A$ versus a $(\gamma^D_L)^{1/2}$ for n-alkanes results in an incremental change of enthalpy of one methylene group, $-\Delta H(-CH_2-)$. This value was 4.21, 7.55 and 7.01 kJ/mol for bleached kraft softwood, bagasse and aspen, respectively. It should be mentioned that 4.21 kJ/mol, the value of $-\Delta H(-CH_2-)$ obtained in this work for bleached kraft softwood, is close to 4.10 kJ/mol reported by Chtourou and Riedl (72).

Linearity is always observed for $-\Delta H_A$ versus $a(\gamma^D_L)^{1/2}$ when the number of carbons is increased in the case of all untreated and oxidised fibres (Figs. 4.58 to 4.63). (Figs. 4.58 to 4.63). The values of $-\Delta H(-CH_2-)$ for C9 were slightly higher for softwood and bagasse fibres than for the three other alkanes. This could be due to the following reasons. The values of $-\Delta G(-CH_2-)$ for C9 were slightly higher for softwood and bagasse fibres than for the other three alkanes. This could be due to the following reason: Nonane is a product with a high molecular weight. Penetration of this probe to the solid stationary phase take longer time than the other alkanes. So its retention time would be usually more as compared with that of hexane, heptane or octane. This was already observed in reference (133).

Linearity of $-\Delta H_A$ versus C6, C7 and C8 was observed for all samples. Straight line of alkanes passing through these three regular points were traced for all of the untreated and treated fibres. Then the $-\Delta H^{SP}_A$ of the samples were measured by the difference between $-\Delta H_A$ values of polar probes and the above straight line. This has been schematically illustrated in Figs. 4.58, 4.60 and 4.62.
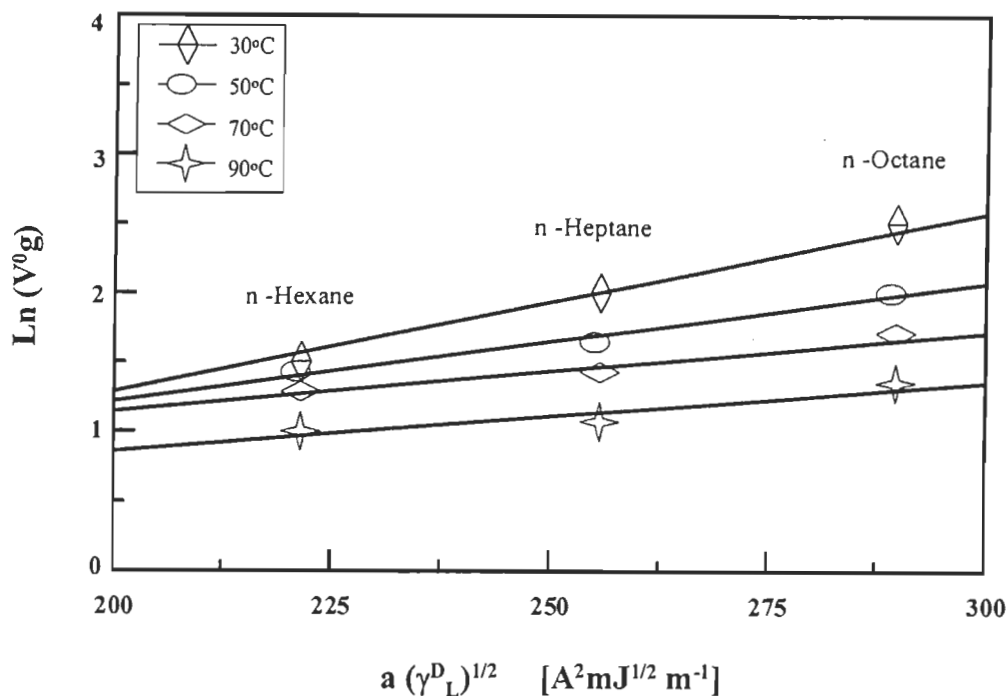
FIGURE 4.46 Linearity between ln (V^0_g) and $a(\gamma^D_L)^{1/2}$ for the number of carbons of the alkane probes of the untreated bleached kraft softwood fibres.
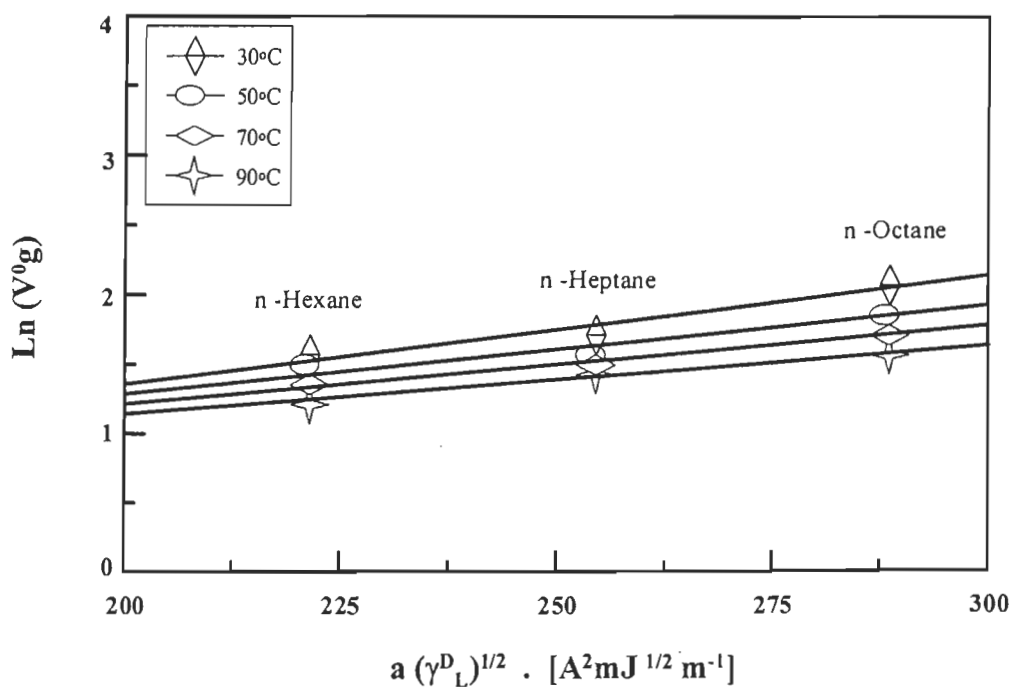
FIGURE 4.47 Linearity between ln (V^0_g) and $a(\gamma^D_L)^{1/2}$ for the number of carbons of the alkane probes of the oxidised bleached kraft softwood fibres with 2.5% N_2O_4.
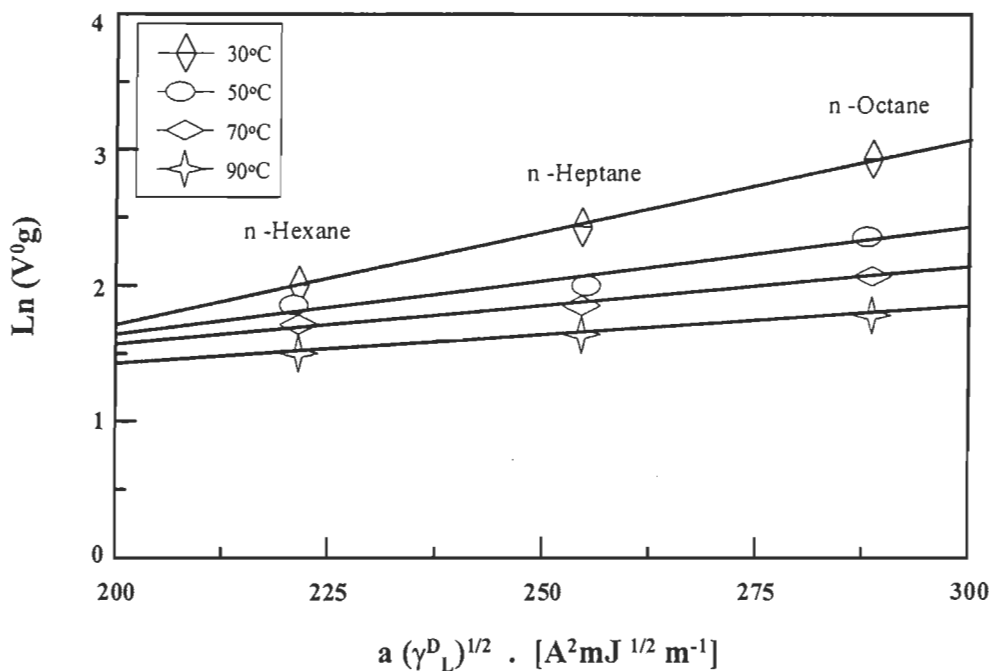
FIGURE 4.48 Linearity between ln (V^0_g) and $a(\gamma^D_L)^{1/2}$ for the number of carbons of the alkane probes of the untreated bleached kraft bagasse fibres.
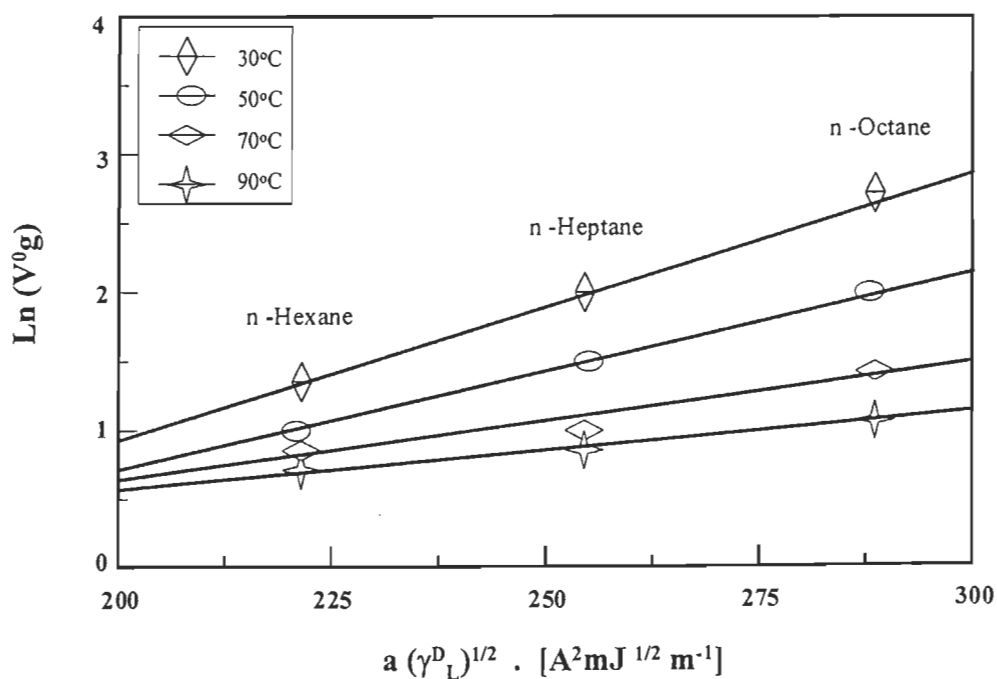
FIGURE 4.49 Linearity between ln (V^0_g) and $a(\gamma^D_L)^{1/2}$ for the number of carbons of the alkane probes of the bleached kraft bagasse fibres with 2.5%N_2O_4.
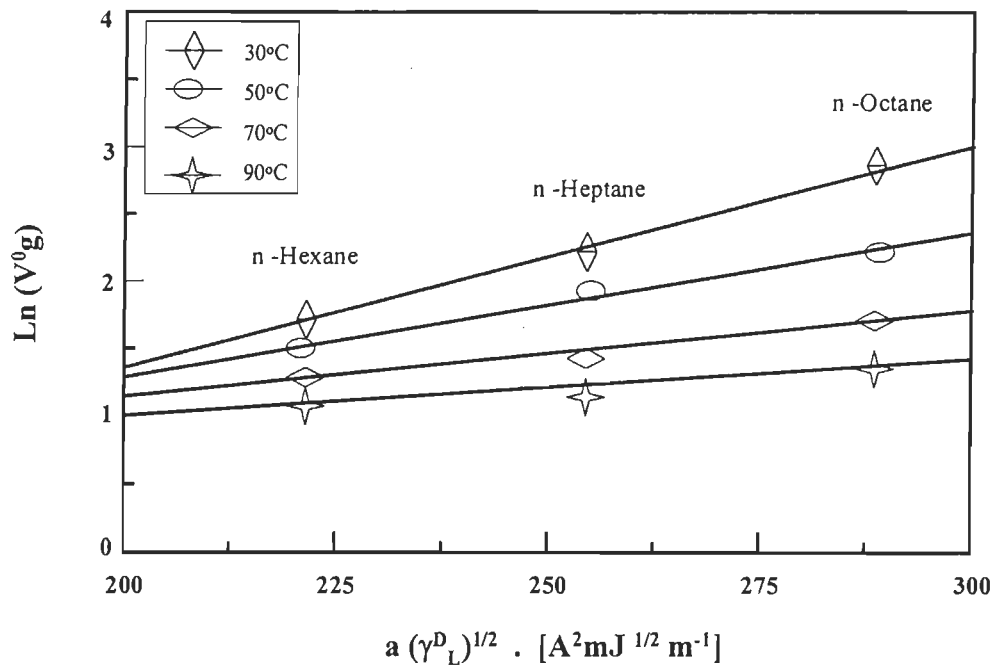
FIGURE 4.50 Linearity between ln (V^0_g) and $a(\gamma^D_L)^{1/2}$ for the number of carbons of the alkane probes of the untreated bleached kraft aspen fibres.
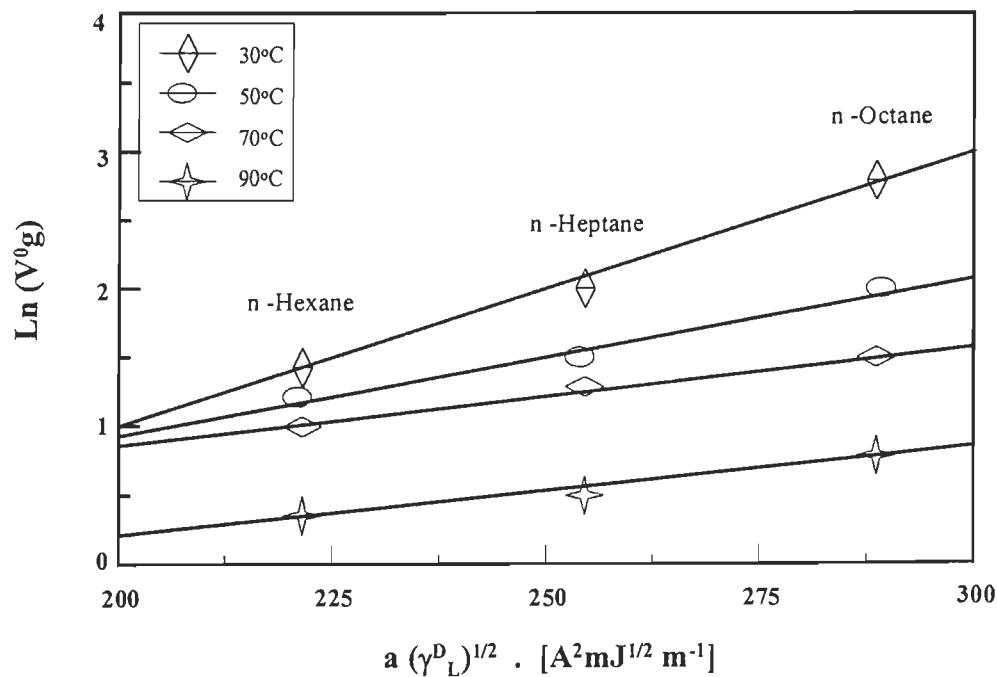
FIGURE 4.51 Linearity between ln (V^0_g) and $a(\gamma^D_L)^{1/2}$ for the number of carbons of the alkane probes of the bleached kraft aspen fibres with 2.5%N_2O_4.
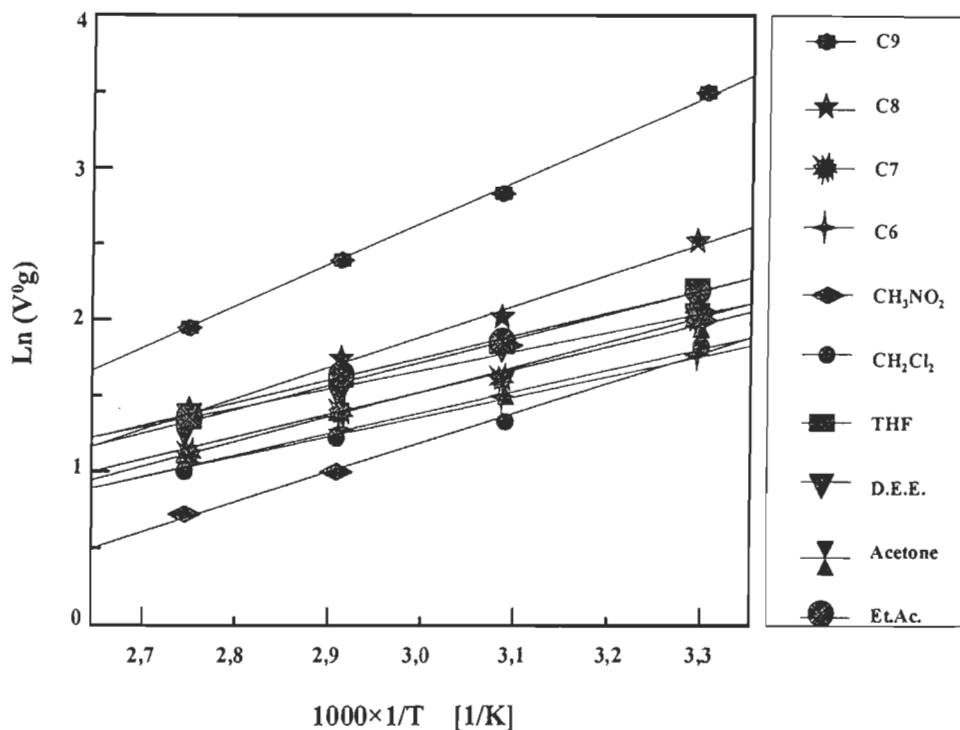
FIGURE 4.52   Linearity of ln (V^0_g) versus the inverse temperature of injection of the alkane and polar probes to the untreated softwood fibres.
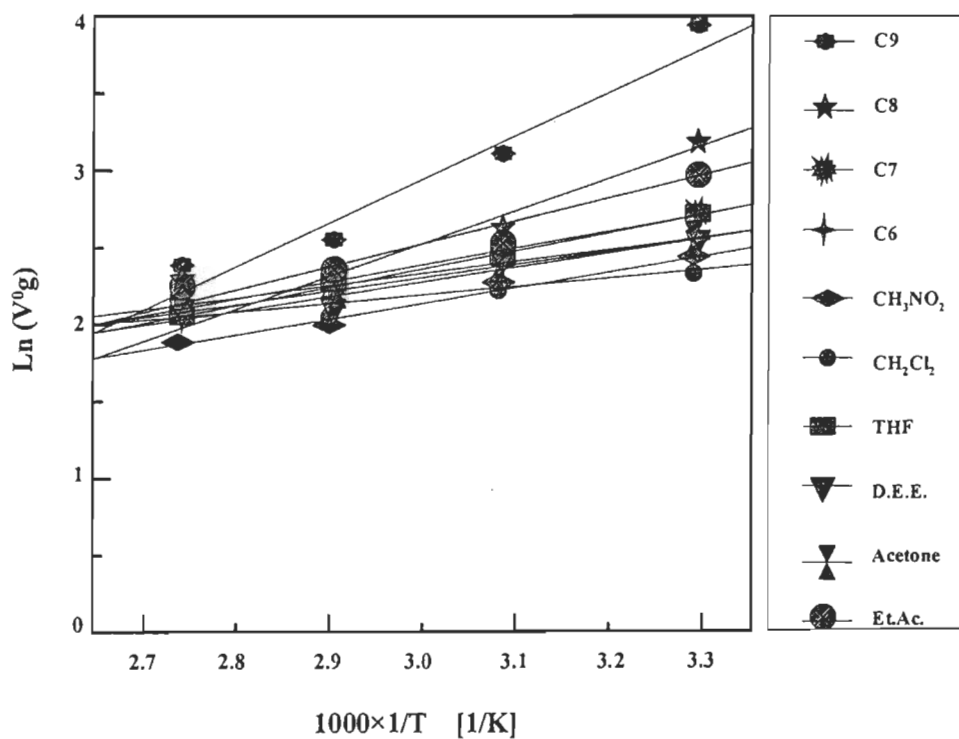
FIGURE 4.53   Linearity of ln (V^0_g) versus the inverse temperature of injection of the alkane and polar probes of the oxidised softwood fibres with 2.5% N_2O_4.
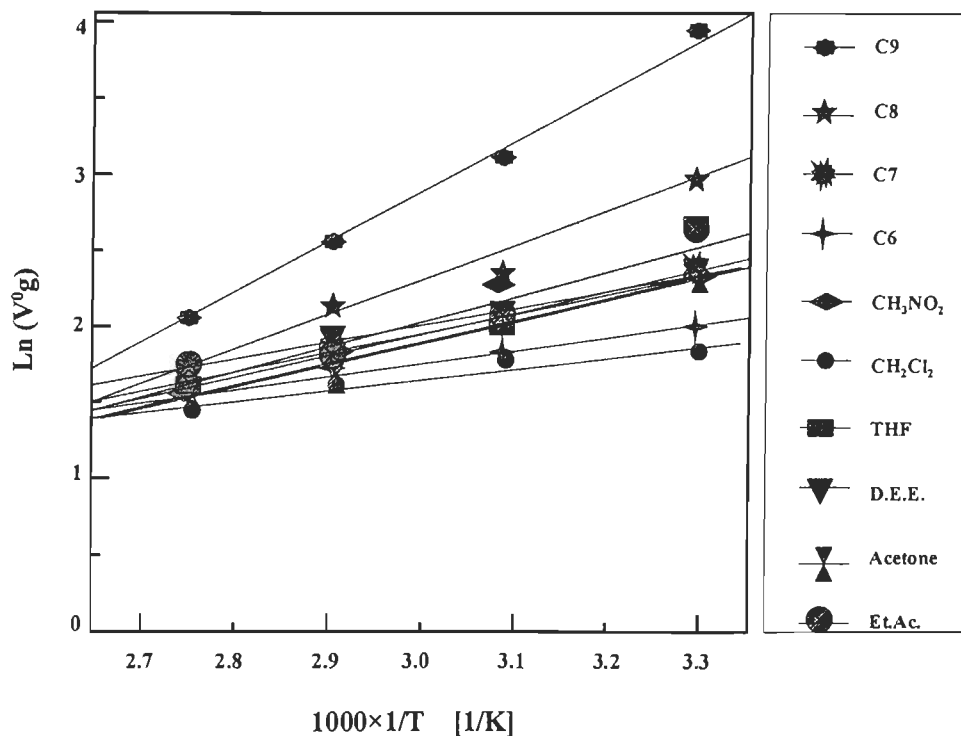
FIGURE 4.54   Linearity of ln (V^0_g) versus the inverse temperature of injection of the alkane and polar probes of the untreated bagasse fibres.
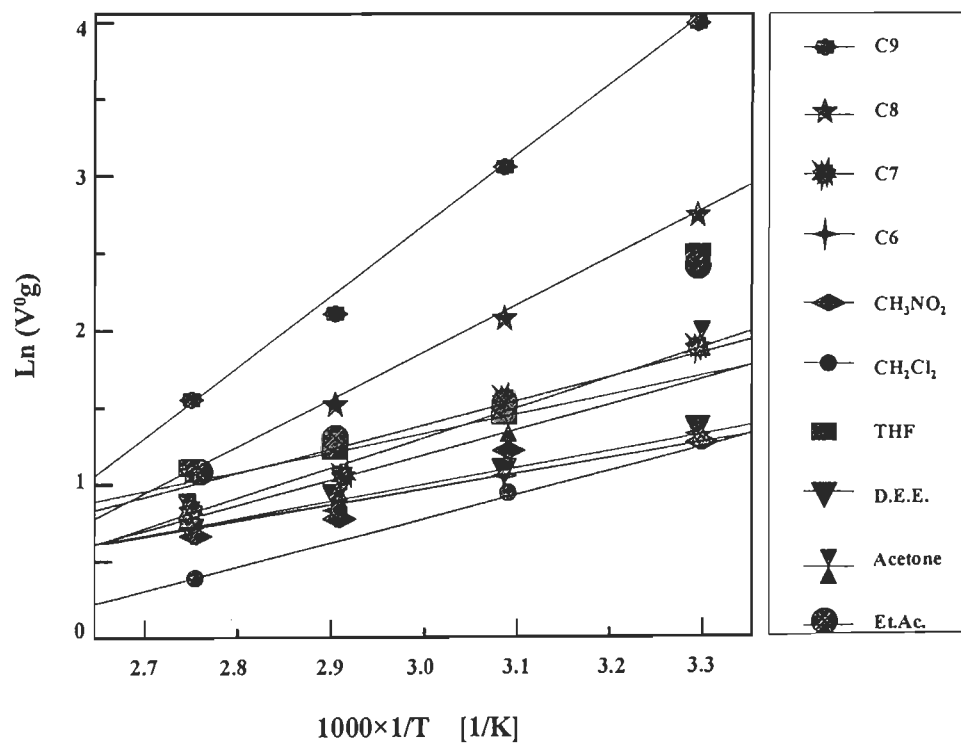
FIGURE 4.55   Linearity of ln (V^0_g) versus the inverse temperature of injection of the alkane and polar probes of the oxidised bagasse fibres with 2.5% N_2O_4.
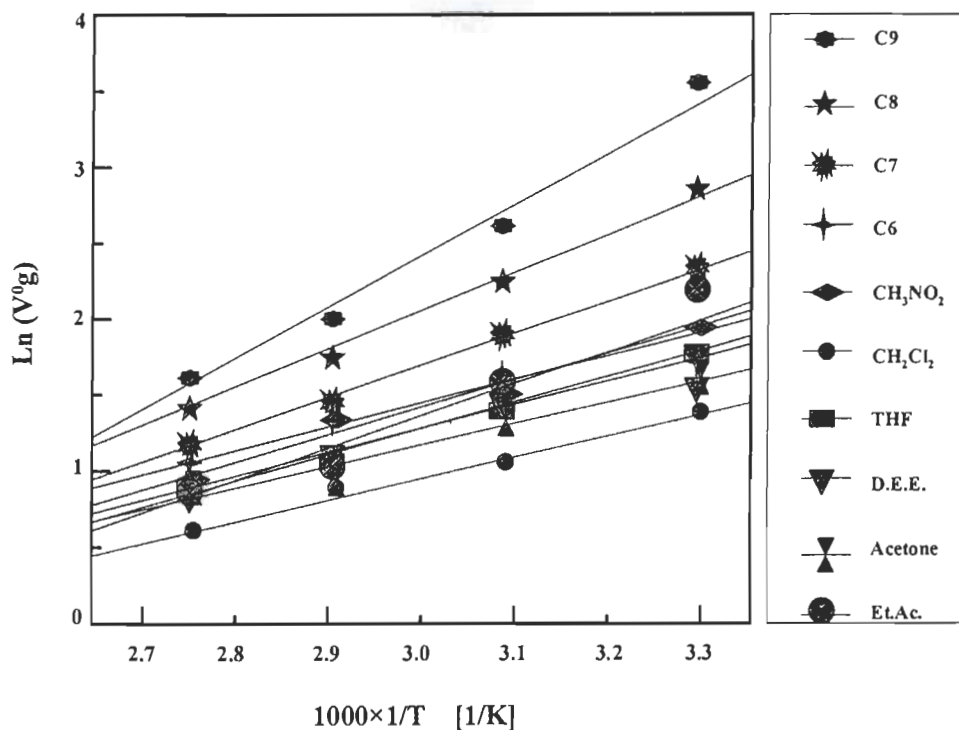
FIGURE 4.56 Linearity of ln (V^0_g) versus the inverse temperature of injection of the alkane and polar probes of the untreated aspen fibres.
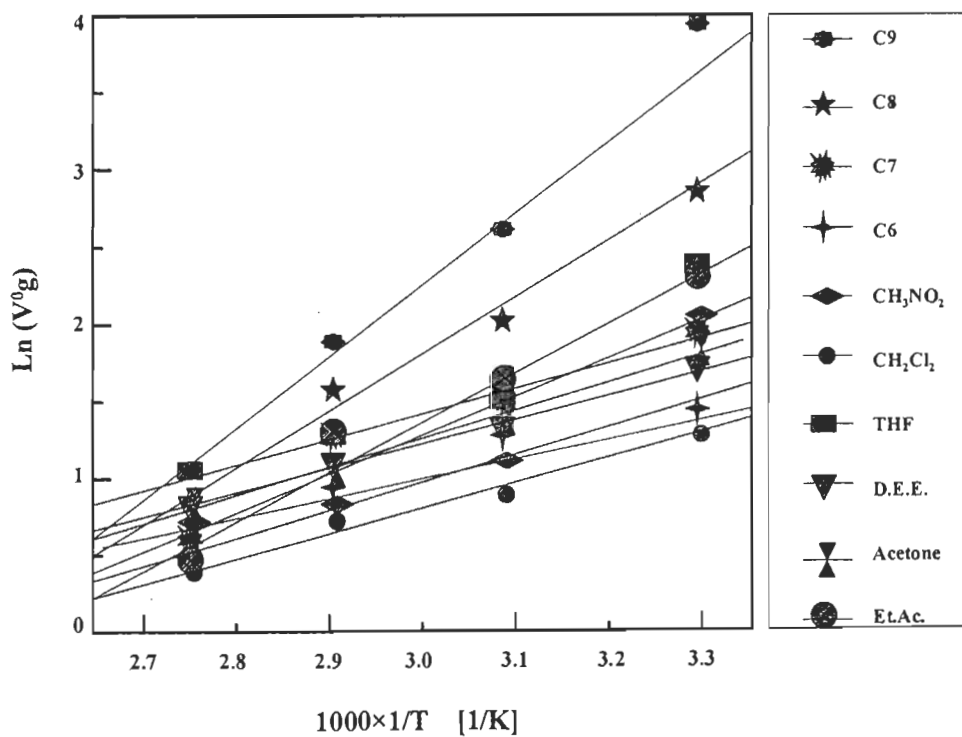
FIGURE 4.57 Linearity of ln (V^0_g) versus the inverse temperature of injection of the alkane and polar probes of the oxidised aspen fibres with 2.5% N_2O_4.

TABLE 4.9 Standard enthalpies for zero–coverage adsorption on the stationary phases of bleached kraft fibres.

N$_2$O$_4$ oxidation	$-\Delta H_A$ (kJ/mol)														
	Softwood					Bagasse					Aspen				
	S-0	S-1	S-2	S-3	S-4	B-0	B-1	B-2	B-3	B-4	A-0	A-1	A-2	A-3	A-4
C6	10.3	8.1	7.8	2.7	4.1	6.8	8.6	7.6	6.8	10.3	9.5	5.5	7.4	4.6	13.7
C7	12.4	10.8	8.8	4.5	8.4	10.2	10.8	13.8	14.0	17.5	16.7	14.2	15.2	9.5	18.8
C8	14.6	13.6	11.3	8.8	13.8	15.7	16.5	22.1	22.8	25.1	23.7	24.1	21.	16.0	29.2
C9	22.7	20.8	15.3	19.1	25.0	30.5	21.7	34.2	32.8	41.9	30.6	32.9	25.9	25.9	41.1
CH$_3$NO$_2$	40.0	14.5	10.9	24.3	10.7	14.6	14.2	49.0	14.5	20.9	11.2	9.9	7.5	16.8	16.9
CH$_2$Cl$_2$	10.3	9.0	9.9	3,5	4.2	7.6	15.5	20.1	10.2	12.2	11.1	7.2	6.6	3.8	11.7
THF	9.7	10.4	7.5	10.7	9.2	13.7	18.9	18.1	13.8	18.2	14.6	11.1	14.7	12.1	16.5
D.E.E.	7.1	6,4	9.8	3.2	7.1	6.4	9.1	10.3	11.5	10.6	8.9	6.7	6.4	3.3	9.1
Acetone	8.9	8.8	10.3	4.6	6.2	7.6	12.3	15.0	9.6	11.9	9.9	8.1	14.5	6.5	11.0
Ethyl Ace.	11.1	10.0	8.7	6.3	10.0	11.6	15.1	18.9	14.2	18.5	21.0	15.9	13.7	8.2	24.3

TABLE 4.10   Specific enthalpies of adsorption of untreated and oxidised bleached kraft fibres.

N_2O_4 oxidation	$-\Delta H^{SP}_A$ (kJ/mol)														
	Softwood					Bagasse					Aspen				
	S-0	S-1	S-2	S-3	S-4	B-0	B-1	B-2	B-3	B-4	A-0	A-1	A-2	A-3	A-4
CH_3NO_2	32.0	12.5	3.8	24.5	11.1	11.7	9.5	48.0	14.9	16.5	8.6	10.0	5.8	16.5	11.2
CH_2Cl_2	4.7	8.8	3.1	5.7	8.1	8.7	14.4	24.5	16.0	13.1	13.7	13.8	9.2	8.1	12.0
THF	1.0	4.4	3.2	9.1	5.8	8.5	11.1	11.8	8.2	8.5	6.9	6.0	8.0	9.0	5.1
D.E.E.	0.8	5.0	2.5	4.2	8.0	4.9	5.0	10.5	13.0	8.0	7.9	9.3	5.7	4.5	5.1
Acetone	2.3	7.2	4.8	6.8	9.0	7.3	9.0	17.0	13.6	10.9	10.8	13.0	15.9	9.8	9.5
Ethyl Ace.	2.2	4.4	1.9	5.0	8.0	6.8	9.1	13.0	10.0	10.0	13.0	11.8	8.10	9.0	13.0
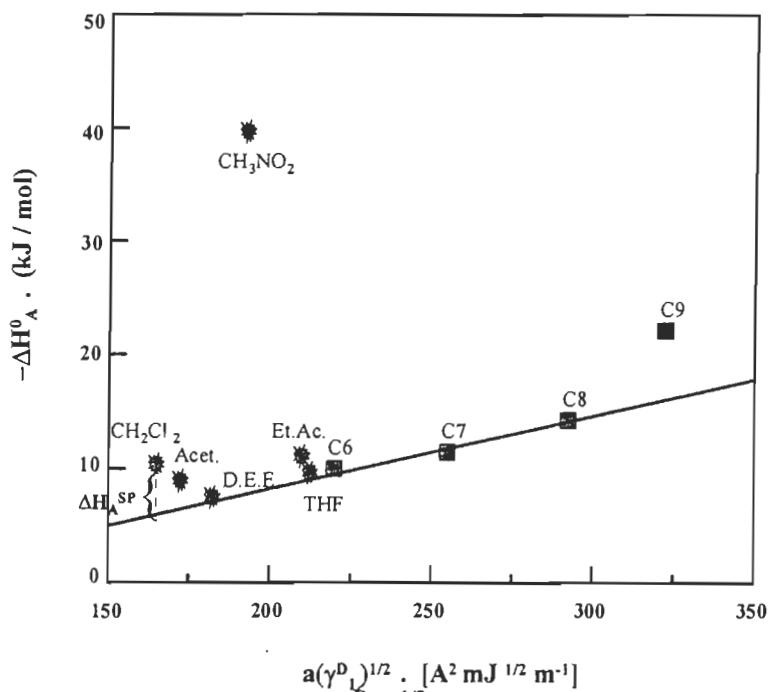
FIGURE 4.58 Plot of $-\Delta H_A$ versus a $(\gamma^D_L)^{1/2}$ of the alkane and polar probes of the untreated bleached kraft softwood fibres.
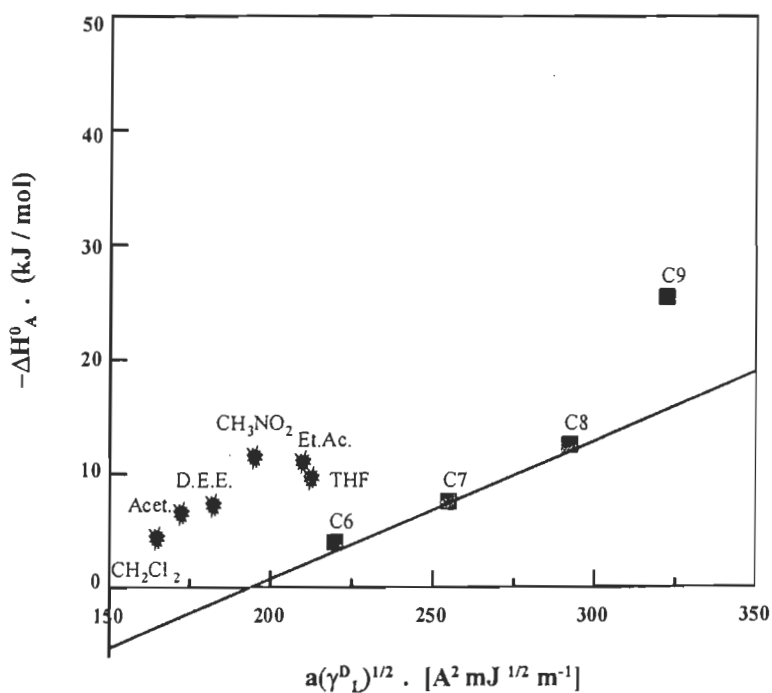
FIGURE 4.59 Plot of $-\Delta H_A$ versus a $(\gamma^D_L)^{1/2}$ of the alkane and polar probes of the oxidised bleached kraft softwood fibres at 2.5% N_2O_4/fibre.
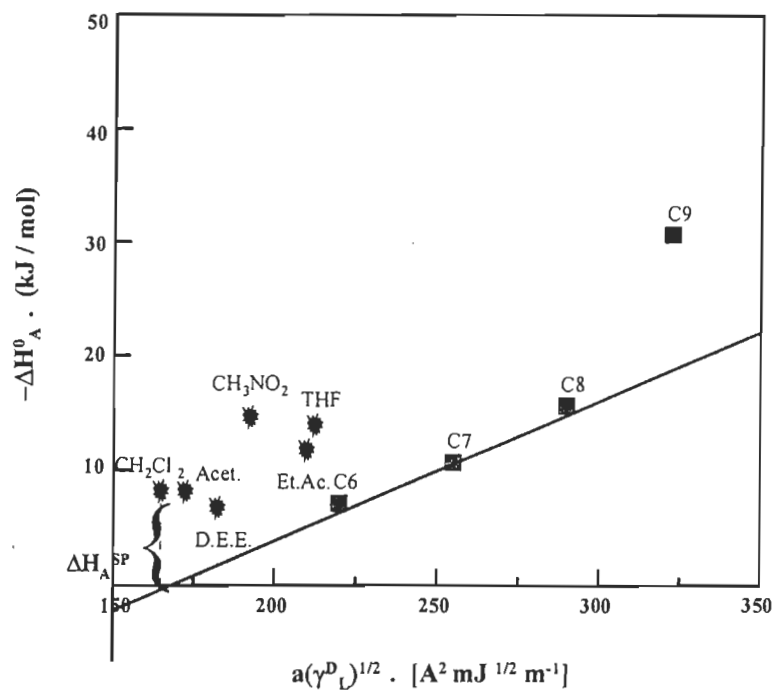
FIGURE 4.60   Plot of $-\Delta H_A$ versus a $(\gamma^D_L)^{1/2}$ of the alkane and polar probes of the untreated bleached kraft bagasse fibres.
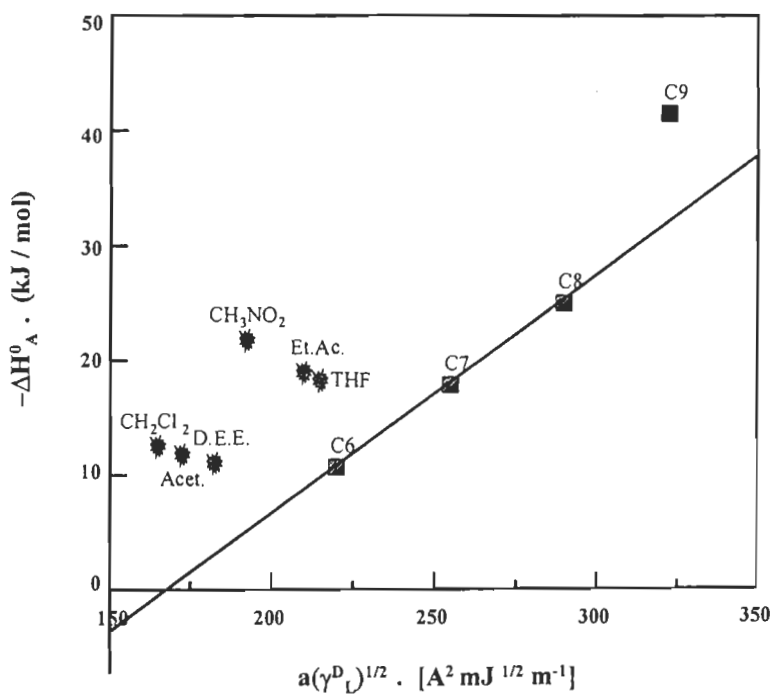
FIGURE 4.61   Plot of $-\Delta H_A$ versus a $(\gamma^D_L)^{1/2}$ of the alkane and polar probes of the oxidised bleached kraft bagasse fibres at 2.5%N_2O_4/fibre.
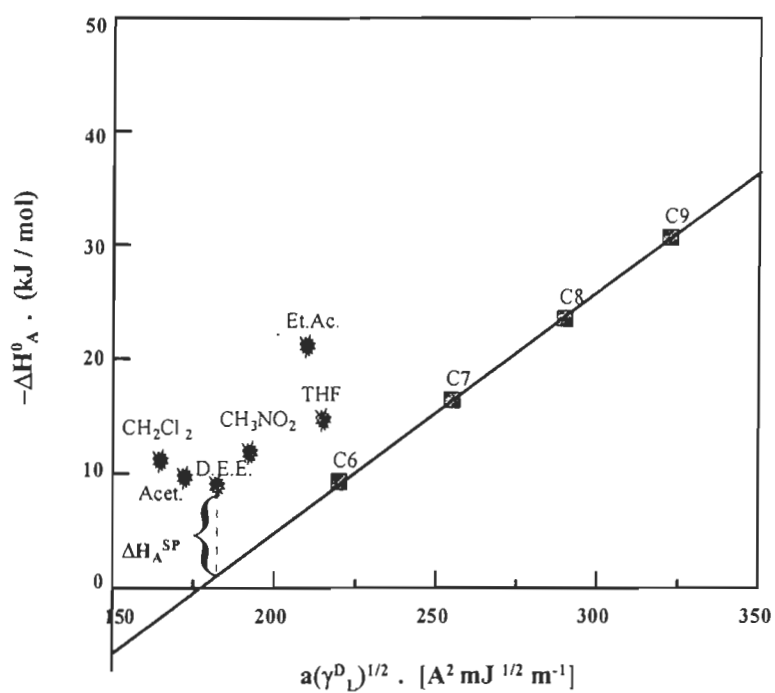
FIGURE 4.62 Plot of $-\Delta H_A$ versus a $(\gamma^D_L)^{1/2}$ of the alkane and polar probes of the untreated bleached kraft aspen fibres.
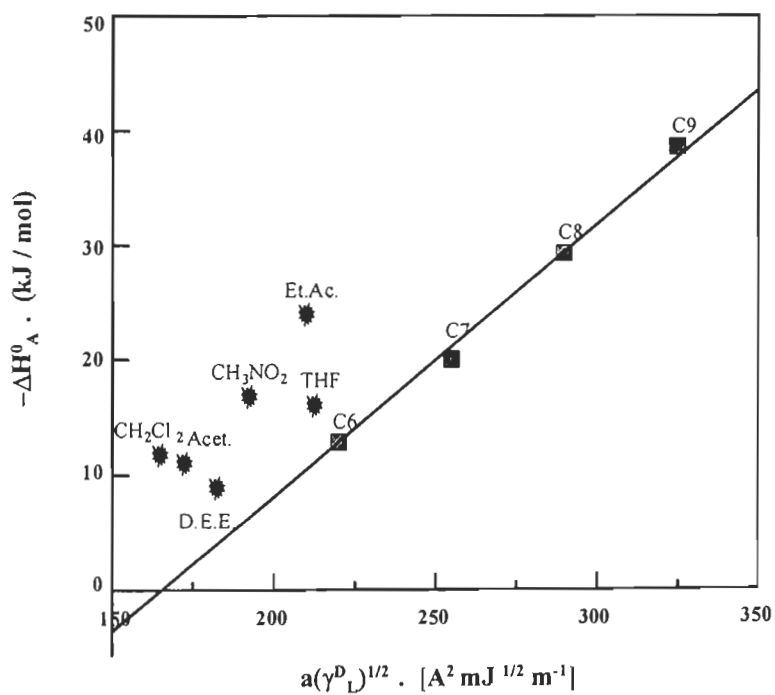
FIGURE 4.63 Plot of $-\Delta H_A$ versus a $(\gamma^D_L)^{1/2}$ of the alkane and polar probes of the oxidised bleached kraft aspen fibres at 2.5%N_2O_4/fibre.

4.4.1.4   Acid-base interaction constants, K_A and K_B

The $\Delta H^{SP}{}_A$ for the various polar probes were computed based on their position regarding the straight line for the alkane probes in the $\Delta H^0{}_A$ graphs (as illustrated in Figs. 4.58, 4.60, and 4.62). These are summarised in Table 4.10. The acid number values, AN* for the probes used in this work were determined according to the method proposed by Riddle and Fowkes (103) and the plots shown in Figures 4.64 to 4.69 corresponding the $\Delta H^{SP}{}_A$/AN* versus AN*/DN were generated. It can be clearly observed that the slope and intercept of all three fibres had increased due to the N_2O_4 treatment. This means the acid-base interaction was increased by the oxidation. The values of K_A are represented by the slopes, while the K_B values are represented by the intercepts of the curves. These are reported in Table 4.11.

Considering that the direction and the amount of changes in K_A and K_B due to the oxidation are not linear, I_{SP} were also calculated to provide a better understanding of the over-all specific acid-base interactions. This value permits comparison of the acid-base characteristics of the different fibres and is given by (68).

$$I_{SP} = 2\,K_A \times K_B$$

The K_A and K_B values obtained for softwood fibres in Table 4.11 indicate that these fibres are amphotheric (K_A=0.49, K_B=0.55), whereas the bagasse fibres are more basic (K_A=1.7, K_B=2.25) and the aspen fibres are more acidic (K_A=2.9, K_B=1.90). Even though the specific interaction of the fibres was increased by the oxidation, the strength properties were not increased due to the simultaneous cellulose degradation (hydrolysis) (see the strength properties graphs of the oxidised fibres in section 4.5).
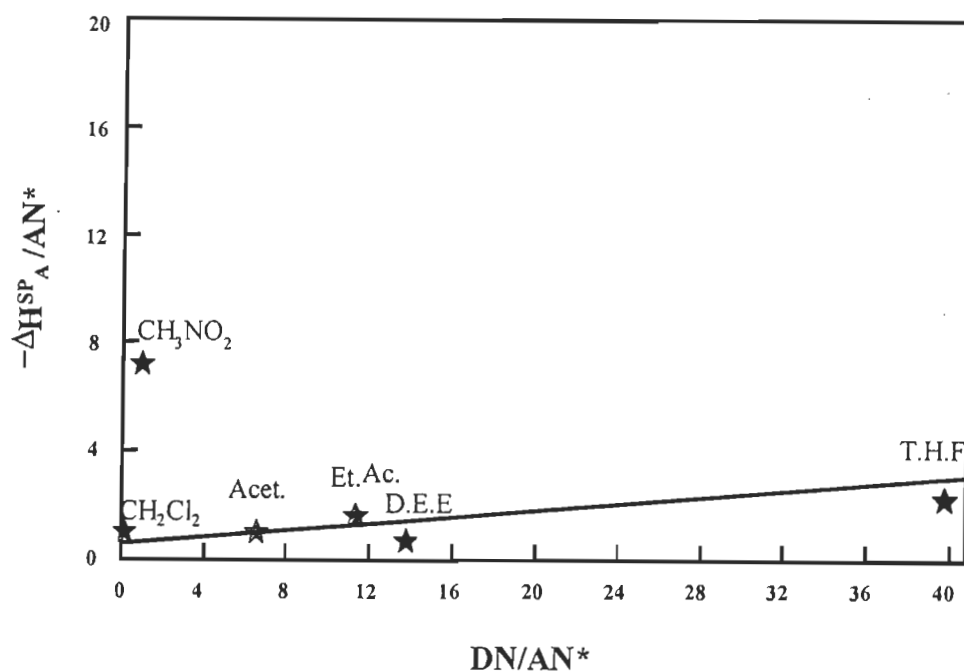
FIGURE 4.64 Plot of $-\Delta H^{SP}_A/AN^*$ versus DN/AN* for the untreated bleached kraft softwood fibres allowing the determination of the acceptor constant, K_A and donor constant, K_B.
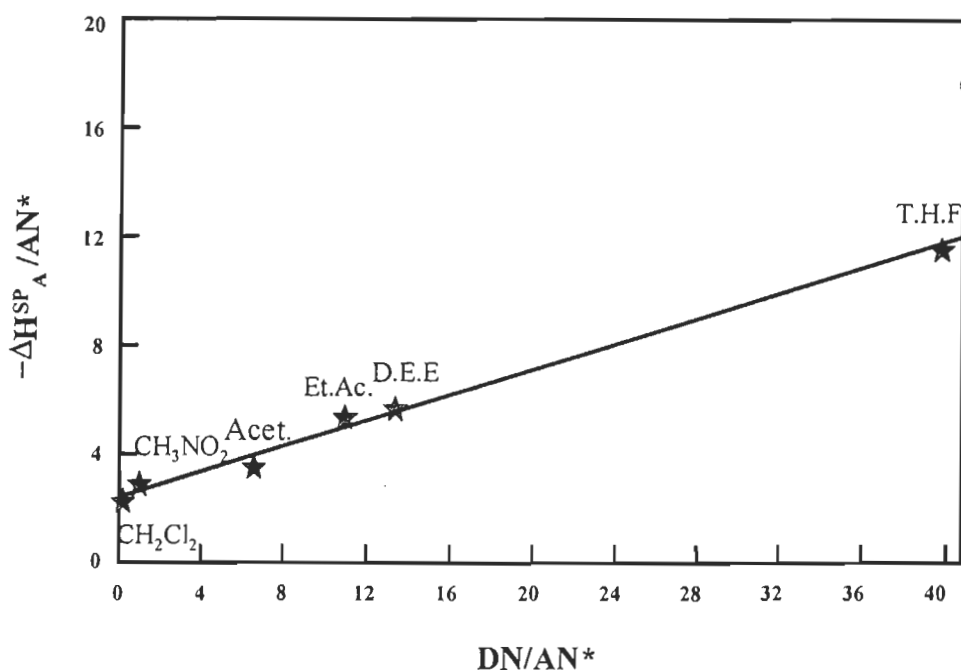
FIGURE 4.65 Plot of $-\Delta H^{SP}_A/AN^*$ versus DN/AN* for the oxidised bleached kraft softwood fibres with 2.5 % N_2O_4 allowing the determination of the acceptor constant, K_A and donor constant, K_B.
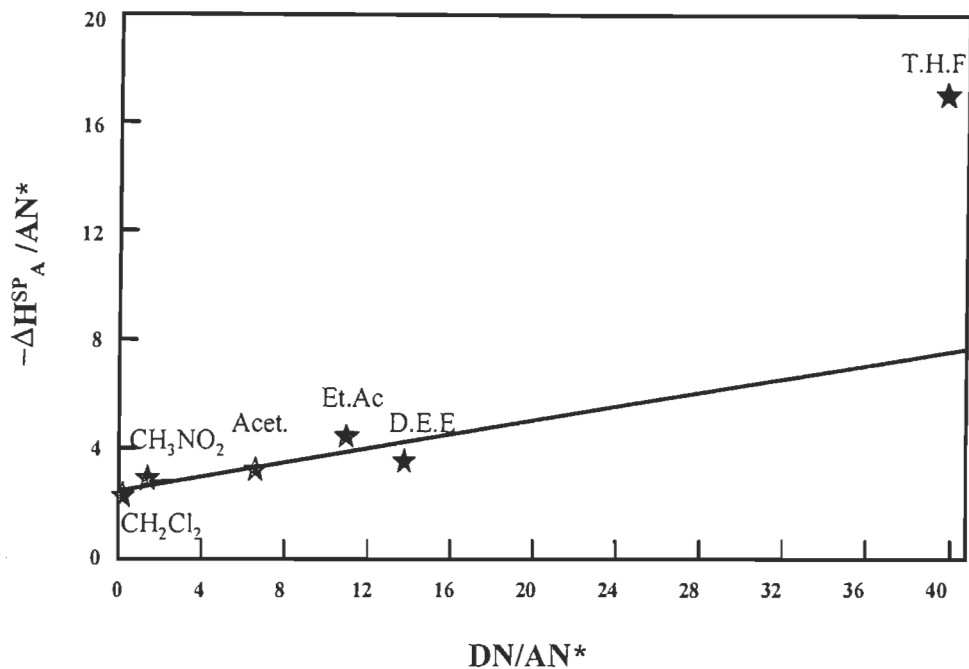
FIGURE 4.66 Plot of $-\Delta H^{SP}_A/AN^*$ versus DN/AN* for the untreated bleached kraft bagasse fibres allowing the determination of the acceptor constant, K_A and donor constant, K_B.
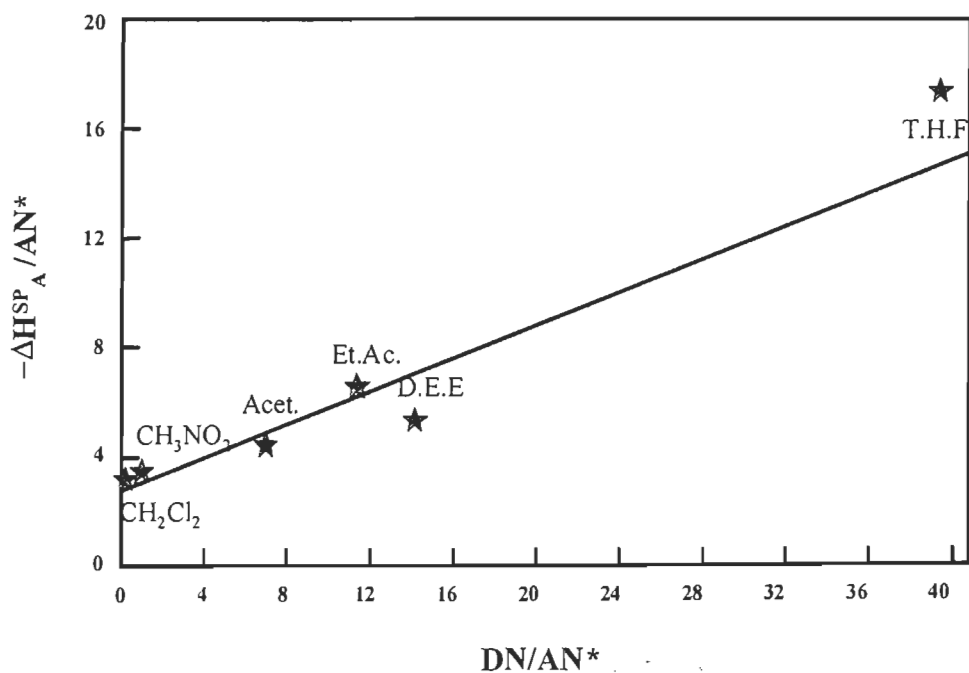
FIGURE 4.67 Plot of $-\Delta H^{SP}_A/AN^*$ versus DN/AN* for the oxidised bleached kraft bagasse fibres with 2.5 % N_2O_4 allowing the determination of the acceptor constant, K_A and donor constant, K_B.
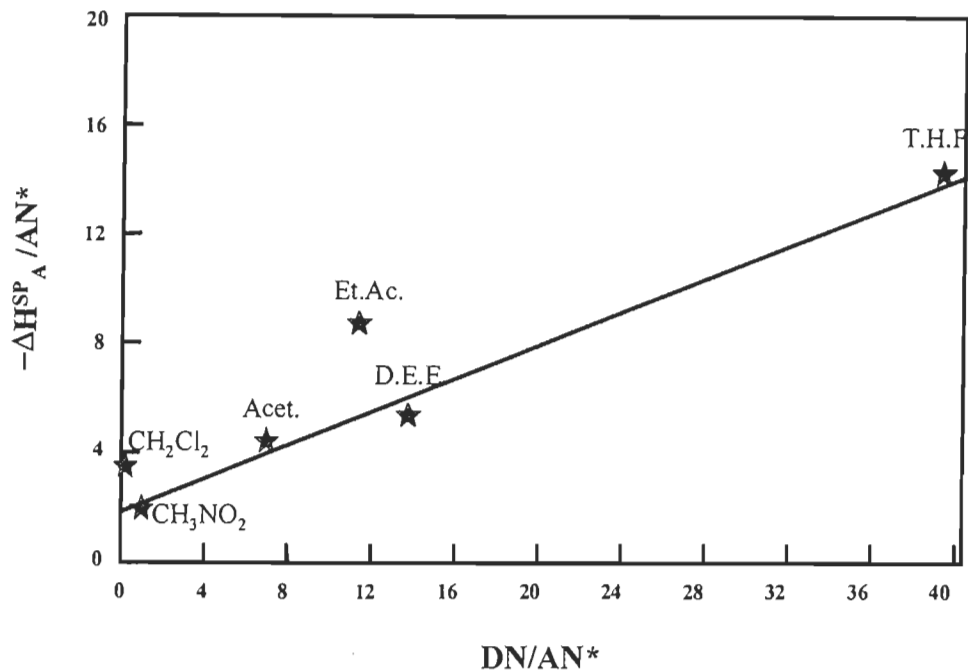
FIGURE 4.68 Plot of $-\Delta H^{SP}_A/AN^*$ versus DN/AN^* for the untreated bleached kraft aspen fibres allowing the determination of the acceptor constant, K_A and donor constant, K_B.
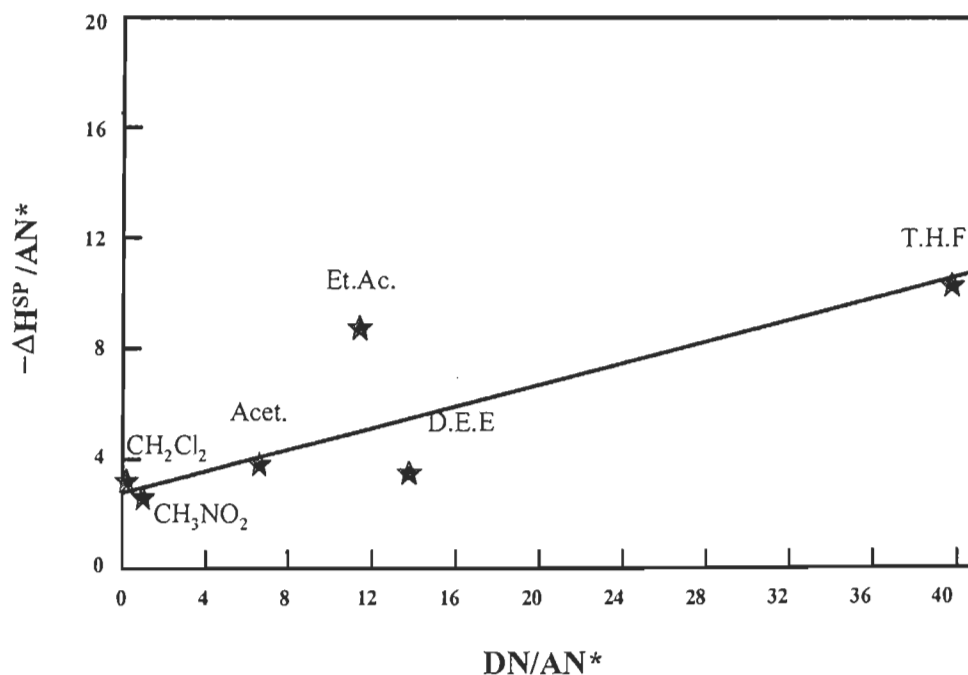
FIGURE 4.69 Plot of $-\Delta H^{SP}_A/AN^*$ versus DN/AN^* for the oxidised bleached kraft aspen fibres with 2.5 % N_2O_4 allowing the determination of the acceptor constant, K_A and donor constant, K_B.

TABLE 4.11 Acid-base constants and specific interaction of untreated and oxidised fibres.

Sample	Description		K_A	K_B	I_{SP}
Softwood	**S-0**	Untreated	**0.49**	**0.55**	**0.54**
	S-1	0.83 %N_2O_4	1.2↑	1.95↑	4.7
	S-2	1.25 %N_2O_4	0.7↑	0.7↑	1.0
	S-3	1.66 %N_2O_4	1.1↑	1.4↑	2.9
	S-4	2.50 %N_2O_4	2.4↑	2.3↑	11.0
Bagasse	**B-0**	**Untreated**	**1.7**	**2.25**	**7.7**
	B-1	0.83 %N_2O_4	3.6↑	1.5↑	10.8
	B-2	1.25 %N_2O_4	2.1↑	5.5↑	23.1
	B-3	1.66 %N_2O_4	3.3↑	3.2↑	21.1
	B-4	2.50 %N_2O_4	2.6↑	2.9↑	14.8
Aspen	**A-0**	**Untreated**	**2.9**	**1.90**	**11.0**
	A-1	0.83 %N_2O_4	2.2↓	3.5↑	15.6
	A-2	1.25 %N_2O_4	3.7↑	1.5↓	11.1
	A-3	1.66 %N_2O_4	2.8↓	2.1↑	11.7
	A-4	2.50 %N_2O_4	1.9↓	2.8↑	10.8

In the case of bagasse fibres, its acidic and basic characters (K_A and K_B) are more than that of softwood (1.7, 2.25 compared to 0.49, 0.55). This might be the indication of higher H-bonding potential of untreated bagasse fibres. On the other hand, the basic character of untreated bagasse fibres lends itself well to the N_2O_4 oxidation since it is an acidic treatment.

When observing the relation between the γ^D_S variation with the O/C ratio during the oxidation (Fig. 4.70 – 4.72), it can be clearly concluded that by the increasing the oxidation ratio, the the γds decreases. This is because the γ^D_S, the dispersive component of the fibres, representing non polar components, the hydrocarures, such as the extractives and fatty acids of the fibres, that was partially removed by the oxidation. This was observed for the softwood as well as for the bagasse fibres, but not for the aspen fibres as expected. In contrast, the polar component, representing the hydrophility of the fibres was increased, what can be seen by the increase in the O/C ratio. This type of relationship between γ^D_S and O/C ratio have also been reported by Kadmem and Riedl in the case of woodfibres grafted by poly methyl metacrylate (96).

The same time, the specific acid-base interaction I_{SP} were increased during the N_2O_4 oxidation, due to the formation of carboxyl groups and improvement in hydrogen bonding (Fig. 4.70 – 4.72) and (Table 4.11). These increases are in agreement with the increase of the COOH intensity of IR peaks. This shows that there is a positive relation between the formation of COOH, O/C ratio and I_{SP}. In the case of the aspen fibres , oxidation did not increased significantly the formation of the COOH. Consequently, no improvement was observed in O/C ratio, neither in the I_{SP} values.(Fig.4.72).
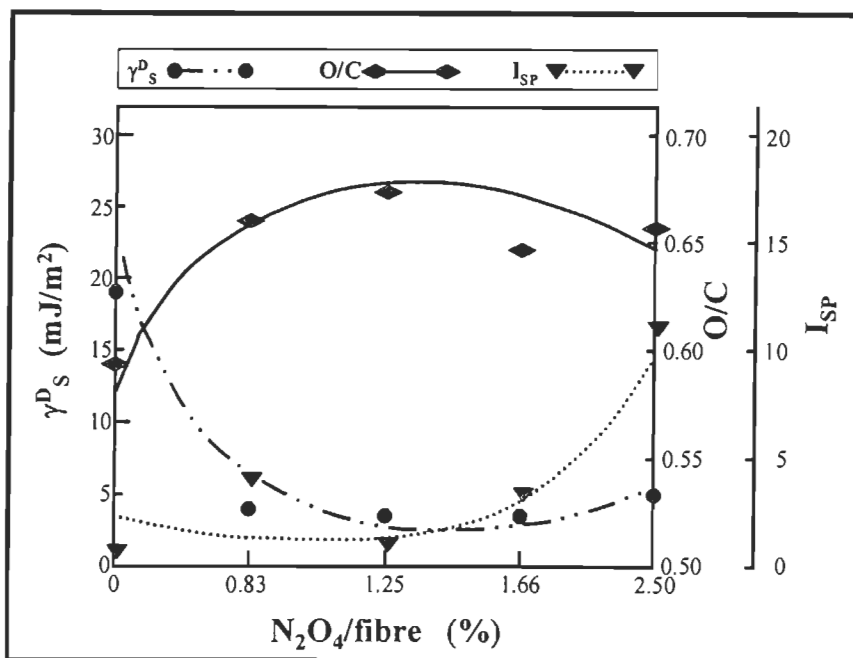
FIGURE 4.70 The relation between γ^D_S with the O/C ratio and the I_{SP} as the function of the percentage of N_2O_4/fibre for the softwood oxidised fibres.
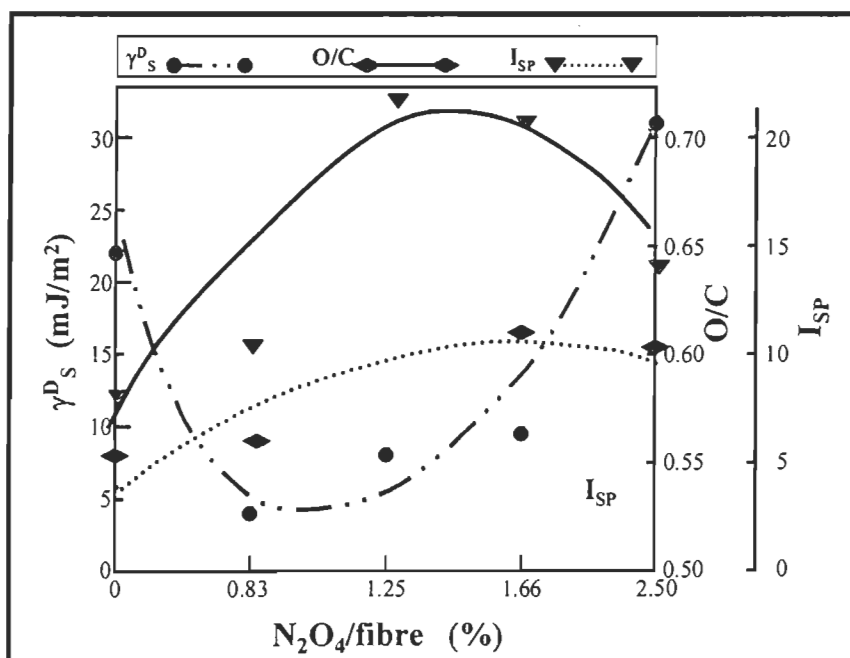
FIGURE 4.71 The relation between γ^D_S with the O/C ratio and the I_{SP} as the function of the percentage of N_2O_4/fibre for the bagasse oxidised fibres.
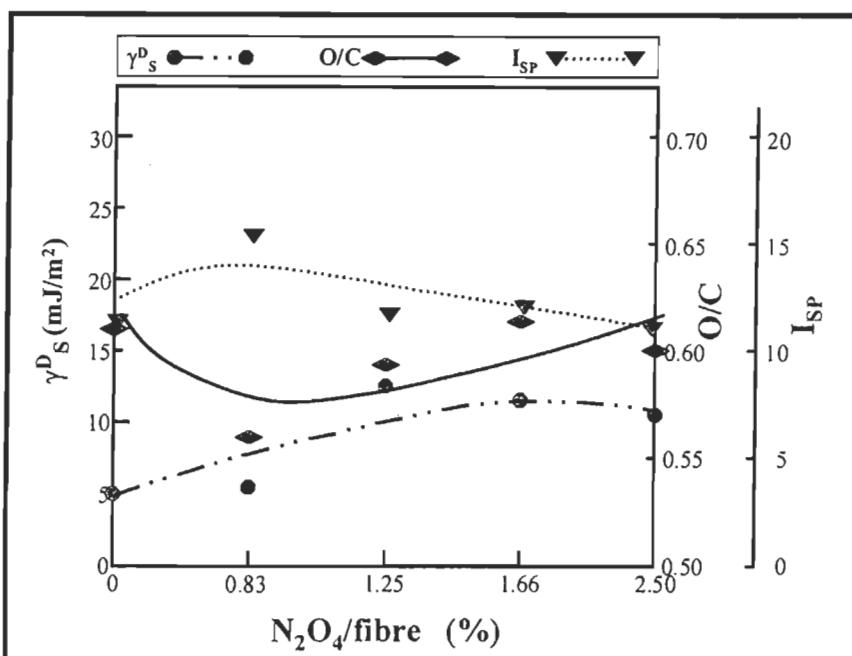
FIGURE 4.72   The relation between $\gamma^D{}_S$ with the O/C ratio and the I_{SP} as the function of the percentage of N_2O_4/fibre for the aspen oxidised fibres.

4.4.2   The effect of the addition MgCO$_3$ during N$_2$O$_4$ oxidation

4.4.2.1   Dispersion component of the surface energy of the fibres

The $-\Delta H^0{}_A$ (-CH$_2$-) and $\gamma^D{}_S$ values of oxidised softwood and bagasse fibres in the presence of 1% MgCO$_3$ are reported in Table 4.12. The $-\Delta H^0{}_A$ (-CH$_2$-) and $\gamma^D{}_S$ decrease with an increase in the temperature of the column. Linearity between $LnV^0{}_g$ and $a(\gamma^D{}_L)^{1/2}$ and between $LnV^0{}_g$ and 1/T are also confirmed.

Some differences in $\gamma^D{}_S$ due to the addition of 1%MgCO$_3$ may be observed. Figures 4.73 and 4.74 are plots of the $-\Delta H^A$ of the alkanes and polar probes versus a $(\gamma^D{}_L)^{1/2}$ for the different oxidation fibres of softwood and bagasse. It can be observed that the position of the polar probes related to the straight line of alkanes is higher for bagasse fibres than for softwood fibres. This indicates higher values of specific enthalpy of adsorption, $-\Delta H^{SP}{}_A$ for bagasse fibres than for the softwood fibres. The values of $-\Delta H^{SP}{}_A$ were measured by the previous procedure and $-\Delta H^{SP}{}_A$/AN* was plotted versus

TABLE 4.12 Column description, $-\Delta G^0_A$ (-CH$_2$-) and γ^D_S obtained from IGC measurements for oxidised bleached kraft fibres using 1% MgCO$_3$.

Samples	W (g)	Q^0(50°C) (ml/min)	J	Q(50°C) (ml/min)	$-\Delta G^0_A$(-CH$_2$-) (kJ/mol)				γ^D_S(mJ/m^2)			
					30 (°C)	50 (°C)	**70** (°C)	90 (°C)	30 (°C)	50 (°C)	70 (°C)	90 (°C)
S-0	1.603	34.6	0.80	28.5	2.5	2.1	1.7	1.6	27.3	19.2	13.8	11.
S-1	1.410	28.8	0.96	28.4	1.3	1.2	1.0	0.8	7.6	6.3	4.4	3.5
S-2	1.445	29.4	0.98	29.1	2.1	1.3	0.5	0.5	19.7	7.3	1.5	1.2
S-3	1.634	28.5	0.99	28.8	2.0	0.9	0.3	0.2	17.1	3.8	0.6	0.4
B-0	1.634	34.6	0.95	34.6	3.0	2.2	1.1	1.0	37.5	21.9	5.3	4.9
B-1	1.484	31.2	0.97	31.7	1.3	0.9	0.5	0.2	7.4	3.5	1.2	0.1
B-2	1.457	31.5	0.94	31.1	1.7	1.1	0.5	0.3	11.9	5.7	1.2	0.5
B-3	1.600	27.8	0.95	27.6	1.6	0.9	0.8	0.7	11.2	3.4	2.9	2.3

DN/AN* for all samples in order to calculate the K_A and K_B values. Figures 4.75 and 4.76 show that these curves are similar to the curves related to the N_2O_4 oxidation in the absence of Mg CO_3.

4.4.2.2   Acid-base interaction constants, K_A and K_B

Figs. 4.75 and 4.76 show that both K_A and K_B increase during N_2O_4 oxidation in the presence of 1% $MgCO_3$. This increase was smaller than that during the oxidation by N_2O_4 alone especially at 2.5% N_2O_4. This is in agreement with the lower COOH peaks in the FTIR spectra and lower O/C ratio measured by ESCA for oxidised fibres in the presence of $MgCO_3$.However, at low rates of oxidation (0.83 and 1.25%N_2O_4), where the degradation was low, the value of I_{SP} has increased more than 10 times for softwood fibres. At the same time, it is observed that the strength properties have increased significantly at these points (part 4.5). This indicates that the effect of acid-base interaction was more significant when the amount of degradation was low.

TABLE 4.13   Acid-Base constants and specific interactions for different fibres.

	Sample	Description	K_A	K_B	I_{SP}
Softwood	**S-0**	**Untreated fibres**	**0.49**	**0.55**	**0.54**
	S-1	0.83 %N_2O_4 +1%$MgCO_3$	1.4↑	1.87↑	5.2
	S-2	1.25 %N_2O_4 +1%$MgCO_3$	2.7↑	2.14↑	11.6
	S-3	2.50 %N_2O_4 +1%$MgCO_3$	2.3↑	1.57↑	7.2
Bagasse	**B-0**	**Untreated fibres**	**1.7**	**2.25**	**7.7**
	B-1	0.83 %N_2O_4 + 1% $MgCO_3$	4.5↑	2.30↑	20.7
	B-2	1.25 %N_2O_4 + 1% $MgCO_3$	3.6↑	2.80↑	20.1
	B-3	2.50 %N_2O_4 + 1% $MgCO_3$	2.3↑	2.70↑	12.4
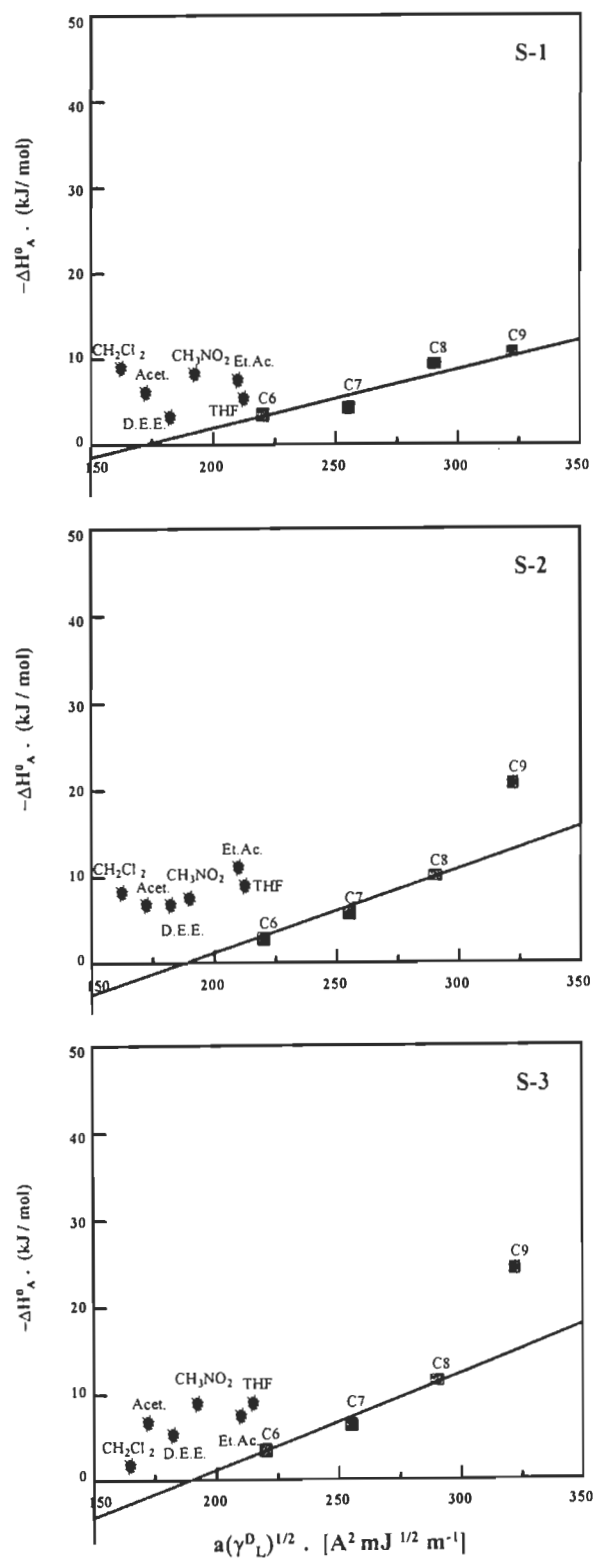
FIGURE   4.73 Plot of $-\Delta H_A$ versus $a(\gamma^D_L)^{1/2}$ for the softwood bleached kraft fibres oxidised at 0.83%, 1.25% and 2.5 % N_2O_4 (S-1, S-2 and S-3) plus 1% $MgCO_3$.
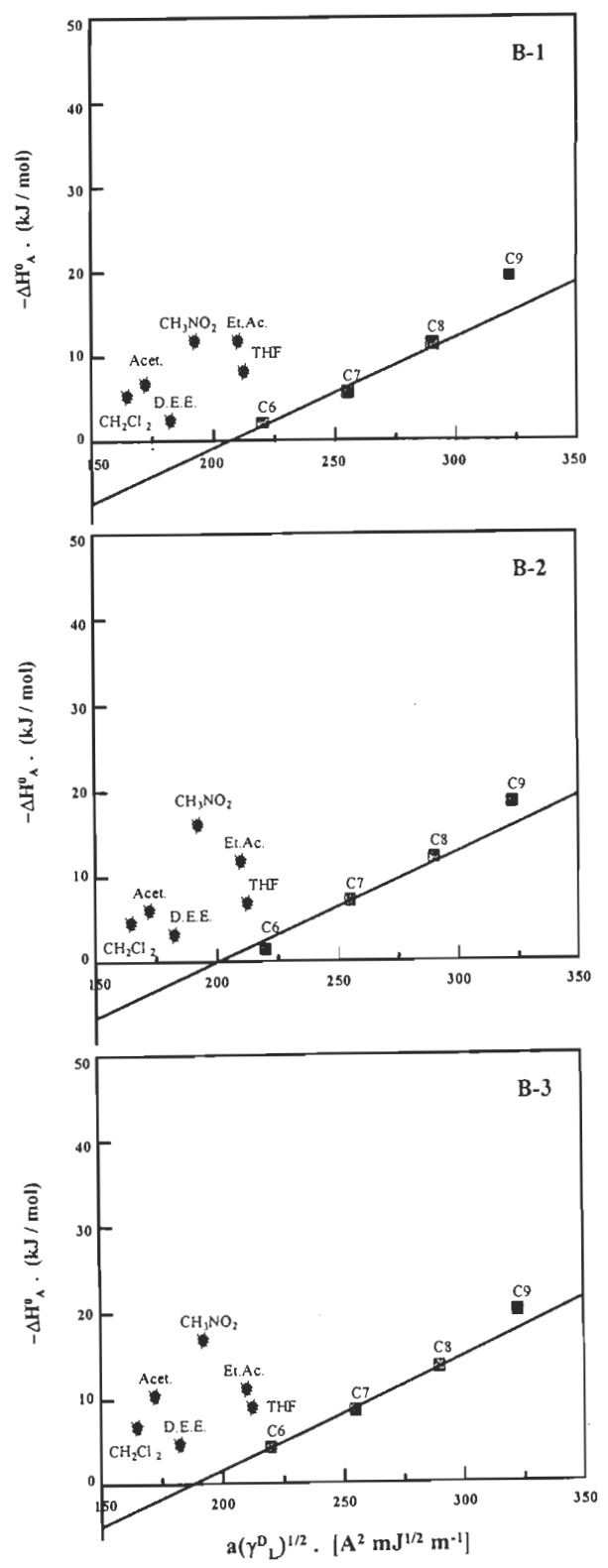
FIGURE 4.74 Plot of $-\Delta H_A$ versus $a(\gamma^D_L)^{1/2}$ for the bagasse bleached kraft fibres oxidised with 0.83%, 1.25% and 2.5 % N_2O_4 (B-1, B-2 and B-3) plus 1% $MgCO_3$.
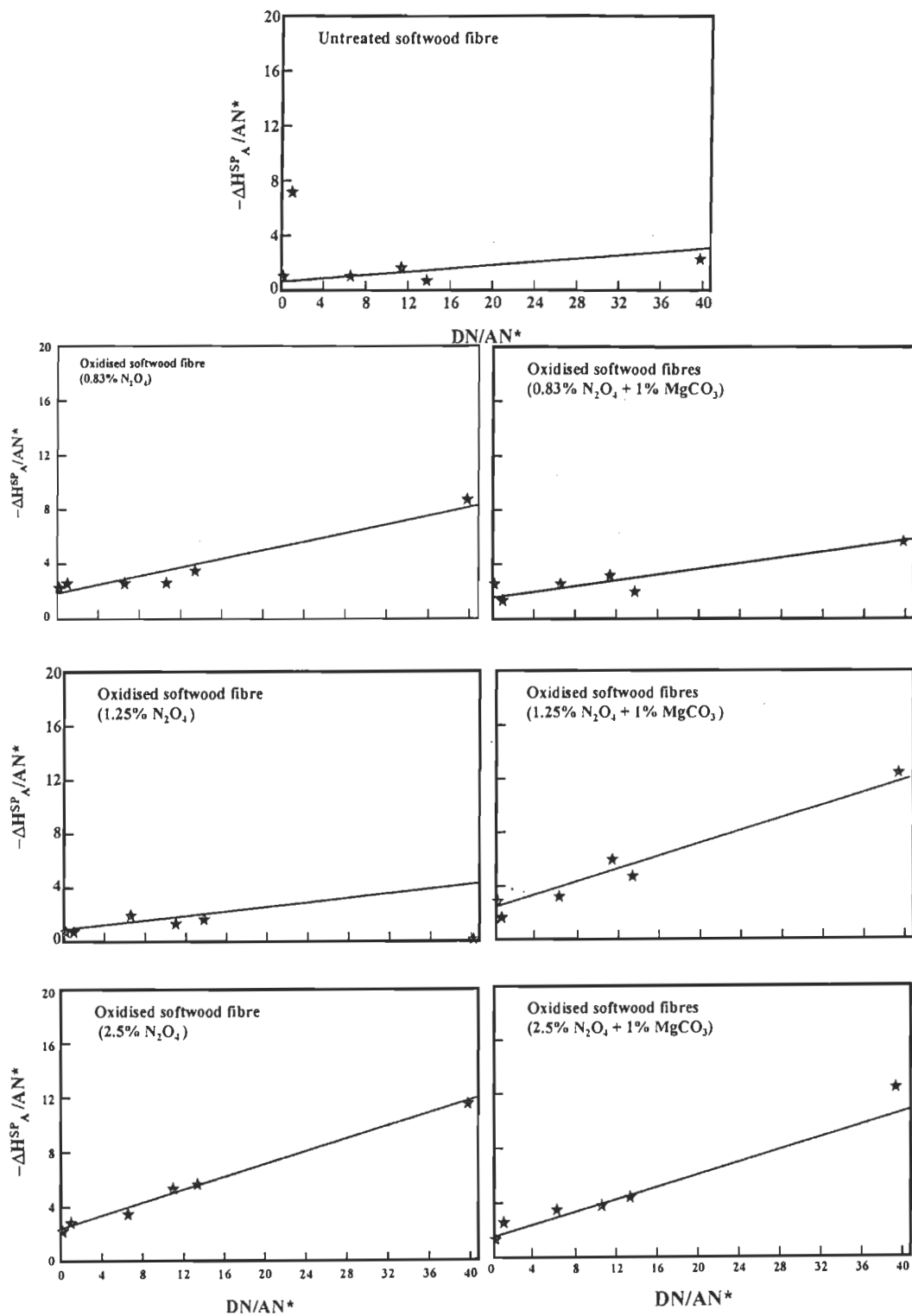
FIGURE 4.75 Plot of $\Delta H^{SP}_A/AN^*$ versus DN/AN* for untreated and oxidised softwood fibres without $MgCO_3$ (left side) and in presence of $MgCO_3$ (right side).
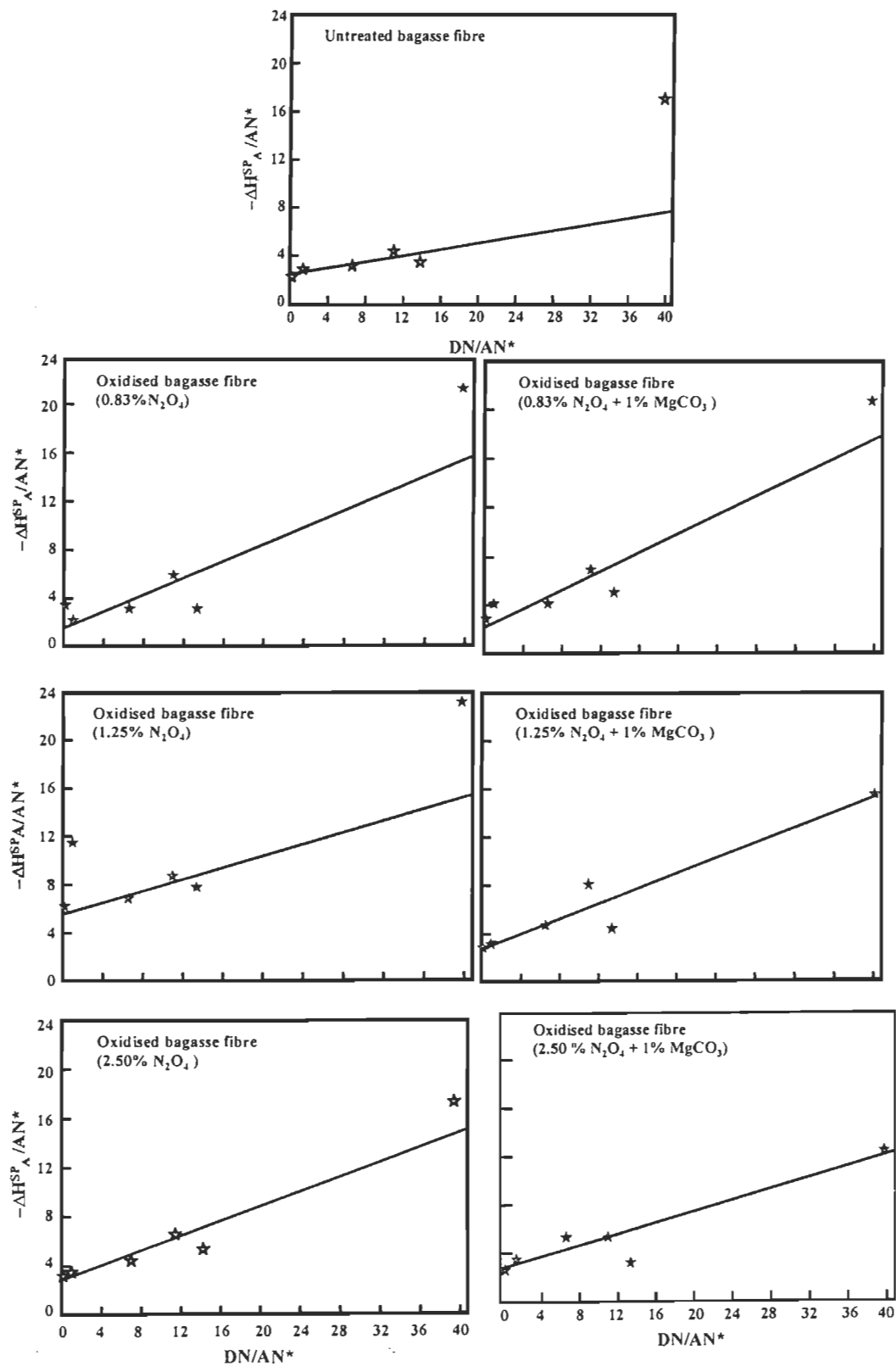
FIGURE 4.76 Plot of $\Delta H^{SP}_A/AN^*$ versus DN/AN* for untreated and oxidised bagasse fibres without $MgCO_3$ (left-side) and in presence of $MgCO_3$ (right-side).

4.4.2.3   Discussion

In the case of bleached kraft softwood, an increase in the oxidation ratio to 1.25% N_2O_4/fibre produces a decrease in the dispersive surface energy, γ^D_S of the fibres. It is improved at higher rates, but never reaches the initial values (Table 4.8). The tendency of $-\Delta H^{SP}_A$ reflects the formation of hydrogen bonds and was more or less the same. It might be suggested that since the dispersive energy decreases up to 1.25% N_2O_4, the total enthalpy decreases and glucosidic breakage is higher. At the same time, due to the formation of carboxyls groups at C6, the values of $-\Delta H^{ab}_M$, and consequently of K_A and K_B increased.

The specific interaction was improved due to an increase in H-bonding, but this did not compensate for the effect of glucosidic breakage. This is in agreement with the strength property evaluation of bleached kraft softwood in Figs. 4.83, where the lowest strength is observed at 1.25% N_2O_4. Above 1.25% N_2O_4, the glucosidic chain breakage was lower, and the influence of the formation of COOH was more noticeable. Consequently, an increase in the acid-base interaction was observed (Figs. 4.65, and the values of K_A and K_B at 2.5% N_2O_4 /fibre in Table 4.11). These could result in an increase in ΔH_A.

In the case of bagasse fibres, the situation was totally different. First, its acidic and basic constants (K_A and K_B) are higher than those of softwood (1.7, 2.25 for bagasse fibres and 0.49, 0.55 for softwood fibres). Secondly, due to its high hemicellulose content (22%) and high lignin percentage (0.42%), there was less cellulose degradation than for softwood (17% viscosity reduction for bagasse fibres as compared to 54% for softwood fibres at 1.25% N_2O_4), since these components acted as a buffer. At the same time, the amount of specific enthalpy of interaction ΔH^{ab}_A, of the oxidised fibres due to higher carboxyl content is higher than that for the untreated baggasse fibres. This lead to a higher increase in K_A and K_B for the oxidised fibres of bagasse. It is observed that aspen fibres are more acidic than the bagasse and softwood (K_A/ K_B ratio of 2.90 /1.90 as compared to 1.70 /2.25 for bagasse and 0.49 /0.55 for the softwood fibres). Secondly,

the reduction in viscosity (up to 1.25-% N_2O_4) is lower than for the two other fibres. However, there was a great reduction in the strength properties (sharp reductions were observed in the z strength and in the tensile index), except for the zero-span strength (Fig. 4.82).

This is in agreement with the lower intensity of the COOH peaks of FTIR (Fig.4.29), and with a reduction in the O/C ratio for the aspen fibres. (Table 4.3). These are also in full agreement with the values of K_A and K_B and $I_{sp,}$ which did not change during oxidation. This indicates that the number of carboxyl groups was lowest in the oxidised aspen fibres, which in turn resulted in a lower specific acid-base interaction. It can be briefly concluded that the IGC technique cannot be used to determine the chemical compositions of these fibres. However, it permits measurement of the acid-base constants of the oxidised fibres. This in turn enables the evaluation of the oxidation treatment and verification of whether the surface adhesion of the fibres has been improved. It was further found that the dispersive component, γ^D_S, of fibres was reduced as a result of an oxidation. This is especially true for the softwood. On the other hand, the acid base constants and the specific interaction of the oxidised fibres increased during the oxidation treatment, except in the case of aspen fibres.

The simultaneous increase in the acidity and basicity of fibres is an indication of the improvement in the surface adhesion of the fibres due to an increase in H-bonds. Thus, it can be concluded that the H-bond force of the oxidised fibres improved due to the formation of carboxyl groups. However, this increase in the acid-base interaction could not compensate for the losses resulting from reduction in the fibre strength due to the breakage of glucosidic bonds resulting in viscosity loss.

$MgCO_3$ treatment was found to modify the value of the dispersive component of the surface energy and the acid base constants of oxidised fibres. Increases in the acidity and basicity were also observed, thus giving an indication of the improvement of the acid-base interactions during N_2O_4 oxidation. In fact, during N_2O_4 oxidation, the presence of $MgCO_3$ mainly reduces the degradation amount of the cellulosic fibres. At the same time a reduction in the acid-base interaction was also observed.

4.5   **Fibre characteristics and paper properties**

The N_2O_4 oxidation conditions listed in Table 3.2 were repeated twice, once with and once without the addition of $MgCO_3$. The results are therefore presented in two parts in each section, as follows:

4.5.1 N_2O_4 oxidation of the bleached kraft fibres

4.5.2 N_2O_4 oxidation of the bleached kraft fibres in presence of 1% $MgCO_3$

4.5.1   **N_2O_4 oxidation of the bleached kraft fibres**

The characteristics of the oxidised fibres are reported in Tables 4.14, 4.15 and 4.16. The effects of the oxidation on the chemical and physical characteristics of the fibres and on the mechanical and optical properties of handsheets are discussed below.

4.5.1.1   **Viscosity and COOH evaluation**

Figs. 4.77, 4.78 and 4.79, show the changes in viscosity and the increases in carboxyl groups due to the oxidation treatment. The decrease in viscosity is representative of a scission of the gucosidic C1-C4 bond which is the major reason for loss of strength in the resulting paper. The decrease in viscosity due to the scission of the cellulosic chains, and consequently the reduction in the degree of polymerisation, DP was demonstrated in the intrinsic resistance (zero span) reduction of handsheets. This in turn was reflected in their tensile strength (Figs 4.83 to 4.85). The reaction mechanism is similar to that which occurs in ozone bleaching, during which the formation of alkali-labile carbonyl groups results in the degradation of cellulose by scission (134). Two methods of limiting this degradation have been used. One is the transformation of carbonyl to carboxyl by further oxidation with $HClO_2$(134). The other is the transformation of the carbonyl to an alcohol group by a reducing agent such as $NaBH_4$ (118).

TABLE 4.14   Characteristics of bleached kraft softwood fibres oxidised by N_2O_4.

Run no.		Pure	1	2	3	4	5
N_2O_4/Fibre	(%)	0	0.42	0.83	1.25	1.66	2.50
COOH	(m mol/kg)	44.40	45.04	51.52	57.4	59.51	56.15
St.dev.		±0.7	±1.0	±1.1	±1.7	±1.4	±1.3
Intrinsic viscosity	(dm^3/kg)	1347	993	881	620	598	498
St.dev.		±59	±50	±41	±37	±32	±27
C.S.F	(ml)	728	739	739	710	733	746
St.dev.		±8	±9	±7	±6	±8	±10
W. A. F. Length	(mm)	2.36	1.995	1.409	1.359	1.059	1.422
St.dev.		±0.005	±0.0005	±0.001	±0.0015	±0.0003	±0.0003
Fines	(%)	3.88	4.64	4.75	5.56	7.04	4.86
St.dev.		±0.020	±0.012	0.036	0.039	0.080	0.110
Zero-span	(km)	12.10	6.88	3.97	3.25	3.41	4.25
St.dev.		±0.14	±0.9	±0.05	±0.06	±0.06	0.09
Z Strength	(kPa)	159.7	134.4	109.1	100.0	124.3	112.3
St.dev.		±6.10	±5.97	±4.17	±4.36	±6.39	±6.48
Density	(g/cm^3)	0.491	0.475	0.436	0.469	0.492	0.447
St.dev.		±0.10	±0.12	±0.10	±0.11	±0.13	±0.09
Burst Ind.	(kPa.m^2/g)	7.83	3.32	3.25	2.86	3.00	2.78
St.dev		±0.24	±0.17	±0.16	±0.17	±0.20	±0.16
Tens. Ind.	(mN.m/g)	21.09	14.16	10.09	4.92	8.05	11.68
St.dev.		±2.05	±1.57	±1.96	±1.20	±1.49	±1.27
Brightness	(%ISO)	85.7	86.15	85.57	85.84	85.68	85.23
St.dev.		±0.13	±0.11	±0.10	±0.12	±0.12	±0.11
Opacity	(%ISO)	71.09	74.33	74.37	76.52	74.82	75.44
St.dev.		±1.01	±0.83	±0.98	±1.39	±1.78	±2.40
L.Scat.Coef.	(m^2/kg)	30.0	34.4	35.5	33.9	35.3	38.0
St.dev.		±0.23	±0.25	±0.26	±0.26	±0.33	±0.27

TABLE 4.15   Characteristics of bleached kraft bagasse fibres oxidised by N_2O_4.

Run no.		Pure	1	2	3	4	5
N_2O_4/Fibre	(%)	0	0.42	0.83	1.25	1.66	2.50
COOH	(m mol/kg)	52.9	63.99	64.53	63.80	64.04	68.90
St.dev.		±1.0	±1.5	±1.7	±1.4	±1.3	±1.7
Intrinsic viscosity	(dm³/kg)	726	684	656	602	468	452
St.dev.		±36	±37	±33	±27	±22	±22
C.S.F	(ml)	590	577	600	648	665	680
St.dev.		±5	±7	±7	±5	±6	±8
W. A. F. Length	(mm)	0.782	0.733	0.780	0.676	0.545	0.746
St.dev.		±0.0002	±0.0003	±0.0002	±0.0001	±0.0001	±0.0001
Fines	(%)	16.54	18.45	16.27	16.70	21.68	16.01
St.dev.		±0.015	±0.025	±0.018	±0.061	±0.050	±0.106
Zero-span	(km)	6.63	6.36	5.89	3.11	2.86	3.78
St.dev.		±0.06	±0.07	±0.08	±0.11	±0.28	±0.14
Z Strength	(kPa)	538.0	532.2	484.4	271.5	259.8	305.5
St.dev.		±43.1	±32.8	±38.0	±17.6	±14.1	±20.2
Density	(g/cm³)	0.542	0.586	0.568	0.479	0.485	0.466
St.dev.		±0.12	±0.14	±0.14	±0.10	±0.08	±0.04
Burst Ind.	(kPa.m²/g)	10.96	8.61	8.09	3.08	2.69	3.48
St.dev		±0.69	±0.44	±0.25	±0.15	±0.17	±0.28
Tens. Ind.	(mN.m/g)	38.05	34.91	33.02	14.32	11.75	15.83
St.dev.		±1.24	±1.16	±1.21	±1.06	±1.20	±1.17
Brightness	(%ISO)	72.25	71.76	72.38	74.80	73.31	75.00
St.dev.		±0.67	±0.65	±0.63	±0.37	±0.34	±0.42
Opacity	(%ISO)	85.77	86.21	86.18	88.40	89.50	88.75
St.dev.		±0.47	±0.54	±0.32	±0.68	±0.52	±0.31
L.Scat.Coef.	(m²/kg)	43.6	45.4	46.0	57.3	59.7	57.3
St.dev.		±1.10	±1.15	±1.08	±1.04	±1.23	±1.05

TABLE 4.16   Characteristics of bleached kraft aspen fibres oxidised by N_2O_4.

Run no.		Pure	1	2	3	4	5
N_2O_4/Fibre	(%)	0	0.42	0.83	1.25	1.66	2.50
COOH	(m mol/kg)	57.4	68.1	67.5	65.4	65.30	63.52
St.dev.		±1.1	±1.7	±1.7	±1.4	±1.3	±1.3
Intrinsic viscosity	(dm^3/kg)	1164	1162	1098	619	657	468
St.dev.		±53	±50	±46	±32	±34	±30
C.S.F	(ml)	670	676	674	689	660	713
St.dev.		±8	±8	±6	±10	±7	±7
W. A. F. Length	(mm)	0.761	0.738	0.746	0.711	0.695	0.728
St.dev.		±0.0006	±0.0007	±0.0003	±0.0004	±0.0001	±0.0003
Fines	(%)	4.56	5.19	4.67	5.21	5.67	4.90
St.dev.		±0.045	±0.045	±0.020	±0.011	±0.022	±0.015
Zero-span	(km)	12.34	11.20	9.69	3.90	2.98	4.00
St.dev.		±0.09	±0.08	±0.8	±0.05	±0.04	±0.5
Z Strength	(kPa)	227.5	75.54	72.12	34.82	42.63	45.79
St.dev.		±12.7	±9.7	±7.6	±3.6	±3.1	±4.1
Density	(g/cm^3)	0.518	0.473	0.481	0.387	0.392	0.397
St.dev.		±0.10	±0.07	±0.07	±0.05	±0.6	±0.05
Burst Ind.	(kPa.m^2/g)	4.35	3.0	2.47	1.1	1.33	1.6
St.dev		±0.23	±0.21	±0.14	±0.12	±0.10	±0.11
Tens. Ind.	(mN.m/g)	19.36	10.14	8.22	4.13	4.61	5.25
St.dev.		±0.78	±0.63	±0.46	±0.21	±0.37	±0.35
Brightness	(%ISO)	75.10	74.82	75.13	78.35	77.21	77.82
St.dev.		±0.49	±0.22	±0.29	±0.14	±0.15	±0.19
Opacity	(%ISO)	82.03	86.86	85.85	85.32	86.22	86.33
St.dev.		±0.73	±3.20	±0.44	±0.41	±0.35	±0.14
L.Scat.Coef.	(m^2/kg)	46.01	53.7	50.4	54.3	54.9	54.0
St.dev.		±0.60	±0.76	±0.70	±0.56	±0.64	±0.62

The reduction in viscosity is much lower for bagasse fibre than for the others (17% viscosity reduction for bagasse fibre as compared with a 54% for softwood and 47% reduction for aspen fibres at 1.25-% N_2O_4). This can be explained by its higher hemicellulose content and slightly higher lignin content of the untreated bagasse fibres. These amorphous polymers are more reactive and less resistant to the oxidation and should therefore be degraded before the cellulose is attacked significantly (39).

Figs. 4.77, 4.78 and 4.79 show that the carboxyl content (COOH) is not linearly related to the oxidation rate. Even though the formation of COOH was increased by the N_2O_4 oxidation, it was relatively constant above 1.25-1.66% N_2O_4. The variations of the last two points are within the standard deviation ($\pm$ 2.8-m mol/kg).
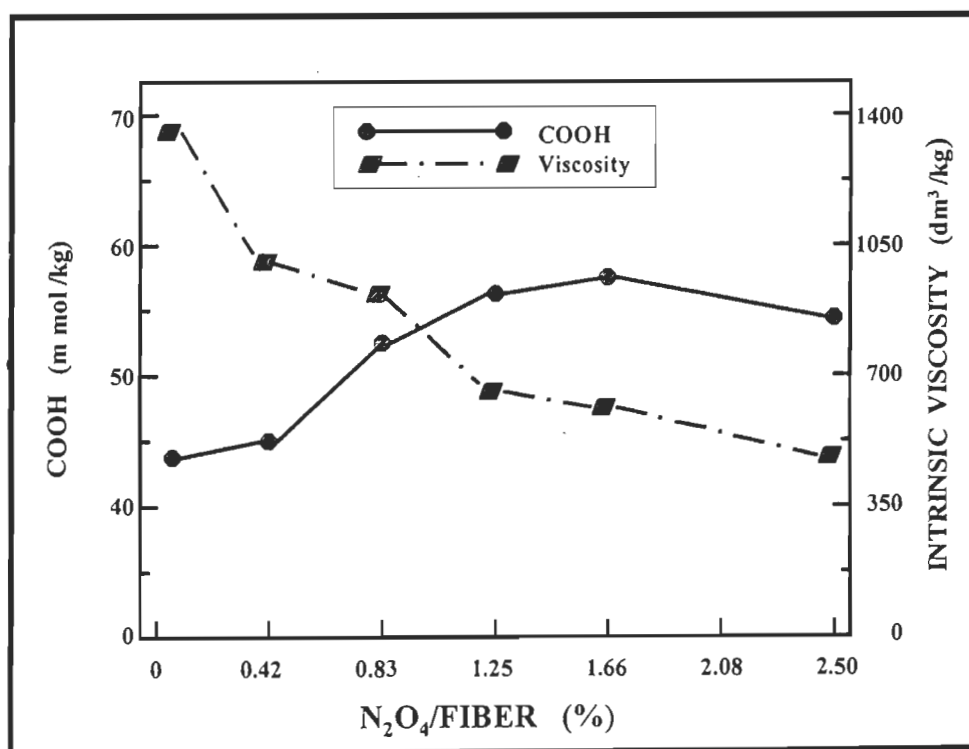
FIGURE 4.77 The variations of intrinsic viscosity and COOH of the oxidised bleached kraft softwood fibres as a function of the percentage of N_2O_4/fiber.
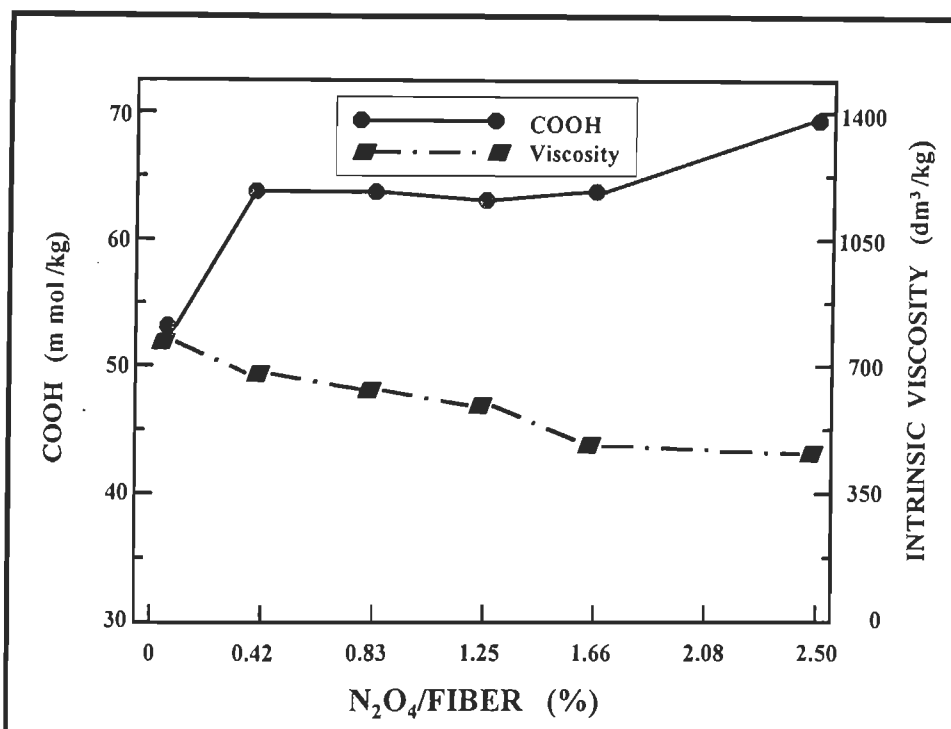
FIGURE 4.78 The variations of intrinsic viscosity and COOH, of the oxidised bleached kraft bagasse fibres as a function of the percentage of N_2O_4/fiber.
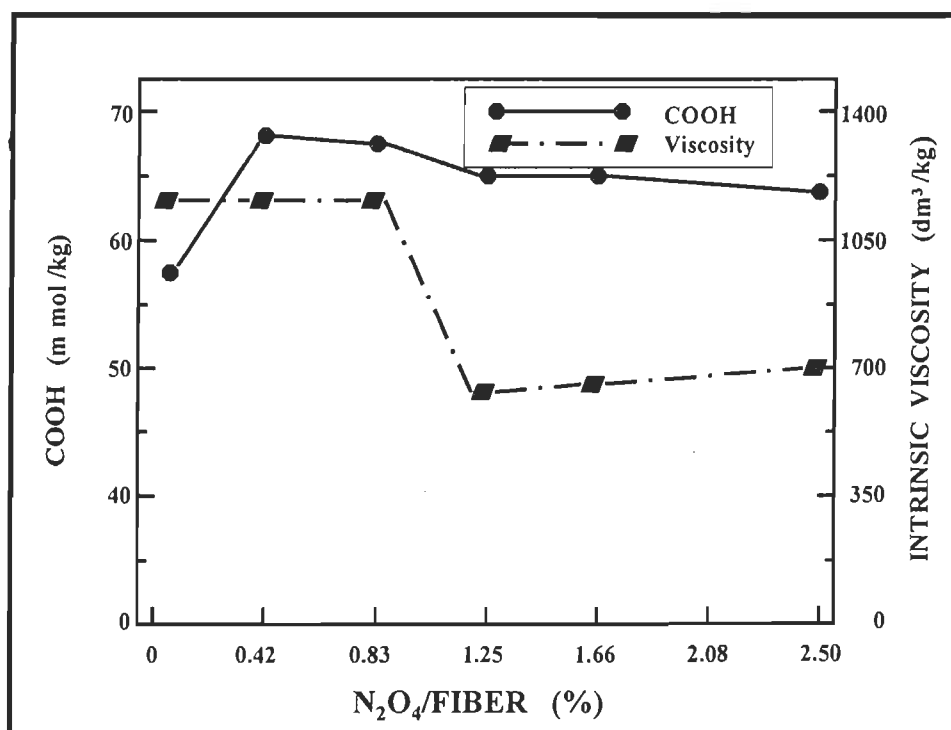
FIGURE 4.79 The variations of intrinsic viscosity and COOH of the oxidised bleached kraft aspen fibres as a function of the percentage of N_2O_4/fiber.

4.5.1.2   The physical properties of fibres

N_2O_4 oxidation also affects the physical properties and morphology of the fibers. As the oxidation rate increases there is a decrease in fiber length and an increase in the percentage of fines (Figs 4.80, 4.81 and 4.82). However, the decrease of the fiber length in the oxidized softwood fibers was greater than that in the two other short fibers. Here again, a maximum reduction in average weighted fiber length, corresponding to a maximum increase in the percentage of fines was observed at 1.25% N_2O_4. Thus, higher chemical degradation produces a lower fiber length. The point here is that above 1.25% N_2O_4, the fiber length is somewhat greater for all three fibers, even though the viscosity due to higher oxidation rate continued to decrease. As fiber length reduction reaches a minimum, the strength properties may gradually recover as in the case for bagasse. This might be explained by the fact that the pH of the reaction medium becomes more acid once the oxidation rate becomes greater than 1.25%. Increasing carboxylic acid due to the nitric acid regeneration was already reported (52).

$$N_2O_4 + H_2O \rightleftharpoons HNO_2 + HNO_3$$

$$RCH_2OH + HNO_2 \longrightarrow RCOOH + NH_2OH$$
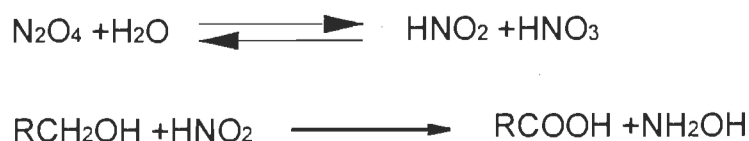
As far as the percentage of fines is concerned, it appears to be inversely related to the weighted fiber length. The variation in the percentage of fines for all the fibres was determined more by the extent of degradation than by the oxidation ratio. It is believed that, more a pulp is refined, there will be more fibrillation and more fines is produced. Consequently the bonding ratio (BR%) and relative bonded area (RBA) increase, resulting in an increase in the Scott-bond and finally in the tensile strength of the sheet. In this work also, it was observed that an increase in the fines percentage, affecting the RBA, resulted to an increase in the bonding strength and tensile strength of bagasse oxidised fibres as compared with those of softwood and aspen oxidised fibres. In the other hand, fibrillation(due to the refining), modifies the surface of the fibres by creating new surface of the fibre on P&S1 layers and more fibrils in the S2 layer .This new

surface participates in fibre to fibre bonding because of the new potential for hydrogen bond (more hydroxyl groups available). That is why the bonding strength and and higher tensile are obtained. In the case of the N_2O_4 oxidation, there is also an increase in the hydrogen bond due to the formation of the carboxyl group. As mentioned earlier the cohesive energy of the hydrogen bonds due the carboxyl groups (COOH). formation is much higher than that of hydroxyl groups (OH), so we expected to have an increase in the bonding strength, B. This could be achieved if there were no degradation of the fibres. Nevertheless the improvement in the bonding strength occurred along with the drastic decrease in the viscosity, lower fibre strength, F. That is why the tensile strength , T, was generally reduced in this condition. In the Tables 4.14 and 4.15, we may observe that higher percentage of fines in bagasse fibres resulted in an increase in z strength, burst and tensile index. This is in agreement with the recent finding of Moss et al(135). that the addition of kraft pulp fines creates a greater fibre bonding potential in paper. It is true, while greater bonding potential leads to higher z strength and tensile strength.

How ever the above assumption did not applied, when oxidation ratio increased and the degradation caused greater percentages of the fines., as degradation effect dominated the effect of the bonding strength for all types of the oxidised fibres. Data presented in Tables 4.14 to 4.16 indicates rather that the strength loss due to the decrease in fibre length (influencing the fibre strength) was greater than the positive effect of the increase in the percentage of the fines, influencing the relative bonded area and bond strength.

Considering the rates of oxidation up to 1.25%-N_2O_4, the reduction in fibre length was lower than for aspen fibres (6.5%) than for the bagasse (13.3%) and softwood (43.3%). Moreover, the viscosity and zero-span of aspen had not dropped very much up to this point. On the other hand, the sheet strength indexes (z strength, tensile strength and burst index) exhibited sharp decreases (Fig 4.85). This indicates that the strength loss for aspen was due to poor bonding, rather than to degradation. This might be related to the low intensities of the IR peak for COOH (section 4.2).
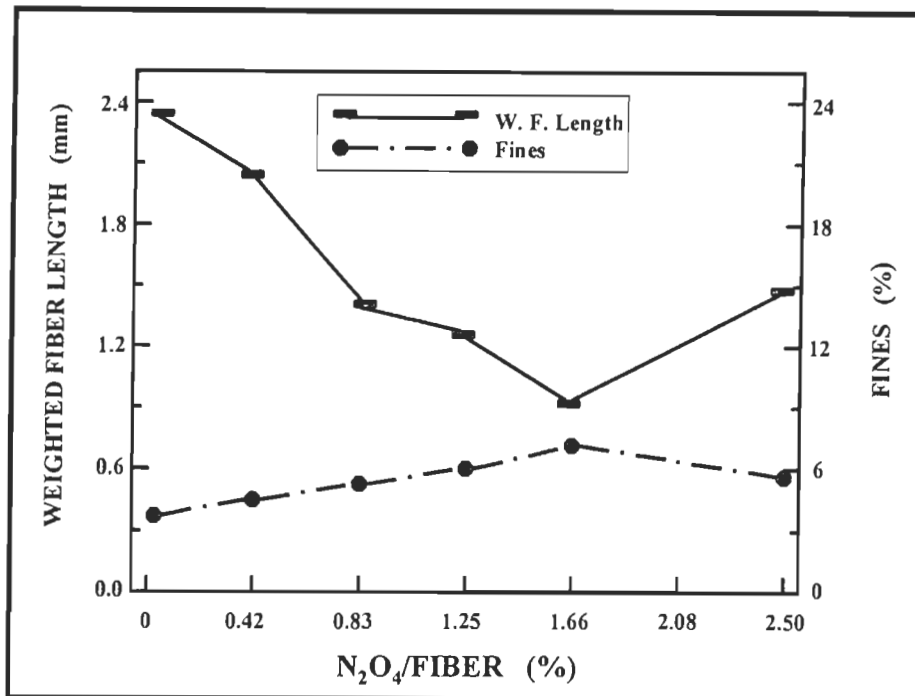
FIGURE 4.80 The variation of the weighted average fibre length and percentage of fines of the oxidised bleached kraft softwood as a function of percentage of N_2O_4/fiber.
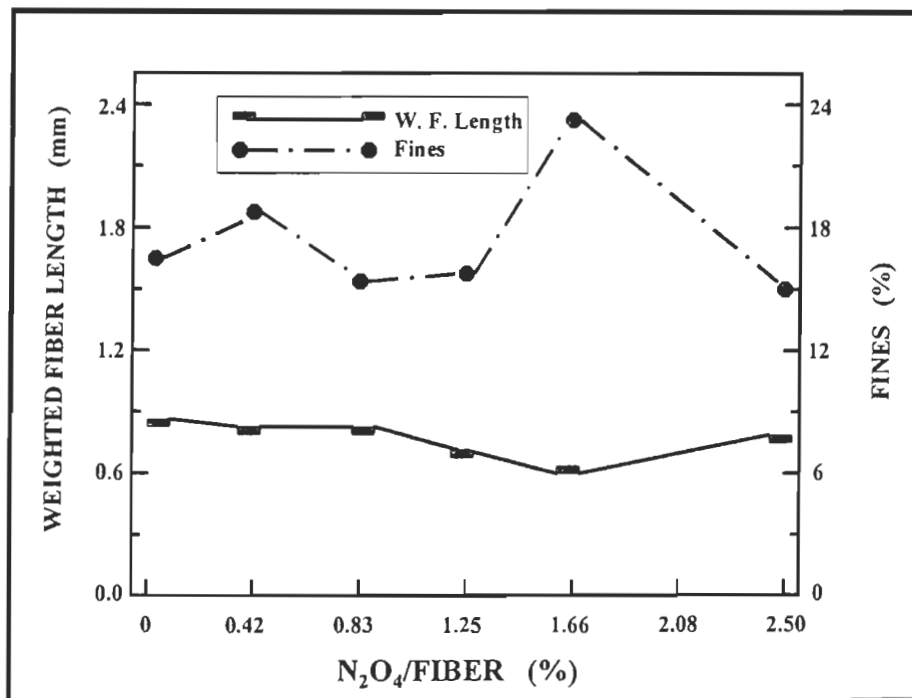
FIGURE 4.81 The variation of the weighted average fibre length and percentage of fines of the oxidised bleached kraft bagasse as a function of percentage of N_2O_4/fiber.
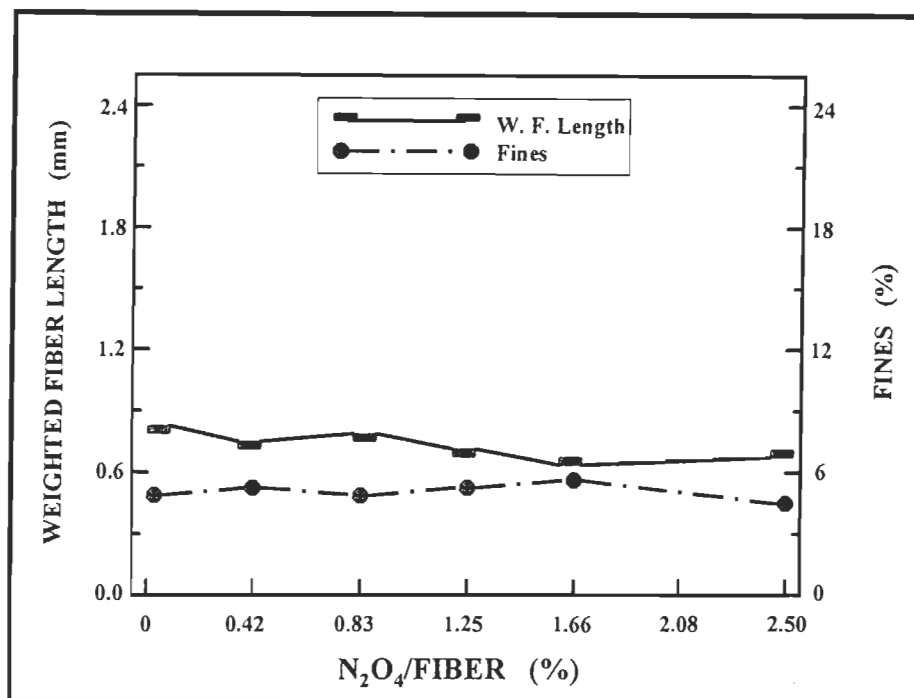
FIGURE 4.82 **The variation of the weighted average fibre length and percentage of fines of the oxidised bleached kraft aspen as a function of percentage of N_2O_4/fiber.**

Furthermore, there was no increase in the O/C ratio (section 4.3), and no change in the I_{SP} values of the aspen fibres (section 4.4). This is in accordance with the hypothesis that the tensile strength of fibres with the same length (such as bagasse and aspen fibres) will only differ if their bonding potentials differ.

4.5.1.3 Strength properties

Figs 4.83, 4.84 and 4.85 show that N_2O_4 oxidation had a negative effect on the strength properties of paper. For all fibres, the strength properties displayed minima in the range of 1.25-1.66%-N_2O_4. This shows that the reductions in fibre length are also greater in this range. Furthermore, the increase in strength properties at higher oxidation rates was significant since the differences exceeded 2 times the standard deviations of the measurements (Tables 4.14 - 4.16).

Hydroxyl radicals are formed by the N_2O_4 oxidation even though there is very little lignin present in the pulp. This could be the cause of the degradation of carbohydrates during oxidation. However, a relatively high lignin content in the bagasse apparently helped to limit the degradation of cellulose. In fact, Magara et al (124) reported that the non-phenolic lignin model compounds (syringaldehyde type of the hardwood pulps) do not produce hydroxyl radicals during ozone bleaching, and that their presence suppresses the degradation of cellulose. As the bagasse lignin is also composed of syringaldehyde, radical formation could be limited, thus resulting in a lower degradation of carbohydrate. This comparison leads to the following conclusion:

a)   The variation in the strength properties was mainly due to the morphological changes induced by oxidation and less influenced by substitution phenomena. At the same time the continually reduction in viscosity is due to the scission of the glucosidic chains of cellulose, which results in a decrease in the fibre strength, F. The reduction in fibre length, L along with the reduction in zero span, Z affect also the fiber strength, F. As the effect of the bonding strength, B is less important than the changes in fibre strength, it leads to a serious reduction in tensile strength, T, which is in agreement with the Page equation of $1/T = 1/F + 1/B$. It is important to note that the CSF was fairly constant for all the treatment conditions since there had been no refining of fibre samples.

b)   Although aspen fibres were less degraded than the two other fibres, the resulting papers were of a lower strength due to the poor improvement of the bonding potential.
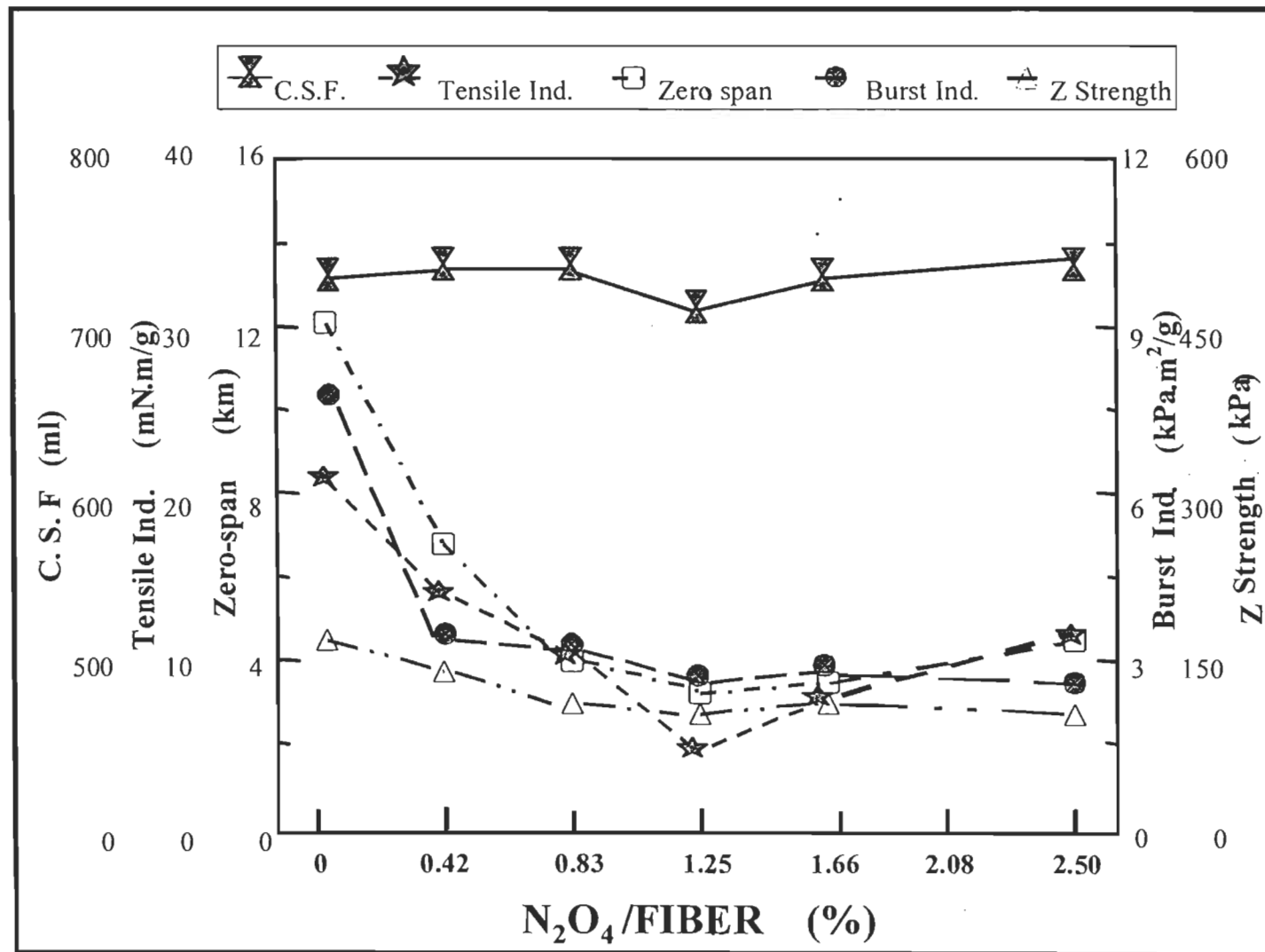
FIGURE 4.83 The variation of CSF, tensile index, zero span, burst index, and z strength of the oxidised softwood bleached kraf fibres as a function of the percentage of N_2O_4/fiber.
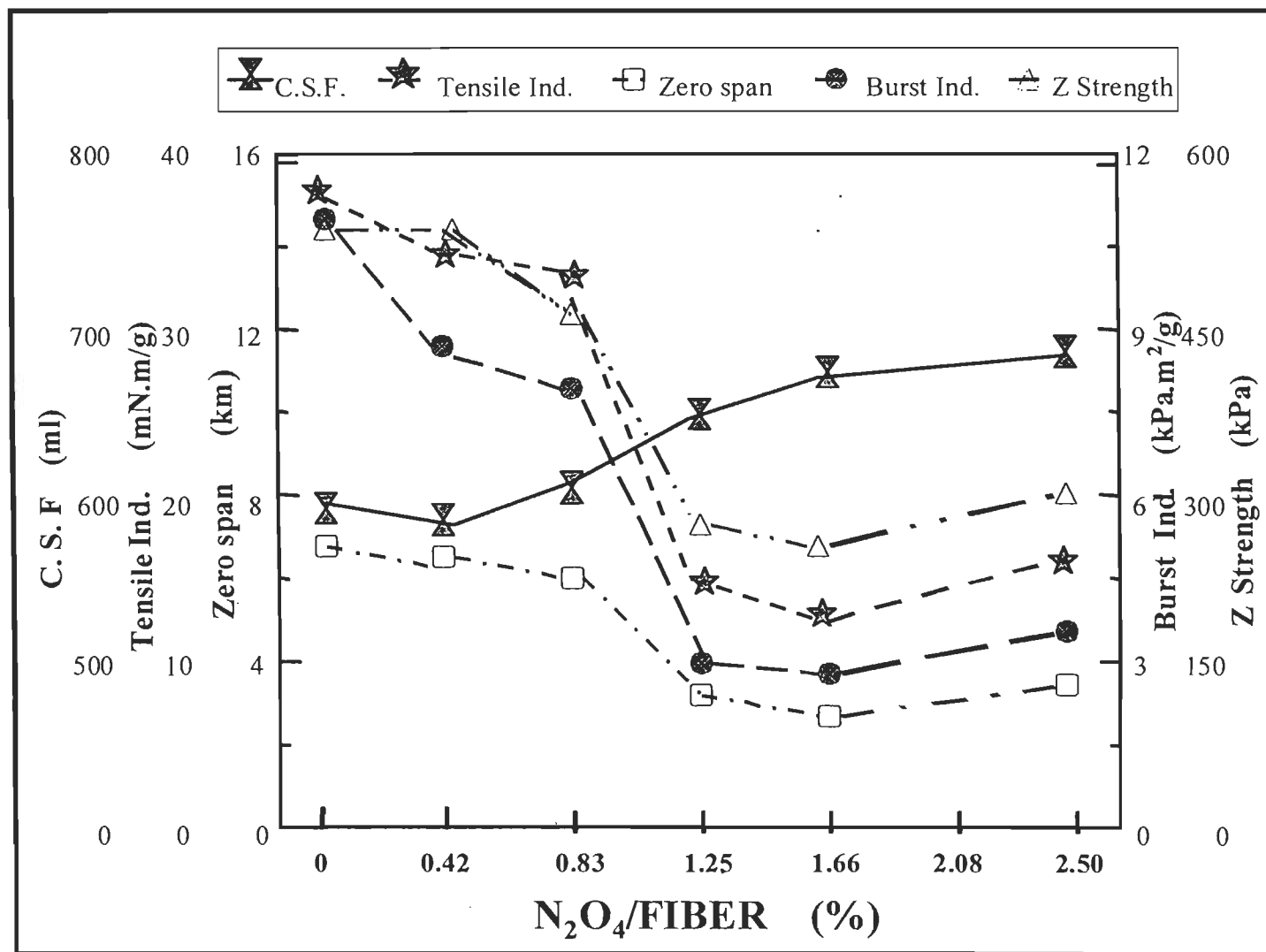
FIGURE 4.84 The variation of CSF, tensile index, zero span, burst index, and z strength of the oxidised bagasse bleached kraft fibres as a function of the percentage of N_2O_4/fiber.
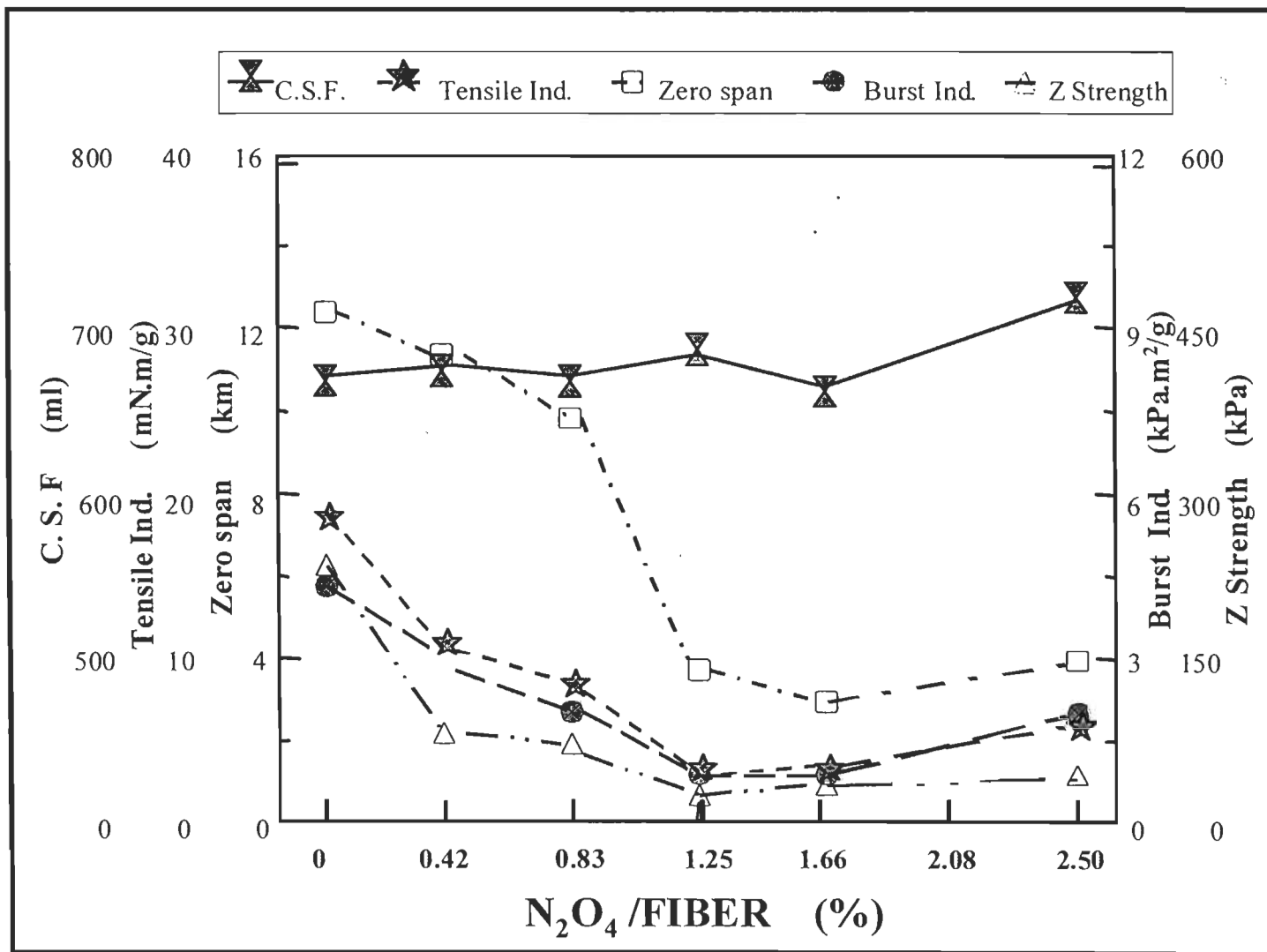
FIGURE 4.85 The variation of CSF, tensile index, zero span, burst index, and z strength of the oxidised aspen bleached kraft fibres as a function of the percentage of N_2O_4/fiber.

c)   Although the initial degree of polymerisation of the softwood fibres was higher than the other ones, it was degraded to a far greater extent than the aspen and bagasse fibres.

d)   Papers made from treated bagasse fibres showed the smallest degradation and reduction in strength properties due to N_2O_4 oxidation. This can be attributed to the higher amount of lignin and hemicellulose content of bagasse fibres.

4.5.1.4   Optical properties

The brightness, opacity and scattering coefficients of the three types of fibres are shown in Figs. 4.86 to 4.88 at different oxidation rates. The softwood pulp was almost at maximum brightness initially since the lignin content was negligible (0.18%). Thus, there was practically no change in brightness after the oxidation treatment. In contrast, the brightness of bagasse and aspen changed from 72.25% to 75%, and 75.1% to 78.35%, respectively, after removal of the lignin (initially 0.42% and 0.5%, respectively).

The mechanism of lignin removal is the formation of radicals upon contact between the N_2O_4 and the lignin, followed by destruction of the lignin structure by these radicals and the subsequent dissolution of the degradation products.

The changes in opacity are different from those of the brightness. The initial opacities are related to the lignin and hemicellulose contents of the fibres, with bagasse being the most opaque and the softwood being the least. Even though the opacity of the untreated softwood fibres (71%) is lower than that of bagasse (86%) and aspen (82%) the increase in opacity was higher due to much greater degradation of the fibres as manifested by lower fibre length and higher percentage of fines. The change in opacity was 5.5 % for the softwood fibres as compared to 4% for the bagasse fibres. Softwood fibre length decreased from 2.36 mm to1.06 mm, while the length of the bagasse fibres decreased from 0.78 to 0.55 mm. Unfortunately, it was not possible to measure the

crystallinity in this study, even though it is known that opacity of paper is also related to the crystallinity of cellulose. The maximum change in opacity of the aspen fibres was 3.3% at 1.25%-N_2O_4. This was the lowest among the three types of fibres, and corresponds to the observation that aspen fibres were the least degraded by the oxidation.

As far as the light scattering coefficient is concerned, its variations were in accordance with changes in the opacity. The light scattering coefficient of softwood was lower than that of aspen at the same percentage of fines. This is likely due to the lower lignin content of the softwood fines (11.8%) compared to the hardwood fines (20.9%) (136). The bagasse had the highest light scattering coefficient, which was probably due to a much higher percentage of fines compared to the others. Since the lignin content of bagasse was similar to that of aspen, the difference in light scattering coefficients for these two fibres can be mainly attributed to the difference in the percentage of the fines.
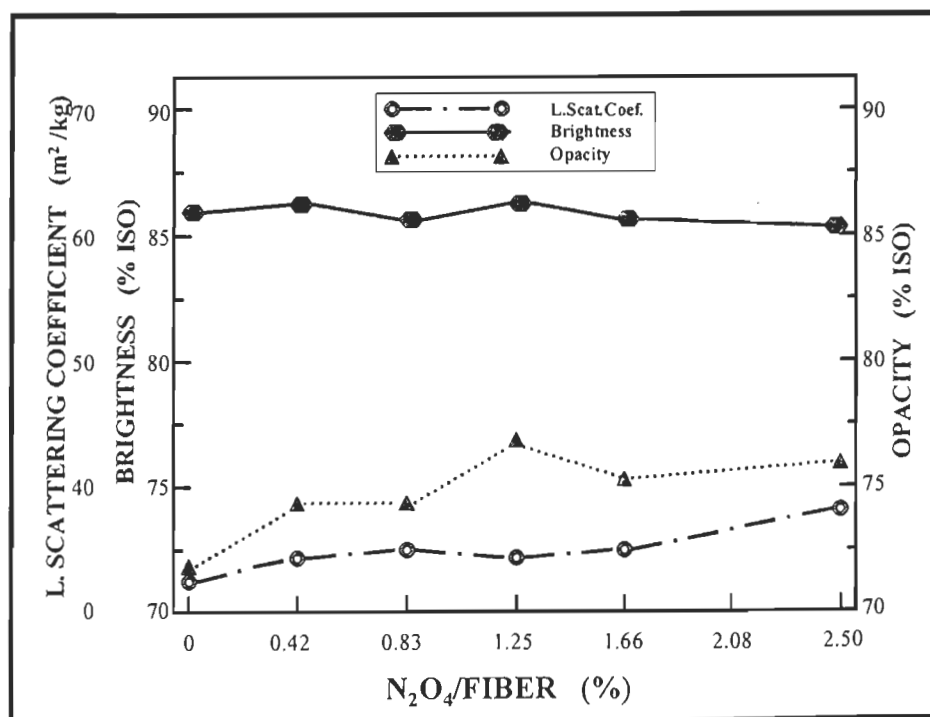
FIGURE 4.86 **Brightness, opacity and light scattering coefficient of the oxidised softwood fibres as a function of the percentage of N_2O_4/fiber.**
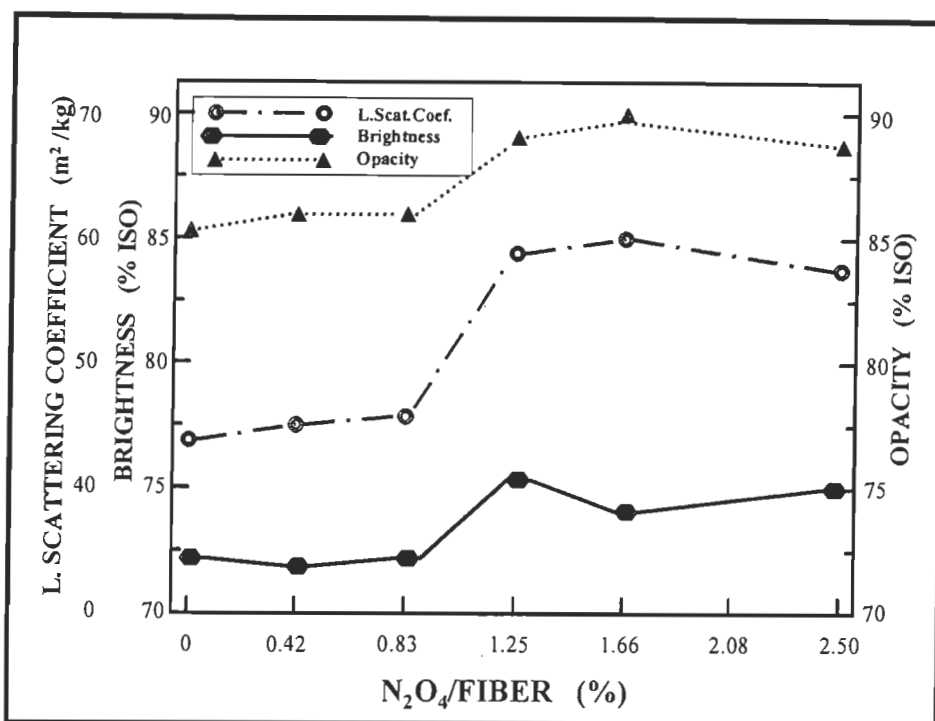
FIGURE 4.87   Brightness, opacity and light scattering coefficient of the oxidised bagasse fibres as a function of the percentage of N_2O_4/fiber.
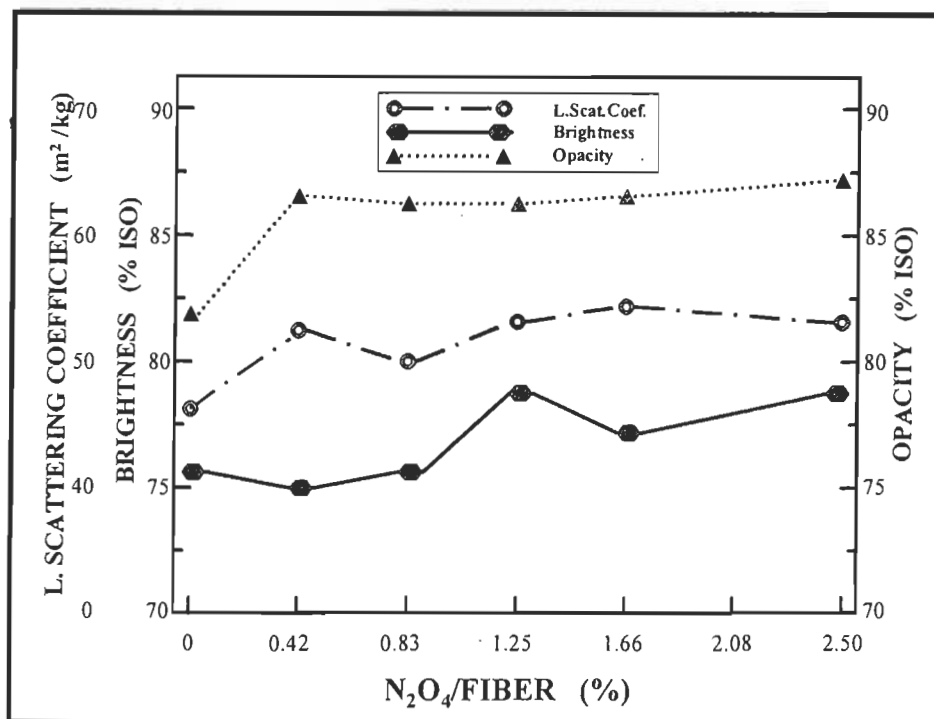
FIGURE 4.88   Brightness, opacity and light scattering coefficient of the oxidised aspen fibres as a function of the percentage of N_2O_4/fiber.

4.5.2   The effect of the addition of Mg CO_3 during N_2O_4 oxidation

The lack of a positive effect of the carboxyl substitutions on the strength properties of the paper sheets was mainly due to the simultaneous viscosity loss caused by the cellulose degradation. The mechanical and optical properties of the sheets and fibres after oxidation are compared to ones with and without addition of 1% $MgCO_3$ in Tables 4.17 and 4.18 for the softwood and bagasse, respectively. The influence of $MgCO_3$ for the two types of fibres are presented graphically for comparison. The data for the viscosity, fibre lengths and fines are given in figs. 4.89, 4.90 and 4.91. Strength properties are given in Figs. 4.92 to 4.95. Finally, the effects on optical properties are compared in Figs. 4.96 to 4.98. Since the differences in freeness values of the oxidised fibres were lower than 10% (60ml), the measured properties could be considered comparable.

4.5.2.1   Viscosity

The major effect of the addition of $MgCO_3$ was the limitation in the reduction of viscosity for both softwood and bagasse fibres during oxidation (Fig.4.86). Consequently, the values obtained for the viscosity in this case were considerably higher than in the absence of $MgCO_3$ (Tables 4.17 and 4.18).

4.5.2.2   The physical properties of fibres

a)   Weighted average fibre length

Softwood fibres, having higher weighted fibre length, lose their fibre length more than bagasse fibres during the oxidation, and in turn regain them more than bagasse fibres in the presence of $MgCO_3$ in turn, However the fibre length values could not achieve the same value for the untreated fibres. Contrary, the loss in fibre length for bagasse fibres was surprisingly higher in the presence of $MgCO_3$.

TABLE 4.17 The Fibre characteristics of softwood bleached kraft fibres oxidised by N_2O_4 in presence of 1% $MgCO_3$.

Run No.	0	1		2		3	
N_2O_4/Fibre	0	0.83		1.25		2.50	
$MgCO_3$ addition	0	0	1%	0	1%	0	1%
COOH (m mol/kg)	44.4	51.52	48.1	57.4	46.7	56.15	49.4
Intrinsic viscosity (dm^3/kg)	1347	881	984	620	833	498	736
C.S.F (ml)	728	739	716	710	694	746	710
W. A. F. Length (mm)	2.36	1.409	1.681	1.359	1.659	1.422	1.764
Fines (%)	3.88	4.75	4.66	5.56	5.50	4.86	3.26
Zero-span (km)	12.1	3.97	11.84	3.25	11.36	4.25	9.75
Z Strength (kPa)	159.7	109.1	154.8	100.0	125.8	112.3	79.2
Density (g/cm^3)	0.491	0.436	0.488	0.469	0.468	0.447	0.445
Burst Index ($kPa.m^2$/g)	7.83	3.25	8.76	2.86	7.21	2.78	4.29
Tensile Index (mN.m/g)	21.09	10.09	26.32	4.92	22.32	11.68	12.99
Brightness (%ISO)	85.7	85.57	85.94	85.84	85.55	85.23	85.6
Opacity (%ISO)	71.09	74.37	76.10	76.52	77.09	75.44	76.09
L.Scattering Coef. (m^2/kg)	30.5	35.5	31.5	33.9	31.7	38.0	34.5

TABLE 4.18   Fibre characteristics of bagasse bleached kraft fibres oxidised by N_2O_4 in presence of 1% $MgCO_3$.

Run No.	0	1		2		3	
N_2O_4/Fibre	0	0.83		1.25		2.50	
$MgCO_3$ addition	0	0	1%	0	1%	0	1%
COOH (m mol/kg)	52.9	64.53	54.8	63.79.	50.2	68.9.	56.2
Intrinsic viscosity (dm^3/kg)	726	656	657	602	653	452	581
C.S.F (ml)	590	600	570	648	597	680	620
W. A. F. Length (mm)	0.782	0.780	0.702	0.676	0.634	0.746	0.692
Fines (%)	16.54	16.27	20.49	16.70	22.50	16.01	21.38
Zero-span (km)	6.63	5.89	6.18	3.11	5.68	3.78	6.38
Z Strength (kPa)	538.0	484.4	403.8	271.5	370.3	305.5	414.8
Density (g/cm^3)	0.542	0.568	0.554	0.479	0.519	0.466	0.578
Burst Index $(kPa.m^2/g)$	10.96	8.09	10.80	3.08	9.08	3.48	12.32
Tensile Index (mN.m/g)	38.05	33.02	35.40	14.32	32.58	15.83	40.07
Brightness (%ISO)	72.25	72.38	71.16	74.85	71.51	75.00	70.59
Opacity (%ISO)	85.77	86.18	88.59	88.40	90.14	88.75	89.50
L.Scattering Coef. (m^2/kg)	43.6	46.0	47.1	57.3	50.4	57.3	46.6

b)   The percentage of fines

After the addition of 1% $MgCO_3$, the percentage of fines was reduced in the case of softwood fibres, after the addition of $MgCO_3$. This is mainly due to an increase in fibre length. In contrast, for bagasse fibres, after the addition of 1%$MgCO_3$ the percentage of fines increased as the fibre length was reduced more.
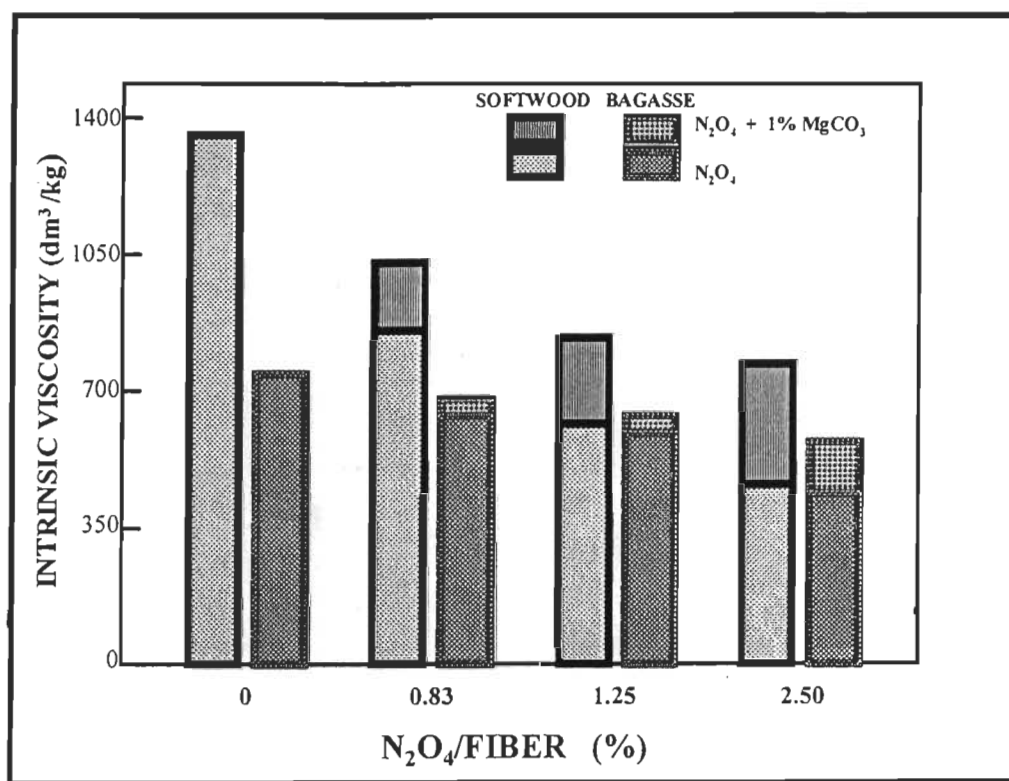
FIGURE 4.89   The effect of the addition of 1.0 % $MgCO_3$ on viscosity during oxidation by N_2O_4.
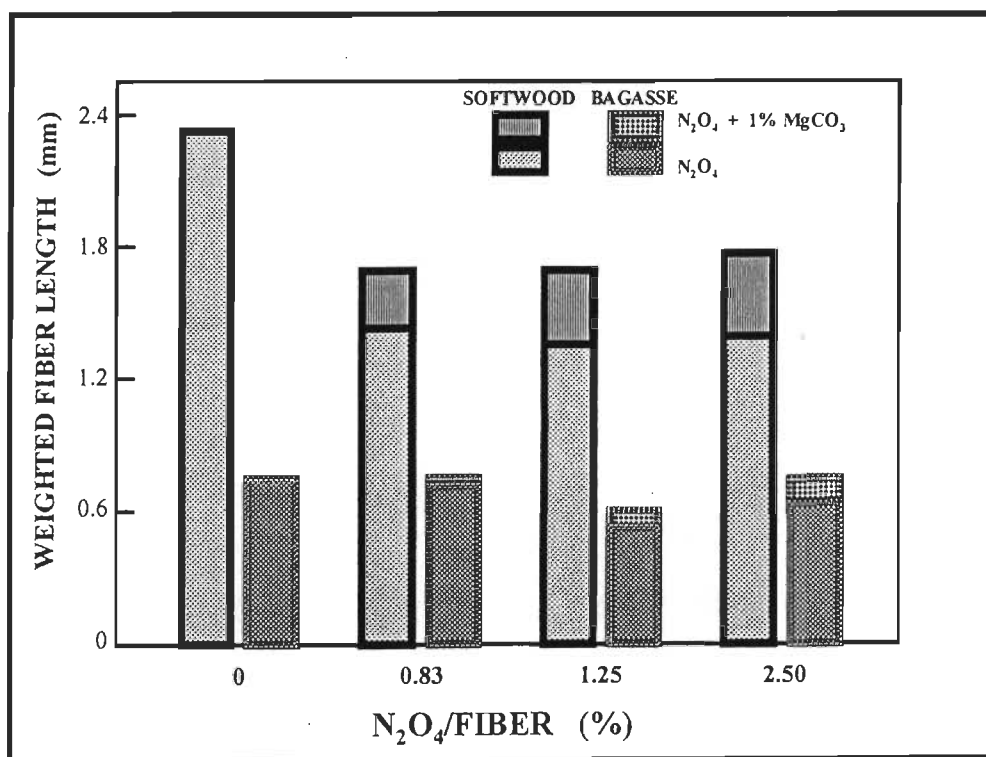
FIGURE 4.90 The effect of the addition of 1.0 % MgCO₃ on weighted fibre length during oxidation by N₂O₄ .
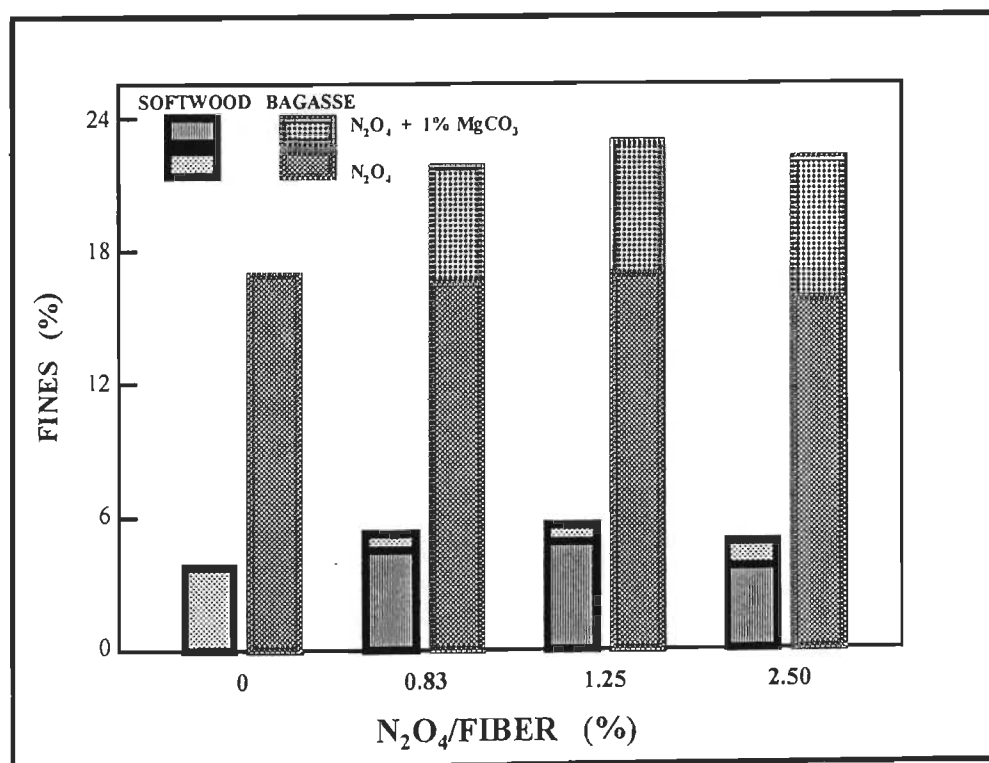
FIGURE 4.91 The effect of the addition of 1.0 % MgCO₃ on percentage of fines during oxidation by N₂O₄.

4.5.2.3   Strength properties

The results of this comparison brought out several interesting features. First, the presence of 1.0% $MgCO_3$ reduced the viscosity drop at all tested conditions for both the softwood and the bagasse fibres. Nevertheless, there was a reduction in the viscosity compared to the initial value in all cases, and one would expect a corresponding drop in paper strength due to this factor alone. However, at various oxidation rates, certain strength properties were equal to or higher than those of the sheets made from the untreated pulp. The significance of this is that these increases could be directly attributed to the increase of carboxyl groups and inter-fibre hydrogen bonding caused by the oxidation treatment, as initially hypothesised. Given that some losses in strength would still occur due to the lower but observable cellulose degradation, these are more than compensated for by the carboxyl group formation.

Secondly, the increase in carboxyl groups during oxidation in the presence of $MgCO_3$ was always slightly lower than without this salt. Since the strength increases that occurred more than compensated for the cellulose degradation at the given conditions, the importance of carboxyl group formation and a resulting increase in hydrogen bonding on the strength properties of paper becomes all the more evident.

a)   Tensile Index

Fig. 4.92 shows that the tensile index of softwood fibres at 1.25 % N_2O_4 was higher than for the untreated fibre. In the case of bagasse this occurred at 2.5% N_2O_4. The increases in the strength properties in the presence of $MgCO_3$ are significant since they are greater than the standard deviation due to the experimental error. For example, the increase in tensile index for softwood fibres at 0.83% N_2O_4 was 6.23, whereas the standard deviation at this point was ±1.96. Similar examples can be observed for the bagasse fibres (Tables 4.17 and 4.18).

b)   Burst index

Fig. 4.93 shows similar effects of the addition of $MgCO_3$ on the burst index. Here the burst index for softwood fibres surpassed the initial value at 0.83% N_2O_4. For bagasse fibres the burst index at 2.5% N_2O_4 was over 3 times higher than that in absence of Mg CO_3. Thus, it can be concluded that the oxidation of the softwood fibre should be done at a lower rate (0.83%-1.25% N_2O_4 /fibre) than the bagasse fibre (1.25%-2.5% N_2O_4 /fibre).

c)   Zero-span

Fig. 4.94 shows that the zero-span values were also increased in the case of the addition of $MgCO_3$. The best case for softwood fibres was at 0.83%N_2O_4, whereas it occurred at 2.5% N_2O_4 in the case of bagasse. The other point is that, as the zero- span drop was greater for softwood fibres than for bagasse ones, and the regain due to the salt was also greater for the softwood.
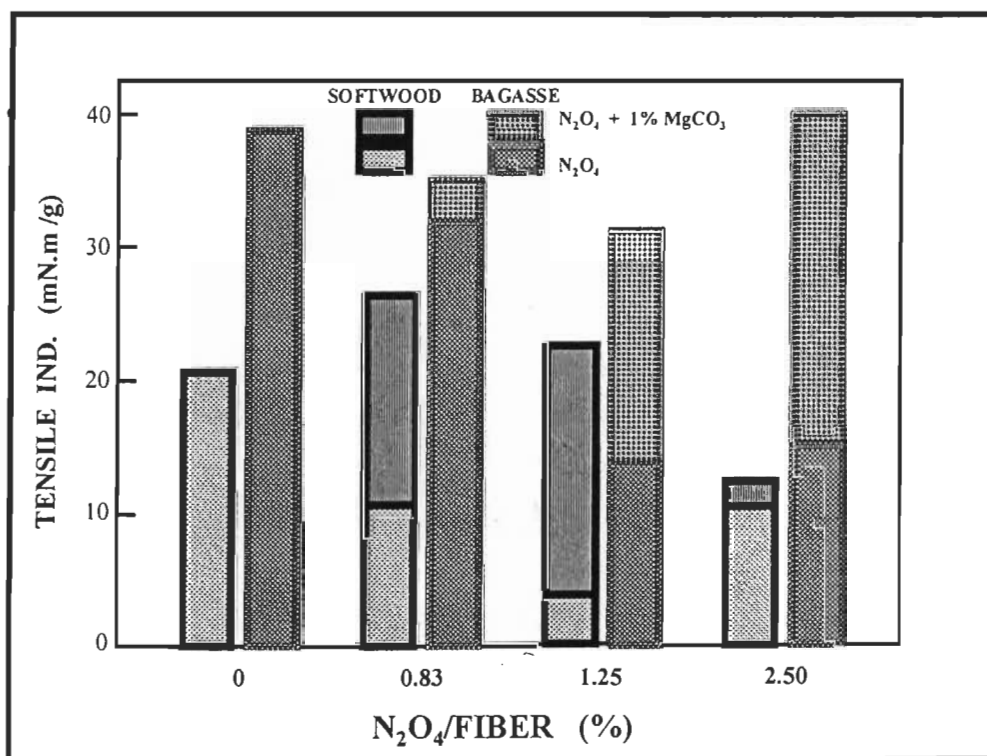
FIGURE 4.92   The effect of the addition 1.0 % $MgCO_3$ on tensile index during oxidation by N_2O_4 .
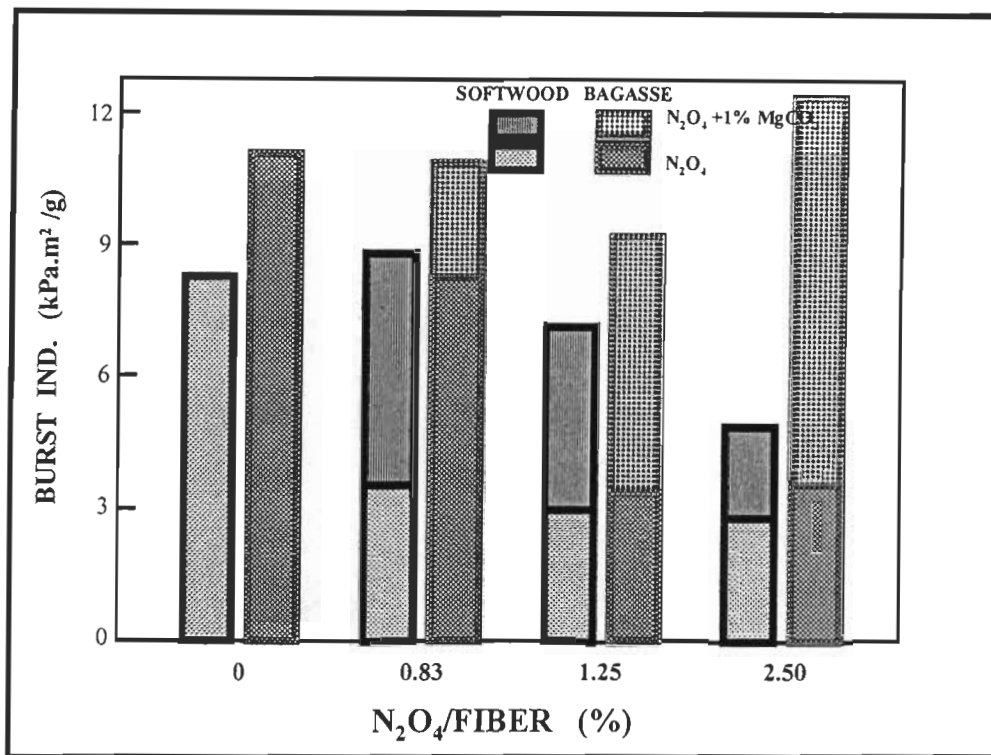
FIGURE 4.93 The effect of the addition 1.0 % MgCO₃ on burst index during oxidation by N₂O.
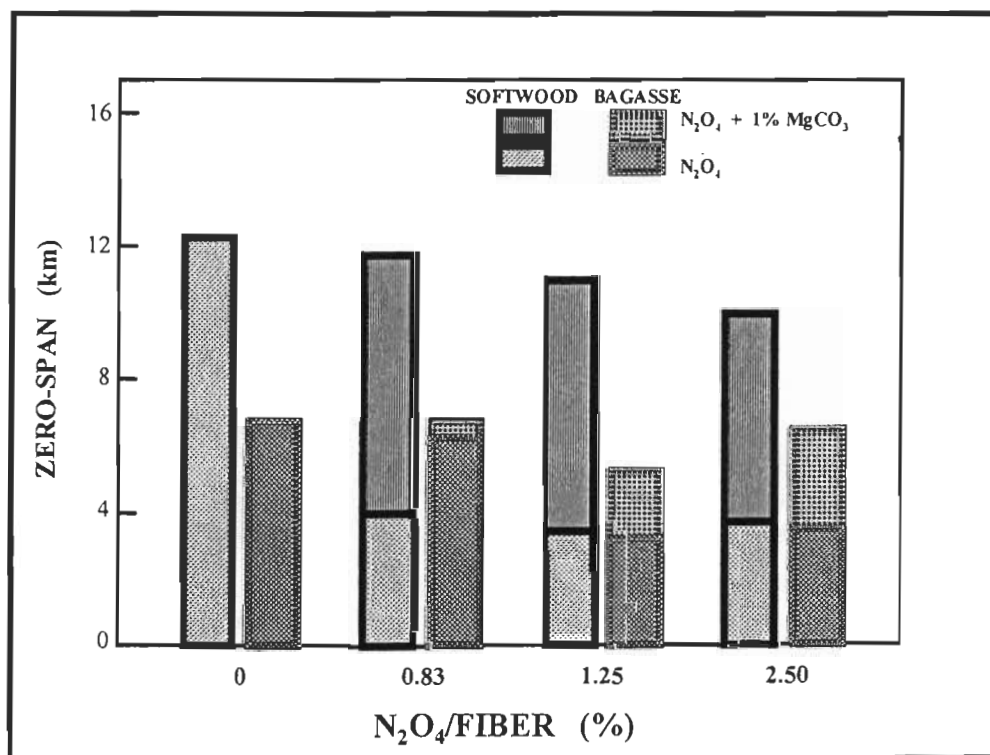
FIGURE 4.94 The effect of the addition 1.0 % MgCO₃ on zero-span during oxidation by N₂O₄.
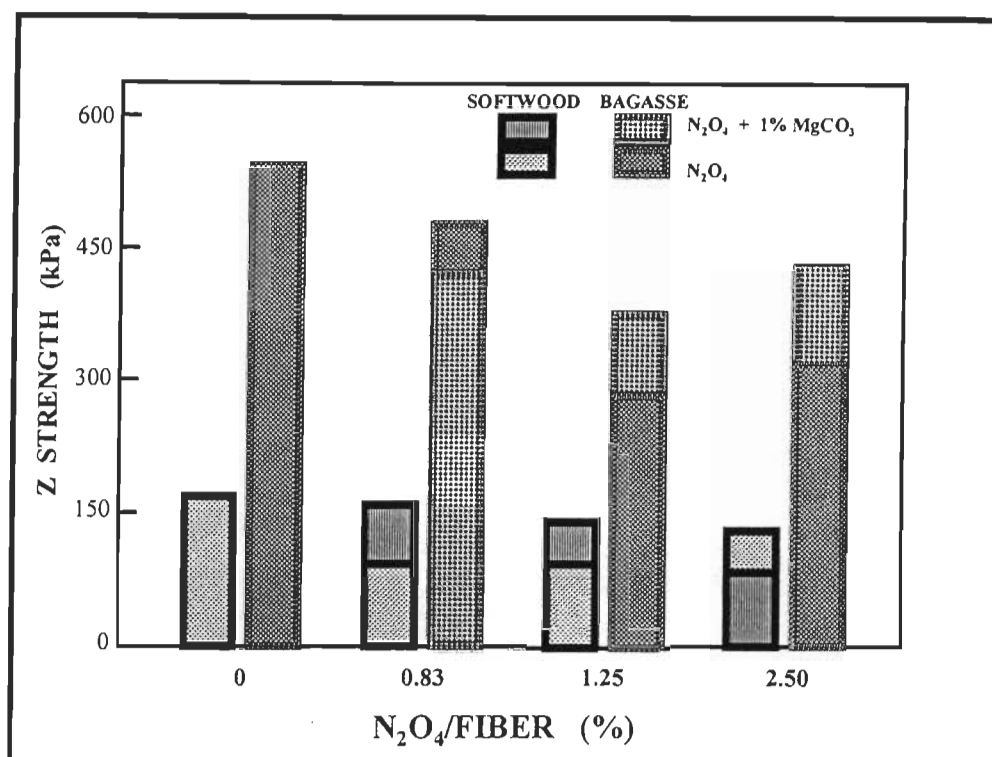
FIGURE 4.95 The effect of the addition 1.0 % MgCO₃ on z strength during oxidation by N₂O₄ .

d) Z strength

Figure 4.95, shows that the z strength, which is an indication of fibre to fibre bonding, responded to the Mg salt in similar fashion as the other strength properties.

4.5.2.4   Optical properties

a)   Brightness

Figure 4.96 shows that the brightness of the softwood fibres did not increase significantly due to the addition of 1%MgCO₃, as would be expected since the brightness was initially near its maximum. In contrast, the brightness of bagasse decreased significantly from 75 %ISO to 70.59%ISO at an oxidation rate of 2.5% N₂O₄ /fibre. This unexpected result might be explained as follows. In the presence of Mg ions, N₂O₄ produced certain radicals which broke chromophormous units of the lignin. These

units of lignin precipitated on the pulp and caused the reduction in brightness. This precipitation of chromophormous units could be eliminated by washing the oxidised fibres immediately after the treatment.

b)   Opacity

Figure 4.97 indicates that the addition of $MgCO_3$ increased the opacity of both the softwood and bagasse sheets. Since the opacity of untreated softwood fibres was much lower than the opacity of untreated bagasse fibres, the increase due to addition of $MgCO_3$ was lower than in the case of the bagasse sheets.
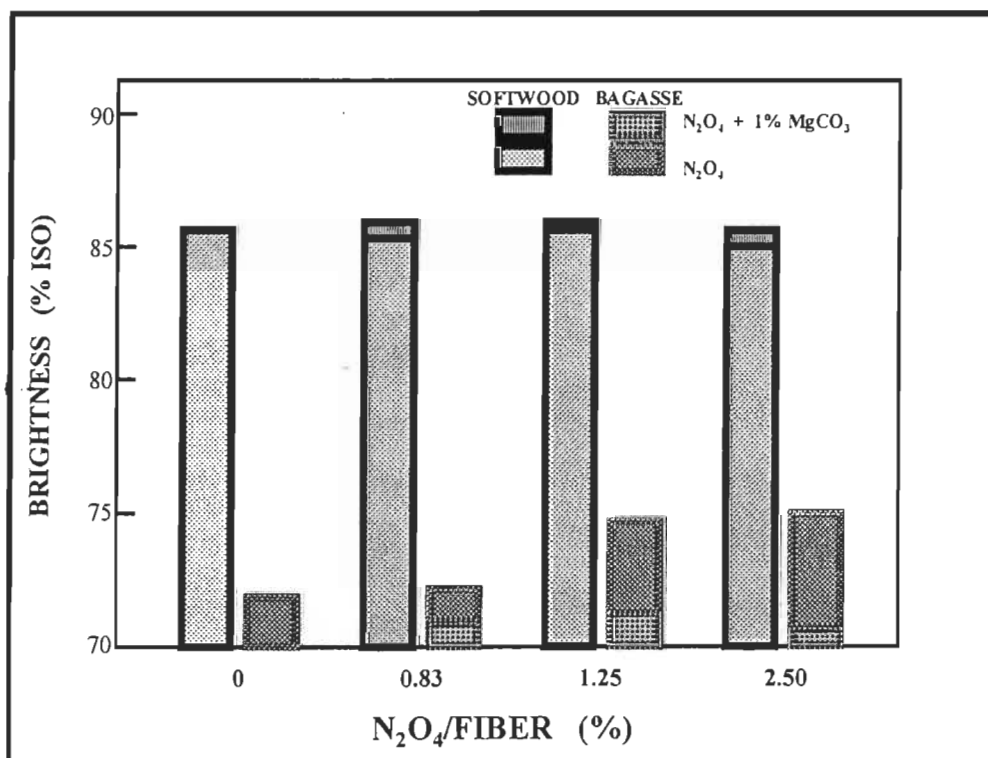
FIGURE 4.96   The effect of the addition 1.0 % $MgCO_3$ during oxidation by N_2O on brightness.

178
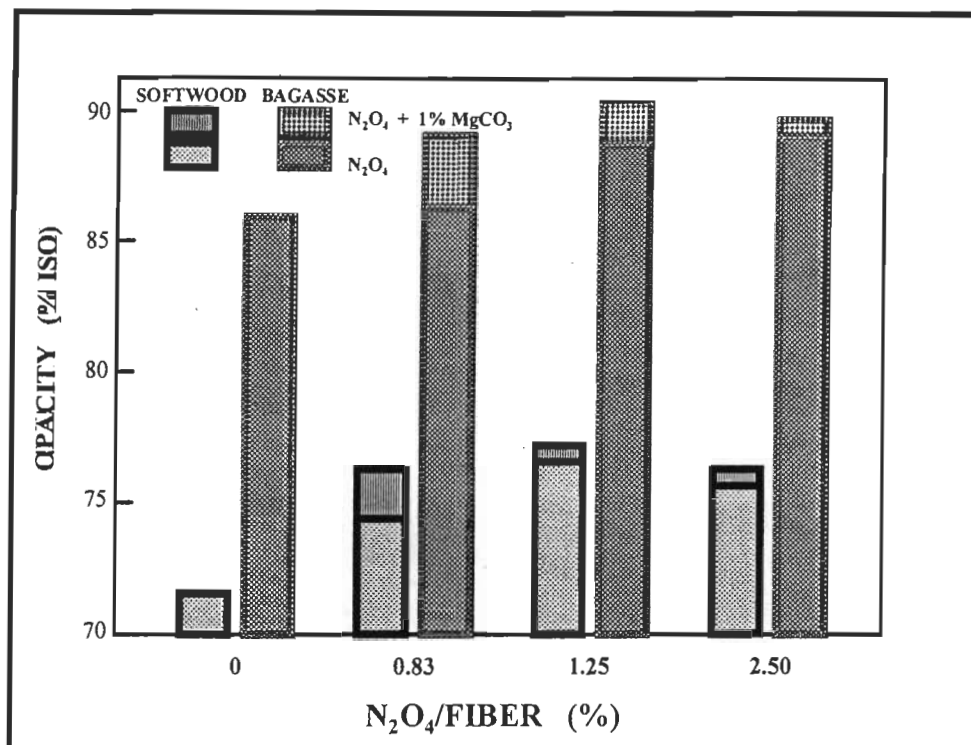
FIGURE 4.97 The effect of the addition 1% MgCO₃ during oxidation by N₂O₄ on opacity.
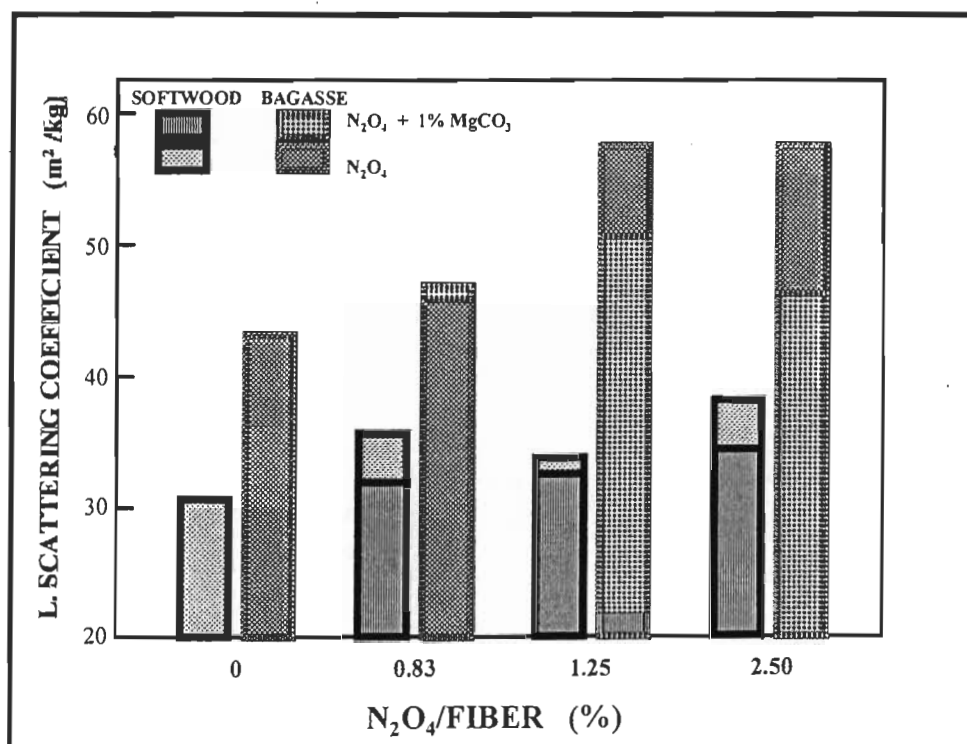
FIGURE 4.98 The effect of the addition 1% MgCO₃ during oxidation by N₂O₄ on light scattering coefficient.

c) Light scattering coefficient

A fairly large reduction in light scattering coefficient was observed for softwood fibres as well as for bagasse fibres (Fig. 4.98). The important point is that the greatest reduction in light scattering was observed at 0.83% N_2O_4 for softwood fibres (4.0 m^2/kg), and at 2.5 %N_2O_4 for bagasse fibres (10.7 m^2/kg). The decrease in the light scattering coefficient means an increase in relative bonded area, RBA, which is an indication of better fibre to fibre bonding. In other word, the higher strength properties. These are the points at which the softwood and bagasse fibres exhibited their maximum tensile and burst indices (Table 4.17 and 4.18). This confirms the influence of RBA on the tensile strength upon equation 2.1. The decrease in scattering coefficient or an increase in the RBA is any how agreeed with the increase in the percentage of the fines in this case, as it is proved in the litterature (25,137).

From all of the results presented so far, it can be pointed out that the N_2O_4 oxidation always causes some degradation of cellulose in the bleached kraft pulps. The maximum degradation appears to occur at about 1.5% N_2O_4 /fibre. At greater oxidation rates there is less degradation, as indicated by higher fibre length. This results in small but significantly higher strength properties than at 1.5% N_2O_4 /fibre, especially for bagasse fibres. This could be due to a higher pH at the higher oxidation rates, which has the effect of pushing the HNO_2 equilibrium to lower concentrations.

The use of 1% $MgCO_3$ during N_2O_4 oxidation clearly reduced cellulose degradation, as indicated by higher viscosities at the same oxidation rates. At certain oxidation rates, it was found that the strength properties increased beyond the initial values, rather than decreasing as was the case for oxidation without the salt. The results also showed the importance of hydrogen bonding due to carboxyl substitution on the strength properties of paper, once the effect of cellulose degradation on these properties was taken into account. The results indicate that the optimal conditions for nitrogen tetroxide oxidation in the presence of $MgCO_3$ are about 0.83 -1.25% N_2O_4 for softwood and 1.25-2.5% N_2O_4 /fibre for bagasse.

4.6 Mathematical evaluation of the data

There are three sets of variables involved in this study. For a given type of fibre prior to oxidation, the set of independent variables is that which describes the oxidation conditions. The characteristics of the oxidised fibres are dependent on the conditions, but may be considered to be independent variables in relation to the properties of the papers that are made from them. The three sets of variables that this study was concerned with are shown in Figure 4.96, according to the conceptualisation of Carrasco (110). This approach was used to develop the regression model using those data obtained from oxidation trials with 1%MgCO$_3$, since it is only in those trials that improvement of paper strength occurred.

Fiber characteristics
(Independent variables)

x1   C.S.F.
x2   Weighted fiber length
x3   Viscosity
x4   Carboxyl content (COOH)
x5   O/ C ratio
x6   C3/ C1 ratio
x7 I_{SP}

Oxidation conditions

z1 N_2O_4 /Fiber (%)
        + 1% $MgCO_3$

z2   Softwood and
        bagasse fibres

Paper properties
(Dependent variables)

y1   Tensile index
y2   Burst index
y3   Z strength
y4   Zero-span
y5   Brightness
y6   Opacity
y7   L.Scattering Coef.

Figure 4.99   Conceptual diagram of Carrasco model relationships between oxidation conditions, fibre characteristics and paper properties.

According to the Carrasco approach, one would designate the oxidation conditions by z, the fibre characteristics by x, and the paper properties by y. Then, the following expressions apply: $y = f(z)$ and $y = f(x)$. Since the changes in z determine the particular values of x, it is possible to use $y = f(x)$ instead of $y = f(z)$ for analysing the effect of z on the final responses (y) Table 4.19 shows the fibre characteristics resulting from the different oxidation rates. Table 4.20 further illustrates the mechanical and optical properties of the handsheets made from the treated fibres.

TABLE 4.19   Fibre characteristics

	No.	N_2O_4 /fibre (%)	C.S.F (ml)	Fibre L (mm)	Viscosity (dm^3/kg)	COOH (mmol/kg)	O/C ratio	C3/C1 ratio	Isp
			x1	x2	x3	x4	x5	x6	x7
SOFTWOOD	S-0	0	728	2.36	1347	44.4	0.593	0.249	0.43
	S-1	0.83	716	1.681	984	48.1	0.608	0.297	5.2
	S-2	1.25	694	1.659	833	50.7	0.662	0.317	11.6
	S-3	2.50	710	1.764	736	49.4	0.612	0.342	7.2
BAGASSE	B-0	0	590	0.782	726	52.9	0.568	0.188	7.7
	B-1	0.83	570	0.702	657	54.8	0.592	0.313	20.7
	B-2	1.25	597	0.634	653	50.2	0.581	0.291	20.1
	B-3	2.50	620	0.692	581	56.2	0.579	0.362	12.4

As a first step, each of the paper characteristics y_i was modelled as a linear function of each of the fibre characteristics, x_i. Eight sets of data points were involved in each of these models since the y_i from both types of fibres were used for the 4 rates of oxidation. The coefficients of determination, R^2, were computed for each of these 49 regressions to determine which of the fibre characteristics had the most significant influence on the paper properties (Table 4.21). The criterion used was the average R^2 taken over the seven paper characteristics, as seen in the table. The same thing was then done for the 21 possible 2-factor models (two-x models);

TABLE 4.20 Mechanical and optical properties of paper (y).

	No.	N_2O_4 /fibre (%)	Tensile Ind. (mN.m/g)	Burst Ind. (kPa.m²/g)	Z Strength (Kpa)	Zero-Span (km)	Bright-ness (%ISO)	Opacity (%ISO)	L.Scatt. Coef. (m²/kg)
			y1	y2	y3	y4	y5	y6	y7
SOFTWOOD	S-0	0	21.09	7.83	159.7	12.1	85.70	71.09	30.5
	S-1	0.83	26.32	8.76	154.8	11.84	85.94	76.10	31.5
	S-2	1.25	22.32	7.21	125.8	11.36	85.55	77.09	31.7
	S-3	2.50	12.99	4.29	79.2	9.75	85.60	76.09	34.5
BAGASSE	B-0	0	38.05	10.96	538.0	6.63	72.25	85.77	43.6
	B-1	0.83	35.40	10.80	403.8	6.18	71.16	88.59	47.1
	B-2	1.25	32.58	9.08	370.3	5.68	71.51	90.14	50.4
	B-3	2.50	40.07	12.32	414.8	6.38	70.59	89.50	46.6

TABLE 4.21 Coefficients of determination (r^2) obtained for the one-x models.

	f(x1)	f(x2)	f(x3)	f(x4)	F(x5)	f(x6)	f(x7)	Mean	Sum
y1	0.693	0.691	0.244	0.584	0.404	0.038	0.240	0.413	2.894
y2	0.549	0.554	0.164	0.541	0.342	0.020	0.164	0.333	2.334
y3	0.834	0.734	0.294	0.598	0.554	0.138	0.230	0.483	3.382
y4	0.899	0.899	0.648	0.725	0.641	0.009	0.575	0.628	4.396
y5	0.925	0.888	0.490	0.728	0.481	0.005	0.498	0.574	4.015
y6	0.889	0.978	0.695	0.742	0.295	0.010	0.677	0.612	4.286
y7	0.882	0.903	0.592	0.661	0.410	0.002	0.646	0.585	4.096
Mean	0.810	0.807	0.447	0.654	0.447	0.032	0.433		
Sum	5.671	5.647	3.127	4.579	3.127	0.222	3.030		

that is, each paper characteristic was modelled in terms of the data corresponding to 2 fibre characteristics at a time, using the data from both fibre types and all oxidation conditions (Table 4.22). Finally, this procedure was used for the 18 possible three-x

TABLE 4.22 **Coefficients of determination (R^2) obtained for the most important two-x models.**

	f(x2x3)	f(x2x5)	f(x1x7)	f(x2x7)	f(x1x5)	f(x1x3)	(x4x6)	f(x3x5)	f(x4x5)
y1	0.881	0.748	0.757	0.774	*0.730*	*0.718*	0.723	0.547	0.653
y2	0.768	0.698	0.625	0.652	*0.588*	*0.587*	0.641	0.432	0.590
y3	0.881	0.857	0.971	0.848	*0.906*	*0.865*	0.907	0719	0.747
y4	0.899	0.933	0.900	0.899	*0.915*	*0.928*	0.759	0.901	0.774
y5	0.935	0.945	0.930	0.894	*0.955*	*0.925*	0.799	0.815	0.803
y6	0.979	0.979	0.909	0.981	*0.889*	*0.936*	0.751	0.847	0.750
y7	0.904	0.927	0.892	0.899	*0.898*	*0.893*	0.673	0.837	0.715
Mean	0.892	0.857	0.855	0.850	0.840	0.836	0.750	0.728	0.719
Sum	6.244	5.999	5.985	5.950	5.881	5.852	5.250	5.098	5.032

TABLE 4.23 **Coefficients of determination obtained for the most important three-x models.**

	f(x2x3x7)	f(x4x5x7)	f(x3x4x7)	f(x3x5x7)	Mean	Sum
y1	0.916	0.671	0.694	0.591	0.718	2.872
y2	0.811	0.592	0.711	0.464	0.645	2.578
y3	0.945	0.772	0.649	0.740	0.777	3.106
y4	0.899	0.939	0.828	0.767	0.892	3.571
y5	0.936	0.927	0.824	0.905	0.898	3.592
y6	0.983	0.942	0.893	0.946	0.941	3.764
y7	0.915	0.967	0.818	0.977	0.919	3.677
Mean	0.915	0.830	0.774	0.770		
Sum	6.405	5.810	5.417	5.390		

models (Table 4.23).The variables of the one x-models that are most highly correlated with the paper characteristics are CSF (x1) weighted fibre length (x2) and carboxyl content (x4), in that order (Table 4.21). The least important variable is the C3/C1 ratio (x6) with an r^2 of 0.032. Here it should be emphasised that the morphological parameters are more important to the mechanical properties than are the chemical differences, carboxyl content (COOH), oxygen carbon ratio (O/C) and specific acid-base interaction

(I_{SP}). This initial step ignores possible interactions between variables and leaves a limited understanding of the processes involved.

When the 2-x models are considered, the combination that most influences the paper properties is seen to be fibre length and viscosity, f(x2x3), which had an average R^2 of 0.892. Thus, any variation in these two can cause major changes in the strength properties of paper. Wherever the viscosity was reduced, the paper strength decreased correspondingly as a result of N_2O_4 oxidation even in the presence of $MgCO_3$, although to a lesser extent in the absence of the salt. This also applies to fibre length.

The lowest average R^2 presented in Table 4.22 corresponded to the combination of carboxyl content with O/C ratio, f (x4x5) (R^2=0.719). This indicates that the strength properties of paper are not easily predictable by the O/C ratio of the oxidised fibres. However their influence on the strength properties is not negligible (r^2 = 0.719). The other independent variable which was modified by the N_2O_4 oxidation, is the specific acid-base interaction, I_{SP}, referred to as x7. The combination of this factor with CSF, f(x1x7) and with fibre length f (x2x7) also yielded significant r^2 values, 0.855 and 0.850, respectively. This implies that the variation in I_{SP} values of the fibres has a definite effect on strength properties, even though this influence is lower than that obtained for the fibre length.

Higher coefficients of determination were obtained for the three-x models which permit observation of the effects of both the fibre and hydrophilic characteristics of the fibre surface. The four convenient combinations are shown in Table 4.23. The greatest R^2 was that associated with f(x2x3x7), which includes fibre length, x2, viscosity x3, and specific acid-base interaction, x7 (R^2 = 0.92). However, three other fibre characteristics involving COOH (x4), O/C (x5) ratio and I_{SP} (x7) which were improved due to the N_2O_4 oxidation with viscosity (x3) result the following combinations: f(x4x5x7), f(x3x4x7) and f(x3x5x7), that exhibited reasonable R^2 (0.830, 0.774 and 0.770 respectively). This indicates that, even though the increase in the hydrophilic character and acid-base interaction (x4, x5 and x7) of the oxidised fibres as compared to the fibre length and

viscosity have lower effect on the physical properties of the sheet, this correlation is also noticeable with an R^2 about 0.83. The means and sums in the right-hand column of Table 4.23 show that the burst index $(R^2 = 0.65)$ is the least predictable by the three-x model while the opacity $(R^2 = 0.94)$ is the most predictable variable. In general, the optical characteristics are more affected and predictable by the N_2O_4 oxidation.

Reminding the Page equation, we may classify the factors influencing the fibre strength, and those which affect the bonding strength during N_2O_4 oxidation in presence of MgCO3. Then the final effect on the tensile strength could be well elucidated as follows; The degree of polymerisation, DP has a direct effect on the viscosity of the pulp. The reduction in viscosity due to the N_2O_4 oxidation produces the reduction in the zero-pan of the fibres. This means the reduction in the fibre strength. In other hand, fibre length reduction during the oxidation is another indication of the reduction in the fibre strength (F). These reflect in turn in the reduction in the tensile strength of the sheet, what has been observed during N_2O_4 oxidation alone.

There are some other factors that were modified during the oxidation which have an important effect on the bonding strength. These are the formation of carboxyl groups proved by the IR peaks, the increase in the O/C ratio of the fibre surface observed by ESCA, as well as the increase in I_{SP} the specific acid base interaction which by increasing the number of H-bond, hydrophilic character and the surface adhesion of the fibres, affect directly the bonding strength (B) of the oxidised fibres. The increase in the fines percentage during the oxidation has also direct effect on relative bonded area, RBA. This in its part also has a positive effect on the tensile strength of the sheet. During the N_2O_4 oxidation of the fibres in presence of 1% $MgCO_3$, we can easily observe that, even though the factors affecting fibre strength, such as fibre length and viscosity were reduced 11 to 29% and 20 to 27% respectively as shown in Table 4.24, but an increase in the factors affecting the bonding strength such as the COOH content, O/C ratio, I_{SP} and fines percentages was achieved (Fig.4.97 and 4.98). Consequently, the burst index and tensile strength were increased up to12% and 25% respectively, as compared with same values of the untreated fibres (Fig 4.99). This was obtained at an

oxidation rate of 0.8% N_2O_4 for the softwood fibres and at 2.5% for the bagasse fibres. The above results demonstrated the important role of the bonding strength of the fibres in the tensile strength of the sheet, which was improved during the N_2O_4 oxidation in presence of 1%$MgCO_3$ (the validity of the Page equation).

TABLE 4.24 **The effect of fibre characteristics(strength) and bonding strength on the paper strength during the N_2O_4oxidation in presence of 1% $MgCO_3$.**

		Softwood			Bagasse		
	N_2O_4/fibre	0%	0.8%	± %	0%	2.5%	± %
	C.S.F (ml)	726	716	-2	590	620	+5
Factors affecting Fibre strength	Fibre length (mm)	2.36	1.681	-29	0.782	0.702	-11
	Viscosity (dm³/kg)	1347	984	-27	726	581	-20
	Zero-span (km)	12.1	11.84	-3	6.63	6.38	-4
Factors affecting Bonding strength	COOH (m mol/kg)	44.4	48.1	+8	52.9	56.2	+6
	O/C ratio	0.593	0.608	+3	0.568	0.579	+2
	I_{SP}	0.54	5.2	+863	7.7	12.4	+61
	Fines (%)	3.88	4.66	+20	16.54	21.38	+29
Paper strength	Density (g/cm³)	0.491	0.488	0	0.542	0.578	+7
	Burst ind. (kPa.m²/g)	7.83	8.76	+12	10.96	12.32	+12
	Tensile ind. (mN.m/g)	21.09	26.32	+25	38.05	40.07	+5
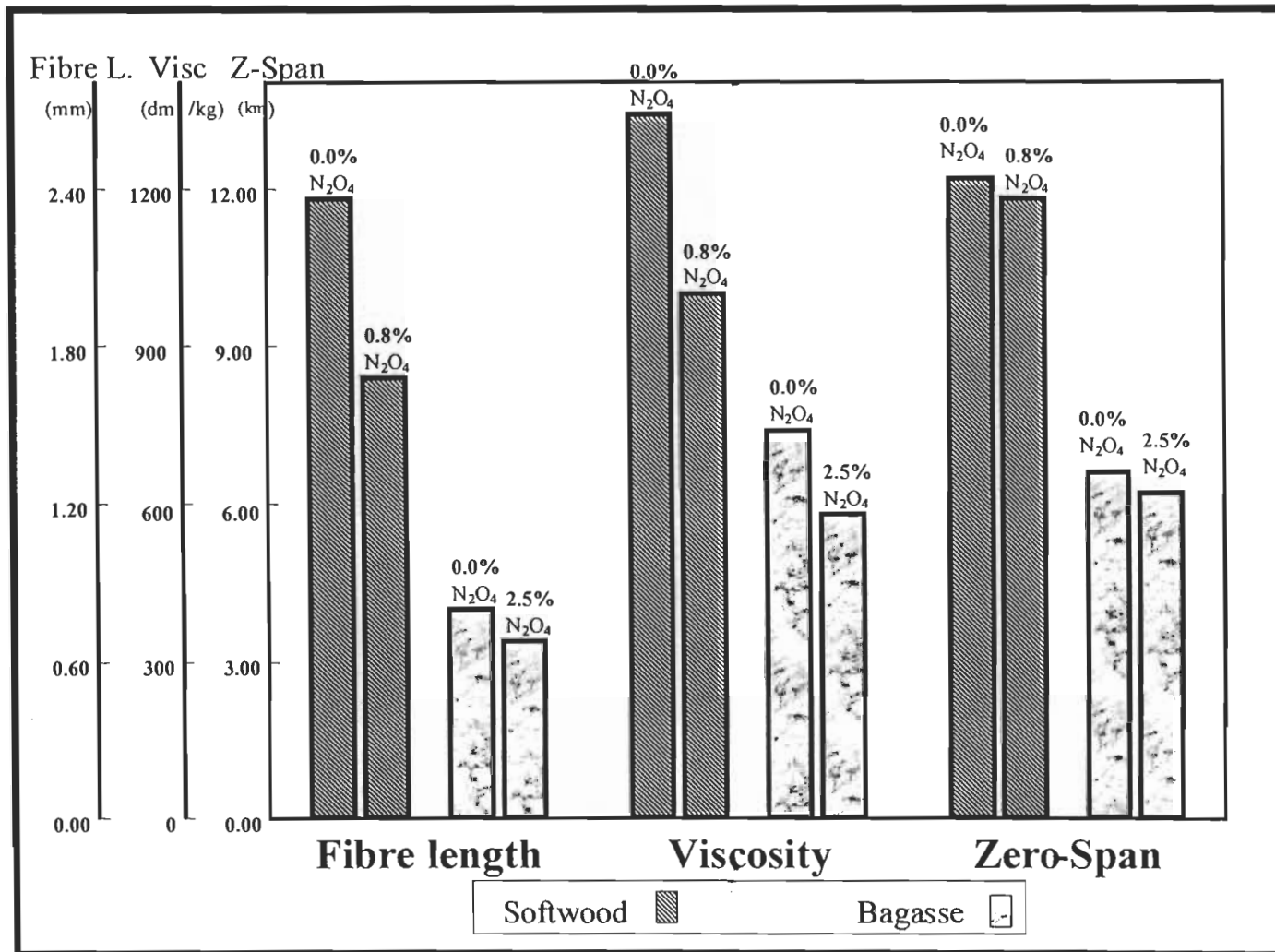
FIGURE 4.100 Factors affecting fibre strength of softwood and bagasse fibre oxidised by N_2O_4 in presence of 1% $MgCO_3$.
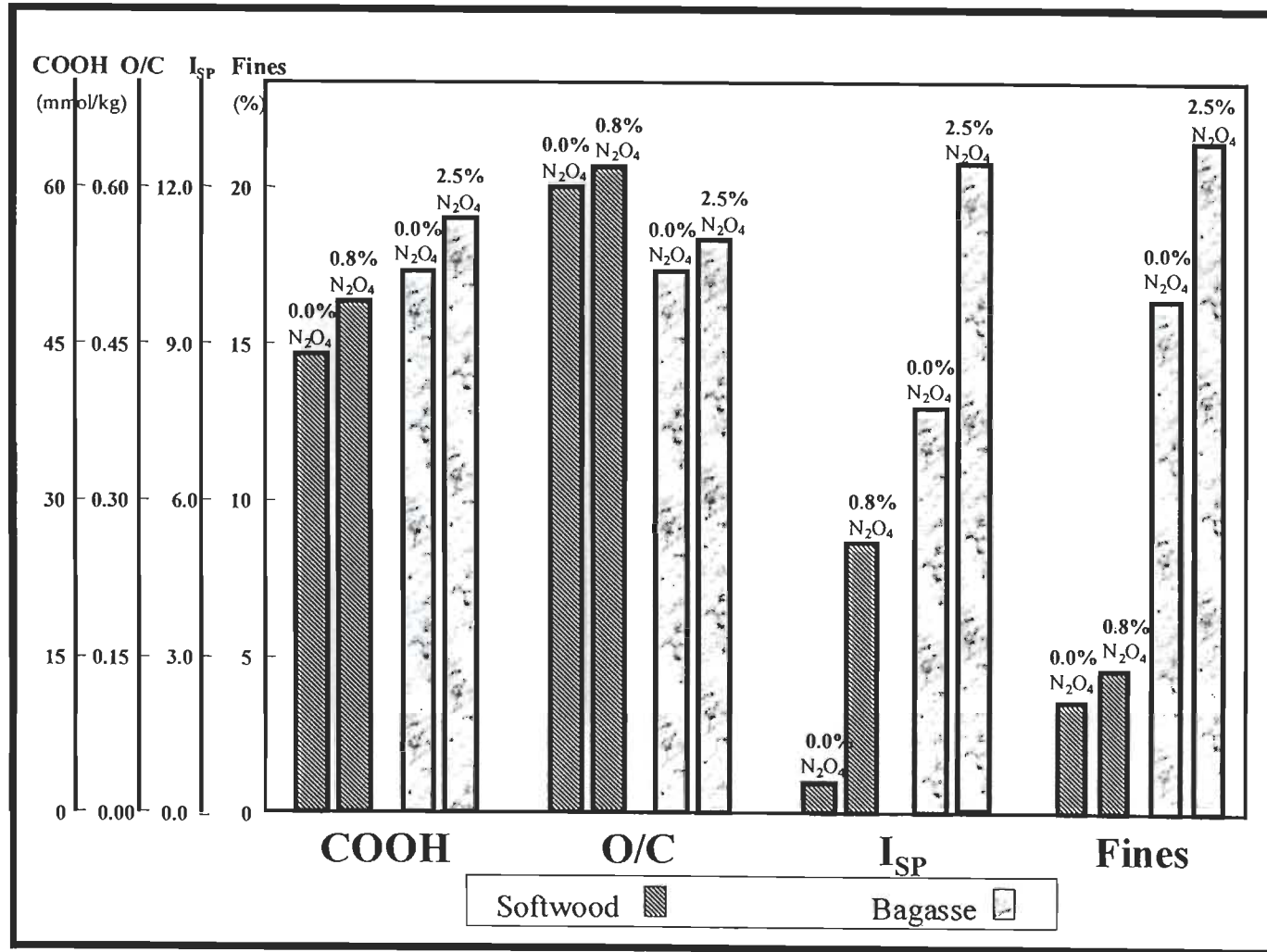
FIGURE 4.101 Factors affecting bonding strength of softwood and bagasse fibres oxidised by N_2O_4 in presence of 1% $MgCO_3$.
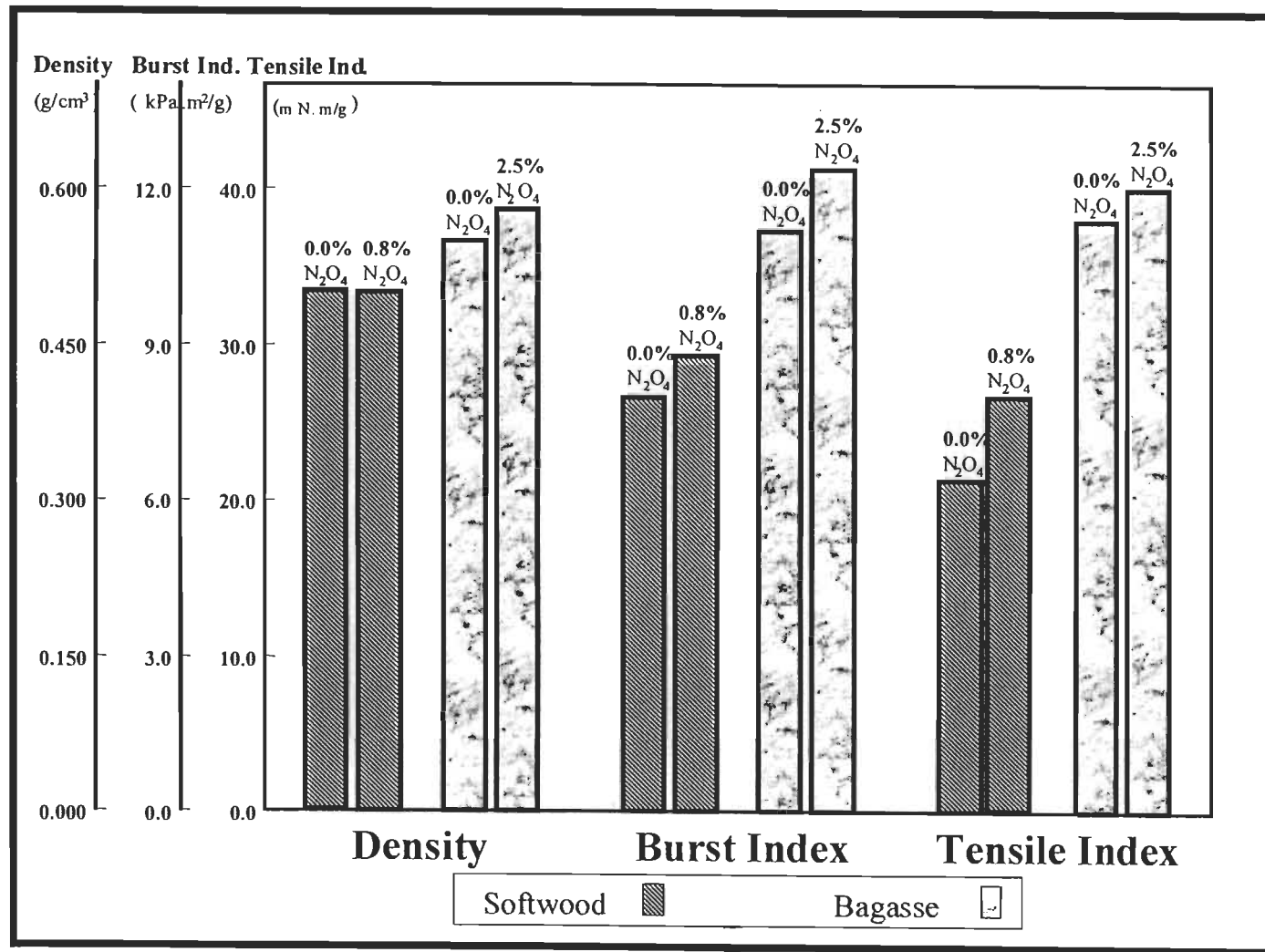
FIGURE 4.102 Strength properties improvement of the sheets made by the softwood and bagasse fibres oxidised by N_2O_4 in presence of 1% $MgCO_3$.

4.6.1 **Prediction equations**

Table 4.25 shows the three-x models with the average coefficient of determinations; R^2 =0.915 for f(x2x3x7), R^2 =0.830 for f(x4x5x7), R^2 =0.774 f(x3x4x7) and R^2 =0.770 for f (x3x5x7) and their prediction equations for each paper property.

TABLE 4.25 **Prediction equations of the correlation between of the oxidised fibres characteristics and paper properties (convenient combinations).**

y=f(x2x3x7)	R^2
y1= 41.567 - 24.833 x2 + 0.029 x3 - 0.426 x7	0.916
y2= 12.011 - 6.695 x2 + 0.008 x3 - 0.128 x7	0.811
y3= 616.616 - 449.439 x2 + 0.432 x3 -16.382 x7	0.945
y4= 3.926 + 4.129 x2 - 0.0005 x3 - 0.0064 x7	0.899
y5= 68.574 +15.500 x2 - 0.013 x3 + 0.047 x7	0.936
y6= 92.401 -11.140 x2 + 0.003 x3 + 0.122 x7	0.983
y7= 46.697 -12.827 x2 + 0.0087 x3 + 0.207 x7	0.915
y=f(x4x5x7)	R^2
y1= 43.030 +1.065 x4 - 117.5 00 x5 + 0.235 x7	0.671
y2= 5.339 + 0.354 x4 - 24.184 x5 +0.016 x7	0.592
y3=1270.379 + 15.443 x4 - 3035.608 x5 - 4.922 x7	0.772
y4= -2.811 - 0.210 x4 + 40.685 x5 - 0.210 x7	0.939
y5= 41.788 - 0.619 x4 + 122.179 x5 - 0.500 x7	0.927
y6= 83.93 + 0.683 x4 - 71.703 x5 + 0.608 x7	0.942
y7= 99.803 +0.302 x4 - 139.663 x5 + 0.766 x7	0.967
y=f(x3x4x7)	R^2
y1= -131.826 + 0.027 x3 + 2.648 x4 + 0.476 x7	0.694
y2= -40.714 + 0.009 x3 + 0.809 x4 + 0.119 x7	0.711
y3= - 2241.794 + 0.336 x3 + 43.443 x4 +5.739 x7	0.649
y4= 32.093 - 7.520 x3 - 0.430 x4 - 0.156 x7	0.828
y5= 180.579 - 0.013 x3 + 1.093 x4 + 0.522 x7	0.824
y6= 20.584 + 0.001 x3 + 1.093 x4 + 0.522 x7	0.893
y7= - 36.713 + 0.006 x3 + 1.269 x4 + 0.669 x7	0.818
y=f(x3x5x7)	R^2
y1= 138.712 - 0.005 x3 - 184.031 x5 + 0.428 x7	0.591
y2= 36.777 - 0.001 x3 - 47.115 x5 - 0.101 x7	0.464
y3= 2706.00 - 0.166 x3 - 3911.999 x5 + 5.295 x7	0.740
y4= - 23.538 + 0.005 x3 + 50.452 x5 - 0.156 x7	0.967
y5= -15.982 + 0.007 x3 + 156.851 x5 - 0.502 x7	0.905
y6= 149.558 - 0.012 x3 - 106.387 x5 + 0.514 x7	0.946
y7= 129.935 – 0.007 x3 – 153.081 x5 + 0.671 x7	0.977

In Table 4.26, the influence of the hydrophilic and surface character of the oxidised fibres (x4x5x7)to the mechanical strength and optical properties are summarised. In the same way the influence of combination of the fibre characteristics and surface adhesion character (x2x3x7) with the same mechanical and optical properties is illustrated.

Table 4.26 Coefficient of determination (degree of dependence) of the mechanical strength and optical properties of the sheet to the fibre characteristics COOH, O/C, I_{SP} and to the fibre length, viscosity, I_{SP}.

		Mechanical Strength (R^2)	Optical properties (R^2)
COOH, O/C, I_{SP}	(x4 x5 x7)	0.59 - 0.67	0.93 - 0.97
Fibre length, Viscosity, I_{SP}	(x2 x3 x7)	0.81 - 0.92	0.94 - 0.98

The paper properties, concerned to the $y = f(x2x3x7)$, fibre length, viscosity and specific acid-base interaction are plotted against the experimental data in Figures 4.103 to 4.109. The proximity of the data points to the regression lines is to be expected due to the high coefficients of determination. However, the fact that there are few outliners is also noteworthy, since it is an indication that there were few procedural problems in the experiments. For example, Figure 4.103 shows the experimental data and the values of tensile index predicted by the equation based on fibre length, viscosity and the acid base interaction. The fact that the data points are all very close to the regression line indicates the suitability of the model. Fig. 4.104 shows the worst case, which was for the burst index. Even here, the regression was quite good. Essentially, these plots can lead to a further evaluation of the data set. For example, differences in behaviour of properties of the softwood and bagasse fibres for brightness and opacity can be easily observed. It would be interesting and necessary to validate these regression equations with a different kind of fibre, in particular one that would have post-oxidation characteristics falling within the range of the two fibres used in this work.
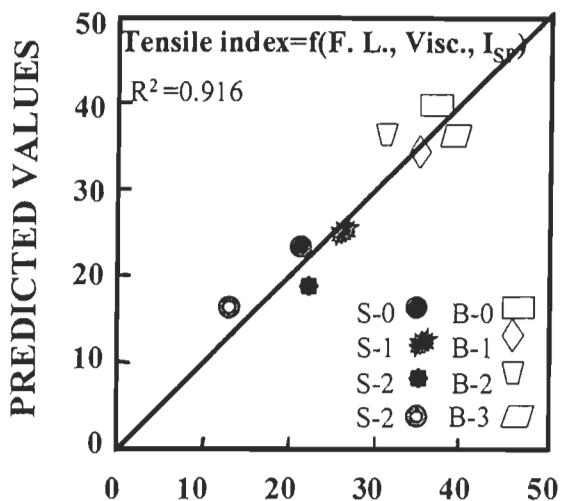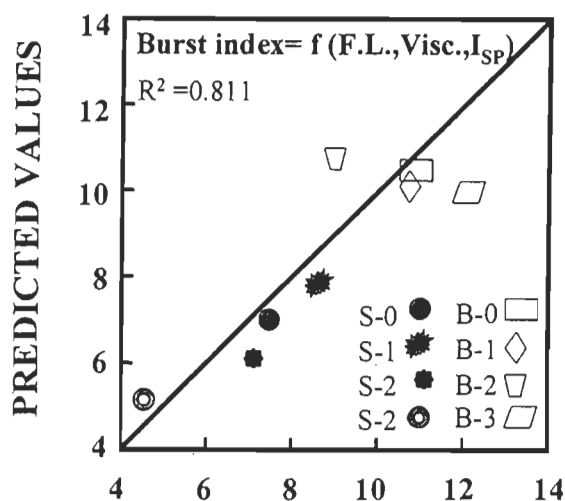
FIGURE 4.103 & 4.104 Correlation between the experimental and predicted values of the tensile index (Fig. 4.103) and the burst index (Fig. 4.104) of softwood and bagasse fibres oxidised by N_2O_4 in the presence of $MgCO_3$
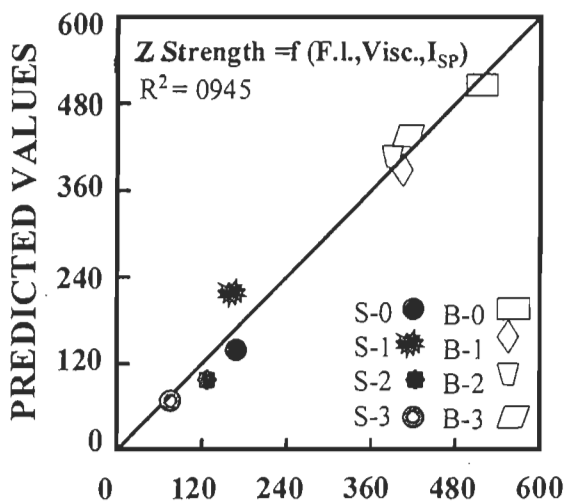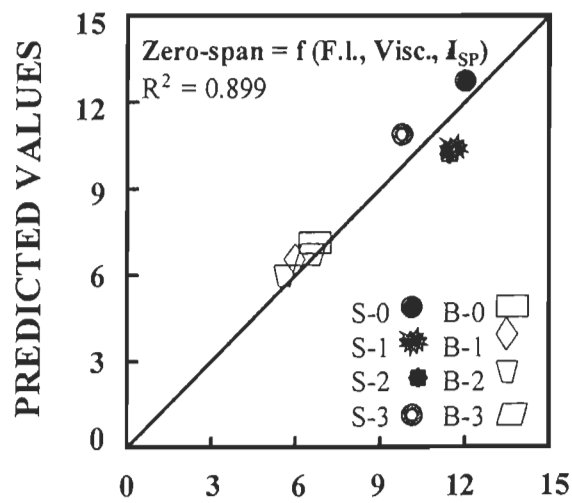
FIGURE 4.105 & 4.106 Correlation between the experimental and predicted values of the z strength (Fig. 4.105) and the zero span (Fig. 4.106) of softwood and bagasse fibres. These were oxidised by N_2O_4 in presence of $MgCO_3$.
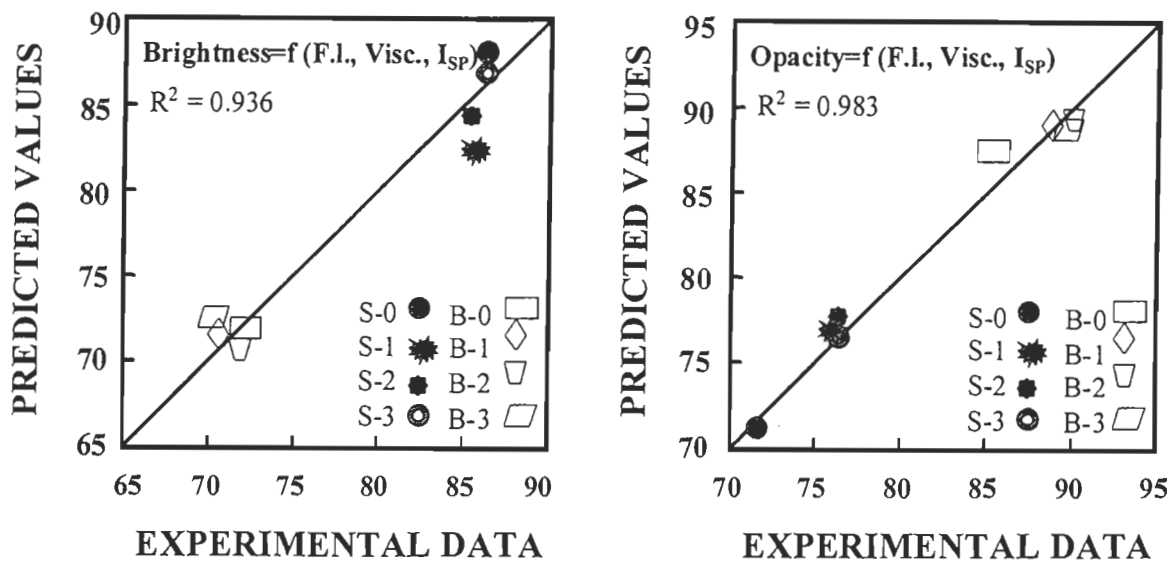
FIGURE 4.107 &4.108 Correlation between the experimental and predicted
values of the brightness (Fig. 4.107) and the opacity
(Fig.4.108) of softwood and bagasse fibres oxidised by
N_2O_4 in the presence of $MgCO_3$.
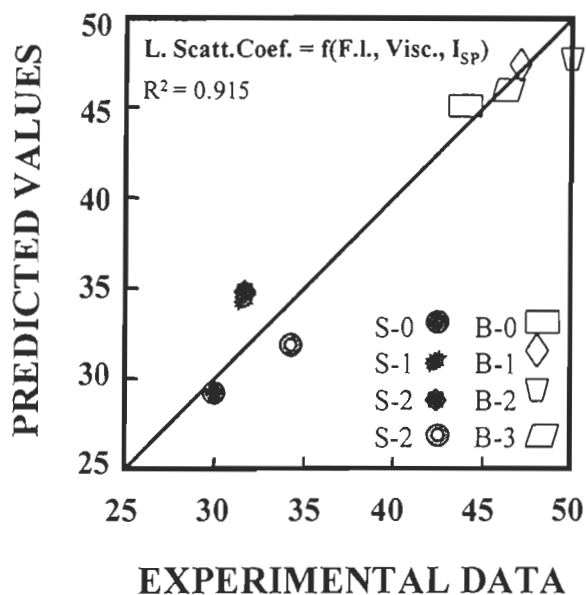
FIGURE 4.109 Correlation between the experimental and predicted values of the
light scattering coefficient of softwood and bagasse fibres oxidised
by N_2O_4 in the presence of $MgCO_3$.

CHAPTER V

CONCLUSION

The objective of this work was to evaluate the effect of N_2O_4 oxidation on the formation of carboxyl groups and on the surface adhesion of fibres. Another objective was to verify the hydrophilic character of the oxidised fibres. The latter was expected to change the internal bond strength of the fibres. In the other word, our aim was to verify the effect of the N_2O_4 oxidation on the bonding strength as well as the fibre strength . This is because both of them are affected by the oxidation, and can lead to an increase in the tensile strength of the sheet, using the Page equation. As the effect of using N_2O_4 under form of NO_2 has been already studied as a pre-treatment of oxygen bleaching for unbleached pulp, so in this work its effect was studied on the bleached kraft pulp. We were interested to evaluate the effect of the formation of the carboxyl groups (COOH) on the cellulose fibres et its influence on the fibre to fibre bonding, That is why it was preferred to chose the *bleached kraft* to eliminate as possible the interference of the lignin during treatment. Decrease in the viscosity of the cellulose by the oxidation was already mentioned in the literature, but no work was done to verify whether it is possible to find a certain condition, in which by increasing the bonding potential of the fibres through the formation of the carboxyl groups, the loss in the viscosity be compensate and leads finally to higher strength of the sheet.

At first, the effect of the oxidation parameter were evaluated on the formation of the carboxyl groups and the viscosity changes. The selected parameters to be evaluated were gas flow-rate, oxidation time, pulp consistency and ambient temperature. These parameters can be modified in a laboratory experiments as well as in an industrial operation. The experiments were continued by the oxidation of three-bleached kraft pulps of softwood, bagasse and aspen by N_2O_4 gas at the same selected conditions. Due

to the high losses in the viscosity of the cellulose which during oxidation hardly affected the fibre strength, the same treatments were repeated in the presence of $MgCO_3$.

In the case of the softwood fibres, it was found that the gas flow-rate increases the COOH formation up to a limit. Beyond that point, there is no longer any absorption of the gas, consequently there is no more increase in the formation of COOH. At the temperature of 5° celsious, a 4 - 5 ml/min gas flow-rate was found to be a sufficient amount of N_2O_4 gas to be absorbed by a 30 grams of fibres. The oxidation time is known to increase the formation of COOH. However, above a two-hour treatment, the oxidation causes drastic degradation of the cellulose with a minimum increase in COOH. Low temperature ($5^\circ C$) treatment results in a relatively small decrease in the viscosity and relative increase in the formation of COOH. Low pulp consistency (10%) also results significantly lower decrease in the viscosity, and relatively higher formation of COOH.

With respect to the FTIR spectra of oxidised fibres, it was found that the oxidation reaction produces a COOH peak at 1734-1738 cm^{-1}. The intensity of this peak is generally proportional to the oxidation ratio. At the same time, the intensity of the OH peak at 3333-3361cm^{-1} perturbed as a result of N_2O_4 oxidation. This reaction transforms the hydroxyl groups of the cellulosic chain to aldehyde, ketone and carboxyl groups in different proportions. By the same way the intensity of CH peaks at 2900 cm^{-1} were decreased, confirming the transformation of the hydroxyl function of the cellulose chains to the carbonyl functions.

As the result of the addition of 1% $MgCO_3$, the intensity of the peak at the 1715-1730 cm^{-1} band corresponding to carbonyl groups was significantly reduced. The change s in the CH peak at 2900 and OH at 333-3362 were not considerable. At the same time the intensity of the OH peak of the adsorbed water at 1645 cm^{-1} was hardly reduced in the presence of $MgCO_3$. That confirms the higher adsorption of cellulose water due to the addition of $MgCO_3$. The intensity of the COOH peak at 1734-1738 cm^{-1} also

decreased in the FTIR spectra, as the addition of $MgCO_3$ lowered the amount of the carboxyl groups formation.

In the case of the ESCA analysis of the oxidised fibres, the O/C ratio of softwood and bagasse fibres was increased, but for aspen fibres the opposite was found. This indicates an increase in the hydrophilic aspect of the softwood and baggase fibres as a result of oxidation as compared to the aspen fibres. At the same time the increase in the O/C ratio for the softwood fibres was not accompanied by a corresponding improvement in the strength of the sheet. This was the result of the high percentage of C3 obtained at 1.25% N_2O_4 /fibre. The percentage of C3 representing the carbonyl groups has increased at this oxidation ratio. The positive effect of the addition of $MgCO_3$ was especially important for the softwood fibres, at a low increase in C3 (10.1% compared to 11.2% C3 for softwood at 1.25% N_2O_4/fibre). That means the addition of $MgCO_3$ helped to lower the degradation of cellulose.

The increase in the O/C ratio was again observed for the softwood as for the bagasse oxidised fibres in presence of $MgCO_3$, confirming the improvement of the hydrophilic character of the fibres, resulting greater H-bonds that leads more bonding strength through the fibres. As far as bagasse fibres is concerned, the percentage of C3 increased unexpectedly after the addition of 1% $MgCO_3$ to 9.9% as compared to 8.6% at 0.83% N_2O_4, and to 9.1% as compared to 6.2% at 1.25% N_2O_4 /fibre. Higher carbonyl formation shows that the ESCA spectra are not always in agreement with the FTIR spectra. In other words, the results observed by the ESCA on a fibre surface, 5 μm in depth, might not be a good representation of the bulk composition of oxidised fibres.

With respect to the IGC technique an increase in the temperature of the column produces a decrease in $\Delta G(-CH_2-)$ γ^D_S and ΔH^0_A, for all of the untreated and the oxidised fibres. A linearity was observed for the lnV^0_g versus both the increases in $a(\gamma^D_L)^{1/2}$ and the 1/T for all alkane and polar probes on the fibres. The critical point of the oxidation treatment was also observed by IGC technique through minimum γ^D_S, ΔH^0_A, at 1.25% N_2O_4, in which the strength properties exhibit the minimum. The specific enthalpy of

interactions, ΔH^{SP}_A, representing the H-bonding was increased. The acid-base interactions, I_{SP} and the surface adhesion were increased respectively, which had a determinant effect on the bonding strength of the oxidised fibres. It was specially obvious in the case of the baggase oxidised fibres. These were observed by the increases in the acid-base constants of K_A and K_B of the softwood and bagasse fibres after the oxidation. However, no increase in K_A and K_B constants were seen for the oxidised aspen fibres. This is in agreement with the minimum intensity in the COOH of the IR peaks. It was observed also by the reduction in O/C ratio of the oxidised aspen fibres.

Softwood fibres showed an amphoteric character (K_A=0.49, K_B=0.54), while bagasse fibres exhibited a basic character (K_A=1.7, K_B= 2.25) and aspen fibres acidic character (K_A=2.9, K_B=1.9). Basic character of bagasse fibres might justified its significantly higher values of the acid-base constants, K_A and K_B, as compared with those values for softwood and aspen fibres during N_2O_4 oxidation in the absence or presence of $MgCO_3$. This technique was found to be outstanding to show the effect of the oxidation treatment on the surface adhesion of the fibres, the modification occurs through their specific acid base interaction values.

By observation of of the strength properties of the sheets made from the oxidised fibres, it was found that bagasse fibres were more resistant to the degradation than the softwood fibres. This was due to relatively high lignin and hemicellulose contents of the bagasse fibres, which can justify the lower decrease in the viscosity and in the strength properties of these fibres as compared with the softwood fibres during N_2O_4 oxidation. The reduction in the strength properties was even more significant for aspen than for softwood fibres. At the same time, the increase in brightness, opacity, and in the percentage of fines was more significant for bagasse fibres than for the two other fibre types.

The addition of 1% $MgCO_3$ during N_2O_4 oxidation was found to have an important effect on the degradation of cellulosic fibres. $MgCO_3$ limited considerably the degradation of the cellulose. Consequently, the minimum reductions were observed in

the viscosity, as well as in the tensile index, the burst index, the z strength and in the zero-span. In some cases, the strength property values surpassed even those of the untreated fibres. This was mainly due to the improvement of the bonding strength of the oxidised fibres, resulted by an increase in the hydrophilic character, O/C ratio, in the surface adhesion of the fibres, I_{SP} and in the percentage of the fines. In this case, the increase in the strength properties for the bagasse fibres was more visible than for the softwood fibres.

The evaluation of data concerning the influence of the characteristics of the oxidised fibres on paper properties was done through analysing the coefficient of regression of two-x and three-x models. These analysis revealed that fibre length and viscosity have much greater influence on the tensile strength than COOH content, O/C ratio and specific acid-base interaction, I_{SP}. That means, the fibre length, the viscosity of pulp and the zero-span affect the fibre strength, F, whereas the formation of COOH, the O/C ratio, the I_{SP}, the % of fines, affect the bonding strength, B. This reveals that the Page equation is also valid in the case of the N_2O_4 oxidation in presence of $MgCO_3$. When the reduction in the viscosity was limited by using Mg salt, then the positive effect of the formation of carboxyl groups (COOH), the increase in the O/C ratio and in the specific acid-base interaction reflecting higher H-bonding, hydrophilic character and surface adhesion of the fibres, could clearly be observed by the increase obtained in the tensile strength of the sheet.

Prediction equations were found for the tensile strength as a function of fibre length, viscosity and the specific acid base interaction (three-x models). That means N_2O_4 oxidation in presence of $MgCO_3$ can produce an increase in the tensile strength by considering three factors of fibre length, viscosity and the specific acid base interaction with $r^2 = 0.92$. By the same way the oxidation by the above conditions can increase the opacity and the brightness of the oxidised fibres of softwood and bagasse bleached kraft with $r^2 = 0.94$.

Herewith the *originality* of the work is summarised as follows:

1)   FTIR peak of the bagasse and aspen fibres (non treated and oxidised by N_2O_4)

2)   Acid base constants of the bleached kraft fibres of

	k_A	k_B	acide-base character
Softwood	0.49	0.55	amphoteric
Bagasse	1.7*	2.25*	basic
Aspen	2.9*	1.9*	acid

* indicates of the finding of this work

3)   The effect of the formation of COOH, hydrophilic character, O/C and acid-base Interaction, I_{SP} of the oxidised fibres on the bonding strength of the oxidised fibres.

4)   Application of the Page equation regarding the factors affecting the fibre strength, F and factors affecting bonding strength, B on the tensile strength, T of the sheet in the case of the N_2O_4 oxidation.

5)   Positive effect of the addition of $MgCO_3$ during the oxidation on minimising in the cellulose degradation of the fibres

6)   Prediction equation to derive the effect of the physical and surface parameters to the tensile strength and the opacity of the sheet during the oxidation with a R^2 over 90%.

It can be assumed that this process may have an industrial application, specially for the semi-bleached pulps (contain about 1% lignin), in preference pulp containing some percentage of the hemicellulose such as bagasse pulp, when the bonding strength of the fibre can be increased and the optical properties needed for writing printing paper can be improved without using chlorine base bleaching agents. To achieve this goal following recommendation are proposed for the future researches.

Recommendations for further research

In order to determine the applicability in an industrial setting, further studies will be necessary as follows:

1)   The mechanical and physical properties of the oxidised fibres should be determined at the different levels of refining.

2)   Other oxidation agents such as $NaClO_2$ or $KMnO_4$ could be tried to compare their degradation effect with that of N_2O_4.

3)   The effectiveness of the other salts such as $MgSO_4$ which is cheaper than the $MgCO_3$ could be investigated.

4)   Installation of a pilot plant will be necessary to observe the operational and maintenance concerns.

5)   With the additional information, a cost-benefit analysis should be performed for the above alternatives.

CHAPTER VI

REFERENCES

1   Nedelecheva, M. P., Stoilkov, G. V., "Polyacrylamide Adsorption by Cellulose ", Colloid Polymer Sci., 225 (4): 327-333 (1977).

2   Walecka, J. A., "An Investigation of Low Degree of Substitution. Carboxymethylcelluloses", Tappi 30 (7):458-863 (1956).

3   Harpham, A., Reed, A. R., Turner, H. W.,"The Fine Paper Properties of Cotton Linters ", Tappi 41 (11): 629-631 (1958).

4   Lewin, M., Ettinger, A., "Oxidation of Cellulose by Hydrogen Peroxide ", Cellulose Chem. Technol., 3 (1): 9-20 (1969).

5   Ni, Y., Kang, G.I., Van Heiningen, A.R.P., "Are Hydroxyl Radicals Responsible for Degradation of Carbohydrates During Ozone Bleaching of Chemical Pulp ", J. of Pulp and Paper Sci., 22 (2) February (1996).

6   Lachenal, D., "Mécanisme réactionnels des constituants du bois au cours des cuisson soude oxygène ", Synthèse bibliographique, A. T. I. P, 30 (6): 203-212 (1976).

7   Hon, D. N. S., Shiraishi, N., "Wood and Cellulose Chemistry ", 1st. Ed. Marcel Dekker Inc. New York, U.S.A., pp 90-333 (1991).

8   Kuniak, L., Alince, B., Marsura, V., and Alföldi, J., "Change in Fine Structure of Cellulose upon Oxidation ", Institute of Chemistry, Slovak Academy of Sciences, Bratislava, Czechoslovakia, Svensk Papperstidning, 7 (15): 205-208 (1969).

9   Snyder, S. L., Vigo, T. L., Welch, C. M., "The Oxidation and Methylation of Cotton by Methyl Sulfoxide-Acetic Anhydride ", Carbohydrate Research, (34): 91-98 (1974).

10   Shimizu, Y., Hayashi, J., "Acetylation of Cellulose with Carboxylic Acids ", Cellulose Chem. Technol., 23:661-670 (1989).

11   Mouhlin, U.B., "Cellulose Fiber Bonding, Part 4. Effect of Chemical Modification on Rayon Fiber Bonding ", Sevensk Papperstidning, (10): 273-275 1975).

12 Daneault, C., Kokta, B. V., Cheradame, H., "Oxidation of Kraft Pulp Cellulose by Tetroxide of Ruthenium "., J. Wood. Chem. Technol., 3 (4): 459-472 (1983).

13 Urchaudhari and Bmadhava Rao, "Kinetic and Analytical Studies of Oxidation of Cellulose Acetate and Cotton Linters with Ammonium Hexanitratocerate ", Indian Journal of Textile Research, (12): 184-187 (1987).

14 McGee, P. A, Fowler, W. F., Unruh, C. C., "Investigation of the Properties of Cellulose Oxidized by Nitrogen Dioxide.VI, The effect of Alkali on the Celluronic Acid ", Communication No, 1179, from Kodak Research Laboratories, (70): 2700-2705.

15 Mercer, C., Bolker, H. I, "Keto Groups of Cellulose and Mannan Oxidized by Nitrogen tetroxide ", Carbohyd .Res., (14): 109-113 (1970).

16 Friedlander, B. L., Dutt, A. S., Rapson, W. H., "The Infrared Spectrum of Oxidized Cellulose ", Pulp and Paper Can. (11): 587-591 (1967).

17 Reinhardt, R. M., Fenner, T. W., Reid, J. D., "Oxidation of Partially Etherified Cottons with Nitrogen Dioxide ", Textile Research Journal, (9): 735-742 (1962).

18 Samuelson, O., Ojteg, U., "NO_2 Treatment of Kraft Pulp Followed by Oxygen Bleaching, Influence of Black Liquor ", Tappi (2):141-146 (1990).

19 Ohi, H., Tajiri, M., Iwanaga, Y., "A Pre-treatment with Nitrous Acid for Oxygen Bleaching of Kraft Pulp and Its Bleaching Mechanism ", Japan's Pulp & Paper Inst. (5): 635-644 (1993).

20 Brannland, R., Norden, S., Lindsrom, L.A, " Implementation in a Full Scale, The Next Step for Prenox ", Tappi (5): 231-237 (1990).

21 Kokta, B. V., Maldas, D., Kuruvilla, A., "Graft Copolymerization of Thermomechanical Pulp Treated with Nitrogen-Oxides ", Eur.Polym.J. 26 (3): 349-353 (1990).

22 Henricson, K., "MC Ozone Bleaching". Paper 4-1 intl. Non-Chlorine Bleaching Conf., FL (Mar.1994).

23 Nedelcheva, M. P., Yur'ev, V. I., « The Effect of the Degree of Pulp Oxidation, The Amount and Formation of Adsorbed Metal Cations on its Swelling in Water. II», Nauch. Tr. Leningrad. Lesotekh. Akad.no.121.74-78(1969).

24 Page, H. D., "A Theory for the Tensile Strength of Paper ", Tappi 52 (4): 674-681 (1969).

25 Paavilainen, L., "Bonding Potential of Softwood Pulp Fibers", Paper and Timber, 76 (3): 162-173 (1994).

26 Berger, B. F., Baum, G.A., "Z-direction Properties: The Effect of Yield and

Refining ", Papermaking Raw Materials, Transactions of the Eighth Funds. Res. Symp., Mech. Eng. Publications Ltd, London, England., (1985).

27   Mayhood, C. H., Kallmes, O. J., Cauley, M. M., "The Mechanical Properties of Paper, Part II: Measured Shear Strength of Individual Fiber to Fiber Contact ", Tappi 45 (1): 69-73   (1962).

28   Mouhlin, U.B., "Cellulose Fiber Bonding. Determination of Interfiber Bond Strength ",Sevensk Papperstidning, (4): 131-137 (1974).

29   Van den Akker, J. A., Lathrop, A. L., Voelket, M. H., "Importance of Fiber Strength to Sheet Strength ", Tappi 41 (8): 416-425 (1958

30   Schniewind, A. P., Nemeth, L. J., Brink, D. L., "Fiber and Pulp Properties, 1. Shearing Strength of Single Fiber Crossings ", Tappi 47 (4): 244-248 (1964).

31   Goring, D. A. I., "Surface Modification of Cellulose in a Corona Discharge ", Pulp & Paper Mag. Can. 68 (8): T372-t376 (1967).

32   Hartler, N., Mouhlin,U.B., "Influence of Pulping on Interfiber Bond Strength ", Svensk, Papperstidning, (8): 295-299 (1975).

33   Luzakova,V., Marcinova,T.,"Effect of Pulp Oxidation on Paper Bonding System ", Cellulose. Chem.Technol, (26): 471-477 (1992).

34   Borsa, J., Reicher, S., " Study of Carboxymethylation of Low Degree of Substitution ", Cellul. Chem. Technol., (26): 261-275 (1992).

35   Talwar, K. K., "A Study of Improved Strength in Paper Made from Low-Substitued Carboxymethylcellulose Pulp ", Tappi 41 (5): 207-215 (1958).

36   Abrahamson, K., Samuelson, O., " Consumption of Oxygen and Formation of Carbon Monoxide during NO_2/O_2 Pretreatement of Kraft pulp ", Tappi 67 (12): 77-81 (1984).

37   Carlsmith, L. A., Luthi, o., Barclay, H., " Gaz Phase Ozone Bleaching, Part 1: Rate of Ozone Consumption in Agitated Contractors ", Pulp & Paper Canada, 97 (12): 141-147 1996).

38   Ohi, H., Kishino, M., Ikeda,T., "Mechanism of Delignification by Nitrous Acid. I- Degradation of Nonphenolic Lignin Model Compounds ", Mokuzai Gakkaishi, 40 (4) 452-454 (1994).

39   Lachenal, D., Bokstrom, M.,"Improvement of Ozone Prebleaching of Kraft Pulp ", J. of Pulp and Paper Sci., 12 (2) March (1986).

40   Dillner, B., Peter, W., "Application of MC Ozone Delignification for Bleaching Chemical Pulp ", to be presented at the SPCI 92/ATICELCA, Bologna, May 20, (1992).

41   Chirat, C., Lachenal, D., " Effect of Ozone on Pulp Components, Application to Bleaching of Kraft Pulps ", Holzforschung, Suppl. 133-139 (1994).

42   Sjostrom,E., "Wood Chemistry, Fondamental and Applications ", Academic Press. Inc., Florida, U.S.A., pp 38-55 (1981).

43   Kany, " The Effects of NO_2 Gas on the Structural Change of Cellulose ", Institute of Russian Beilarus, 11: 2476-2480 (1976).

44   Pettersson, S., Samuelson, O., "Carboxyl Groups in Chlorite Oxidized Cellulose before and after Alkali Treatment ", Svensk Papperstidning, II (15 juni): 429-431 (1968).

45   Svetlov, B.S., Lur'e, B.A., Kornilova, G. E., "Kinetics of Cellulose Oxidation by N_2O_4 ", Tr. Mosk. Khim-Technol. Ins. (83): 41-47 (1974).

46   Laisha, G. M., "Oxidation of Cellulose in the Dissolved State with Nitrogen Tetroxide ", Nauch. Tr. Leningrad. Lesotekh. Akad. No. 3-7 (1973).

47   Abrahamson, K., Samuelson, O., " The Influence of Oxygen Pressure during Oxygen Bleaching of Kraft Pulp Pre-treated with Nitrogen Dioxide/Oxygen " Svensk Papperstidning, 85 (3): 27-33 1982).

48   Ramos, J., Davalos, F., Sandoval, J., "High Brightness CMP from Eucalyptus Globulus using a Nitric Acid Pre-treatment ", Tappi, 79 (12):169-177 (1996).

49   Lindstrom, L. A., ′ Prenox-genombrott eller avveckling , Nordisk Cellulosa, (4): 33-34 (1989).

50   Gert, E. V., Torgashov, V. I., Kaputskii, F. N., "Production, Properties, and Structure of High -Substituted Cellulose Nitrite ", Journal of Polymer Science, (27): 393-397 (1989).

51   Grinshpan, D. D., Kaputskii, F. N., Ermolenko, I. N., "New Data on the Mechanism of   Cellulose Oxidation by Nitrogen Oxide ", Dokl. Akad. Nauk BSSR, 17 (12): 117-119   (1973).

52   Gusev, S. S., Grinshpan, D. D., Kaputski, F. N., "Infrared Spectra of Products of Oxidation of Cellulose by Nitrogen Tetroxide ", Zhurnal Prikladnoi Spektroskopii, 24 (4): 716-719 (1976).

53   Boenig, H. V., Missouri, St. L., "Structure and Properties of Polymers ", George Thieme Publishers, Stuttgart, Germany, pp 134-135 (1973).

54   Lide, D. R., CRC, "Handbook of Chemistry and Physics", 73rd.ed. Chemical Rubber Publishing Co., Florida, U.S.A., pp 9.3-9.9 (1992).

55   Brundrup, J., Immergut, E. H., " Polymer Handbook ", 2nd. ed. John Wiley & Sons Inc., New York, U.S.A., pp 338-340 (1975).

56   Ruzinsky, F., Tomasec, M., Kokta, B.V., Garceau, J. J., "Relation Between Ultra-High Yield Aspen Pulp Properties and Fibre Characteristics by Multiple Linear Regression", Cellulose Chem.Technol, 30:267-279 (1996).

57   Koran, Z., "The Effect of Density and CSF on the Tensile Strength of Paper", Tappi 77 (6):167-170 (1994).

58   Pauling, L., "The Nature of Chemical Bonds, The Structure of Molecules and Crystals ",3rd. ed. Cornell Univ. Press, New York, U.S.A., pp 454-481 (1960).

59   McCall, E. R., Morris, N. M., Tripp, V. W., 2 "Low Temperature Infrared Absorption Spectra of Cellulosics ", Applied Spectroscopy, 25 (2): (1971).

60   Fowkes, F. M., "Role of Acid-base Interfacial Bonding in Adhesion ", J. Adhesion Sci. Technol., 1 (1): 7-27 (1987).

61   Chaudhury, M. K., van Oss, C. J., Good, R. J., " Paper presented at 60th Colloid and Surface Science Symposium, Atlanta (1986).

62   Skoog, D. A., West, D. M., Holler, F. J., "Fundamentals of Analytical Chemistry ", 6th.ed., Saunders College Publishing, Orlando, U.S.A., pp 118-127 (1992).

63   Dasgupta, S., J. Appl. Polym. Sci., 41: 233 (1990).

64   Vrbanac, M. D., Berg, J. C., "The Use of Wetting Measurements in the Assessment of Acid-Base Interactions at Solid-Liquid Interfaces ", J. Adhesion Sci.Technol., 4 (4): 255-266 1990).

65   Dorris, G. M.., Gray, D. G., "Adsorption Spreading Pressure, and London Force Interactions of Hydrocarbons on Cellulose, and Wood Fiber Surfaces ", J. of Collid and Interface Sci., 71 (1): 93-106 (1979).

66   Dorris, G. M., Gray, D. G., "Adsorption of n-Alcanes at Zero Surface Coverage on Cellulose Paper and Wood Fibers ", J. Colloid. Interface Sci., 77 (2): 353-362 (1980).

67   Kamdem, D. P., Riedl, B., "IGC Characterization of PMMA Grafted onto CTMP Fiber ", of Wood Chem.&Technol., 11 (1): 57-91 (1991).

68   Chtourou, H., " Evaluation fondamentale et physico-méanique des papiers composites à la base de fibres de polyéthylène et fibres lignocellulosiques ",

Ph. D. Thesis, Univ. Laval, Canada (1994).

69 Borch, J., "Thermodynamics of Polymer-Paper Adhesion: a Review", J. Adhesion Sci. Technol., 5 (7): 523-541 (1991).

70 Felix, J. M., Gatenholm, P., "Characterization of Cellulose Fibers Using Inverse Gas Chromatography", Applied Paper Chemistry, Nordic Pulp and Paper Research Journal   (1): 200-203 (1993).

71 Schultz, J., Lavielle, L., Martin, C., "The Role of the Interface in Carbon Fiber Epoxy Composites", J. Adhesion, (23): 45-60 (1987).

72 Chtourou, H., Riedl., Kokta, B. V., "Surface Characterizations of Modified Polyethylene Pulp and Wood Pulp Fibers Using XPS, and Inverse Gaz Chromatography ", J. of Adhesion Sci. Technol., 9 (5): 551-574 (1995).

73 "Tappi Test Methods 1994-1995", ISBN: 0-89852-212-9, Tappi press, Atlanta, USA (1994).

74 Katz, s., Beatson, D., Scallan, A. M., « The Determination of Strong and Weak Acidic Groups in Sulfite Pulps», Svensk Papperstidning no.6, R 48-53(1984).

76 Koubaa, A., "Amélioration de la résistance des liaisons dans le papier et les cartons par raffinage et par pressage et séchage simultanés ", Thèse doctorat en génie papetièr de l'Univ. du Québec, Trois-Riviéres, Canada (1996).

77 Koubaa, A., Koran, Z., " Measure of Internal Bond Strength of Paper-board ", Tappi., 78 (3): 103-111 (1995).

78 Pavia, D. L., Lampman, G.M., Kriz, jr. G. S., « Introduction to Spectroscopy, A Guide for Students of Organic Chemistry», W.B. Sunders Co., Philadelphia, USA. pp.17-33 (1979).

79 Rouessac, F., Rouessac, A., "Analyse chimique, Méthodes et Techniques Instrumentales Modernes", 2nd ed. Masson, Paris. France pp.139 (1994)

80 Chtourou, H., Riedl, B., Kokta, B. V., Adnot, A., Kaliaguine, S., "Synthetic Pulp Fiber Ozonation, An ESCA and FTIR Study ", J. of Applied Polymer Science, (49): 361-373 1993).

81 Dorris, G. M., Gray, D. G., "The Ssurface Analysis of Paper and Wood Fiber by ESCA ",Part I. Application to Cellulose and Lignin, Cellul. Chem. and Technol., 12 (1): 9-23; and Part II. Surface Composition of Mechanical Pulps. Cellul. Chem. and Technol., 12 (6): 721-734( ).

82 Barry, A. O., Koran, Z., Kaliaguine, S., "Surface Analysis by ESCA of Sulfite Post-Treated CTMP ", J. of Applied Polymer, (39): 31-42 (1990).

83   Hua, X., "Steam Explosion Pulping from Aspen Characterisation using New Analytical Techniques", Ph. D Thesis, Univ.Laval, Canada (1994).

84   Siegbahn, K. C., Nordling, A., Fahlman, R., Nordberg, K., "Atomic Molecular and Solid State Structures Studied by Mean of Electron Spectroscopy", Almquist and Wiksells, Uppsala, (1967).

85   Ahmed, A., Adnot, A., Grandmaison, J.L., Kaliaguine, S., Doucet, J., " ESCA Analysis of Cellulosic Materials " Cellulose Chem. Technol., 21:483-492 (1987).

86   Adnot, A., "Techniques d'analyse de surface", Notes des cours, Faculté des Sciences et de Génie.Université Laval, (1995).

87   Gray, D. G., "The Surface Analysis of Paper and Wood Fibers by ESCA ", Part III. Interpretation of Carbon (1s) Peak Shape., Cellulose Chem. Technol., 12: 735-743 (1978).

88   Reilman, R. F., Msezanea, A., Manson, S. T., " Relative Intensities in Photoelectron Spectroscopy of Atoms and Molecules", J.Electron Spectrosc. 8. 389-394 (1976).

89   Fowkes, F.M., "Acid-base Interactions in Polymer Adhesion " from Microscopic Aspect of Adhesion and Lubrication ", Elsevier Scientific Publishing Co., pp 119-134 (1982).

90   Lavielle, L., Schultz, J., Nakajima, K., " Acid-Base Surface Properties of modified Poly(ethylene Terephtalate) Films and Gelatin: Relationship to Adhesion ", Journal of Applied Polymer Science, 42: 2825-2831 (1991).

91   Dorris, G. M., "Characterization of Low Energy Surfaces by Inverse Gas Chromatography ", Ph.D.Thesis, Univ. McGill, Canada (1979).

92   Gray, D. G., Guillet, J. E., "A Gas Chromatographic Method for the Study of Sorption on Polymers ", Macromolecules, 5 (3): 316-321 (!972).

93   Etxeberria, A., Alfageme, J., Uriarte, C., Iruin, J. J., " Inverse Gas Chromatography in the Characterisation of Polymeric Materials », Journal of Chromatography, 607: 227-237 (1992).

94   Lee, H. L., Luner, Ph., "Characterization of AKD Sized Papers by Inverse Gas Chromatography ", Nordic Pulp and Paper Research Journal, 2: 164-172 (1989).

95   Lundqvist, A., Odberg, L., « Surface Energy Characterization of Pigment Coating by Inverse Gas Chromatography », J. P. P. S. 23 (6): 298-303 (1997).

96   Riedl, B., Kamdem. D. P., «Estimation of the Dispersive component of Surface Energy of Polymer-grafted Lignocellulosic Fibers with Inverse Gas Chromatography», J. Adhesion Sci. Technol.6(9):1053-1067(1992).

97   Ramond, D., "La pratique de la chromatographie en phase gazeuse", Hewlett Packard, Division analytique, Lyon. France. 1077.

98   Conder, J. R., Young, C. L., "Physico-chemical Measurement by Gas Chromatography ", chap. 9, Willey-Interscience, New York, (1979).

99   De Boer, J. H., "The Dynamical Character of Adsorption ", p.115, Oxford Univ. Press Clarendon, London, (1953).

100   Panzer, U., Schreiber, H. P., "On the Evaluation of Surface Interactions by Inverse Gas Chromatography", Macromolecules, 25: 3633-3637 (1992).

101   Saint Flour, C., Papirer, E., . J.Colloid Interface Sci., 91,63 (1983).
        Unbleached Pine and Birch Kraft Pulp Fibers", J.P.P.S. 22 (2): 43-47 (1996).

102   Sawyer, D. T., Brookmann, D.J., Chem., 40, 1847 (1968).

103   Riddle, F. L., Fowkes, F. M., "Spectral Shift in Acid-base Chemistry.1, Van der Waals Contribution to Acceptor Number ", J. Am. Chem. Soc., 112 (9): 3259-3264 (1990).

104   Papirer, J., Schultz, Turchi, C., "Surface Properties of a Calcium Carbonate Filler Treated with Stearic Acid", Eur. Polymer.J. 20 (12):1155-1158 (1984).

105   Papirer, E., Kucynski, J., Shiffert, B., Chromatographia, 23 (6): 401 (1987).

106   Gutmann, V., "The Donor, Acceptor Approach to Molecular Interactions" , Plenum Press: N.Y., 1978.

107   Mayer, U., Gutmann, V., Greger, M., Montash. Chem., 106,1235 (1975).

108   Jensen, W. B., "Overview Lecture. The Lewis Acid-Base Concepts: Recent Results and Prospects for the Future", Acid-Base Interactions: Relevance to Adhesion Science and Technology, Editors: K.L.Mittal and H.R.Anderson, jr. VSP BV, Netherlands, p 3-23 (1991).

109   Schmidt, S. R., Launsby, R. G., "Understanding Industrial Designed Experiments ", 3rd ed., Air Academy Press, U.S.A., pp 3.5-3.31 (1992).

110   Carrasco, F., Kokta, B. V., Ahmed, A., Garceau, J. J., "Ultra-High-Yield Pulping: Relation Between Pulp Properties and Fibre Characteristics by Multiple Linear Regression", Ellis Horwood Ltd, New York, (1993).

111   Barry, A. O., Koran. Z., and Kaliaguine, S., " Infrared Study of Sufonated CTMP Pulp ", Cellulose Chem. Technol., (25): 121-130 (1991).

112   Chapados, C., Trudel, M., Fitzback, L., Gauthier, A., « Problematique et résultats des mesures en DSC et en IR des saccharides », Bulletin numéro 2, Laboratoire

de spectroscopie moléculaire et centre de recherche en pâtes et papiers, UQTR,Canada (1991).

113   Fitzback, L., « Étude par spectroscopie infrarouge et par calorimétrie différentielle à balayage de composants simples du papier», Thèse de maitrise, UQTR, Canada (1992).

114   Zhbankov, R.G., "Infrared Spectra of Polycarbohydrates and Their Model System " Institute of Physics, Byelorussian Academy of Sciences, Minsk, U.S.S.R., Journal of Polymer Science. part c (16): 1629-1643 (1969).

115   Tajmir-riahi, H.A., "Interaction of D-Glucose with Alkalin Earth Metal Ions", Carbohydrate Research, 183:35-46 (1988).

116   Pouchert, C. J., "The Aldrich Library of Infrared Spectra", 2nd .ed. Library of Congress, USA. P.213-255.

117   Pachler, K. G. R., Matlok, F., Gremlich, H. U., "Merk FT-IR Atlas ", VCH publishers, Federal Republic of Germany, pp 38-46 (1988).

118   Chirat, C., Viardin, M-T., Lachenal' D.,"Use of a Reducing Stage to Avoid Degradation of Softwood Kraft Pulp after Ozone Bleaching", Paperi ja puu, Pulp and Paper and Timber 76 (6-7): 417-422 (1994).

119   Ahmed, A., Adnot, A., Kaliaguine, S., «ESCA Study of the Solid Residues of Supercritical Extraction of Populus Tremuloides in Methanol», J. of App. Poly. Sci.(34):359-375(1987).

120   Young, R. A., Rammon, R. M., Kelly, S. S., Gillespie, R. H., "Bond Formation by Wood surface Reaction, Part I- Surface Analysis by ESCA ", Wood Science, 14 (3): 110-119 (1982).

121   Yokoyama, T. , Masumoto, Y., Yasumoto, M., Meshitsuka, G., « Carbohydrates Degradation During Oxygen Bleaching Part. II :Effect of Oxygen Pressure on the Degradation of Lignin and Carbohydrates Model Compounds on the Reaction Selectivity », J. P. P. S. 22 (5): 151-154 (1996).

122   Wan, J. K. S., Depew, M. C., « Effect of NO_x Exposure on Paper, The Role of Free Radicals », J. P. P. S. 22 (5):174-177 (1996).

123   Gronroos, A. J., Pitkanen, M., Vuolle, M., « Radical Formation in Peroxide Bleached Kraft Pulp », J. P. P. S. 24 (9): 286-290 (1998).

124   Magara, K., Ikeda, T., Tomimura, y., Hosoya, S., « Acceleration Degradation of Cellulose in the Presence of Lignin During Ozone Bleaching », J. P. P. S. 24 (8): 264-268 (1998).

125   Fernandez, N., Naranjo, M. L., Alvarez, J., "Research Experiences in Bagasse Pulp Bleaching ", Tappi Proceedings, Pulping Conference, pp 121-130 (1981).

126   Atchison, J. E., " New Developments in Non-wood Plants Fibre Pulping- A Global Perspective ", Tappi Proc.1989 Pulping Conference, p: 781-802

127   Dilk, A., in "Electron Spectroscopy, Theory, Technique and Application", Brundle, C.R., vol.4, Academic Press Inc., N.Y., USA. pp.452-355.

128   Gurnagul, N., Gray, D. G., Can. J. Chemistry, 65, p.1935 (1987).

129   Huang, Y., Gardner, D. J., Chen, M., Biermann, C. J., "Surface Energetic and Acid-Base Character of Sized and Unsized Paper Handsheets", J. Adhesion Sci. Technol., 9 (11): 1403-411 (1995).

130   Dorris, G. M., Gray, D. G., " Adsorption of Hydrocarbons on Silica-Supported Water Surface", J. Phys. Chem., 85, 3628-3635 (1981).

131   Quillin, D. T., Caufield, D. F., Koutsky, J. A., "Surface Energy Compatibilities of Cellulose and Polypropylene ", Mat. Res. Soc. Symp. Proc., 266 (1992).

132   Westerlind, B., Berg, J. C., "Surface Energy of Untreated and Surface Modified Cellulose Fibers ", J. Applied Polymer Sci., (36): 523-534 (1988).

133   Schmitt, P., Koerper, E., Schultz, J., Papirer, E., «Characterization br Inverse Gas Chromatography of the Surface Properties of Calcium Carbonate Before and After Treatment with Stearic Acid », Chromatographia, vol 25(9):786-790(1988).

134   Fuhrmann, A., LI, X-L., Rautonen, R., « Effect of ECF and TCF Bleaching Sequences on the Properties of Softwood Kraft Pulp », J. P. P. S. 23 (10):487-492(1997).

135   Moss. P.A., Retulainen, E., « The Effect of Fines on Fiber Bonding : Cross Sectional Dimensions of TMP Fines at Potential Bonding Sites », J. P. P. S. 23 (8):382-388 (1997).

136   Suurnakki, A., Heijnesson, A., Buchert, J., Tenkanen, M., Viikari, L., Westermark, U., "Chemical Characterization of the Surface Layers of

137   Ingmanson, W., L., Thode, E. F., "Factors Contributing to the Strength of the Sheet of Paper , II: Relative Bonded Area ", Tappi 42 (1): 83-93 (1959).

138   Rydholm, S. A., "Pulping Process", John Wiley & Sons Inc., N.Y., USA. pp. 104-105(1965).

APPENDICES

This section consists of two parts as follows:

a) Tables A.1 to A.6 are related to the treatment conditions and fibre characteristics during the parameters evaluation by three experimental designs which were applied to the softwood bleached kraft fibres.

b) Figures A.1 to A.12 are related the to the IGC experiments on the oxidised fibres of softwood, bagasse and aspen at oxidation rates of 0.83%, 1.25% and 1.66% N_2O_4/fibre. Those figures related to the untreated pulp and oxidised fibres at 2.5% N_2O_4/fibre have already been presented in the section four of chapter 4.

Figures A.1 to A.3 are to confirm the validity of the experiments by the linearity obtained for lnV^0_g as a function of the while the number of carbon of the alkanes increases. Figures A.4 to A.6 show also the linearity between LnV^0_g and the inverse increase in the temperature of the column of IGC containing the fibres. As it can be observed the linearity are found for all types of the oxidised fibres. Figures A.7 to A.9 show values of $-\Delta H^A$ of the alkane and polar probes on different oxidised fibres (the stationary phases) as a function of $a(\gamma^D_L)^{1/2}$ when the number of carbons increased. By these figures we were able to calculate the $--\Delta H^{SP}$. for different fibres. Figures A.10 to A.12 show the plots of $-\Delta H_{SP}/AN^*$ versus DN/AN^* regarding all polar probes used. For each of the oxidised fibres. at least three to four points were considered to draw representative curves. These enable calculation of the values of K_A and K_B. These figures shows how the acid-base interaction constants are increased by the N_2O_4 oxidation. Greater slope and the intercept values obtained for bagasse fibres confirm the higher acid-base interaction representing higher H-bond formation for this fibre during oxidation. Figure A.13 represents the variations in the value of γ^P_S as a function of the temperature of the IGC column, for the untreated fibres of softwood, bagasse and aspen.

TABLE A.1 Oxidation parameters evaluation : Gas flow-rate.

Run No.	1	2	3	4	5	6
Flow (ml/min)	**2.6**	**3.3**	**4.2**	**5.5**	**6.5**	**8.9**
Time (min)	120	120	120	120	120	120
Temperature (°C)	45	45	45	45	45	45
Consistency (%)	10	10	10	10	10	10
COOH (m mol/kg)	62.5	67.64	66.59	57.69	52.01	45.81
Intrinsic viscosity (dm³/kg)	804	617	587	559	567	507
Tensile Ind (mN.m/g)	10.279	8.509	7.922	7.353	8.906	7.104
Z Strength (kPa)	59.46	64.84	61.48	58.40	60.34	59.08

TABLE A.2 Oxidation parameters evaluation : Oxidation time.

Run No.	1	2	3	4	5	6	7	8
Flow (ml/min)	2.6	2.6	2.6	2.6	2.6	2.6	2.6	2.6
Time (min)	**60**	**120**	**240**	**480**	**60**	**120**	**240**	**480**
Temperature (°C)	5	5	5	5	45	45	45	45
Consistency (%)	10	10	10	10	10	10	10	10
COOH (m mol/kg)	62.98	80.04	56.24	54.11	62.07	65.34	58.70	69.30
Intrinsic viscosity (dm³/kg)	698	680	450	411	704	520	470	385
Tensile Ind. (mN.m/g)	11.37	12.32	7.18	5.63	8.64	7.47	6.70	5.48
Z Strength (kPa)	92.70	120.40	89.40	80.60	91.89	119.70	92.40	96.80

TABLE A.3   Oxidation parameters evaluation :Consistency of pulp.

Run No.	1	2	3	4
Flow (ml/min)	2.6	2.6	2.6	2.6
Time (min)	120	120	120	120
Temperature ($^{\circ}$C)	5	5	5	5
Consistency (%)	**10**	**22.5**	**35**	**95**
COOH (m mol/kg)	86.43	60.06	53.59	75.07
Intrinsic viscosity (dm^3/kg)	·698	545	595	504
Tensile Ind (mN.m/g)	9.02	6.49	7.69	5.88
Z Strength (kPa)	128.14	72.51	63.90	63.83

TABLE A.4   Oxidation parameters evaluation :Ambient temperature.

Run No.	1	2	3	4	5	6	7	8
Flow (ml/min)	2.6	2.6	2.6	2.6	2.6	2.6	2.6	2.6
Time (min)	120	120	120	120	120	120	120	120
Temperature ($^{\circ}$C)	5	25	45	65	5	25	45	65
Consistency (%)	10	10	10	10	35	35	35	35
COOH (m mol/kg)	85.04	82.54	53.93	51.85	68.50	61.75	59.69	58.20
Intrinsic viscosity (dm^3/kg)	894	776	730	545	760	772	693	595
Tensile Ind. (mN.m/g)	10.45	8.81	8.70	4.86	8.64	8.35	7.42	6.84
Z Strength (kPa)	112.1	92.54	78.06	68.84	121.09	102.66	98.09	73.90

TABLE A.5 Oxidation parametters evaluation by a Half-Factoril-Design of four factors at two levels 2^{4-1}

Run No.	1	2	3	4	5	6	7	8
Flow (l/min) Time (min) Temperature (°C) Consistency (%)	2.6 30 5 10	2.6 30 45 35	2.6 60 5 35	2.6 60 45 10	6.5 30 5 35	6.5 30 45 10	6.5 60 5 10	6.5 60 45 35
COOH (m mol/kg)	56,45/50,65 /46,87	50.65/52.41 /50.42	59.49/57.38 /60.28	57.81/58.35 /55.25	63.05/64.29 /63.90	59.57/60.75 /61.23	63.60/65.10 /63.13	61.97/60.21 /60.53
Viscosity (dm³/kg)	918/847 /860	848/819 /782	697/720 /705	652/629 /621	682/738 /691	684/665 /603	634/614 /552	605/584 /569
Zero-span (m)	9.44/9.18 /8.11	8.14/8.47 /8.82	7.28/7.62 /7.20	6.69/7.51 /6.75	8.96/8.74 /8.01	7.22/6.58 /6.92	5.06/4.78 /4.50	5.40/4.25 /4.91
Tensile Ind. (mN.m/g)	16.97/15.41 /14.87	15.35/15.42 /14.67	13.64/12.88 /13.97	11.54/12.59 /11.23	13.91/12.09 /14.01	12.92/11.66 /11.08	10.19/10.73 /9.81	8.74/9.05 /8.34
Density (g/cm³)	0.298/0.302 /0.293	0.290/0.299 /0.295	0.319/0.308 /0.306	0.287/0.283 /0.280	0.315/0.309 /0.311	0.302/0.309 /0.303	0.358/0.350 /0.346	0.329/0.332 /0.324
Z Strength (kPa)	85.98/89.02 /86.53	58.69/62.01 /63.02	88.94/84.71 /89.12	88.19/82.02 /86.94	85.40/84.52 /81.51	77.26/74.30 /79.95	135.3/126.0 /129.9	118.4/113.5 /121.4

TABLE A.6 Oxidation parameters evaluation by a CCD of three factors at five levels.

| Run No.	1	2	3	4	5	6	7	8	9	10	11	12	13	14	15	16
Flow (ml/min)	2.6	2.6	2.6	2.6	5.5	5.5	5.5	5.5	4.04	4.04	6.488	16.11	4.04	4.04	4.04	4.04
Time (min)	30	30	60	60	30	30	60	60	45	45	45	45	70.23	19.77	45	45
Temp. (^{o}C)	5	5	5	5	5	5	5	5	5	5	5	5	5	5	5	5
Cons. (%)	10	35	10	35	10	35	10	35	22.5	22.5	22.5	22.5	22.5	22.5	43.52	1.48
COOH (m mol/kg)	52.8	51.6	62.5	58.6	57.8	56.1	54.9	52.1	54.9	56.2	49.7	50.5	53.6	54.5	53.6	56.9
Viscosity (dm^3/kg)	971	983	688	601	648	536	595	500	684	648	492	941	556	678	509	730
CSF (ml)	731	748	744	730	736	739	761	757	755	741	756	729	757	737	762	737
After refining		690	719				733	730	724	714	727		724		688	
Tensile Ind (mN.m/g)	18.49	13.40	13.13	13.03	12.90	13.85	10.80	10.16	16.84	17.56	10.17	18.58	15.27	13.76	10.20	13.79
Brightness (%ISO)	84.3	83.55	84.80	86.10	84.61	85.90	83.65	84.77	83.42	82.99	83.52	85.35	77.62	86.10	83.56	86.64
Opacity (%ISO)	73.27	74.88	75.37	74.83	74.20	73.84	76.87	78.18	77.35	78.07	76.39	73.49	77.99	75.59	75.41	75.67
Scat.Coef. (cm^2)	333.3	358.6	335.5	348.1	333.9	345.	382.5	445.3	380.5	389.	438.2	345.5	366.3	388.9	373.1	376.1
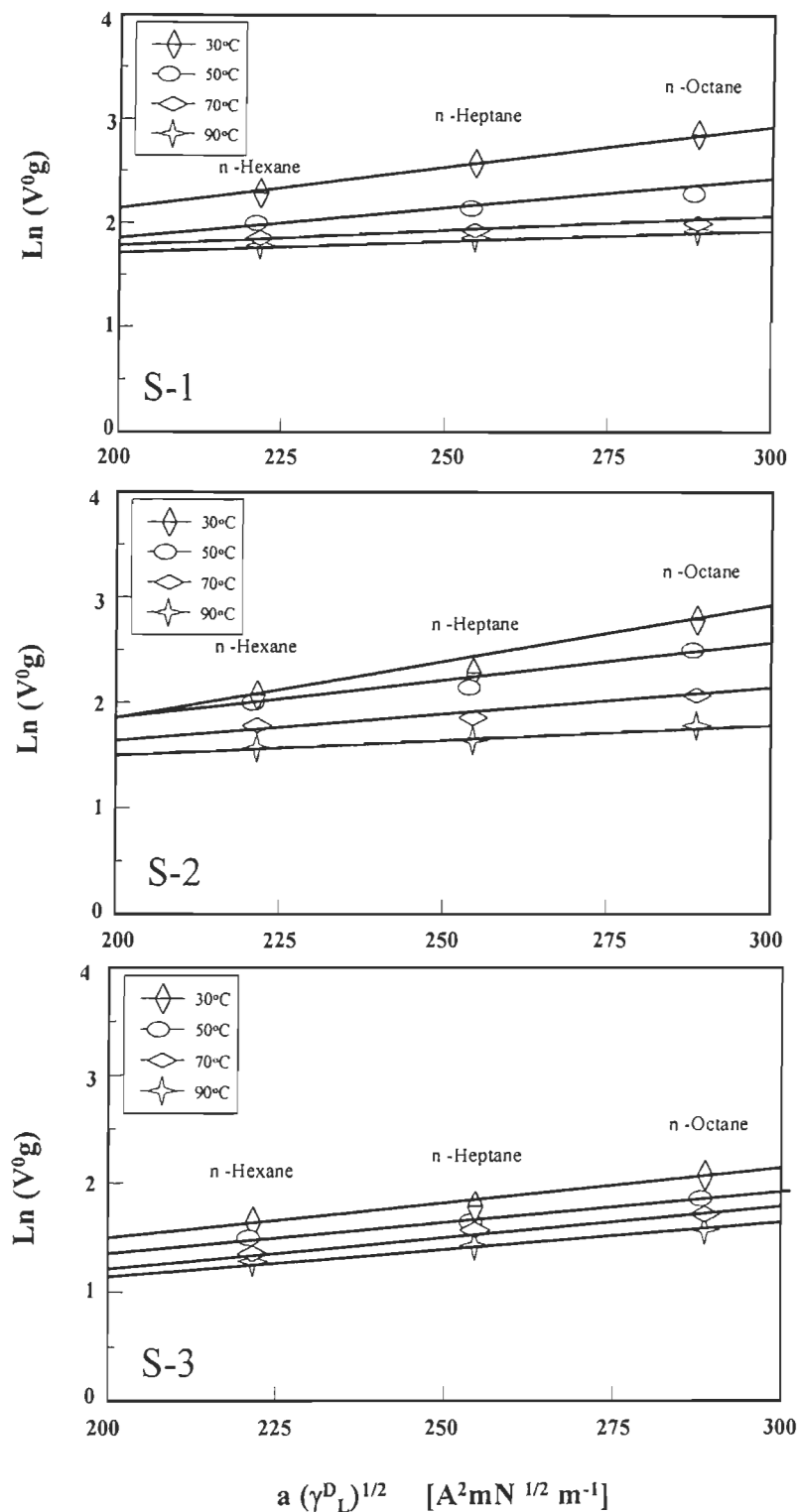
FIGURE A.1 Linearity between $\ln(V^0_g)$ and $a(\gamma)^{1/2}$ for the number of carbon of the alkane probes of the oxidised softwood bleached kraft fibres with N_2O_4 /fibre of 0.8% (S-1), 1.25% (S-2) and 1.66% (S-3).
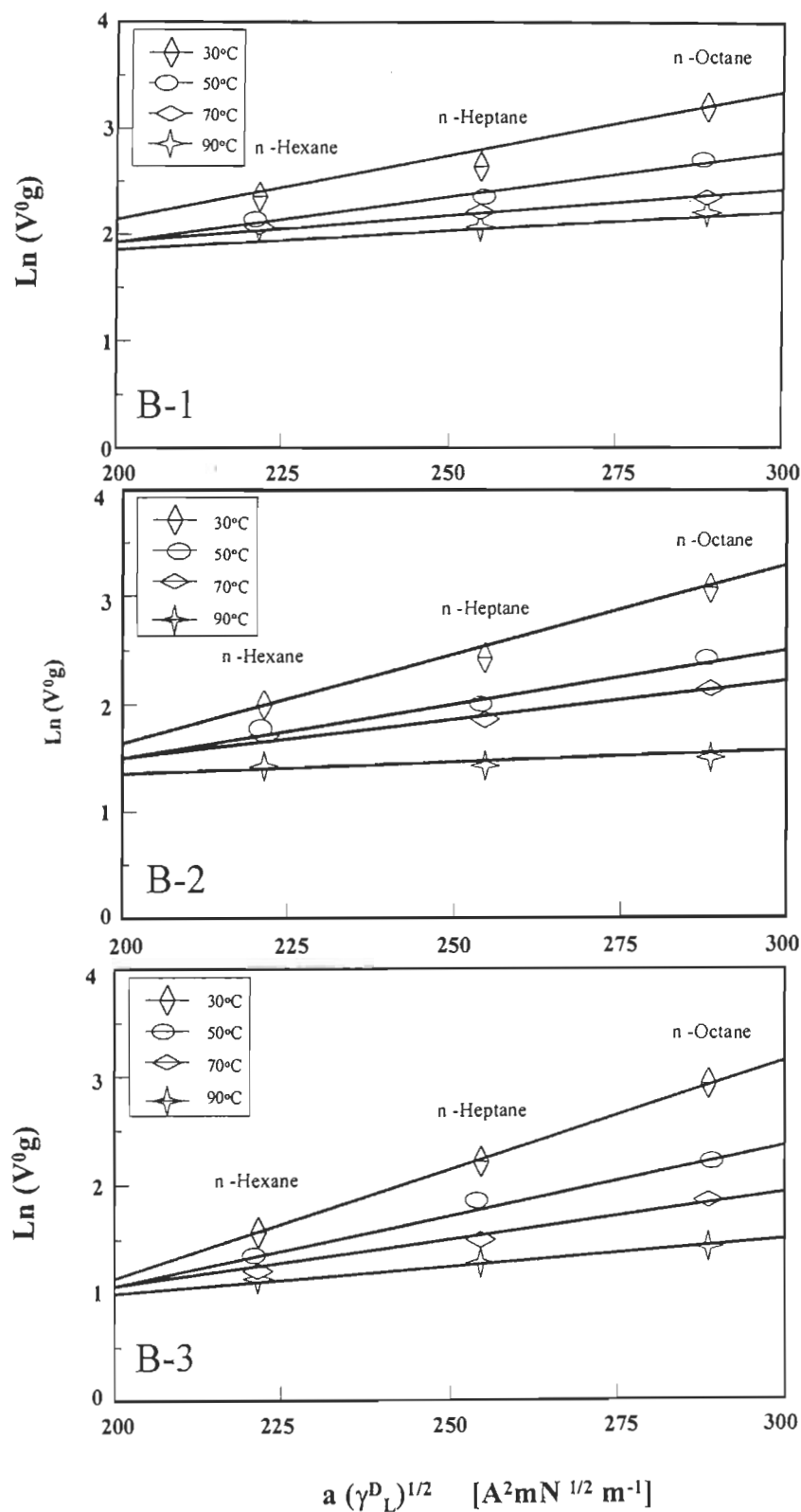
FIGURE A.2 Linearity between $\ln(V^0_g)$ and $a(\gamma)^{1/2}$ for the number of carbon of the alkane probes of the oxidised bagasse bleached kraft fibres with N_2O_4/fibre of 0.83% (B-1), 1.25% (B-2) and 1.66% (B-3).
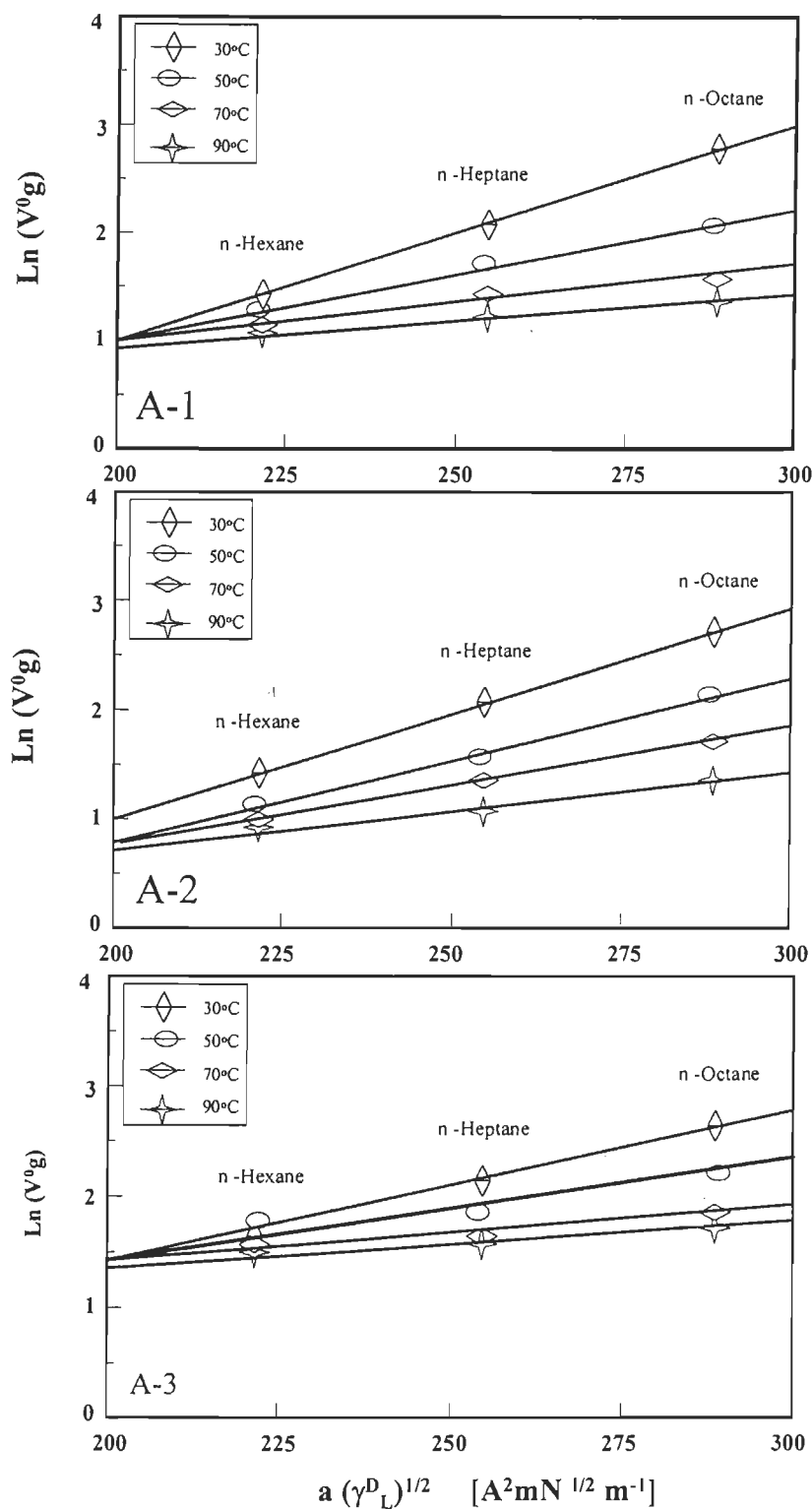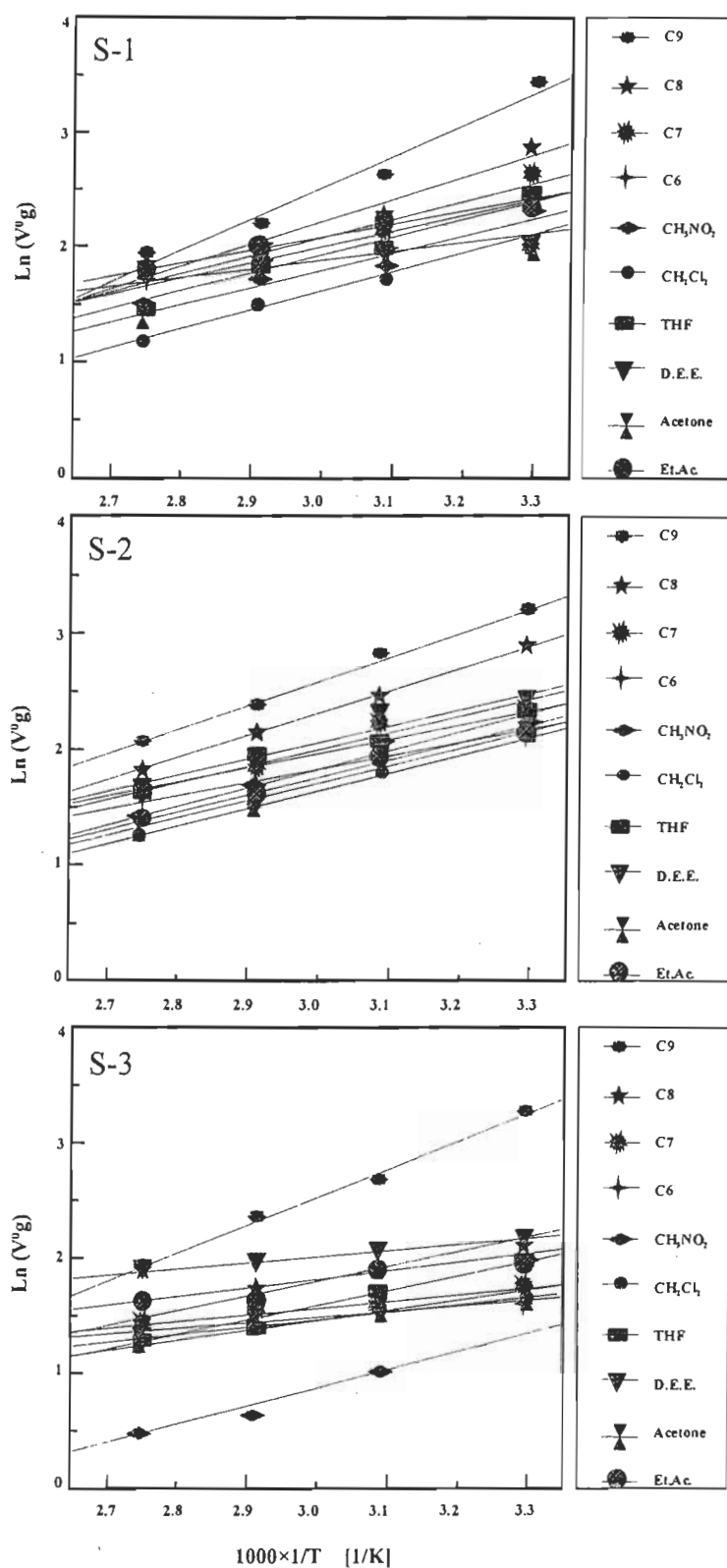
FIGURE A.3 Linearity between $\ln(V^0_g)$ and $a(\gamma)^{1/2}$ for the number of carbon of the alkane probes of the oxidised aspen bleached kraft fibres with N_2O_4/fibre of 0.83% (A-1), 1.25% (A-2) and 1.66% (A-3) .

FIGURE A.4   Linearity of ln(V^0_g) versus the inverse increase in the temperature of the alkane probes of the oxidised softwood fibres with N_2O_4 /fibre of 0.83% (S-1), 1.25% (S-2) and 1.66% (S-3).
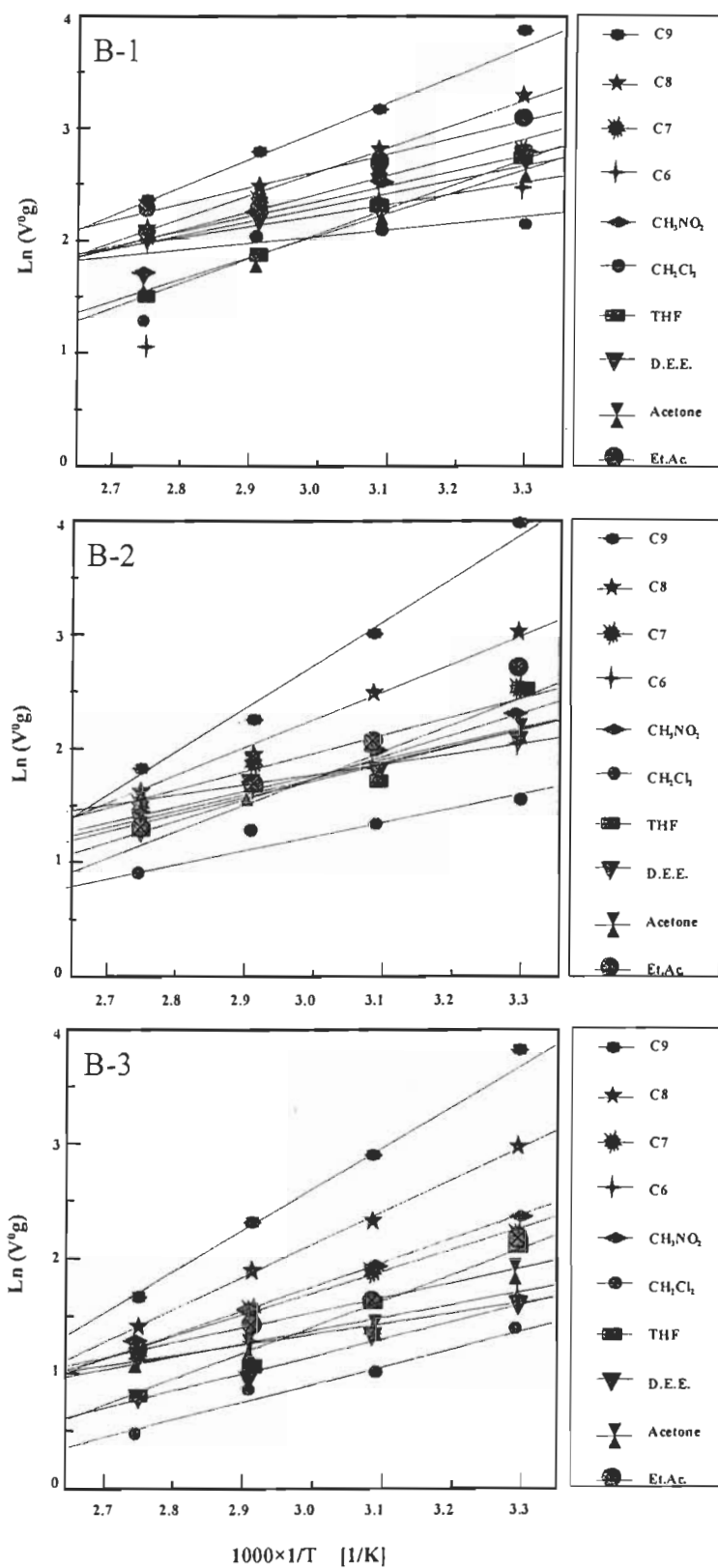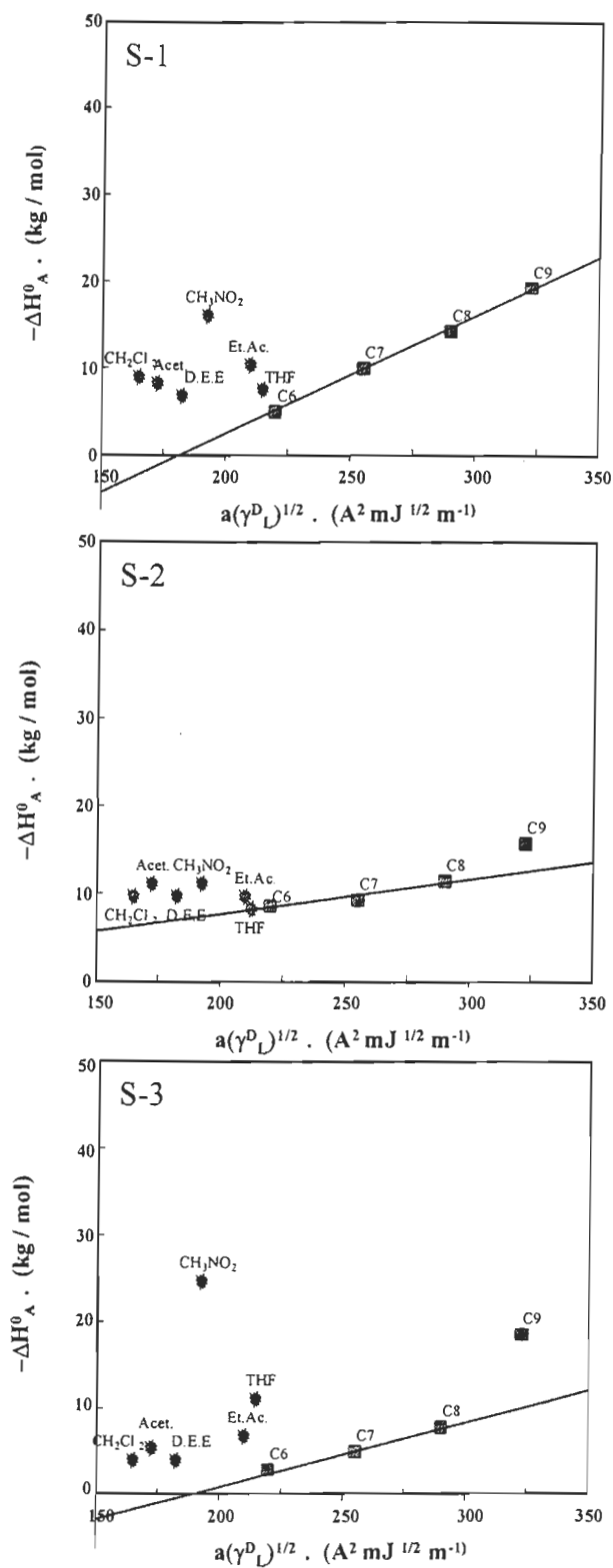
FIGURE A.5 Linearity of $\ln(V^0_g)$ versus the inverse increase in the temperature of the alkane probes of the oxidised bagasse fibres with N_2O_4 /fibre of 0.83% (B-1), 1.25% (B-2) and 1.66% (B-3).
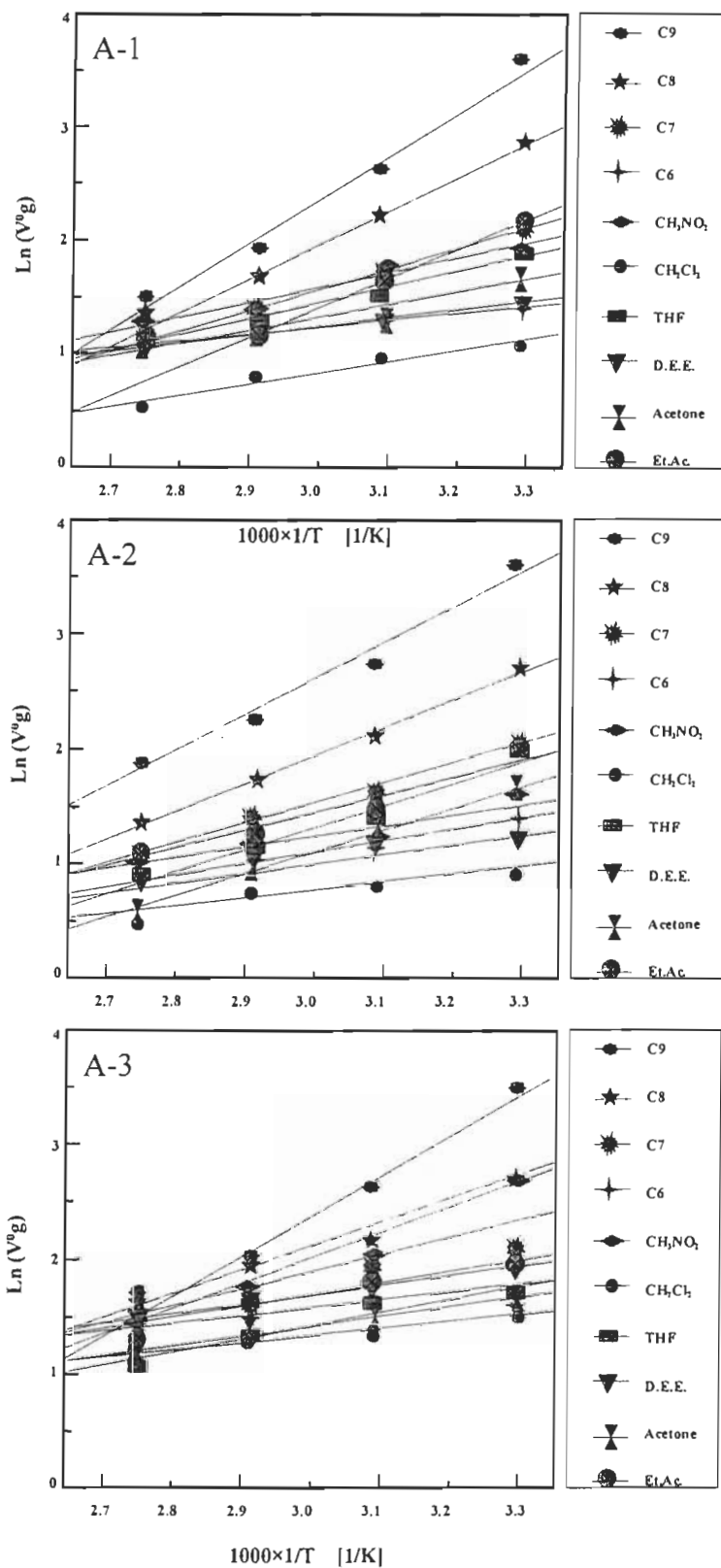
FIGURE A.6 Linearity of $\ln(V^0_g)$ versus the inverse increase in the temperature of the alkane probes of the oxidised aspen fibres with N_2O_4 /fibre of 0.83% (A-1), 1.25% (A-2) and 1.66% (A-3).
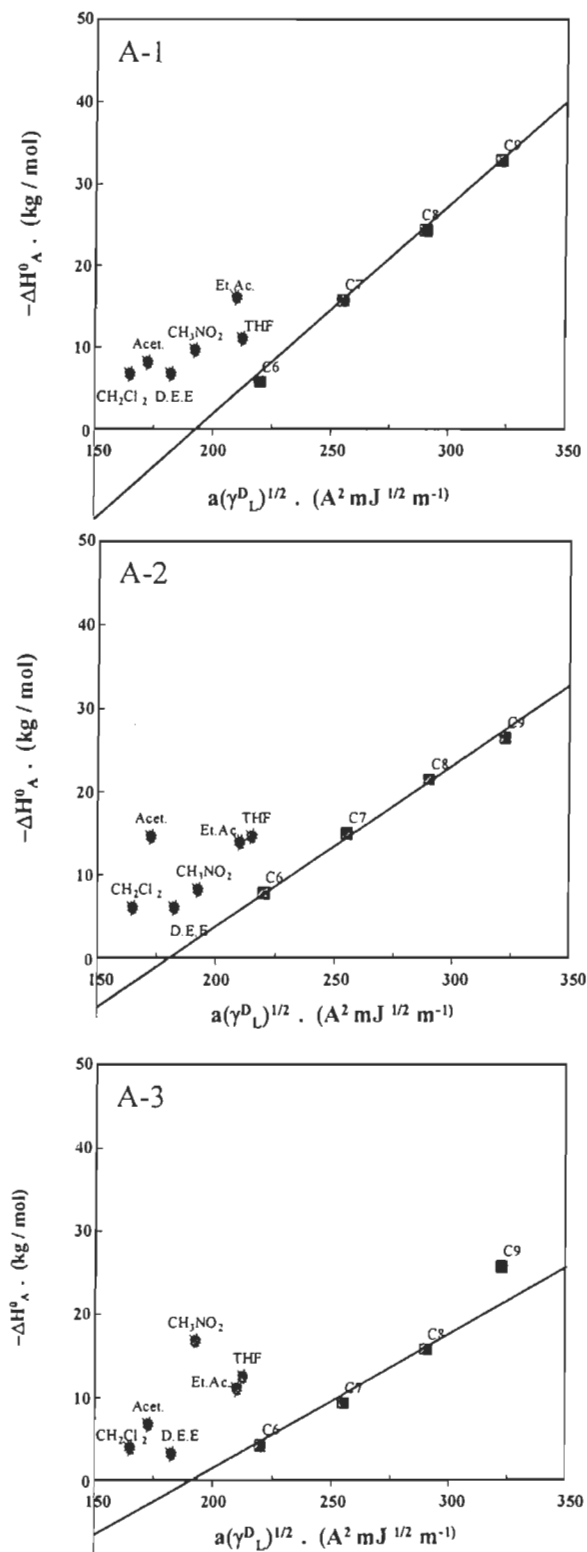
FIGURE A.7 Plot of $-\Delta H_A$ versus $a(\gamma^D_L)^{1/2}$ of the alkane and polar probes of the oxidised softwood bleached kraft fibres at N_2O_4/fibre of 0.83% (S-1) ,1.25% (S-2) and 1.66% (S-3).
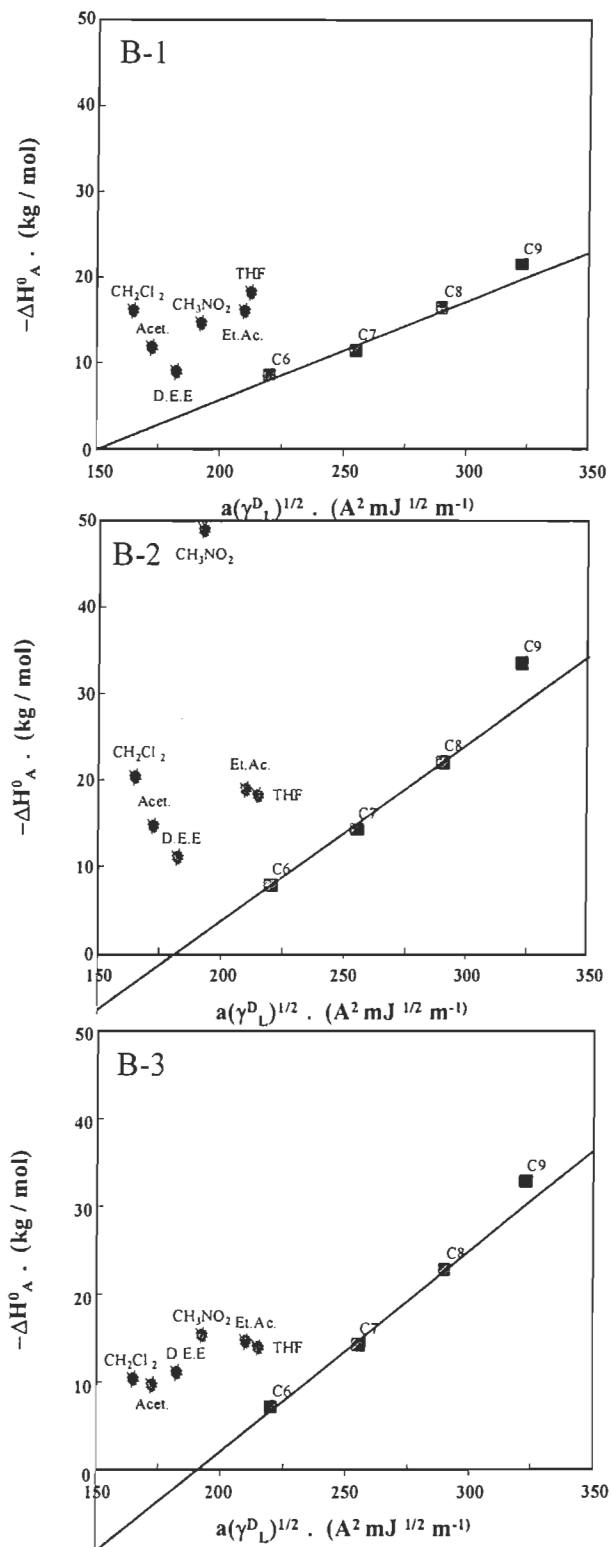
FIGURE A.8   Plot of $-\Delta H_A$ versus $a(\gamma^D_L)^{1/2}$ of the alkane and polar probes of the oxidised bagasse bleached kraft fibres at N_2O_4/fibre of 0.83% (B-1) ,1.25% (B-2) and 1.66% (B-3).

FIGURE A.9 Plot of $-\Delta H_A$ versus $a(\gamma^D_L)^{1/2}$ of the alkane and polar probes of the oxidised aspen bleached kraft fibres at N_2O_4/fibre of 0.83% (A-1) ,1.25% (A-2) and 1.66% (A-3).
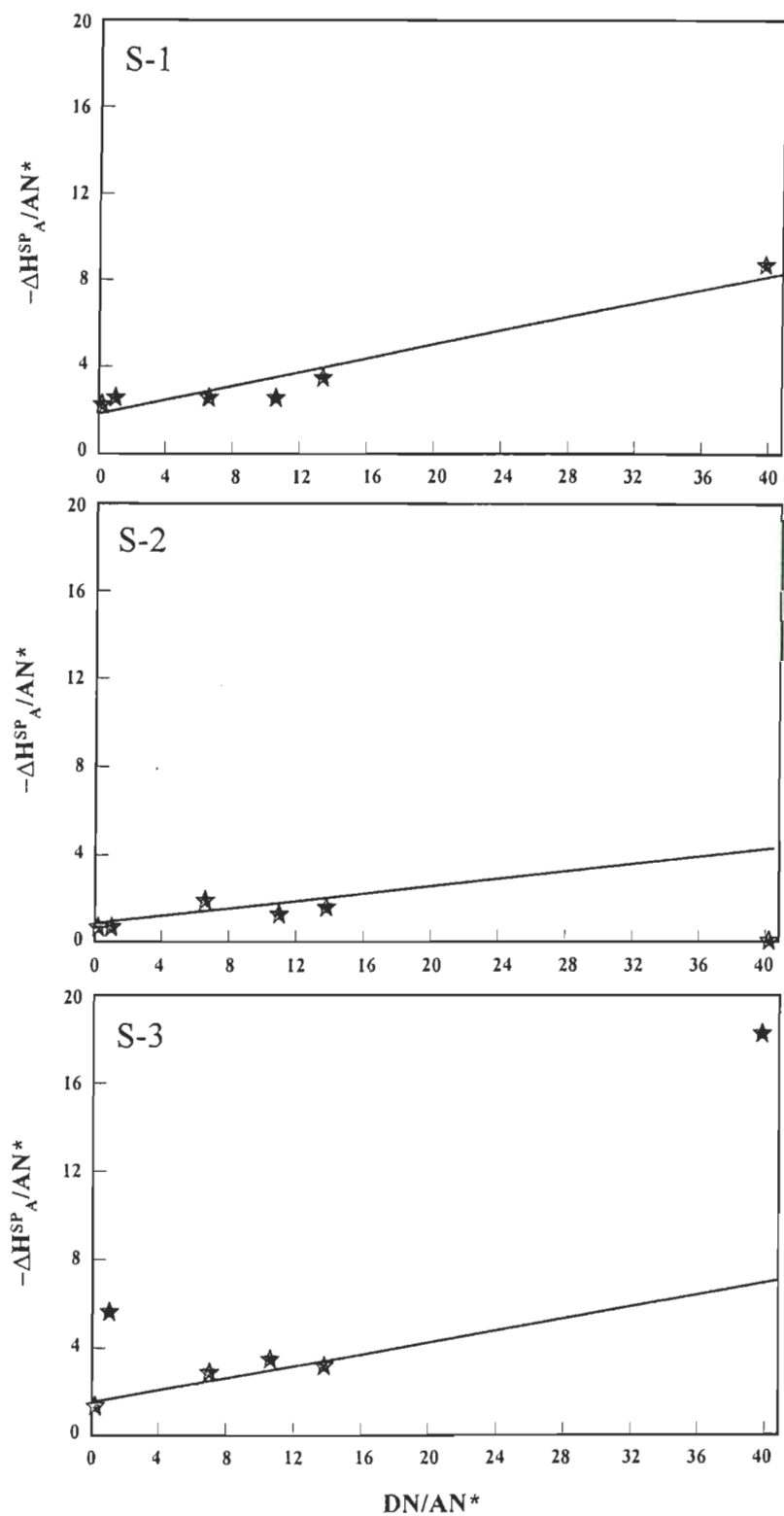
FIGURE A.10   Plot of -ΔH^{SP}_A/AN* versus DN/AN* for the oxidised softwood
bleached kraft fibres at N_2O_4/fibre of 0.83% (S-1), 1.25% (S-2) and
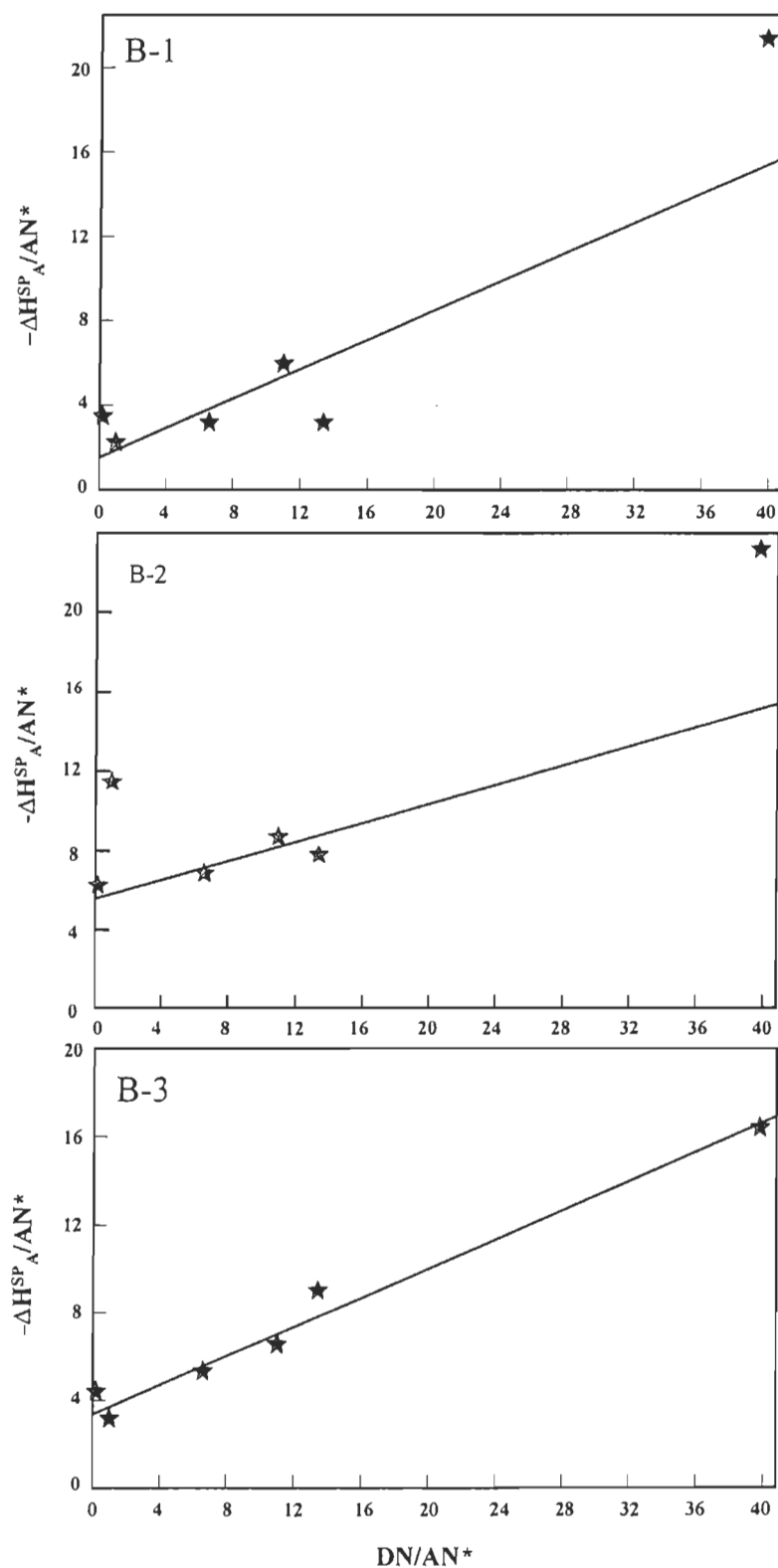1.66% (S-3), allowing the determination of K_A and K_B.

FIGURE A.11   Plot of -ΔH^{SP}_A/AN* versus DN/AN* for the oxidised bagasse bleached kraft fibres at N_2O_4/fibre of 0.83% (B-1), 1.25% (B-2) 1.66% (B-3), allowing the determination of K_A and K_B.
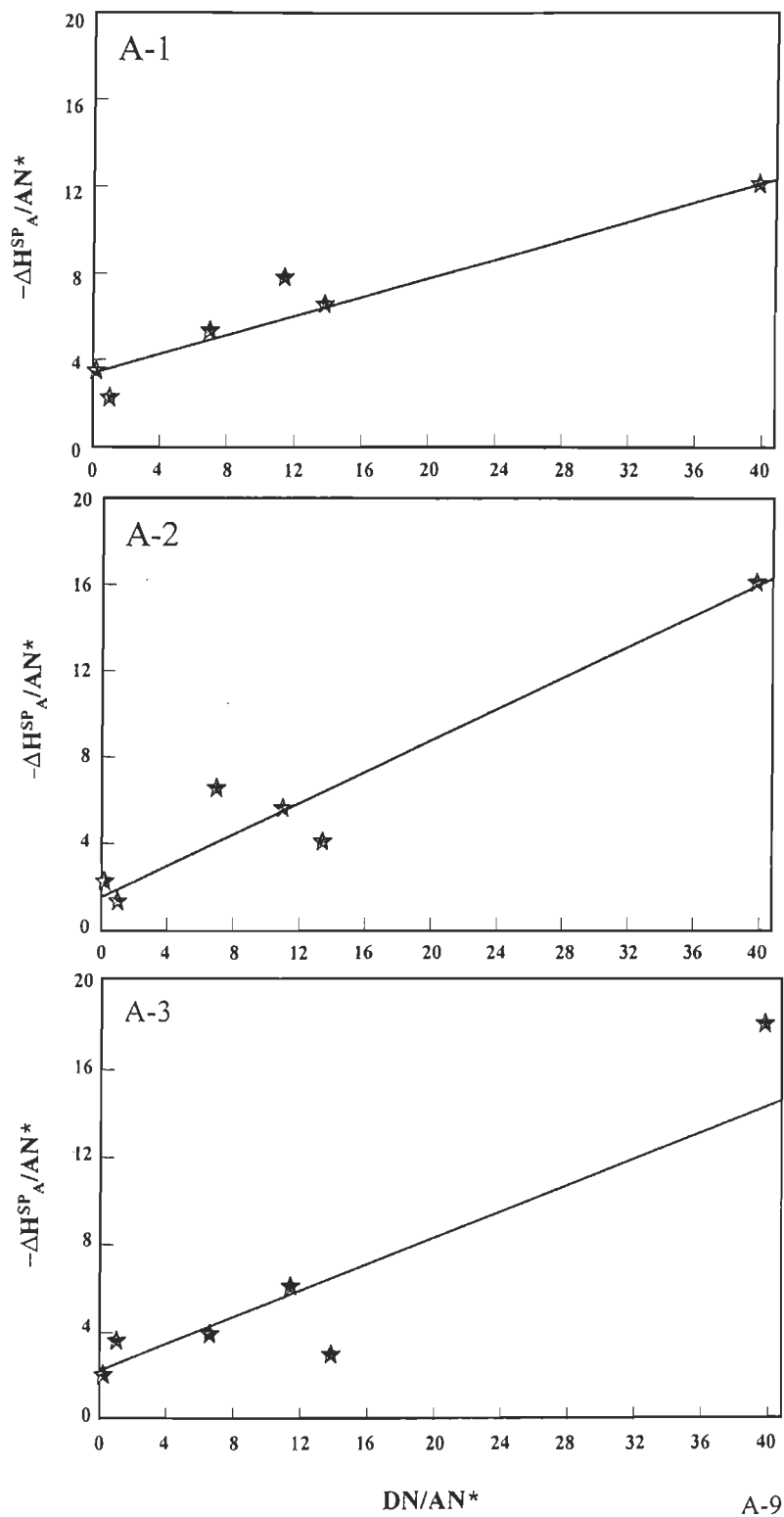
FIGURE A.12 Plot of $-\Delta H^{SP}_A/AN^*$ versus DN/AN^* for the oxidised aspen bleached kraft fibres at N_2O_4/fibre of 0.83% (A-1), 1.25% (A-2) and 1.66% (A-3).
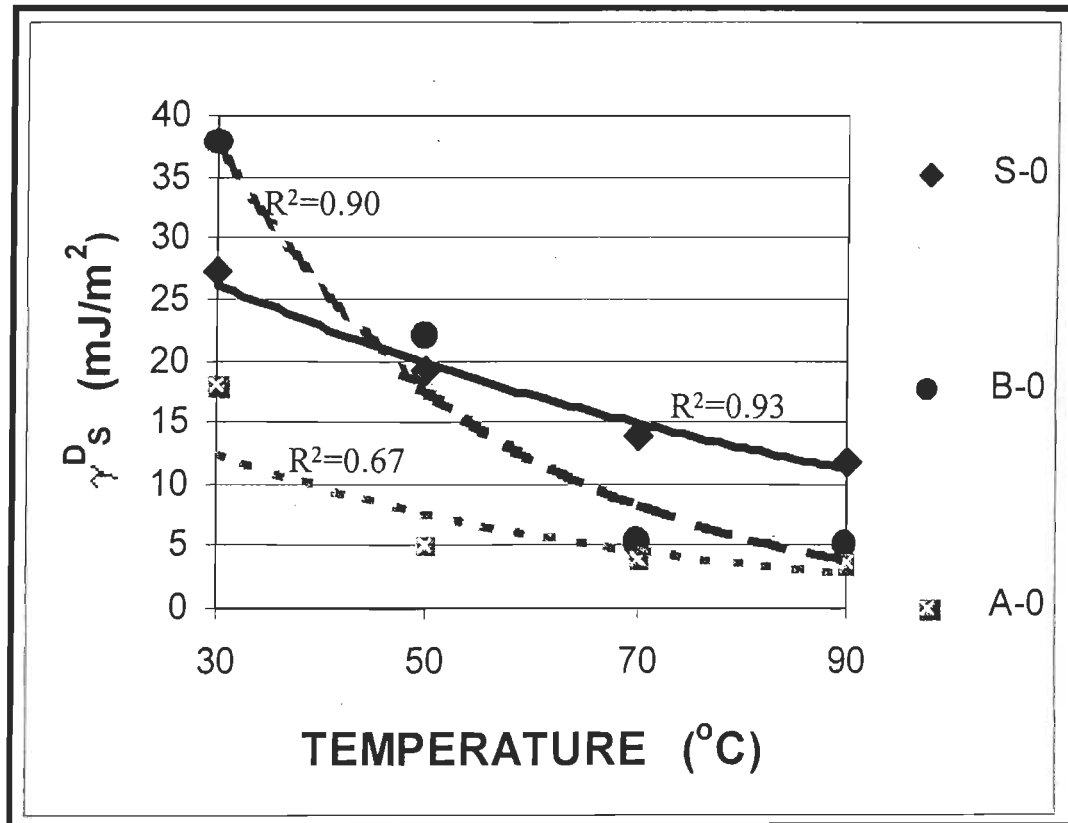
FIGURE A.13 Variations in the value of γ^D_S as a function of the temperature of the IGC column for the untreated softwood (S-0), bagasse (B-0) and aspen (A-0) fibres.